Renal Perfusion in Human Septic Shock

Watchorn, Jim

Awarding institution:
King's College London

Renal Perfusion in Human Septic Shock

Thesis submitted for the degree of Doctor of Philosophy

James C Watchorn

King's College London
School of Immunology & Microbial Sciences
Faculty of Medicine and Life Sciences
King's College London

2023

In memory of Dr Gordon Fryers who inspired me to study medicine and to always ask questions.

Abstract

Sepsis is the dysregulated host response to infection and with resultant organ impairment carries a mortality rate of between 15 and 25%. It is a leading cause of acute hospital admissions. Septic shock, the severe end of the sepsis spectrum is identified by persistent lactataemia and vasoplegia. Hypoperfusion distinguishes patients with this condition, its timely identification being critical to their management. Organ impairment is fundamental, with renal impairment being most frequently observed and independently associated with mortality. Despite its prevalence, the mechanisms underlying renal impairment in septic shock are unclear. Inflammation, metabolic alterations and cell cycle arrest are all implicated but alterations in renal perfusion are also contributory. Animal models are limited and the extent to which alterations in renal blood flow and perfusion occur in humans has not been determined.

Novel methods of studying renal perfusion are necessary as traditional cross-sectional imaging in early septic shock is difficult. The utility of bedside ultrasound in combination with dynamic contrast enhancement (DCE-US) is a potential tool to study these changes but has yet to be tested in detail. This thesis examines the extent to which renal perfusion is altered in both early and persistent septic shock and between patients who develop acute kidney injury and those who do not. It argues that these changes are fundamental to AKI development, anchoring them to biomarker profiles of renal and endothelial injury and inflammatory profiles.

Following a review of the background and a methodology of relevant techniques, Chapter 3 describes the development of the DCE-US technique and assesses its suitability for the study of critically ill patients, validating the developed method by the same user and between two users in a cohort of healthy controls. This study defines normal values of renal perfusion, previously unreported, and informative for the future assessment of patients. It describes my development of the outpatient

radiology-based technique to one that is more suitable for bedside assessments in the intensive care unit (ICU), addresses reliability of contrast data analysis, by the same user (R=0.77-0.9) and between users (R=0.52-0.74) and develops a method of quantifying renal blood flow.

Chapter 5 compares the DCE-US variables in a patient study, addressing correlations between the variables and in combination with the healthy control data, compares and contrasts, aiming to gain greater insight into the strengths and weaknesses of the individual variables. The data presented here suggests a limitation of intensity-based measures. It introduces a grouping variable used throughout the thesis, that of renal perfusion status, dichotomized by those with above and below average values.

Chapter 6 describes the demographic data from the main patient study and compares baseline characteristics. The key differences are the higher vasopressor requirements and sickness severity in those who develop severe AKI. (day zero results: noradrenaline dose severe AKI 0.35(0.26-0.51)mcg/kg/min vs non-severe 0.21(0.14-0.3)mcg/kg/min, $p<0.001$; SOFA scores severe 11.3±3.28 vs non-severe 9.3±1.9, $p<0.05$).

Chapter 7 examines the primary outcome, that of renal microvascular alterations in sepsis. It compares renal perfusion according to the development of severe AKI and looks for longitudinal alterations in perfusion following a septic insult as patients either develop AKI or not. It demonstrates that patients with more pronounced impairment of renal cortical perfusion develop more severe AKI (day zero data mean transit time: severe AKI 10.2(6.5-23.2)sec vs non-severe 5.5(4.7-6.5)sec, $p<0.05$).

Chapter 8 examines haemodynamic data as renal perfusion and AKI manifests. It examines renal blood flow, measures of left heart function and cardiac output and right heart function with venous pressure and congestion assessment. This chapter demonstrates that renal perfusion alterations are intrinsic,

generated by specific renal mechanisms and not secondary, captive to alterations in systemic haemodynamics.

Chapter 9 contrasts renal perfusion with systemic tissue perfusion and the wider examination of shock and its severity. It uses multiple assessments of global tissue perfusion, including sublingual incident dark-field microscopy and biochemical assessments. Further mechanistic data are presented from markers of endothelial and glycocalyx injury. This chapter provides insight into the distinct nature of renal hypoperfusion, its weak association with systemic alterations and its persistence, in contrast to the early resolution of global parameters.

Chapter 10 looks at the relationship between inflammation, renal perfusion and AKI development. It identifies an association with inflammation which occurs later during AKI and is associated with persistence (day 4 IL-8 values maintained perfusion group 32(15-62)ng/ml vs hypoperfusion perfusion group 69(45-154) ng/ml, $p<0.05$) and angiopoietin ratios by day 4 (maintained perfusion group 0.88(0.27-1.53) vs hypoperfusion group 2.11(1.86-5.82), $p <0.05$), these between group differences are not present on admission. Chapter 11 follows on from the previous chapter by examining renal perfusion in previously described AKI subphenotypes. These subphenotypes are differentiated by their inflammatory profiles and have differing outcomes following the use of vasopressors, suggesting a vascular aetiology.

Chapter 12 looks for correlations between renal biomarkers and perfusion, as novel markers are specific to the site of injury, associations may inform the areas of the nephron most affected by alterations in perfusion and longitudinal data demonstrates differing patterns over time, but the close association between tubular alterations and hypoperfusion. This chapter also examines the ability for perfusion assessment to predict severe AKI, demonstrating similar results when compared to novel

biomarkers (AUROC perfusion index 0.84 vs AUROC NGAL*albuminuria 0.78).

Chapter 13 describes longer term data in relation to renal perfusion and whether hypoperfusion is more likely to result in persistent AKI and disease progression. It finds that hypoperfusion can predict the time spent on RRT and the development of acute kidney disease (admission mean transit time for those who spend <7 days on RRT 6.255(4.602-8.2) sec vs more 10.477(7.157-25.387) sec, $p<0.05$).

Chapter 14 compares alterations between septic shock and another severe infection without the septic phenotype, COVID-19 associated AKI. This provides a second cohort of critically ill patients to compare those with sepsis to and demonstrates the utility of DCE-US assessment.

This work describes the development and use of DCE-US as a novel tool, creating a window to assess renal status in sepsis associated AKI. This technique provides utility beyond that provided by novel biomarkers. Renal hypoperfusion appears to be fundamental to, and persistent in all patients with septic shock in combination with downregulation of tubular epithelial cells (TECs) but more so in those who develop the clinical manifestations of AKI. Patients with renal hypoperfusion have worse renal outcomes and a greater mortality. DCE-US accurately identifies these patients on admission and this thesis provides a foundation for future study.

Contents

Abstract 3
Contents 7
Table of Figures 11
Table of Tables 14
Acknowledgements 15
1 Introduction to themes and review of relevant literature 16
1.1 Sepsis 16
1.2 Microcirculation 17
1.2.1 Overview and Physiology 17
1.3 Acute Kidney Injury 19
1.3.1 Overview and Definitions 19
1.3.2 Epidemiology 19
1.4 Sepsis associated AKI 21
1.4.1 Overview 21
1.4.2 Difficulties in studying sepsis associated AKI 22
2 Methodology and Critical Appraisal of Applied Techniques 24
2.1 Imaging in AKI 24
2.1.1 Overview 24
2.1.2 Ultrasound Imaging 25
2.1.3 Contrast Ultrasound 33
2.2 Renal Biomarkers 55
2.2.1 Conventional biomarkers 55
2.2.2 The Search for Novel Biomarkers 56
2.2.3 Predictive Ability of Biomarkers 58
2.2.4 Biomarkers used in this thesis 60
2.3 Endothelial Biomarkers 69
2.4 Methods of examining tissue perfusion and microcirculatory flow 73
2.4.1 Biochemical assessment 73
2.4.2 Handheld Video Microscopy (HVM) 81
Summary of introduction and basis for studies 94
Hypotheses examined in this thesis 96
3 Development of a dynamic contrast enhanced ultrasound technique suitable for intensive care and its validation in healthy controls 97
3.1 Introduction 97

3.2 Method 98
3.3 Results 104
3.4 Discussion 107
4 Introduction and methods of the MICROSHOCK RENAL study: Macro and micro haemodynamic responses to septic shock in the renal and systemic circulations. 112
4.1 Introduction 112
4.2 Overall Method For the Microshock Renal Study 113
5 Time-based variables appear superior to intensity-based variables: a comparison using patient data 123
5.1 Introduction and method 123
5.2 Results 124
5.2.1 Correlation between individual variables 124
5.2.2 Generating a new grouping variable: High and low perfusors 126
5.3 Discussion 128
6 Patients with severe AKI have higher vasopressor requirements and a higher burden of organ failure: Descriptive and Demographic Results of the Microshock Renal Study 130
6.1 Introduction 130
6.2 Results 130
6.3 Discussion 134
7 Patients with more severe cortical hypoperfusion have more severe AKI: Alterations in the renal ***micro***vasculature in sepsis associated AKI 136
7.1 Introduction 136
7.2 Results 137
7.2.1 Differences between individual stages of AKI 139
7.3 Discussion 139
7.3.1 Nitric oxide and its role in regulation of perfusion 144
8 Cortical hypoperfusion is not associated with cardiac output, renal blood flow or markers of venous hypertension: Alterations in the renal and systemic ***macro***vasculature 146
8.1 Introduction 146
8.2 Results 149
8.2.1 Right heart function and venous congestion 149
8.2.2 Left heart function and afterload 152
8.2.3 Changes in renal blood flow 154
8.3 Discussion 155
8.3.1 Key findings 155
8.3.2 RBF in sepsis associated AKI 155
8.3.3 Cardiac function 156
8.3.4 Venous assessment and right heart 157

8.3.5 Fluid balance and volume administration 157
8.3.6 The renal effects of select inotropes and vasopressors 158
9 Cortical hypoperfusion is not associated with systemic shock: A comparison with traditional markers 161
9.1 Introduction 161
9.2 Results: 163
9.2.1 Sublingual microcirculation 163
9.2.2 Alterations in biomarkers 165
9.2.3 Analysis of supply adequacy and oxygen consumption by blood gases 167
9.2.4 Correlation between shock indices 169
9.3 Discussion 170
10 The relationship between inflammation, renal perfusion and AKI development 174
10.1 Introduction 174
10.2 Results 176
10.2.1 AKI groups 176
10.2.2 Perfusion groups 177
10.3 Discussion 178
10.3.1 Key findings 178
10.3.2 The interaction between TECs and the immune system 178
10.3.3 The emerging interaction of immunological resistance and tolerance mechanisms 179
10.3.4 Endothelial and glycocalyx involvement in AKI development 180
10.3.5 Cellular immune response in AKI 180
10.3.6 Bioenergetic Adaption and mitochondrial function 181
11 AKI subphenotypes: A reassessment using data from the Microshock Renal study 184
11.1 Introduction 184
11.2 Methods 185
11.3 Results 187
11.4 Discussion 189
12 Biomarker Profiles and Renal Perfusion 192
12.1 Introduction 192
12.2 Results 193
12.2.1 Correlation between DCE-US variables and biomarkers 195
12.2.2 Prediction of AKI using DCE-US 195
12.2.3 Proenkephalin A 198
12.3 Discussion 200
12.3.1 Predicting AKI 201

12.3.2 Normalisation to urinary creatinine 202
12.3.3 PENK 202
13 Renal hypoperfusion is associated with an increased risk of death and prolonged duration of RRT 204
13.1 Introduction 204
13.2 Results 206
13.2.1 Alterations in baseline function 207
13.2.2 Outcome data for patients with better or worse renal perfusion 208
13.3 Discussion 210
14 Patients with COVID-19 associated acute kidney injury have reduced renal perfusion and reduced renal blood flow despite preserved cardiac output. A case-control study 213
14.1 Introduction 213
14.2 Materials and Methods 215
14.3 Results 218
14.4 Discussion 222
14.5 Conclusion 225
15 Final Discussion and Conclusion 226
15.1 Limitations 233
15.2 Conclusion and suggestions for further work 235
16 References 237

Table of Figures

Figure 1 Quantification of pulsatile flow within a vessel. 31

Figure 2 Stylised SonoVue microbubble. 34

Figure 3 Ultrasound dual-mode mode image of a kidney. 37

Figure 4 The contents of the SonoVue contrast kit. 39

Figure 5: DCE-US kinetics 44

Figure 6: Gain settings and DCE-US 48

Figure 7: Graph demonstrating maximum coefficient of variation in DCE-US. 50

Figure 8 graph demonstrating the time course of novel urinary biomarkers 58

Figure 9: Site of injury leading to alterations in novel biomarkers. 59

Figure 10 Schematic drawing of the endothelial glycocalyx layer 70

Figure 11 The relationship between oxygen extraction and venous oxygen saturations. 75

Figure 12 The differences between admission ScvO2 in the EGDT studies 76

Figure 13, The carbon dioxide dissociation curve 78

Figure 14 ROC curves for biochemical shock variables 80

Figure 15 Schematic of handheld video microscopy. 83

Figure 16 Determination of Microvascular Flow Index quadrant score. 89

Figure 17; (A) example of an HVM video image 90

Figure 18 Comparison between the signal from the cortex. 103

Figure 19 Bland Altman analysis of the four DCE-US variables 105

Figure 20 Boxplots demonstrating the variation between ROI area and DCE-US variables . 106

Figure 21 Principal methods of assessing the macro- and microvasculature 113

Figure 22 Investigation patient timeline for the MICROSHOCK RENAL study. 116

Figure 23 Correlation coefficients of the DCE-US parameters. 124

Figure 24 Population distributions for variables generated by DCE-US 125

Figure 25 3D correlation plot of day 0 observations 126

Figure 26 3D correlation plot, rotated from Figure 25 127

Figure 27: Descriptive data for the Severe and Non-severe AKI groups 132

Figure 28 CKD stage on admission and admission DCE-US variables. C 133

Figure 29 Differences in renal perfusion variables between severe and non-severe 138

Figure 30 Perfusion variables on admission and the most severe stage of AKI 139

Figure 31Diagram illustrating the presence of peritubular arterio-venous shunts.....142

Figure 32 Boxplots of alterations in sublingual perfusion 163

Figure 33 Handheld video microscopy findings in the sublingual mucosa.....164

Figure 34 Shock biomarkers between those with severe and non severe AKI. 165

Figure 35 Boxplots of angiopoietin ratio, arterial blood lactate and syndecan. 166

Figure 36 Correlation between individual perfusion variables and cardiac output. 169

Figure 37 Inflammatory cytokine levels in patients with and without severe AKI 176

Figure 38: Boxplots demonstrating differences between inflammatory cytokine profiles. .177

Figure 39 3D clustering of inflammatory groups. 186

Figure 40: Biomarker boxplots between higher and lower renal perfusion. 194

Figure 41 ROC analysis for DCE-US (CEUS) variables in the prediction of severe AKI. 196

Figure 42 ROC charts of admission biomarker levels to predict severe AKI.....197

Figure 43 Mixed graphic summarising the key findings of proenkephalin-A (PENK) 199

Figure 44 Kaplan-Meier graph for hospital survival by KDIGO AKI stage. 205

Figure 45 Ability of admission biomarkers to predict RRT requirement for greater than or equal to 7 days 206

Figure 46 Admission values and the ability to predict higher creatinines after discharge. ..207

Figure 47 Kaplan-Meir curves for high and low perfusion groups 209

Figure 48 Boxplots comparing patients with sepsis, covid and controls.....221

Table of Tables

Table 1 Commercially available contrast agents 38

Table 2 Average values of normal renal cortical perfusion in healthy controls 104

Table 3 A comparison of dynamic contrast ultrasound variables at two minutes 106

Table 4 Noradrenaline doses and presence of a second inotrope, by day 133

Table 5 Longitudinal perfusion data from day 1 through day 4. 139

Table 6 Assessments of right heart function and venous congestion. 150

Table 7 Assessments of right heart function and venous congestion. 151

Table 8: Indicators of left ventricular function, cardiac output and afterload 152

Table 9 Proportion of patients with severe AKI intubated per day 153

Table 10 Indicators of left ventricular function, cardiac output and afterload 153

Table 11: Renovascular variables 154

Table 12 Renovascular variables, between perfusion groups 154

Table 13 Number of patients alive by day 164

Table 14 Blood gas analysis values for those with severe and non-severe AKI. 167

Table 15 biochemical measures of shock severity 168

Table 16 Comparative data between Bhatraju et al and the present study 185

Table 17 Differences in cortical perfusion between high and low inflammatory groups 187

Table 18 Trends in haemodynamic variables in low and high inflammatory subgroups. 188

Table 19 correlation between biomarker and perfusion index on day 0 195

Table 20 Ability of admission values to predict an RRT requirement beyond 7 days 207

Table 21 Demographic and baseline patient characteristics 218

Acknowledgements

I would like to thank the following people, without whom I would never have achieved this, a feat at times I thought beyond me:

Dr Sam Hutchings, my supervisor. A constant source of excellent ideas and inspiration, a mentor and a critic. It has been a pleasure to study under your direction.

Dr Kate Bramham, co-supervisor. Always encouraging and supportive, always opening doors and creating networks; an excellent sounding board and sage advice.

Dr Dean Huang, Radiologist and imaging expert. Thanks for the time you took training me and developing this project together.

The ACET team at King's College Hospital, particularly Lt Cdr Su Jeffreys QARNNS. For helping me with the administration and running these studies, for helping in the lab and for your general support.

The Defence Deanery, Col David Woods, Gp Capt Ed Nicol and Brig Duncan Wilson for allowing me to undertake a dedicated period of research, for being supportive of my aims and for the resources which enabled me to complete my studies.

My parents for their support and indomitable curiosity. For always encouraging me to inquire and understand the world in which we live.

Charlotte, Evie, Connie and Hetty. Thank you for your love, your encouragement and your patience.

1 Introduction to themes and review of relevant literature

1.1 Sepsis

Sepsis presents a massive global disease burden. In 2017 there were an estimated 48.9 million cases (95% uncertainty interval 38.9-62.9) and 11.0 million deaths (UI 10.1 – 12.0m). Although trends are probably reducing worldwide, as better treatment strategies emerge, it disproportionally effects children and low-income countries, particularly in Africa and South Asia, where both the incidence and mortality rates are higher and advanced healthcare is unavailable[1]. In high-income countries sepsis still presents a major disease burden. A large point prevalence study demonstrated 51% of ICU patients were classed as infected and 71% were receiving antibiotics[2].

Definitions of sepsis and septic shock have altered over time from an original reliance on blood pressure, through a focus on overt organ failure requiring organ support, to the status of identifying circulatory impairment and persistent tissue hypoxia through hyperlactataemia[3,4]. Changing definitions are beneficial by increasing precision and geographical comparability but reduces temporal comparisons meaning the incidence of sepsis and septic shock over time is unclear.

The latest definition of septic shock, SEPSIS-3[5] requires a persistently elevated blood lactate, hypotension requiring vasoactive drugs and the presence of infection and has identified a more specific but sicker cohort of patients than the previous definition. A recent meta-analysis using sepsis-2 criteria demonstrated that septic shock accounts for approximately 10% of ICU admissions but by Sepsis-3 criteria 6.5% of ICU admissions have

septic shock[6]. In high-income countries the mean ICU mortality using previous definitions of septic shock is 37.3% but 52% if Sepsis-3 criteria are used [6].

1.2 Microcirculation

1.2.1 Overview and Physiology

Abnormal tissue perfusion has been recognised since antiquity; Hippocrates commented:

"First of all the doctor should look at the patient's face […], the following are bad signs […] hollow eyes, cold ears, dry skin on the forehead, strange face colour such as green, black, red or lead"[7].

In 1740 the first recorded use of *shock* was made by Henri Françóis-LeDran following haemorrhage[8]. *Choc* became gradually accepted in English as shock and refined to describe an inability to provide sufficient tissue perfusion, with a variety of accepted causes.

1.2.1.1 Regulation of the microcirculation

The microcirculation is the vascular network responsible for substrate exchange, recognised as vessels under 20µm. The microvascular unit comprises the terminal arteriole, 15-20 capillaries and the collecting venule[9]. The terminal arteriole and collecting venule are generally between 20-100µm and involved in the regulation of flow within the capillaries. Increased oxygen consumption from cellular work is fed back by the capillary endothelium and signalling from venule metabolites including changes in oxygen extraction. Additional feedback is generated by haemodynamic forces exerting transmural pressure on arteriolar smooth muscle and luminal shear stress on the capillary endothelium. Capillaries regulate their own supply depending on conditions through the production of vasodilatory substances,

including NO, prostacyclin and oxygen, whilst vasoconstrictors such as endothelin and platelet activating factor provide the opposite[10]. Diffusion of metabolites from venules lying near arterioles provide additional vasoactive feedback. These paracrine homeostatic signalling loops and a local neural network induce changes in the proximal arteriole, maintaining uninterrupted flow despite alterations in supply and able to respond to changes in demand. Feedback loops induce vasodilatation of the terminal arterioles until completely vasodilated, at which point the locus of blood flow control shifts proximally to induce vasodilatation in the proximal arterioles and arteries[11]. Sympathetic fibres also course in the opposite direction, from the artery to the terminal arteriole and induce vasoconstriction through noradrenaline release, inhibiting vasodilatation. Regulatory control is therefore provided by multiple levels, all of which can affect the delivery of oxygen and its extraction.

1.3 Acute Kidney Injury

1.3.1 Overview and Definitions

Acute kidney injury is an abrupt deterioration in renal function, disrupting metabolic, electrolyte and fluid homeostasis within hours or days[12]. As with sepsis, the defining criteria of AKI have changed over time, making the understanding of temporal and geographical trends more difficult. Prior to the early 2000s more than 35 different criteria had been published and such diversity was unacceptable for investigators[13]. The 2004 Acute Dialysis Quality Initiative's (ADQI) RIFLE criteria[14] and the 2007 updated version published by the Acute Kidney Injury Network, the AKIN criteria[15], represented the first consensus definitions, becoming widely accepted by the medical community[16]. Alongside the new definition came the term "acute kidney injury" and "acute renal failure" became obsolete. In 2013 the previous definitions were refined further to form the current Kidney Disease Improve Global Outcomes KDIGO classification, modifying stage 3 from the AKIN criteria and allowing a rolling baseline creatinine value[17,18]. Limitations remain however, definitions rely on relative changes in creatinine from a baseline value which may be unknown, whilst serum creatinine is insensitive and urine output is non-specific. The defining criteria are based on the recognition of a failure in filtration and novel biomarkers have not been adopted. Despite its imperfection, the KDIGO classification and its predecessors represent a monumental step forward in the care and study of AKI, providing a common language and enabling comparison.

1.3.2 Epidemiology

In low to middle income countries AKI is predominately community-acquired but hospital-acquired in higher income countries. In Europe community-acquired complicates 8.3% of

ambulatory patient encounters, whilst hospital-acquired AKI occurs in 20.0-31.7% of inpatients in one meta-analysis of >3,000,000 patients [19,20]. Risk factors for AKI are multiple and causes are typically multifactorial. Environmental factors include poor sanitation and endemic infections whilst patient factors include chronic disease such as heart failure, existing CKD, volume depletion, hypotension and nephrotoxin exposure amongst others[21].

In developed countries AKI is predominately hospital acquired and occurs in 21% of hospitalised adults and 33% of children, with a decreasing mortality rate and an inverse relationship between mortality and GDP, according to a systematic review of 49 million patients[20]. Despite the revisions to the diagnostic criteria there is good evidence that the incidence of AKI is increasing over time[22,23]. In the UK the incidence has been reported as 577 per 100,000 population[24]. A large multinational observational study determined the epidemiological characteristics of severe AKI within the ICU, demonstrating a period prevalence of 5.7%, of which septic shock caused 50%, crude in-hospital mortality was 60% and dialysis dependence on discharge 13%[25]. Another reported observational data across 17 Finnish ICUs, demonstrating an incidence of 39% for all AKI severity and 14% for severe, in-hospital mortality for stage 3 was 39% and 11% remained dependent on RRT at day 90[26]. A third study demonstrated similar results, incidence of RRT in ICU admissions was 6.8% and population-based incidence of severe AKI was 19.2 per 100,000 population[27]. A large international study of 97 centres and 1802 patients reported an incidence of 57% for all-severity AKI[28]. The incidence of ICU AKI is increasing by 2.8% per year, whilst the mortality is reducing by 3.8% per year[29]. The aetiology of AKI in developing countries differs from that of developed, with increased infectious disease, trauma and obstetric complications. As a result, patients in developing countries are typically younger, present later, occur in rural

areas and have a greater mortality[30].

1.3.2.1 Cost

Renal replacement is amongst the greatest expenditures of intensive care units. Costs vary depending on geography and modality, but the daily cost of continuous renal replacement (CRRT) is approximately £1200, being more expensive per day than intermittent (IRRT) [31–33]. There is some evidence to suggest that patients treated with IRRT spend longer on renal replacement than CRRT but overall the effect is considered negligible[34,35].

1.4 Sepsis associated AKI

1.4.1 Overview

Sepsis is frequently reported to be one of, if not the most common cause of AKI in the community, the hospital and the ICU[25,28,36]. Sepsis occurs in 15-27% of ICU admissions although the rate increases to 37% if only emergency admissions are studied[37–39]. Mortality from septic shock is approximately 30%, increasing to 40%-60% in those with AKI[25,37]. Mortality is consistently greater in patients with septic shock and AKI than those without AKI[28,40].

A group of investigators, all of whom have published widely in sepsis associated AKI produced a unified theory of the pathogenesis in 2014[41]. They proposed three principles which underpin the development of sepsis associated AKI: abnormal inflammation, alterations of cellular bioenergetics and microcirculatory flow abnormalities. These findings

have broad support across the literature. They propose that following inflammatory danger signals, renal cells undergo an adaptive response, favouring cell survival through maintenance of membrane potentials and cell cycle arrest at the expense of gross renal functions such as filtration and tubular transport. These three pillars of inflammation, metabolic adaptation and particularly microcirculatory alterations are discussed in greater depth in the appropriate sections of this thesis.

1.4.2 Difficulties in studying sepsis associated AKI

There is a paucity of human tissue data from sepsis associated AKI. Performing a biopsy in critically unwell patients is technically demanding, involving issues with coagulopathy, positioning and ethical considerations amongst others. Histological data can be gathered post-mortem but end-stage multiorgan failure, in combination with the dying process and cold ischaemia may confound the results and limit information on the early pathogenic mechanisms. A 2008 meta-analysis reported histopathological data from a total of 184 septic patients and only 22% had features of acute tubular injury, once thought the predominant mechanism. The majority of findings were in fact normal and this finding was consistent between humans, primates and other large and small animal models[42]. A later rapid post-mortem study of 44 septic patients demonstrated oedematous mitochondria without mitochondrial membrane disruption. This study reported regions of focal ATI in 78% of patients, particularly at the corticomedullary junction with KIM-1 positivity. The findings were mild and most renal tubules were normal, leading the investigators to conclude that the degree of organ dysfunction was not explicable by the tissue findings[43]. A recent study demonstrated a constellation of histopathological features with no one mechanism predominant, suggesting the occurrence of dysregulated biological processes[44].

Another study of 19 post-mortem septic patients with anuric AKI, of whom 7 had DIC, reported monocyte infiltration in glomeruli and interstitial capillaries with 3% of tubular epithelial cells (TECs) being apoptotic[45]. A meta-analysis of experimental data showed ATI as a predominant feature in low cardiac output states. Hyperdynamic sepsis experimental models, a more realistic model of human sepsis demonstrated tubular vacuolisation, swelling and brush border injury[46]. Interestingly Tran and colleagues demonstrated that the presence of tubular vacuolisation was associated with mitochondrial damage[47]. Other issues with experimental models include the short lifespan of some animals which does not mimic the often-protracted course of human septic shock. Large animals are generally required for the accurate measurement of renal haemodynamics and rodents have a relative resistance to endotoxin infusion[48]. As a results novel methods are required to investigate these changes in clinical septic shock. Experimental studies have provided a wealth of data, but inference to humans has limitations and such methods do not lend themselves to practice. Confirmatory studies are therefore necessary.

2 Methodology and Critical Appraisal of Applied Techniques

2.1 Imaging in AKI

2.1.1 Overview

Investigating acute kidney injury presents unique challenges. Although often mild and self-limiting, AKI complicates approximately 25% of acute hospital admissions and only if detected early would intervention be most effective, reducing severity and long-term morbidity[49]. Imaging in AKI is currently only indicated for the following reasons [1] to exclude obstruction, although this only accounts for 10-13% of cases[50] [2] to identify structural renal abnormalities [3] to help differentiate AKI from CKD and [4] to assess the vasculature, surrounding tissues and end organs for the sequalae of renal disease[51].

The commonality of AKI and the relatively low incidence of obstructive nephropathy - the main indication for imaging, dictates that investigations are in the main, relatively simple to perform, have a cost consideration and no associated harm. Ultrasound has been the mainstay, able to reliably identify reversible causes, such as obstruction, pyelonephritis and renovascular disease. It is low cost and simple. In addition it has the advantage of portability, particularly useful for acutely unwell patients. However, the combination of greyscale ultrasound and clinical laboratory tests prove insufficient to diagnose most causes of AKI, often with a delay between injury and investigations. Cross sectional imaging is infrequently performed in clinical practice; iodinated contrast agents frequently exacerbate renal injury limiting the role of CT. Perfusion MRI uses gadolinium and due to the occurrence of nephrogenic systemic fibrosis is contraindicated, which is unfortunate as it has the power to

reveal precise anatomical and physiological information[52].

As a greater understanding of AKI pathophysiology emerges and the search for potential treatments continues, new imaging techniques which provide functional data are needed. Advancements in multiple imaging modalities now provide detailed physiological and anatomical data, although largely used for research purposes, they hold promise for future translation. These methods include multi-parametric functional MRI, scintigraphy, elastography and molecular imaging[53] but are largely unsuitable for studying the early changes of critical illness and the changes of sepsis associated AKI in humans, as they are often in remote research centres, require patient stability and have a substantial cost consideration.

2.1.2 Ultrasound Imaging

2.1.2.1 Principles and Physics

Propagation

Ultrasonic piezoelectric crystals act as an interface between electrical and sound energy and vice versa. Most medical piezoelectric crystals are fabricated from a polycrystalline ferroelectric ceramic material such as lead zirconate titanate (PZT). Initially the particles are randomly orientated and PZT is electroplated with sliver or chrome-gold. The composite material is heated just above its Curie temperature, the temperature at which its magnetic properties are lost, and cooling occurs slowly whilst exposed to a strong magnetic field causing alignment of the ferroelectric grains within the PZT. When the electroplated surface of the crystal is exposed to a voltage it causes the crystal to deform and when the voltage is removed the crystal returns to its resting form. The kinetic energy produced by the vibration

of the crystal is emitted as a sound wave and ultrasound imaging utilizes high frequency sound waves in the region of 1.5-15MHz[54].

Ultrasonic pulses produced by the transducer move through the patient tissues, if the propagated wave is reflected by a structure, a returning wave contacts the transducer, inducing vibration within the piezoelectric crystals which in turn creates a voltage and a signal is detected. The same crystals therefore act to send and receive. Usually only a small proportion of the wave is reflected, the remaining wave continues along its beam line to detect deeper structures. More reflective structures appear brighter in brightness mode (B mode) imaging. A transducer propagates many small coplanar beams, sequentially across the face of the probe. Each pulse accounts for a small fraction of a frame and multiple beams are therefore required to produce each frame. The usual frame rate for medical ultrasonography is 20-40 per second[55].

Soft tissues act as a liquid in relation to sound wave propagation, with a speed equal in both of 1540m/sec, although varies slightly depending on the stiffness of the tissue. Propagation in air is approximately five times slower and in bone is much faster (4080m/sec)[56]. This makes imaging of all soft tissues possible but other media are outside the detectable range for usual medical imaging. As the soundwave velocity (v) is a fixed property of the substance through which it travels, the frequency (f) of the propagated wave is inversely proportional to the wavelength (λ) as described by the universal wave equation:

$$v = f\lambda$$

Typical wavelengths range from 0.1 to 0.77mm, shorter wavelengths are more likely to collide

with a small reflector, hence shorter wavelengths or higher frequencies increase spatial resolution. The fixed speed of sound in tissue permits the calculation of distance, being directly proportional to the time between pulse transmission and detection of the reflected wave. The likelihood of wave reflection depends on the density of the tissue through which it travels, referred to as the acoustic impedance. Particles oscillate longitudinally in the same direction as the wave propagation; where two media of different impedance meet, the wave creates regions of compression and rarefaction which results in a specular reflection; the sum of the transmitted and reflected pulses equal the energy of the initial pulse, thus energy is conserved. The greater the difference in acoustic impedance, the greater the reflection, hence why ultrasound is unable to penetrate a tissue-air interface as it is almost all reflected and why ultrasound gel is necessary as a bridge between the transducer and the body[55].

The wave loses energy during propagation, this attenuation occurs as reflection, scattering, beam divergence and friction. This loss is proportional to both the distance travelled and wavelength, as a certain amount of energy is lost per cycle. Particles close to the transducer are exposed to more ultrasound energy than distant ones and higher frequencies provide better spatial resolution at the expense of depth penetration.

Detection

Ultrasound transducers contain multiple crystals, the arrangement of which is dependent on the transducer (array) type. For example, curvilinear arrays cover a wide field of view, but phased array cardiac transducers have fewer elements with slight offsets in excitation timing able to steer the beams at non-perpendicular angles. This allows beams to propagate from a small transducer footprint, allows a higher frame rate and provides the ability to concentrate

beams to converge at a particular depth which provides a focal distance.

Echoes detected by the receiving crystals are amplified at several stages, immediately by the transducer, by gain setting and by software processing known as time-gain compensation which is amplification dependent on the depth of the echo received, providing a uniform brightness for the field of view, to compensate for the lower energy delivered to and from distant structures. Further processing steps act to reduce the ratio of the received signal, thus removing signal extremes using logarithmic compression. The resulting signal provides the dynamic range[57].

Another physical property of the propagated wave, particularly pertinent to the research undertaken for this thesis, is its power, this is a measure of the wave's strength; how much energy is contained within the wave and is expressed in watts. The power per unit area is known as the intensity, which may be expressed as pressure but due to its high variability is expressed after logarithmic transformation using the decibel scale. The amount of negative acoustic pressure within an ultrasonic field imparted on the tissues is quantified using mechanical index (MI) and aims to describe the biological destructive power of the sound energy[58]:

$$MI = \frac{peak\ rarefaction\ pressure}{\sqrt{central}\ wave\ frequency}$$

Different manufacturers arrive at MI values via different approaches and generally MI values are not interchangeable between machines[59]. However low MI modes are typically <0.2 and even as low as 0.04[60]. Normal MI ranges from 0.2-0.5 and high MI >1.0. The FDA requires the

MI to be always visible on the screen and limits the maximum to 1.9.

2.1.2.2 Advantages of Ultrasound

Ultrasound provides multiple advantages in comparison to other imaging modalities. It is non-ionizing and presents no significant risk to patients, the risk of heat from vibration of tissues and cavitation of gas filled structures at the exposed intensities of typical medical usage is insignificant. The portability of ultrasound makes the study of unstable patients easier than cross sectional imaging. Imaging occurs in real-time allowing data collection over a period of time, (eg a number of heart beats or breathing cycles) and also permits repeatability. It provides structural data but also functional and temporal data and the use of Doppler ultrasound permits velocity and flow measurements.

2.1.2.3 Doppler-Based Assessments of Renal Perfusion

Measurement of Renal Blood Flow

The combination of time, distance and velocity measurements enables ultrasound to quantify flow and is used routinely in clinical practice, including cardiac output and cardiac valve area estimations. It should be seemingly straight forward to use a flow calculation in the renal artery using the formula below:

$$Flow = cross\ sectional\ area \times velocity \times time$$

$$\therefore Flow = \pi(renal\ artery\ diameter/2)^2 \times time\ averaged\ velocity$$

In practice this approach is problematic. Multiple assumptions are made including a 50:50 left to right split of RBF and one renal artery per kidney, although up to one third of patients may have multiple supplies[61]. Any error in the measurement of diameter becomes a square error

in the above calculation and the diameter of the renal artery may vary in its anatomical course and with pulsatility; measuring velocity at the same location reduces but does not eliminate the variability[62]. The RA is often not clearly visible with B-mode ultrasound particularly in patients who are obese or oedematous, sub-optimally positioned due to immobility or from renal respiratory motion. Colour Doppler enhances the view of the RA but may lead to an overestimation of its diameter from aliasing outside the vessel wall. Ultrasound contrast, confined to the intravascular space, may provide a more reliable view of the diameter and is a promising alternative.

Velocity quantification depends on the flow-type within the vessel. In smaller vessels parabolic flow may be more likely and time averaged mean velocity (TAMV) quantifies all velocities within the vessel, slower speeds at the vessel edge and the faster in the centre. In large vessels such as the left ventricular outflow tract laminar flow is more likely, velocities throughout the area of the vessel can be treated equally as the effect of the flow reductions at the vessel edge becomes negligible. The maximum frequency of the Doppler profile can therefore be used to generate the time averaged peak velocity (TAPV)[62].

Figure 1 demonstrates the differences between TAPV and TAMV. TAPV is comparatively higher than TAMV and the appropriate use of either depends on the likely flow profile[62]. In arteries such as the RA, early and late components of systolic flow are thought to be parabolic

and mid- systole predominately laminar[63].

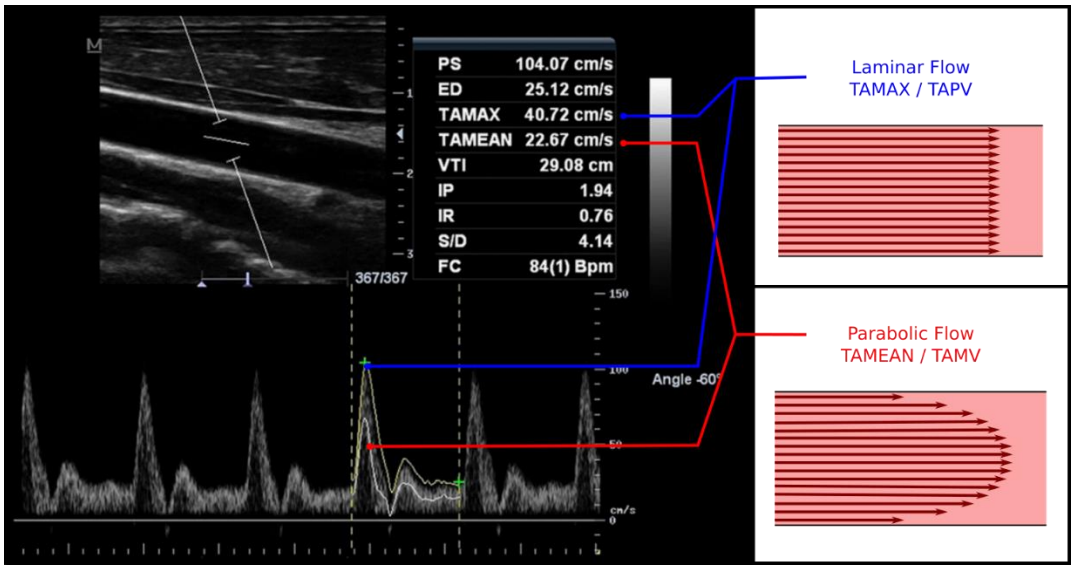

Figure 1 Quantification of pulsatile flow within a vessel. TAPV (TAMAX above) measures the area under the peak velocities of the Doppler profile, appropriate for laminar flow. TAMV (TAMEAN) quantifies the maximum signal intensity of the Doppler flow profile, appropriate for parabolic flow[62].

Variation between Doppler flow and an invasive gold-standard is therefore likely. In an experimental study in sheep, Doppler derived parameters of renal blood flow correlated poorly with those derived by transit-time flow probes and failed to identify changes in RBF more than 20%[64], whereas a study in dogs demonstrated a good correlation with invasive measurements[65]. Quantification of RBF by Doppler assessment is technically difficult and has multiple potential weaknesses, but in critically ill patients may still be meaningful, particularly if relative change or between-group differences are measured rather than absolute values.

2.1.2.3.1 Renal Resistive Index (RI)

$$Renal\ Resistive\ Index = \frac{Peak\ Systolic\ Velocity - End\ Diastolic\ Velocity}{Peak\ Systolic\ Velocity}$$

RI is derived from the pulsatility flow velocity waveform within an intrarenal artery, using the above ratio[66]. As O'Neill comments in a 2014 editorial, the naming is inaccurate as the index

is reflective of pulsatility and has little to do with resistivity, it would be more appropriately termed an impedance or compliance index[67]. RI is a velocity ratio and has previously been suggested to be reflective of flow, however the diameter of the vessel may vary and flow and velocity are not equivalent[64]. Being relatively simple to perform it is repeatable, regardless of the operator's experience[68]. The normal range for RI is 0.55-0.7 and values above this range are encountered across a range of pathologies, including progressive dysfunction in CKD[69], prior adverse cardiovascular events, renal graft loss and recipient death in transplantation[70,71].

RI demonstrates good predictability for AKI, comparable with plasma NGAL concentrations in one study and better than Cystatin-C in another [72–78]. In predicting persistence of AKI, results of a small study were favourable (AUROC = 0.88), but a follow-up multicentre study demonstrated very little predictive power (AUROC = 0.58)[79,80]. A meta-analysis in 2015 reported pooled sensitivity and specificity of 0.83 and 084 respectively but with significant heterogeneity among the 9 selected studies[81].

RI correlates with blood pressure in some studies[72] but not in others[79]. Others reported the correlation only existed in those who went on to develop AKI[75]. Some have suggested it could be used to titrate vasopressor dosage[76]. The correlation with vasopressor dosage is however variable, demonstrating correlation in some studies[76] but not others. In the assessment of renal perfusion Harrois demonstrated superiority of CEUS parameters, probably as they

provide a more direct measure of the microcirculation[82].

Several authors suggest caution in the interpretation of RI; whilst it has repeatedly demonstrated predictability for AKI and recovery, the cause of alterations in the systolic and diastolic velocities are multiple and not always apparent[75]. Changes in vascular compliance may either reflect long standing vascular stiffness, as occurs with differences in age and gender or in the presence of arterial disease, diabetes or hypertension. Otherwise variation in these parameters may represent subcapsular pressure from venous congestion, interstitial oedema, volume overload or hydronephrosis[83–86]. Variation in RI may therefore just reflect this rather than identifying a causal linkage between arterial velocity and renal injury.

2.1.3 Contrast Ultrasound

2.1.3.1 Principles of contrast enhanced ultrasound

Gramiak described the first use of contrast for ultrasonography in 1969 using a rapid intracardiac injection of multiple substances and noted "echoes at the site of injection and downstream […] permitting identification of the cardiac chambers"[87]. The rheological properties of small bubbles have since been shown to mimic the behaviour of red blood cells and can be used as a reliable tracer for blood flow and blood pool imaging[88].

Although small air bubbles were initially used for ultrasound contrast, Lindner theorised that microbubbles with a lower solubility would have a longer lifespan and demonstrated this with microbubbles of perfluorocarbon gas[89]. This study was the first to demonstrate that microbubbles larger than 5µm did not distribute freely, becoming lodged in the microvasculature. Smaller bubbles are more likely to collapse however, according to Laplace's

law of surface tension, where internal bubble pressure (p) is inversely proportional to the bubble radius (r) and σ represents the surface tension[90]:

$$p = \frac{2\sigma}{r}$$

As the maximum bubble size must remain less than 5µm, investigators wishing to prolong bubble half-life had to reduce the bubble surface tension to prevent collapse. Multiple attempts led to thick albumin shells to enclose air, although these did not deform under ultrasound and produced little backscatter[91]. The second approach was to fill microbubbles with a poorly-soluble gas such as sodium hexafluoride or perfluorocarbons which reduces the diffusion out of the bubble shell and found this technique successful, these agents make up the current commercially available products, a typical microbubble is presented in Figure 2[92].

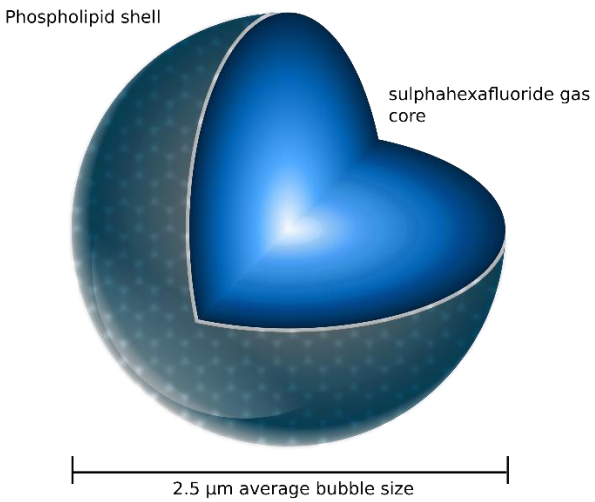

Figure 2 Stylised SonoVue microbubble, comprising a phospholipid (Dipalmitoylphosphatidylglycerol) shell, approximately 2nm thickness and a sulphahexafluoride (SF6) gas core. Average bubble size 2.5µm (90% <6µm, 99%<11µm)[90].1ml SonoVue contains 4x10[7] microbubbles and 1.5µl of SF6 [93].

Pure low solubility gas cores provide an additional theoretical hurdle, having the potential to equilibrate dissolved ambient gases from the blood, particularly nitrogen and oxygen with the

potential of bubble expansion within the vasculature. Currently available solutions overcome this by preparation under a head of low solubility gas with a small amount of air included, the air reducing the in-vivo gas partial pressure difference. The vial spike also contains a 5µm filter to provide a suspension of bubbles below the maximum safe size. Theoretically patients breathing oxygen will have a lower partial pressure of dissolved nitrogen, as a result the nitrogen within the bubble will be lost more rapidly into solution, causing a reduction in bubble size and a recommendation that experimental studies utilize a standardized inhaled gas mixture, this has not been demonstrated to be significant in clinical studies however[94]. Over time gas is lost from the bubble causing its shell to contract and eventually the external compression overcomes the internal pressure maintaining bubble integrity and it collapses, the gas is free within the blood to be exhaled and the lipid shell is metabolised. 80-90% of sulphur hexafluoride from SonoVue is detectable outside the body within 11 minutes and the half-life is not dose dependent[95].

Microbubble destruction occurs continually though both dissolution and cavitation from ultrasound energy. The proportion of bubbles destroyed by ultrasound is subject to the acoustic energy imparted in them; once a threshold is reached bubble integrity is lost causing rapid fragmentation. Whilst seemingly detrimental, this permits microbubble behaviour to be controlled and bubble fragmentation utilised for the assessment of tissue perfusion, holding potential for the use of bubbles as a vehicle for targeted drug delivery[90] which has previously been demonstrated using microbubble cavitation to open the endothelial component of the blood-brain barrier and in the same process, release nanoparticles to reach the target site[96,97].

Like red cells, microbubbles demonstrate slower flow along the vessel periphery and faster

central flow, this slower peripheral flow provides the possibility of further applications of microbubbles such as molecular targeting with bubble-ligand complexes, binding endothelial receptors. The formation of ligand-receptor bonds can anchor the microbubble, allowing real-time identification of molecular expression and provide a potential bedside molecular imaging technique[98].

Standard B-mode ultrasound has several drawbacks when imaging contrast agents, the wave power may cause bubble destruction, particularly at lower frequencies, according to the mechanical index equation above. In addition, tissues are highly echogenic, making contrast difficult to differentiate from background signal. Fortunately the acoustic properties of bubbles are quite different to tissues and have enabled equipment manufacturers to preferentially identify them. At low power non-linear oscillations occur in microbubbles where rarefaction is greater than compression due to the highly compliant shells of modern agents. Strong signal harmonics are produced when insonated, even at low-power and they can produce high signals at the second and third harmonic frequencies. Equipment manufacturers can both filter out the fundamental frequency and make use of low-power ultrasound where insonation of tissues produces little signal[99]. These techniques provide a specific Contrast Mode, which at baseline is predominately black, with little background noise but displays signal from bubble insonation on delivery of contrast. Newer scanners can send alternating low-MI, and normal-MI pulses, dividing the frame rate by two, to create two side-by-side images, one contrast specific and one standard B mode. This allows contrast data to be displayed alongside anatomical B-mode data but at powers less than the threshold for bubble destruction[89] An example of this side-by-side imaging is presented in Figure 3. Oscillatory frequencies and bubble destruction thresholds are agent specific and therefore

mechanical indices will vary slightly.

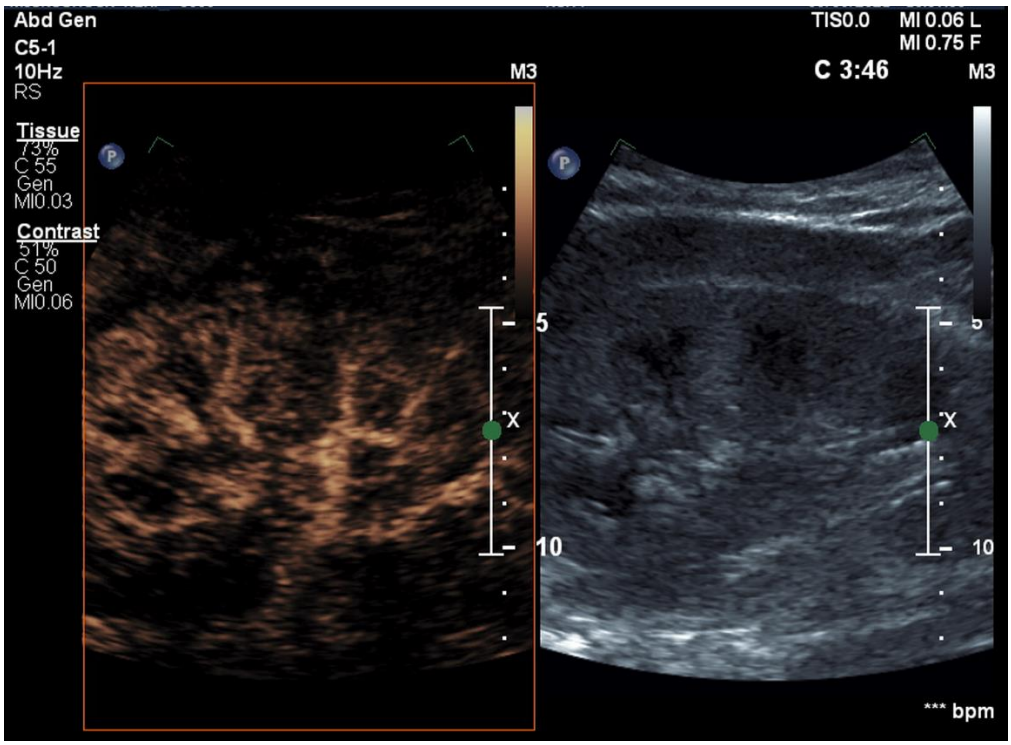

Figure 3 Ultrasound dual-mode mode image of a kidney. Contrast mode is displayed on the left with microbubble specific signal preferentially filtered and B-mode is displayed on the right

2.1.3.2 Contrast Agents

Agents and Preparation

A summary of the available contrast agents is presented in Table 1. Sonovue contrast (Bracco, Milan, Italy) was utilized as the contrast agent for the research presented in this thesis. It has similar characteristics to other ultrasound contrast agents (UCAs) and is possibly the most used agent for renal imaging. It is also commonly used by our collaborating radiology department. SonoVue is sold as a kit as shown in Figure 4, containing a vial with phospholipid lyophilisate in a sulphur hexafluoride (SF_6) atmosphere, a prefilled syringe with 4.8ml of 0.9% saline and a minispike transfer system[93]. Preparation is straight forward and involves

attachment of a plunger to the saline syringe, connecting this to one end of the minispike transfer system and attaching the phospholipid vial to the other. The saline injected and mixed with the phospholipid lyophilisate by vigorous shaking within the SF_6 atmosphere and the microbubble solution produced is drawn back into the syringe suitable for injection or infusion. Each millilitre of the 4.8ml pharmacologically inert substance contains approximately $2x10^8$ microbubbles and 8µl of SF_6. The mean bubble diameter is 2.5µm and 99% of microbubbles are <10µm. The solution remains stable for administration for 6 hours[93].

Agent	Shell	Gas Core	Bolus dose	Elimination half life	Manufacturer	Notes
SonoVue	Lipid	Sulphur hexafluoride (SF_6)	1.2-2.4ml	12 min	Bracco, Milan, Italy	Marketed as Lumason in the USA
Optison	Albumin	Perflutren (C_3F_8)	0.5ml	1.3min	GE Healthcare, Milwaukee, USA	
Luminity	lipid	Perflutren (C_3F_8)	0.2-0.3ml	1.3min	Lantheus Medical Imaging, N. Billerica, USA	Marketed as Definity in the USA
Sonazoid	egg phosphatidyl serine	Perflurobutane (C_4F_{10})	0.5-1.0ml	30-45min	GE Healthcare, Milwaukee, USA	Currently only available in Asia

Table 1 Commercially available contrast agents

Figure 4 The contents of the SonoVue contrast kit. From left to right: Minispike transfer system, phospholipid lyophilisate in a sulphur hexafluride atmosphere, prefilled saline syringe (plunger attached)

Safety Profile

Sonovue is a widely used, licensed pharmaceutical agent with 2.5 million doses administered by 2013 (manufacturer sales data). Reported adverse events following UCAs are rare and mostly mild, with headache and nausea most common but in less than 1% of patients. Serious adverse events occur at a rate of 0.03% and anaphylactoid reactions between 0.004 and 0.009%. Such events are typically not IgE mediated and therefore no prior exposure is required[100]. Product labelling for UCAs continue to warn against their administration in pulmonary hypertension, however several prospective studies have examined this, of which two were in conjunction with the Federal Drugs Administration. A number of these studies were performed with concurrent right heart catheterisation and all studies have demonstrated stable haemodynamics and no safety concerns[101–104]. As a result many investigators administer UCAs to patients with pulmonary hypertension, as currently no evidence exists to the contrary, despite the product warning[100]. The warning also covers UCA use in acute respiratory distress syndrome. UCAs have seen limited use in paediatric populations and the safety profile is unknown. The same is true of pregnancy and UCAs are

not routinely administered in either group[105]. Being of similar dimensions to a red cell, UCAs are blood pool contrast agents and are not filtered across the glomerular basement membrane and are not secreted by the tubules. They have no known renal interactions and are not nephrotoxic; a distinct advantage for the study of renal disease over intravenous contrast agents of other imaging modalities[106].

Administration

The principal use of UCAs are to provide anatomical detail of the vasculature, referred to as contrast enhanced ultrasound (CEUS). UCAs can be administered to model perfusion kinetics, referred to as dynamic contrast enhanced ultrasound (DCE-US), both terms are used interchangeably in the literature which can be confusing[106]. For the purposes of this thesis CEUS is used as an overall term whilst DCE-US specifically applies to perfusion kinetics. UCAs may be administered either by bolus intravenous injection or by infusion and has been demonstrated to closely correlate with invasive measures of tissue perfusion[107]. For renal imaging a good view of the kidney is needed with ultrasound in B-mode prior to enabling contrast mode, preferably displaying B-mode and contrast-mode side by side, which aids in detecting movement of the transducer and finalising the view before administration[59]. Maintaining a B-mode image alongside provides a continual image, as prior to UCA administration contrast-mode imaging is dark and lacks detail. For bolus administration a standard volume (typically 1.2 to 2.4ml of Sonovue) is given either centrally or peripherally followed by a 10ml saline flush and a recording is taken from start to finish[59]. The contrast image enhances as the microbubbles arrive within the insonated region providing an arterial

wash-in phase, a microvascular perfusion phase and a venous wash-out phase.

When given by infusion, typically 1ml/min of neat Sonovue is infused. A slower wash-in phase occurs due to the slower rate of injection, until a plateau and steady-state is achieved. The field of view is then pulsed with a high mechanical index pulse which causes mass fragmentation of microbubbles and the field of view darkens until it is re-perfused, from which time-intensity curves (TICs) can be created. The faster and brighter the signal returns, the better the perfusion. Previous investigators have diluted the UCA infusion with saline with no detrimental effects observed from a 1:20 dilution[108]. Neat contrast was diluted 1:4 in this thesis.

2.1.3.3 Analysis of ultrasound contrast kinetics

Off-line processing of CEUS imagery is performed by dedicated software. Several proprietary platforms are available as are bespoke programmes written for a specific research purpose[109–111].

VueBox (Bracco, Geneva, Switzerland) is a commonly used analysis system for perfusion quantification and the platform used by our institution and in this thesis. Other available software includes MATLAB (The MathWorks, Natick, MA, USA) and QLAB (Advanced Technology Laboratories, Philips, NY USA). Several ultrasound manufacturers have added contrast analysis software to their carts, including the GE TIC Analysis module and Seimens CDx analysis module[112]. Many of these systems use black-box modelling algorithms, each producing reassuring accuracy figures but at the expense of reproducibility with different

platforms. In VueBox, files are imported from the ultrasound machine in digital imaging and communications in medicine (DICOM) format. These files are imaging-converted video data, log-compressed and palletised as grey-scale or colour-coded 8-bit data[113]. Once imported linearisation occurs, the process of converting the log-compressed DICOM files back to linear signal for analysis. After the file is loaded an overall region of delimitation is selected and motion compensation applied. If motion occurs within a clip it is usually the result of respiratory motion (a frequent issue in renal imaging) or probe movements. Automatic motion correction corrects in plane motion by spatially realigning anatomical structures in a user-selected reference image[114]. If uncorrected, motion can prevent analysis in 30% of data[115]. Regions of interest (ROIs) are selected and time-intensity curves created to generate a line of best fit according to a mathematical model; the shape of the TIC and variables produced are software specific due to the individual algorithms within the programs and also dependent on whether UCAs are administered by bolus or infusion.

A constant UCA infusion is required to produce destruction-replenishment kinetics and this is the method used in this thesis. In renal imaging steady state is achieved in one to two minutes, with signal intensity proportional to the relative blood volume. Large vessels produce the greatest signal and cortical signal is uniform in health, although may be attenuated towards the poles and nearer the pelvis as signal is scattered by other bubbles[116]. Provided regions of interest are within well-visualised parenchymal tissue, the exact shape, size or location of the ROI makes little difference to the reproducibility of the results[117,118]. This makes the examination of renal perfusion by DCE-US in longitudinal clinical studies more of a possibility.

Medullary signal is heterogenous, calyces produce no signal as UCAs are not filtered, however

vascular regions have high signal. Medullary parenchymal tissue receives approximately one tenth of cortical blood flow and enhances more slowly[119]. The complex arrangement of the vasculature within the renal medulla and the associated anisotropy makes clinical quantification of perfusion challenging regardless of the imaging method including fMRI. Quantification of medullary perfusion by DCE-US is therefore challenging and further work is needed to determine if it can be done reliably.

Once steady state is achieved a high mechanical index pulse (>1.0) can be delivered by the operator, with mass bubble destruction and replenishment. TICs are generated off-line and the steeper the replenishment gradient and more intense the signal, the greater the perfusion. ROIs are plotted and the variables created by VueBox for both destruction-replenishment and bolus-transit kinetics are demonstrated in Figure 5. Bolus kinetic variables are provided in the figure legend for interest but are otherwise not used in this thesis. Destruction-replenishment kinetics include the wash-in rate (WiR) which is the initial gradient and the mean transit time (mTT) which describes half the time to signal plateau, both variables are thought representative of blood velocity / flow. Relative blood volume (RBV) describes signal intensity and is calculated from plateau signal minus background signal; perfusion index (PI), a composite variable is a computed by the division of RBV by mTT and aims to provide a single number representing tissue perfusion[120]. According to the central volume theory (see reference) the perfusion of a tissue can be calculated by this ratio,

although is measured in arbitrary units, 2D ultrasound being unable to quantify volume[113].

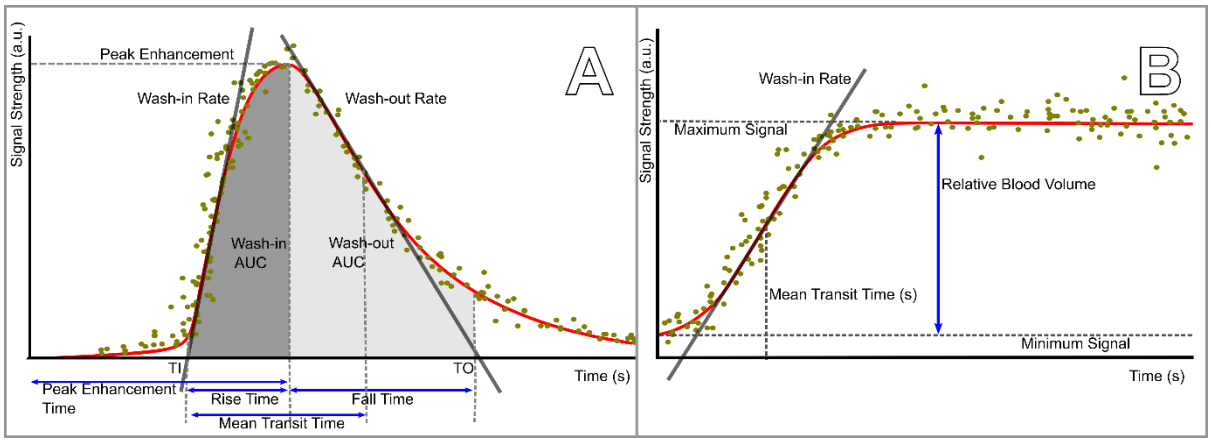

Figure 5: (A) Bolus-transit kinetics. Assessed values: (1) Maximum wash-in rate (WiR) and (2) maximum wash-out rate (WiR) are measured using the maximal slope and both the gradients and x-axis intercepts are used to the quantification. TI= Time In, defined as maximum wash-in rate x-axis intercept; TO= Time Out defined as maximum wash-out rate x-axis intercept. (3) Mean Transit Time (mTT)= wash-in rate x-axis intercept to mid-point wash-out rate. (4) Wash-in Area Under the Curve (WiAUC) = AUC (TI: peak enhancement time). (5) Wash-out Area Under the Curve (WoAUC) = AUC(peak enhancement time: TO). (6) Rise Time= peak enhancement time – TI. (7) Fall Time= TO- peak enhancement time. (8) Wash-in Perfusion Index = WiAUC/Rise Time

(B) destruction-replenishment kinetics. Assessed values: (1) Relative Blood Volume (rBV) =maximum signal – minimum signal. (2) Wash-in Rate (WiR) = gradient of maximum slope. (3) Mean Transit Time (mTT) = time to half maximum signal. (4) Perfusion Index (PI) = rBV / mTT

2.1.3.3.1 Mathematical Modelling of CEUS Data

The sigmoidal mathematical model adopted for perfusion quantification by destruction-replenishment was initially described by Lucidarme et al[121]. Earlier empirical negative-exponent models failed to fully reflect perfusion measurements during Wei's series of invasive experimental studies[122,123]. Krix adapted a similar mathematical description after taking experimental measurements from tumours and was able to demonstrate equivalent, if not better results to the initial Wei mono-exponent model[124]. The sigmoidal model was

subsequently developed by Arditi[125] and further refined by Hudson[126]. This model assumes a multiple-vessel vascular network may be simplified with fractal branching geometry of the vascular tree, whose distribution of vessel sizes and associated flow rates is given by a lognormal velocity distribution, please see referenced texts for greater detail[127]. The Arditi-Hudson lognormal model improves on previous models in several ways. It explicitly considers the velocity distribution within the regions of interest rather than assuming homogenous flow profiles, more reflective of in vivo perfusion than a pre-mixed volume model. It accounts for the character of the ultrasound beam which affects the shape of the TIC. It models different components of the region of interest separately such as larger vessels and this realistic microvascular geometry permits more accurate perfusion quantification[126]. Hudson demonstrated better correlation with implanted flow meter measurements, in comparison with the previous mono-exponential models described[128]. In a further study, the group demonstrated the new model had greater test-retest reliability using different planes and different operators[129].

2.1.3.4 Limitations of contrast ultrasound

Many authors have identified the reproducibility of CEUS as a potential issue with both bolus and infusion methods, particularly the quantification of signal intensity[118,130–132]. Potential sources of error have been well described in previous reviews and may be broadly subdivided into issues with microbubbles, ultrasound scanner settings and patient characteristics[133]: A summary of the sources of error is given below:

1. **Contrast mixing within the syringe:** Bubble separation occurs after a period of stasis. To counter this dedicated oscillatory infusion pumps are available for prolonged

periods of imaging.

2. **Uniform mixing of contrast with blood** within the cardiac chambers, a potential issue for bolus infusion but unimportant with steady-state infusions[134].

3. **Patient blood volume:** A standard rate of UCA is administered regardless of the size, gender, age or fluid balance of the patient, where blood volume may vary by a significant degree, leading to variation in the bubble : blood dilution ratio[135]. This is likely to be more of an issue for intensity-based variables than time-based.

4. **Respiratory motion and transducer movement:** May alter the stability of the ROIs if not carefully accounted for. In healthy volunteers and able patients, breath holding can be utilized[126] or in-plane motion correction software. The dual-screen B-mode and contrast-mode display allows the operator to visualise anatomical landmarks providing a visual reference and more able to keep a still image[59,120]. Averkiou et al have also described a respiratory-gated ultrasound technique for the evaluation of liver metastases[136].

5. **Field of view and organ depth:** A reliable, unobstructed view of the kidney is required for accurate quantification, rib shadows are commonly encountered. Other acoustic shadows are more problematic at low MI and should be carefully assessed. Microbubbles can be imaged up to 15cm from the transducer, more distant images require lower frequency insonation or higher mechanical indexes, both of which may increase bubble destruction in the near-field [59]. Organ depth may affect the reliability of measurements, particularly those dependent on signal intensity. Ignee et al recommends not undertaking DCE-US examinations at all at less than 4cm and not measuring intensity variables at greater than 6cm due to unacceptable variation[118], in

clinical renal studies this will affect TICs in obese populations.

Ultrasound Settings: Settings including depth, gain, frame rate, frequency, dynamic range and focus have all been shown to alter the shape of TICs. The focal point should be positioned just beyond the target organ, producing a more uniform acoustic field within the ROI and reducing bubble destruction[136]. Gain should be set to provide slight background signal before contrast administration, with adequate visualisation of bubbles in both the macro- and microvasculature. Figure 6 demonstrates how under or over-gained images result in clipping of the signal and loss in data. The dynamic range settings should provide contrast between the micro and macrocirculation. For perfusion quantification a wide dynamic range is preferred to avoid signal saturation[59]. The frame rate should be >10Hz to achieve sufficient data points to plot replenishment kinetics from highly vascular regions, which may have returned to steady state within a few seconds

after destruction.

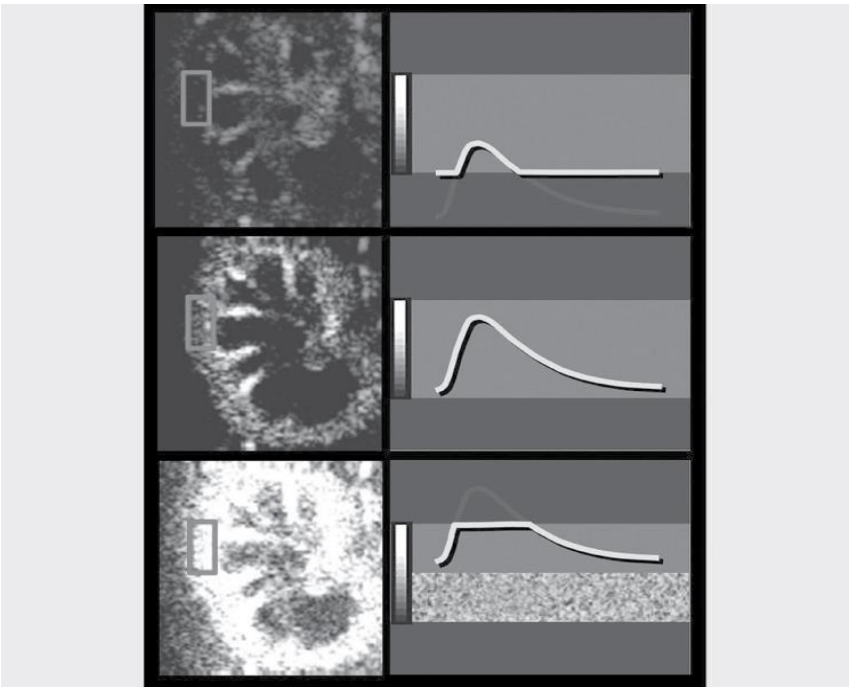

Figure 6: Reproduced from reference [59]. Top image: gain setting too low results in an underestimation of the microbubble concentration within the microcirculation, only flow in the large vessels is quantified. Middle image: Appropriate gain settings to achieve detail from both micro- and microcirculatory flow. Bottom image: gain too bright making macro- / microcirculation differentiation difficult.

6. **Data export:** The process of image transfer by DICOM format creates an issue with data loss both in compression by different ultrasound machines and decompression (linearisation) by different processing software. DICOM files are log-compressed raw (linear) data imaging files used as a standard filetype for medical imaging. However different developers linearise DICOM files using different methods, which has led to calls for an industry-wide standard from the Quantitative Imaging Biomarker Alliance (QIBA) of the Radiological Society of North America[112]. Linearisation, the process of removing the logarithmic compression, is thought to be accurate provided the dynamic range and gain settings were optimised in the original capture[137]. This issue

is akin to other compression-decompression processes such as RAW to jpeg for photography, where jpeg formats make adequate photographs but much of the embedded modifiable data has been removed in the process, making off-line manipulation limited. Other authors have exported raw data, negating the need for compression and subsequent data loss[138]. Ultrasound developers such as Seimens and GE have embedded analysis software within the machine, again avoiding the issue. This issue hampers multicentre trials where different equipment may be used by different centres[136]. Peronneau compared raw and compressed DICOM data and found time dependent variables to be equivalent, but intensity variables demonstrated significant variability between the two file formats [139].

7. **Mathematical modelling:** Different software manufacturers have different algorithms to fit the sum of least squares from the data to the Arditi-Hudson lognormal model, creating a more representative line of perfusion. Proprietary software is often a black-box and differs between platforms, creating an issue of reproducibility and comparison between sites in multicentre studies, particularly values of intensity, measured in arbitrary units[136].

2.1.3.5 Reliability

Hudson demonstrated CEUS to be reliable when using the same ultrasound machine in an *in vitro* model; coefficient of variation of 13%[126]. A North American QIBA CEUS Biomarker Committee supported a body of work in 2020 describing an imaging and quantification protocol to promote standardisation across machines and analysis platforms. They also demonstrated similar reproducibility to Hudson *in vivo* but found time dependent variables to be more reliable than intensity based variables, commenting that intensity based variables

could not currently be compared between different systems without standardisation[112]. The main findings of Averkiou's study are presented in Figure 7 noting that this study is in bolus kinetics and the variables are not those used in this thesis. It does however demonstrate time dependent variables being more reliable, a finding which is replicated throughout the existing literature and in the group's previous work[136]. This variability is also recognised by the European Committee in contrast ultrasound, EFSUMB[120]. Intensity parameters vary even when imaged and analysed using the same platform, as both signal saturation from dynamic range settings, microbubble concentration, depth and acoustic shadowing from both microbubbles and native structures can alter them[118].

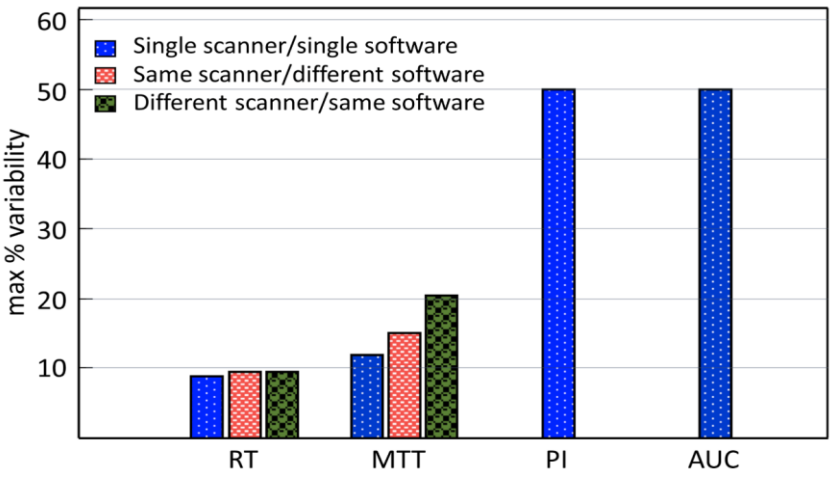

Figure 7: Reproduced from reference[112]. Graph demonstrating maximum coefficient of variation. Variables are from bolus kinetics which are not used in this thesis but demonstrate the principle of reduced reliability of intensity variables when compared with time-based. Rise time (RT) and mean Transit Time (mTT) are time-based variables. Peak Intensity (PI) and Area Under the Curve (AUC) are perfusion-based. Comparisons are annotated within the graphic. Due to alterations in intensity units between platforms, intensity variables cannot be compared between systems.

2.1.3.6 Summary of technical application

Time-intensity curve analysis is user dependent and requires dedicated software. Reproducibility may be problematic, particularly for variables which reflect blood volume and are intensity-based; quantification of flow by time-based variables are more robust, despite

this, expert committees recommend reporting both types[112]. Measured variables differ depending on the analysis platform and the method of contrast delivery. In this thesis destruction-reperfusion kinetics were measured on the Vuebox system, where mean transit time is truly time dependent and relative blood volume is purely intensity-based. Wash-in rate is dependent on the reperfusion gradient and therefore partly influenced by intensity as is the perfusion index.

2.1.3.7 Clinical Applications in Renal Imaging

Despite its limitations, contrast ultrasound has found an expanding role in modern imaging. Qualitative CEUS and the quantifiable DCE-US (particularly the bolus-transit method) have a wide body of literature supporting their use in oncological imaging to differentiate tumour types. Several articles have shown greater sensitivity by CEUS in identifying early vascular changes in tumours in comparison to CT using the Response Evaluation Criteria in Solid Tumours (RECIST). CEUS is frequently used in the evaluation of modern cytostatic chemotherapy agents and other oncological applications[116,120,140–142].

In renal imaging CEUS is recommended by the European Federation of Societies for Ultrasound in Medicine and Biology (EFSUMB) to characterise ischaemic disorders, tumours from pseudo-tumours, complex cysts, indeterminate lesions, abscesses in pyelonephritis and used for follow-up of non-operable masses[116]. For DCE-US, oncological applications predominately use bolus-transit kinetics and perfusion quantification is predominately imaged by infusion and destruction-replenishment.

Clinical development of CEUS has occurred in several renal conditions. These include diabetic

nephropathy, able to identify both early and late microvascular changes with reduced intensity, wash in rate and AUC in diseased kidneys[143] and a correlation between diabetic nephropathy histology and CEUS findings in rats[144]. Acute renal transplant rejection can be identified and pancreatic transplants demonstrate normalisation of CEUS values after successful treatment of rejection[110,145]. It has demonstrated an ability to identify transplant vascular issues in comparison to gold standards[146,147] and is predictive of graft function at 12 months[71]. Other investigators have compared DCE-US values between stages of CKD and healthy volunteers, showing a reduction in both time and intensity variables[148]. The reduction in cortical perfusion measured by DCE-US in CKD correlates with a clinical gold standard, ASL-MRI[149].

DCE-US assessed perfusion has an R value >0.9 when compared with flow probes in rat kidneys[150]. In humans the gold standard for measuring renal plasma flow (RPF) is para-aminohippuric-acid (PAH), but this method is only reliable with stable renal function and does not lend itself to acute kidney injury, oliguria or critically ill patients[151]. Healthy volunteer studies have assessed pharmacological manipulation of renal blood flow using exenatide, a GLP-1 receptor agonist, comparing RPF and cortical perfusion by DCE-US analysis in healthy males, demonstrating a moderate correlation (R=0.533). This finding was echoed in another healthy volunteer study, comparing radionucleotide measurements and PAH with DCE-US [152]. A greater correlation may not be expected however as RPF provides a measure of blood flow at the organ level, but CEUS provides detail of the microcirculation[153]. This point is pertinent to the data presented in this thesis as there is a dissociation between the two. The macro and micro haemodynamic relationship is complex, where gross renal blood flow is not fully

reflective of perfusion.

Reduced time-based variables from improved perfusion has been demonstrated with dopamine infusion[154], valsartan administration[155] and a high protein meal[156] and two of these studies used concurrent assessment with PAH to show a significant correlation, however all three studies demonstrated no significant change in intensity-based variables. A series of publications by Schneider and colleagues showed that pharmacological manipulation of cortical perfusion decreased with angiotensin-2 and increased with captopril[157], however their experimental study in sheep produced unconvincing results; both time and intensity-based variables correlated poorly with invasive measurements but much of the data was compromised by respiratory motion and stomach gas[158]. The same group demonstrated an improvement in cortical perfusion following terlipressin administration in patients with hepatorenal syndrome. Although only 4 patients, CEUS was able to predict the two whose renal function improved[159]. Taken together these studies suggest that manipulating cortical perfusion is possible and importantly it can be monitored with a portable, repeatable imaging modality. When applied to critically ill patients it provides several possibilities. Poor cortical perfusion may identify the early development of AKI and therapeutic interventions to improve hypoperfusion can be monitored. If so, potential targets for renal resuscitation become a possibility[160]. Schneider attempted to manipulate cortical perfusion in critically ill patients with noradrenaline, although severe AKI was excluded from the study. A mean blood pressure of 60mmHg was compared with 80mmHg in a mixed group of 12 patients, all within 48hrs of ICU admission. Changes in cortical perfusion were variable, some increased by 25% whilst others decreased by similar[161], which is in keeping with assessment by other

methods[162] and DCE-US was both feasible and able to identify changes[161].

2.1.3.8 Imaging of Sepsis Associated AKI

Renal perfusion in sepsis associated AKI has been assessed with DCE-US in a small number of studies. Harrois conducted a prospective, longitudinal study comparing 20 patients with septic shock and AKI, patients with septic shock without AKI and ICU patients with neither. Both intensity and time-based measures were abnormal, but intensity variables had greater variability. Mean transit time could identify differences poor perfusion in the AKI group which improved over time but not in the non-AKI group[82]. A larger study by Wang reported bolus-transit kinetics in 90 patients with sepsis[163]. This study had methodological limitations; bolus-transit kinetics are mostly used in oncological imaging where two tissue types can be compared. The measurement of tissue perfusion in this setting lacks a comparator tissue. It therefore produce TICs which are principally indicator-dilution curves and likely to be confounded by cardiac output. The AKI group in Wang's study had a mean serum creatinine of 141 µmmol/l and >2l/24hr urine output, and unusual exclusion criteria such as "patient gave up treatment halfway through". Despite these limitations they identified reduced velocity in the AKI group against comparators.

2.2 Renal Biomarkers

2.2.1 Conventional biomarkers

2.2.1.1 Creatinine

Creatinine, the long-established reference for renal function is easy to measure, cheap and ubiquitous. It is released by the body at a constant rate, freely filtered by glomeruli and secreted by tubules. It also undergoes extrarenal secretion by the intestine[164]. Its serum concentration is influenced by muscle mass, age, sex, race, diet and medications and is an imperfect marker of filtration with a large number of determinants; for example a creatinine of 132 µmmol/l could correspond with a glomerular filtration rate (GFR) between 20 and 90 ml/min/1.73m^2 [164]. The computation of GFR is achieved using one of several formulae, which are reasonably robust if GFR is stable but of limited use in AKI, as the lag between renal insult and creatinine accumulation will initially mask the severity of the injury[165].

As an indicator of tubular function it lacks sensitivity, indeed both chronic and acute tubular injury may occur without elevated plasma creatinine elevation[166] and conversely drugs may block tubular secretion, increasing plasma concentration, but without renal injury.

2.2.1.2 Urine Output

Urine output changes more rapidly than creatinine and is a cheap and effective marker of renal injury and easy to measure, although unreliably measured in practice. Alongside creatinine it has been adopted as a diagnostic component of the KDIGO staging system for AKI, as a sustained reduction for >6 hours is associated with renal injury and urine output

changes occur before alterations in creatinine[167].

Urine output is a by-product of haemostatic volume control, rather than the body's indicator of renal health. As a result the two do not demonstrate perfect harmony, physiological adaptation to hypovolaemia alters sodium and water handling under the influence of antidiuretic hormone and the renin-angiotensin-aldosterone pathways. A reduction in urine output is therefore not specific for AKI, whilst normal or increased urine output does not necessarily indicate normal function as reduced GFR in the presence of tubular injury may occur without oliguria[168]. In the assessment of critically ill patients, multiple causes may reduce the predictive power of urine output, including volume status, intrinsic antidiuretic hormone levels, obstruction and diuretics[169]. Outside of the ICU measurements of urine output are often unreliable, catheters are needed for hourly assessment and clinical workload often prevents its timely recording.

2.2.2 The Search for Novel Biomarkers

The use of creatinine as a gold standard impedes advancement in AKI research, however no other single marker of renal injury can bridge these gaps and a histological diagnosis is usually time consuming and inappropriate. A search for new markers aims to improve on the limitations of creatinine and provide further mechanistic insight, however the assessment of such biomarkers is difficult as creatinine, the "gold standard" comparator is flawed. For example, assuming creatinine has a sensitivity of 80%, specificity of 90% and a disease prevalence of 10% the new marker with a true sensitivity of 100% may only have 47% sensitivity when compared with creatinine[166]. False positives may represent subclinical injury not identified with creatinine detection due to recruitment of renal reserve, whilst false

negatives may reflect haemodynamic (pre-renal) elevations in creatinine, without kidney damage[170]. An experimental study demonstrated better performance of biomarkers than creatinine at diagnosing renal injury when a tissue standard was used[171]. New markers therefore need to be carefully considered before adoption or abandonment and through means other than comparison against creatinine.

Further issues also lie in the study of new biomarkers beyond the limitations of creatinine; the syndrome in question also provides difficulty. AKI is a diverse group of conditions (sepsis, drug-induced, pre-renal) all grouped together and the cause of AKI in any particular patient is often multifactorial. Therefore the search for markers which are sensitive enough to include all true cases, but specific enough to exclude non-renal causes is challenging[25]. The variation in biomarker levels over time following an injury may also alter the perceived sensitivity of the test, especially when the time of injury is unknown. As demonstrated in Figure 8, taken from Malyszko et al[172], markers which rise and fall within a few hours will not be detectable several days afterwards once creatinine has peaked, further complicating the study of potential candidate molecules. Malyszko makes the point that if timing of injury and baseline renal function are accounted for AUROC can increase from 0.59-0.67 to 0.85-0.94.

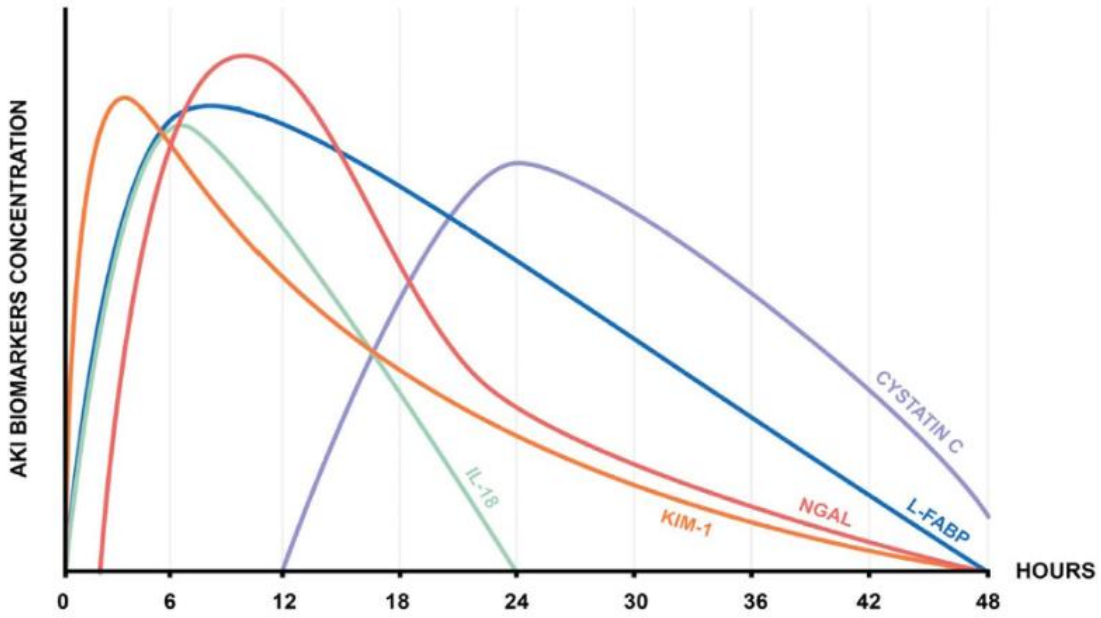

Figure 8 graph demonstrating the time course of novel urinary biomarkers[173]

2.2.3 Predictive Ability of Biomarkers

Both renal injury from AKI and functional change without renal injury, such as pre-renal azotaemia may elevate creatinine, but biomarkers are hoped to increase specificity and assist this distinction[174]. Biomarkers have demonstrated a moderate to excellent ability to discriminate between pre-renal, intrinsic AKI, CKD and normal function, depending on the marker in question[175]. Elevated biomarkers in the presence of normal creatinine also increases the risk of adverse outcomes, by potentially identifying occult renal injury.

Despite the number of candidate markers, no one marker is perfect. The ideal biomarker should accurately diagnose tubular injury, the most common form of AKI in the hospital setting, aid with risk stratification by predicting the need for RRT, as well as the duration of

AKI and renal recovery[176]. In reality the cause of AKI is often complex and multifactorial; despite its unifying designation as acute kidney injury, it is not a single entity unlike its frequently used comparator, acute coronary syndrome. Different regions of the nephron are affected by different injuries. The interpretation of multiple biomarker profiles may prove to be a more powerful tool in the assessment of AKI, rather than one renal "troponin". As demonstrated in Figure 9 also taken from Malyszko et al[173], biomarker levels provide not only the severity of injury but functional data regarding the location.

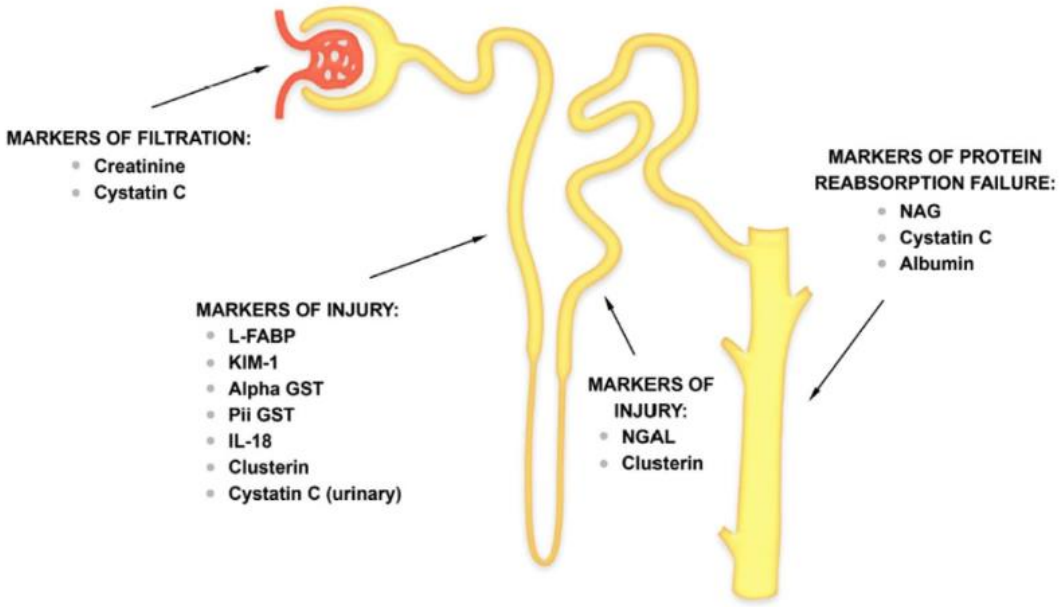

Figure 9: Site of injury leading to alterations in novel biomarkers[173].

In addition to multiple biomarker profiling, recent studies have demonstrated an increase in the predictive power of biomarkers if predictive models incorporate clinical factors. The renal angina index (RAI) is a composite score of an individual's AKI risk and the early signs of injury, it aims to risk stratify patients in whom biomarker measurement would be beneficial and informing the pre-test probability of biomarkers. The inclusion of the RAI with multiple biomarker profiles increases the power of the model (RAI AUROC 0.8 vs RAI and biomarker

AUROC 0.84-0.88).

Despite the limitations of current biomarkers, research into biomarkers is prolific with over 1700 publications in the past 5 years alone[170] and has led ADQI to provide a consensus statement on the clinical use of biomarkers[177]. A summary of relevant studies is presented below, whilst not all-encompassing or systematic, it aims to provide a general description from the current evidence for the markers measured in this thesis.

2.2.4 Biomarkers used in this thesis

2.2.4.1 Neutrophil Gelatinase-Associated Lipocalin (NGAL)

Overview

In 2003 a transcriptome-wide interrogation strategy was undertaken to identify genes induced by renal ischaemia. Seven were identified of which one was a short peptide resistant to proteases which increases sample stability and makes potential identification easier. The concentration of neutrophil gelatinase-associated lipocalin (NGAL) was also found to be proportional to the degree of renal ischaemia and it became a promising candidate biomarker[178]. Since its description it has shown moderate predictive ability for AKI in both blood (pNGAL) and urine (uNGAL). A meta-analysis published in 2018 considered 12 studies of uNGAL and 22 studies of pNGAL with a pooled AUROC of 0.72 and 0.755 respectively. The AUROC improved to 0.76 once the urinary levels were normalized to creatinine concentration.

Characteristics

NGAL was first identified as a bacteriostatic agent in neutrophil function in the 1990s, binding

siderophores, small iron-binding molecules present on prokaryotes[179]. It is usually expressed at very low levels but is rapidly induced by epithelial injury after NF-κB binding the promotor region[180]. It functions as an acute phase protein and is secreted in the ascending limb of the loop of Henle and tubular cells[181]. It rises within 2 hours and peaks about 10 hours after injury and is easily measured either by ELISA or with commercial immunoassay[173]. It has the advantage of being detectable in both the urine and plasma and has been extensively validated as a marker of tubular injury in cardiac surgery[182], critical illness[183], contrast induced nephropathy[184], delayed graft function[185] and it has demonstrated an ability to differentiate pre-renal azotaemia from tubular injury[186]; arguably it has the greatest evidence base of any novel biomarker.

Performance

Plasma NGAL can be influenced by coexisting variables such as CKD and hypertension, it also increases to a lesser extent in other conditions such as lupus nephritis and IgA nephropathy[181]. The interpretation of NGAL in acutely unwell patients is complicated by its concurrent increase in sepsis; a 2016 meta-analysis reviewed 15 studies of sepsis associated AKI and demonstrated pooled sensitivities of 0.83 (95% CI: 0.77-0.88) for pNGAL and 0.80 (95% CI: 0.77-0.83) for uNGAL but a specificity of 0.57(0.54-0.61) and 0.8(0.7-0.86) respectively[187]. A multinational collaborative group undertook a series of studies to better describe the role of biomarkers. The TRIBE-AKI consortium investigated the predictive ability of pNGAL and uNGAL to identify AKI in 1219 post-operative patients. The study demonstrated a moderate predictive power to identify AKI, with an AUROC between 0.67 and 0.74 but with only modest improvement over creatinine[188]. Another study in ICU admissions demonstrated both uNGAL and pNGAL were good predictors of AKI development in 632 patients with an AUROC between

0.77±0.05 and 0.88±0.04 depending on the severity of renal injury[183], but such promising results have not always been repeatable, a subsequent study of 451 patients demonstrated a slightly worse predictive ability of uNGAL to identify AKI development on ICU admission (AUC ROC of 0.71 (95% CI: 0.63-0.78))[189].

Despite initial promise and a comprehensive body of investigation, NGAL is yet to find widespread clinical use in AKI identification or prediction, or in the initiation or cessation of RRT. Common to all novel biomarkers, the strengths may lie in the interpretation of multiple markers to gain a deeper understanding of the injury and phenotype[174].

2.2.4.2 Tissue Inhibitor of Metalloproteinases-2 (TIMP2) and Insulin-Like Growth Factor-Binding Protein 7 (IGFBP7)

Overview

In 2013 a collaborative group of investigators in North America performed two observational studies across 35 sites to identify potential biomarkers. The discovery component identified 340 molecules from the existing literature known to be expressed in renal injury and examined the predictive power of these markers in 522 acutely unwell patients. The second component of the study, the Sapphire validation study enrolled 744 acute patients and examined the two best performing biomarkers from the discovery study. This process identified two cell-cycle arrest biomarkers detectable in urine, tissue inhibitor of metalloproteinases-2 (TIMP2) and insulin-like growth factor-binding protein 7 (IGFBP7). The combination of the two (IGFBP7*TIMP2) demonstrated superior sensitivity to all previous AKI biomarkers (AUROC 0.80, $p<0.002$)[190]. The combination of IGFBP7 and TIMP2 was validated by the same group and demonstrated that a level of >0.3$(ng/ml)^2/1000$ was most able to

identify critically ill patients at imminent risk of severe AKI. When included in a model with clinical variables the AUROC increased from 0.7 for clinical variables alone to 0.86, the negative predictive value ranged from 88 to 96%[191]. The results of these studies led to FDA approval for the biomarker combination to be used clinically as a predictive tool to identify ICU patients at risk of AKI[176].

Characteristics

IGFBP7*TIMP2 levels can be assessed by ELISA or using the Nephrocheck system (Astute Medical, San Diego, CA – now part of BioMérieux, Inc., Lyon), a point of care test licensed for the early detection of AKI in hospitalised patients. Being the product of IGFBP7 and TIMP2 levels are reported as ng/ml^2 and then divided by 1000. A high sensitivity threshold of $0.3(ng/ml)^2/1000$ and a high specificity threshold $2.0(ng/ml)^2/1000$ have been advocated in early studies. Use of IGFBP7*TIMP2 has been reviewed by both the National Institute for Health and Care Excellence and the American Association for Clinical Chemistry's academy but neither have recommended its use, as no improvement in clinical outcome has been demonstrated [192].

Performance

In contrast to the original Sapphire study, an external validation study by Bell et al was unable to demonstrate any predictive power of IGFBP7*TIMP2, NGAL or Cys-C for AKI development in ICU admissions. This study had a low number of AKI cases, of the 94 enrolled, AKI developed

in 19 patients, 15% of the population had sepsis and 47% trauma[193].

The normal range of IGFBP7*TIMP2 in healthy volunteers is 0.04 to 2.25$(ng/ml)^2/1000$ [194]. The high sensitivity marker of 0.3$(ng/ml)^2/1000$ falls in the middle of this range and therefore a number of healthy patients will be identified as positive if used in a binary fashion. Studies with a low proportion of true AKI cases will demonstrate poor performance because of false positives[192] and why Sapphire authors recommend its use only once a reduction in GFR is detected, although to do this would restrict its utility[195].

Discriminatory power to predict RRT following AKI demonstrated a pooled AUROC of 0.857 in a relatively small meta-analysis of 4 studies and 280 patients[196]. The meta-analysis also commented on slightly better performance of TIMP2 to predict sepsis associated AKI and IGFBP7 to predict postoperative AKI, currently the two biomarkers are not used independently. The ability for IGFBP7*TIMP2 to predict renal recovery has been recently investigated in a single centre study; higher levels were associated with a longer time spent on RRT, with 2$(ng/ml)^2/1000$ defining a level of increased risk. Patients with a level <2$(ng/ml)^2/1000$ on admission or in whom levels had become undetectable were able to successfully discontinue RRT. Discontinuation of therapy with persistently positive biomarkers was associated with a 5 times greater risk of failure[197].

An independent study in septic patients examined the ability of biomarkers to predict persistent AKI beyond 7 days and found no biomarkers measured on admission to be predictive. NGAL and IGFBP7*TIMP2 had limited predictive ability 6 hours after admission

(AUROC 0.63 and 0.63) [198], it may be optimistic for admission bloods to accurately predict the clinical status of the patient 7 days later particularly as the use of RRT as an indicator for severe AKI is not perfect. A study by the Sapphire investigators described the predictive ability of IGFBP7*TIMP2 to determine long-term renal outcomes after AKI in critically ill patients. A level of <0.3$(ng/ml)^2/1000$ had a 30% risk of death or dialysis at 9 months, whilst levels >2.0$(ng/ml)^2/1000$ increased the risk to 60%. In the absence of any change in creatinine based GFR the biomarkers levels were unhelpful[195]. Indeed, the incorporation of clinical risk factors with IGFBP7*TIMP2 into a predictive model increased prediction from AUROC 0.66 to 0.75[199].

IGFBP7*TIMP2 is very promising, able to provide insight into severity and duration, when used in isolation it has limitations but the same is true of any test. The incorporation of clinical risk factors improves the pre-test probability and strengthen specificity.

2.2.4.3 Proenkephalin A (PENK)

Cleavage of pre-proenkephalin A yields proenkephalin A and several enkephalins: endogenous opioids, acting primarily on delta opioid receptors. The greatest concentration of delta receptors outside of the central nervous system are within the kidney and appear to have a regulatory role in diuresis and natriuresis, although the full mechanism is not fully elucidated[200]. PENK is stable with a long in vivo half-life and is not affected by age or sex[201]. It is entirely filtered by the glomerulus, not reabsorbed and plasma levels have been shown in several studies to correlate closely with measured GFR by inulin or iohexol clearance at steady state[201]. Enkephalins may also be induced by AKI, in turn increasing PENK production and provide a dual cause of elevation[202]. In non-steady-state settings such as sepsis, PENK correlated more closely with measured GFR than eGFR MDRD estimates (R^2=0.9 vs 0.82)[203].

As a specific marker of filtration, levels correlate closely with renal blood flow and GFR and alter faster than creatinine. There is no tubular handling of PENK, levels do not reflect tubular function and are not associated with tubular biomarkers, this finding adds to its specificity and suggests its potential role amongst other biomarkers is to provide assessment of filtration[204].

As a marker of AKI in ICU admissions, PENK performs similarly to other novel biomarkers with an AUROC of approximately 0.8[205]. PENK provides prognostic information in addition; of 956 patients with sepsis admitted to ICU, PENK demonstrated a close correlation with AKI prediction, improvement, RRT requirement and 90-day mortality[206]. A head-to-head study demonstrated superiority of PENK against IGFBP7*TIMP2 in predicting AKI in 200 ICU admissions, AUROC 0.91 vs 0.66 and in the need for RRT 0.78 vs 0.68[207]. It may be expected that a marker of filtration correlates better with the diagnosis of AKI as creatinine is a fundamental component of staging. Tubular markers inform the degree of tubular damage and likely the combination of both marker types provide greatest insight into the mechanisms of injury.

2.2.4.4 C-C motif chemokine ligand 14 (CCL14)

AKI recovery may occur as distinct phenotypes, early recovery, delayed recovery, relapsing and non-recovery; with the associated 1-year mortality ranging from <10% for early recovery but >60% for non-recovery[208]. Predicting AKI recovery is problematic and current methods rely on the monitoring of urine output and creatinine. No diagnostics reliably provide information regarding recovery and decisions on RRT initiation and cessation are based on creatinine trajectory and clinical opinion. The availability of biomarkers to predict either

recovery or persistence would enable clinicians to time therapy decisions and provide greater input to higher risk phenotypes such as those with persistent AKI and acute kidney disease (AKD), who are at greatest risk of progression[209]. The RUBY study published in 2020 investigated multiple potential biomarkers for their performance at predicting persistent AKI, with a similar design to the SAPPHIRE study and from a similar group of investigators. The RUBY study recruited ICU patients with stage 2 or 3 AKI with the primary endpoint being persistent AKI, that is AKI persisting beyond 72 hours. Levels of candidate molecules with known involvement in apoptosis, endothelial injury or other inflammatory pathways were measured in plasma or urine. A protein not previously identified as a marker for AKI, CCL14, demonstrated the greatest prediction for persistent AKI, AUROC 0.83[210]. A further study demonstrated an AUROC of 0.81 for predicting persistent AKI in a secondary analysis of the SAPPHIRE dataset although persistent AKI only occurred in 28 patients, duration of persistence was proportional to CCL14 levels[211]. A recently published prospective study measured CCL14 levels in 100 patients pre and post cardiac surgery demonstrating an AUROC of 0.92 for predicting persistence[212]. At the time of writing the only three studies available are from the SAPPHIRE/ RUBY investigators.

It is measured in urine by conventional ELISA.

2.2.4.5 Urinary albumin quantification

A simple and cheap test and an independent indicator of RRT risk and death following ICU admission[213,214]. The DAMAGE study followed 257 ICU admissions and demonstrated that a clinical risk prediction model with the combination of urinary NGAL and albumin had the

greatest predictive power of all markers in the study (0.87 AUROC for stage 3 AKI). Like suPAR and DKK3[215,216], pre-insult levels inform the likely severity of injury. The TRIBE-AKI consortium demonstrated preoperative proteinuria provided a graded risk following cardiac surgery with an increased risk of death post-operatively (adjusted hazard ratio 2.85), another study demonstrated patients with elevated urinary albumin were more likely to suffer post-operative AKI and require RRT[217,218]. It does not stand out alone as a biomarker for AKI but in combination with NGAL it does[174], plus it indicates at risk patients prior to insult and informs long-term risk if albuminuria persists after injury.

Normalisation to creatinine

The urinary levels of a biomarker will depend on the rate of release into the urine and the urinary flow rate. In chronic disease states where GFR is stable biomarker quantification such as calciuria and albuminuria are referenced to urinary creatinine as the concentration will depend on both the severity of the disease and the concentration of the urine[219]. However, in AKI GFR is in a state of flux, altering creatinine clearance. Urinary biomarkers for AKI, particularly tubular damage markers are released from a different site of the nephron and therefore the normalisation of biomarkers is controversial. Existing literature is variable but generally publishes crude and normalized values together. The case has been made in a simulation study of creatinine kinetics for using timed values instead, although this approach would only be possible if the timing of renal injury is known, such as transplantation or surgery[220]. Despite the suggested drawbacks, normalising appears to demonstrate superior predictive power to crude values. Both crude and normalised values are presented in this

thesis.

2.3 Endothelial Biomarkers

The following biomarkers are used in this thesis to inform endothelial and inflammatory processes:

2.3.1.1 Syndecan-1

As shown in Figure 10, syndecans are transmembrane anchor proteins, covalently attached to proteoglycans and heparan sulphate and at its core is a central protein with glycosaminoglycan side branches. Heparan sulphates have a multitude of roles in inflammatory processes and syndecans function as integral membrane proteins involved in cell proliferation, cell matrix interactions, cell migration and act as sponges for chemokines and growth factors[221,222]. Syndecan-1 is the most ubiquitous syndecan, expressed at a level of 10^6 per epithelial cell forming a major component of the epithelial glycocalyx[223]. As a result of inflammation, syndecans, heparan sulphate and other components of the glycocalyx are shed and detectable in plasma. Syndecans are excellent markers of this process being stable ex-vivo and reliably detected by ELISA[224]. Syndecan-1 serves as a marker of endothelial injury in multiple research fields including COVID-19[225], CKD[226], diabetes[227], critical illness[228,229] and sepsis[230,231]. Levels correlate with the severity of organ injury and can be used to predict prognosis and mortality in septic shock, increasing up to 9000-fold with severe glycocalyx disruption[232]. Levels are independently associated with acute kidney injury, with moderate predictability of stage 3 AKI after paediatric cardiac surgery[233] and is used in some models to distinguish AKI subphenotypes[234]. Its predominant role is a detectable sheddase for

endothelial and glyocalyx injury.

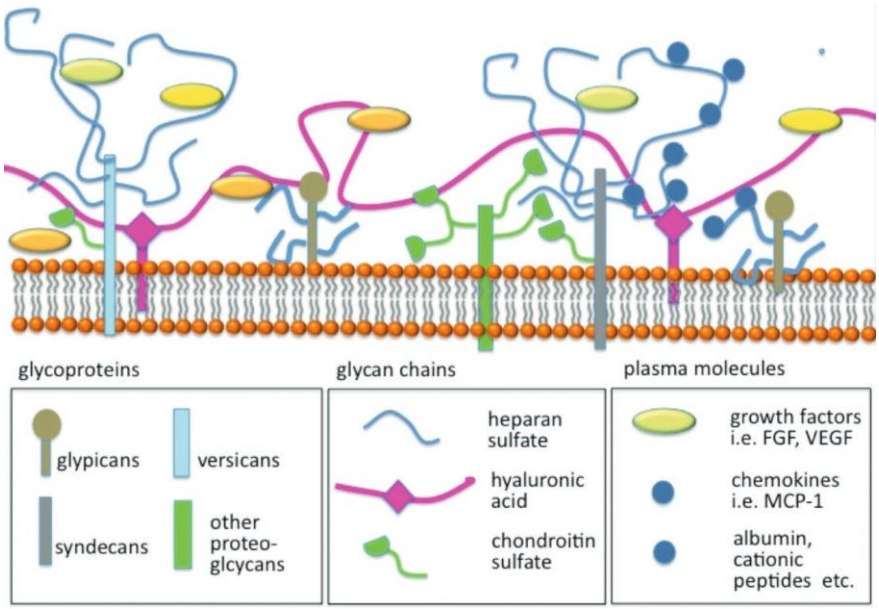

Figure 10 taken from reference [235]. Schematic drawing of the molecular ultrastructure of the endothelial glycocalyx layer

2.3.1.2 Angiopoietin 1 and Angiopoietin 2

Amongst others, angiopoietin-1 and -2 (Ang1 and Ang2) are important growth factors for embryonic vascular neogenesis, Ang1 is responsible for stabilisation of the endothelial barrier and Ang2 destabilises epithelial junctions. The constant assembly-disassembly cycle of the embryonic endothelium incorporates new vessels and enables the construction of a vascular network[236]. These growth factors are also responsible for vascular repair mechanisms in adults. Intuitively elevated Ang2 would be expected with inflammation and vascular damage whilst Ang1 is anti-inflammatory and associated with repair. This association is borne out in studies of critically ill patients with vascular injury, morbidity and mortality associated with an elevated Ang2:Ang1 ratio[237,238]. The agonist/antagonist pair bind to the Tie-2 receptor tyrosine kinase of epithelial cells, with elevated Ang2 and suppressed Ang1 profiles within the septic milieu. Serum from patients with high Ang2 levels disrupts endothelial architecture ex-

vivo and excess Ang2 in mice induces pulmonary leak and the development of ARDS[238].

2.3.1.3 sTNFR1

Tumour necrosis factor alpha (TNFα) is a key inflammatory mediator, functioning through two receptors TNFR1 and TNFR2, expressed on all nucleated cells but predominately epithelial cells and leukocytes[239]. Binding of TNFα to TNFR1 leads to intracellular caspase activation, cellular apoptosis and immune activation mediated via NF-κB[240]. Shedding of the receptor as the soluble form (sTNFR1) occurs via cleavage at the cell surface or through release of a vesicle which includes the receptor. Elevated levels of sTNFR1 are interpreted as a marker of TNFα activation[241]. Levels of sTNFR1 have been shown to correlate closely with conditions including arthritis activity[242], CKD progression[240], diabetic nephropathy progression[243], sepsis severity[244] and as a predictor of AKI in septic shock[245]. sTNFR1 was used by Bhatraju and colleagues in defining AKI subphenotypes, with higher levels present in the inflammatory / endotheliopathy group[234]. Multiple studies have also demonstrated sTNFR1 to be an independent predictor for severe AKI in critically ill adults[241,246,247]. In the kidney TNFR1 is predominately expressed in glomerular and peritubular capillaries[248].

2.3.1.4 Interleukin-8 (IL8)

Activated neutrophils are implicated in the development of AKI and interleukin-8 (IL8) is the endothelially derived chemokine responsible for their recruitment to injured tissue. IL8 also triggers several neutrophil behaviours including degranulation, chemotaxis and respiratory burst[249]. IL8 is independently associated with AKI development after adjustment for clinical factors but is less predictive than the aforementioned biomarkers[249]. Elevated levels correlate with ischaemia-reperfusion injury of allografts[250], prediction of AKI in sepsis[251] and

demonstrate higher levels in non-survivors of septic shock[252]. Levels of IL8 are used by Bhatraju and colleagues to identify the inflammatory / endotheliopathy subphenotype of AKI[234].

2.4 Methods of examining tissue perfusion and microcirculatory flow

Overview

Perfusion and microcirculatory flow are terms often used interchangeably in the literature, strictly microcirculatory flow specifies the movement of blood cells within the capillary network alone, whereas perfusion may include flow within arterioles, venules and the microcirculation.

A wide number of techniques assessing perfusion are described, which generally either provide an average estimate of global perfusion or rely on a specific region or window to reflect the global state – such as the skin, but variability within different tissue beds is common. Any such technique therefore has the potential to under- or over-estimate global perfusion, but provided errors are constant often reliable correlations with outcome exists.

2.4.1 Biochemical assessment

2.4.1.1 Lactate

The supply dependency of oxygen consumption on oxygen delivery is a fundamental concept of shock and its resuscitation. However normalising or supra-normalising systemic oxygen supply through early goal-directed therapy is ineffective and direct observation of the microcirculation confirms that blood lactate levels lag observable changes in tissue perfusion.

The critical supply or DO_2 threshold is the value below which delivery fails to satisfy the metabolic demand for oxygen and is suggested to be altered in sepsis, making septic patients more at risk of tissue hypoxia and the onset of anaerobic metabolism. Nelson et al

identified such an inflection point of oxygen consumption (VO_2) and lactate production through the incremental reduction in supply (DO_2) in a large-animal septic shock model[253].

Widely considered the product of anaerobic metabolism, where oxygen delivery is inadequate for consumption, investigations to identify anaerobic metabolism in patients with septic shock have produced unexpected results. In 1993 Ronco et al attempted to identify the critical supply threshold in critically illness by observing patients after the withdrawal of organ support, a situation where cardiorespiratory function would expectedly fail to meet metabolic demand. Whilst able to demonstrate the critical supply threshold they found no difference in either the threshold or oxygen extraction ratios of patients with septic shock in comparison to critically ill controls and there was no correlation between lactate level and critical DO_2 threshold[254].

Despite this evidence, proponents of the critical supply threshold argue for the presence of occult hypoperfusion in solid organs otherwise unidentified. If solid organ hypoperfusion existed within the kidney, an association with renal perfusion imaging would be expected.

2.4.1.2 Venous oxygen saturations

Overview

Increased oxygen demand will initially increase extraction from the arriving RBCs and is then sensed by multiple pathways and balanced by increasing supply. Beyond the limit of supply, extraction increases more rapidly to compensate until exhausted, at which point the critical supply threshold is reached where consumption becomes supply dependent and hypoperfusion occurs as demonstrated in Figure 11. This forms the basis of measuring

venous oxygen saturations to detect tissue hypoxia, in effect, to identify shock.

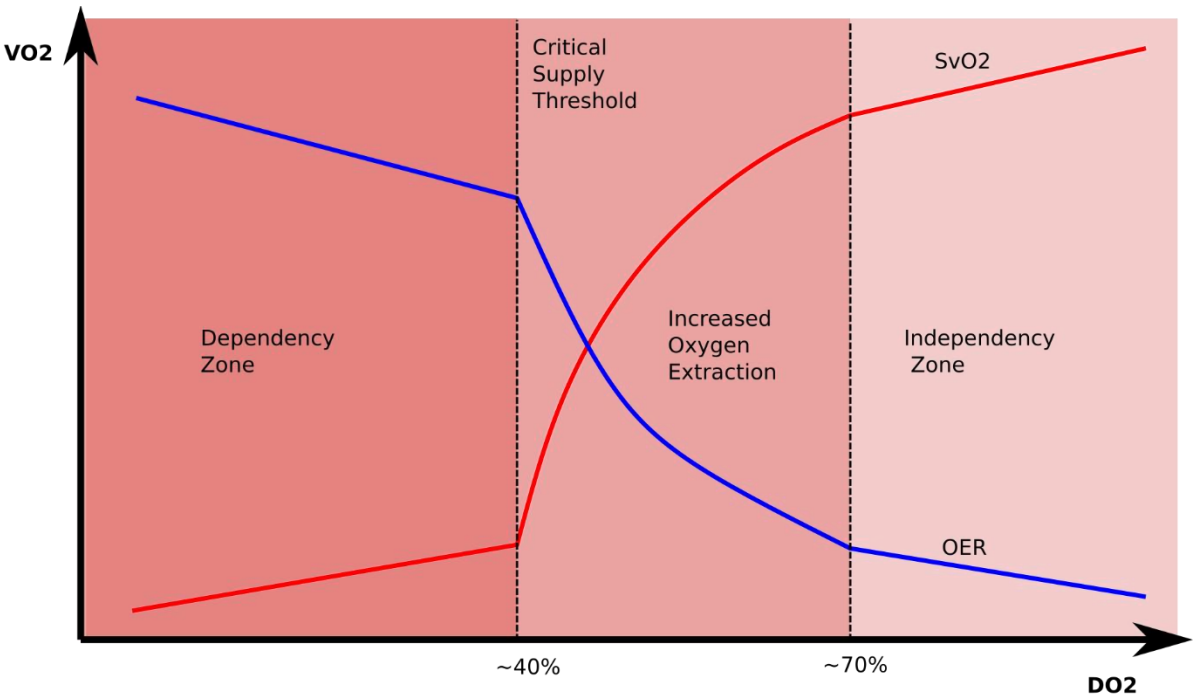

Figure 11 simplified graph of the relationship between oxygen extraction and venous oxygen saturations. As delivery (DO2) reduces for any given consumption (VO2), oxygen extraction (blue line) will increase and venous oxygen saturations (red line) will fall to reflect this. Once the critical supply threshold is passed oxygen extraction is exhausted and tissue hypoxia occurs, with consumption becoming supply dependent. Adapted from [255,256]

Expectedly, lower ScvO2 in sepsis particularly below 60% predicts a worse outcome[257] and generally levels persistently below this are incompatible with life after several hours[254,258]. Much controversy surrounds the significant improvement in mortality demonstrated with EGDT by Rivers et al. in 2001[257], which failed to be reproduced in three large interventional studies thereafter. Whilst the reasons for this may be multiple, Gutierrez makes the point that the admission venous oxygen saturations were much lower in the Rivers study which may reflect a point beyond the critical supply threshold[259], whereas those in the ARISE,

ProCESS and ProMISe study were near normal as depicted in Figure 12[260–262].

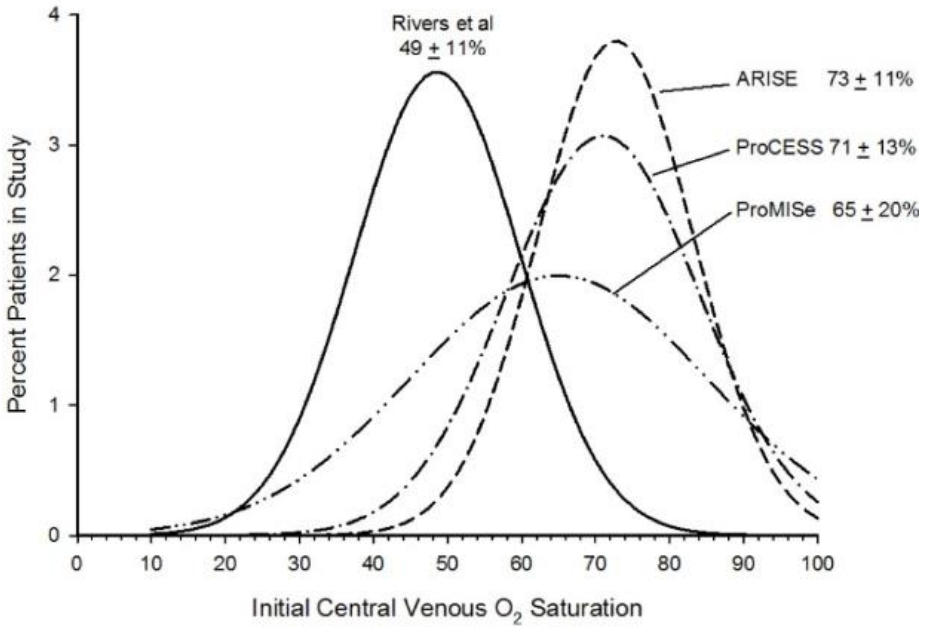

Figure 12 from reference [259]. The study populations above represents the differences between admission ScvO2 in the EGDT studies assuming normal distributions in the samples.

Measurement of venous saturations has a role in identifying at risk groups, as measurements outside the normal range indicate a worse outcome[257,263,264], but they are still poorly predictive of 28-day mortality, with area under the ROC of 0.53 in one study[265]. More recent data suggest the relationship between venous saturations and mortality is U-shaped, values greater than 77% indicating a failure of extraction from microcirculatory shunting, clinical evidence has demonstrated a reduction in mitochondrial activity and mitochondrial distress at values >80% [264,266–268].

The use of venous saturations to assess perfusion assumes homogeneity throughout the body; one value to reflect impaired delivery. Whilst hypoperfusion may be a global phenomenon, organ or regional hypoperfusion is frequently seen in critical illness, or

indeed heterogeneous perfusion within the same tissue bed or even adjacent capillary segments. $ScvO_2$ may be low, normal or high despite the presence of tissue hypoperfusion as outlined in a recent systematic review[269]. Venous saturations are therefore inadequate in isolation and other guides are needed to assess perfusion.

2.4.1.3 Carbon dioxide gap

Overview

As a normalising $ScvO_2$ can be falsely reassuring in shock resuscitation, elevation of other markers such as blood lactate or pCO_2 gap help improve sensitivity[270]. The latter has been suggested as a tool to better characterize a failure of supply, demonstrating closer correlation with cardiac output in several studies[271–275].

Calculation

Carbon dioxide is produced from aerobic metabolism, specifically the oxidative processes of the Krebs cycle. The main determinants of production being the rate of oxidative metabolism (VO2) and the metabolic fuel source, notated by the respiratory quotient R[276]. Under anaerobic conditions CO_2 is also generated, but to a lesser degree than aerobic production. Bicarbonate accounts for most of the anaerobic production, being released from proton buffering and lactic acid production. Decarboxylation of ketoacids provides a minor contribution to CO_2 production[277]. Figure 13 provides a graphical reference demonstrating how haemoglobin binding to CO_2 occurs preferentially in the deoxygenated state; this Haldane effect accounts for the preferential loading of oxygen in the lungs and its offloading in the tissues, with the reciprocal exchange of CO_2[278]. Unlike oxygen, carbon dioxide total carriage and the partial pressure of CO_2 in solution demonstrate a near-linear

relationship, allowing pCO_2 to act as a surrogate for carriage in most circumstances[276]. The relationship is not perfect however and is affected by factors which alter in critical illness including haematocrit, acidaemia and oxygen saturations.

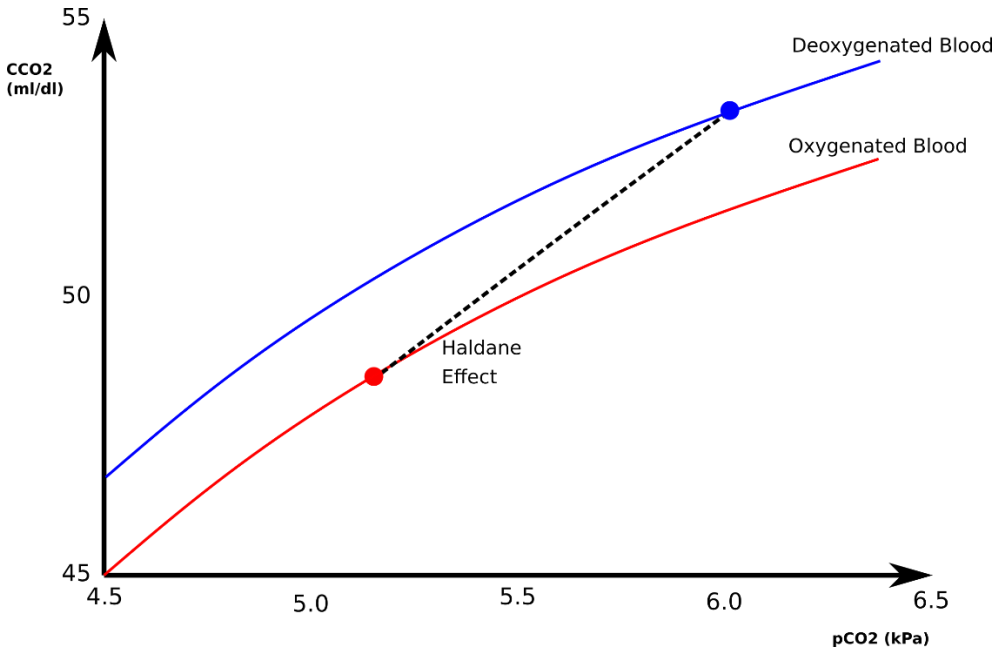

Figure 13, The carbon dioxide dissociation curve, the relationship between CO_2 content and tension. The relationship is curvilinear and determined by acidaemia and the oxidative state of haemoglobin. The dashed line represents the increased affinity for CO_2 binding be deoxygenated haemoglobin

Performance of carbon dioxide gap to identify shock

The normal range for ΔpCO_2 is between 0.27 and 0.67 kPa[279]. As VCO_2 (carbon dioxide production) remains constant at steady state, the change in pCO_2 can reflect alterations in cardiac output. Put another way CO_2 is constantly released into the circulation by cellular metabolism but in circulatory stagnation from low cardiac output, CO_2 accumulates increasing venous $pvCO_2$. Once the higher CO_2 tension is removed by pulmonary washout $paCO_2$ returns to normal, resulting in an increased ΔpCO_2. Multiple experimental and clinical studies have confirmed the association between cardiac output and ΔpCO_2 whilst

highlighting the lack of association between cardiac output and venous oximetry[271–273,280–282].

The assessment of ΔpCO_2 in isolation is not entirely specific for cardiac output assessment however and has led some authors to suggest interpreting elevations in ΔpCO_2 in conjunction with lactate. Elevations in both would indicate insufficient cardiac output, whereas increase in ΔpCO_2 alone may indicate increased oxygen demand alone[276,283]. As a means of determining cardiac output by metabolic assessment certainly ΔpCO_2 is more predictive than $ScvO_2$[275]. It has also been shown as more predictive in the assessment of fluid responsiveness[284] and post-operative complications in some[285,286] but not all studies[287].

Limitations

Limitations include the accuracy of measurement, small differences in pCO_2 need to be detected and the accuracy of blood gas analysis should be considered, particularly when the difference between the normal range and the critical threshold could be as little as 0.3-0.6kPa[279]. Central venous CO_2 tension is a surrogate for mixed CO_2 and excellent correlation was demonstrated in a mixed critically ill population, although a further study reported 95% limits of agreement between -0.62 and 0.58kPa, which is high considering the normal range lies within this[282,288].

2.4.1.4 A combined approach to assess tissue hypoxia

Neither $ScvO_2$ or ΔpCO_2 are sufficient to detect tissue hypoxia in isolation and lactate

kinetics may be biphasic and non-specific. ΔpCO_2 is inversely proportional to cardiac output, whereas $ScvO_2$ detects an oxygen supply and demand imbalance, but not the direction of the imbalance. It has therefore been suggested that the combination of these variables may be more able to identify an oxygen demand issue, detect supply dependency, tissue hypoxia and the potential for further resuscitation. As demand outstrips supply, or supply reduces below demand, anaerobic metabolism commences which utilizes no oxygen and VO_2 rises no further. VCO_2 will rise under anaerobic conditions but more gradually from the contributions of bicarbonate buffering and ketoacid metabolism. Therefore, a ratio of the change in venous to arterial CO_2 carriage ($C_{v\text{-}a}CO_2$) to the change in arterial to venous O_2 carriage ($C_{a\text{-}v}O_2$) may identify tissue hypoxia. Substituting $C_{v\text{-}a}CO_2$ for ΔpCO_2 allows this to used clinically as $\Delta pCO_2 / C_{a\text{-}v}O_2$. As reproduced in Figure 14, Mekontso-Dessap demonstrated how this method performed well at predicting arterial lactate levels >2mmol/L, with an area under the ROC of 0.85±0.03[289].

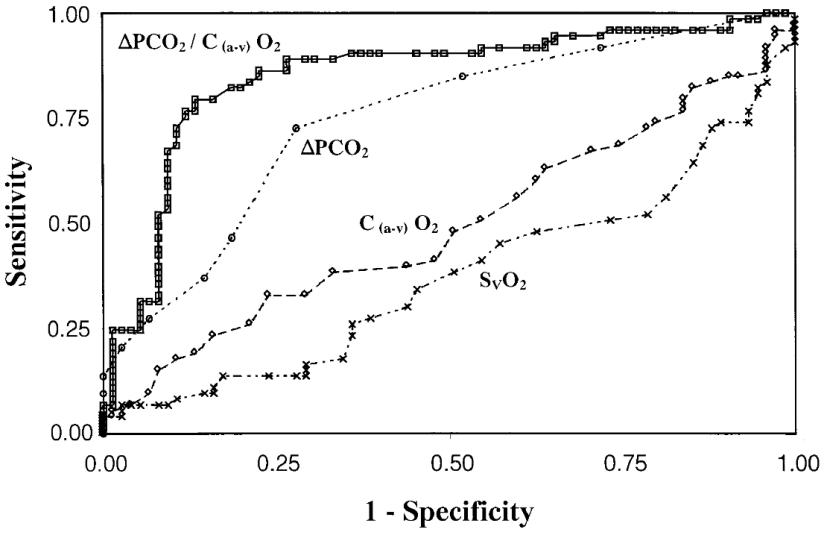

Figure 14 Adapted from [289]. Receiver operating characteristic curves of O2 and CO2 derived parameters for the prediction of hyperlactataemia

The Mekontso-Dessap study used mixed venous values obtained from pulmonary artery

catheterisation. In 2015 Mesquida and colleagues used central $\Delta pCO_2/ C_{a\text{-}v}O_2$ in paired samples to predict future lactate clearance and identified a similar correlation, with an AUROC of 0.82(95% CI 0.73-0.92). Multiple studies have now demonstrated how the admission $\Delta pCO_2/ C_{a\text{-}v}O_2$ ratio predicts subsequent organ failure and mortality in septic shock[290,291] and post-operative complications[292]. A recent post-hoc analysis of the ANDROMEDA SHOCK study demonstrated $\Delta pCO_2/ C_{a\text{-}v}O_2$ reduced in line with other perfusion indices[293]. No study has compared the $\Delta pCO_2/ C_{a\text{-}v}O_2$ ratio with direct observations of the microcirculation.

2.4.2 Handheld Video Microscopy (HVM)

2.4.2.1 Overview

Microcirculatory parameters are reduced in septic shock[294–302], cardiogenic shock[303–305], haemorrhagic shock [306,307], patients on ECMO[308–310], after major surgery[311] and in general critical illness[301,312]. Perfusion parameters also reduce physiologically in the elderly[313]. Perfusion impairment has been demonstrated in the sublingual circulation, in other accessible tissue beds such as stomas[314] and non-accessible regions during surgery, including the brain[315], serosa[316], peritoneum[317] and liver[318]. Preclinical studies have searched for a correlation between sublingual perfusion and clinically relevant tissue beds, to determine if sublingual observations truly reflect global perfusion. In shock models abnormalities can be identified in both beds, but the degree of correlation is limited. Changes in gut perfusion reflected sublingual measurements in two studies[319,320] but not in another[321]; whereas renal and sublingual perfusion barely correlated in one study[322] but did

in another[323].

A reduction in microcirculatory variables is common early in the admission of a shocked patient, with the degree of shock correlating with the severity of the reduction. Generally, impaired tissue perfusion early in the admission highlights the presence of shock but it is the persisting impairment following initial resuscitation efforts that portends surgical complications, morbidity and death, as evidenced in multiple longitudinal studies[298,302,307,311]. Whilst improvement in sublingual microcirculatory parameters precedes clinical improvement in a variety of conditions[295,310].

The microcirculation can be directly imaged using a video microscope. To have clinical application emitted light must be reflected, rather than transilluminated. Incident Dark Field Microscopes (IDF) use polarised light with a wavelength of 530nm, in the green band of the visible spectrum. Light which is reflected but does not pass through an RBC remains polarised and is removed by a polarised filter, Figure 15 illustrates the various types of camera available. IDF devices have the light source positioned next to the lens and synchronised to rapidly cycle between emitting and receiving, the returning beams are directed onto a computer-controlled sensor resulting in superior contrast and

resolution[324,325].

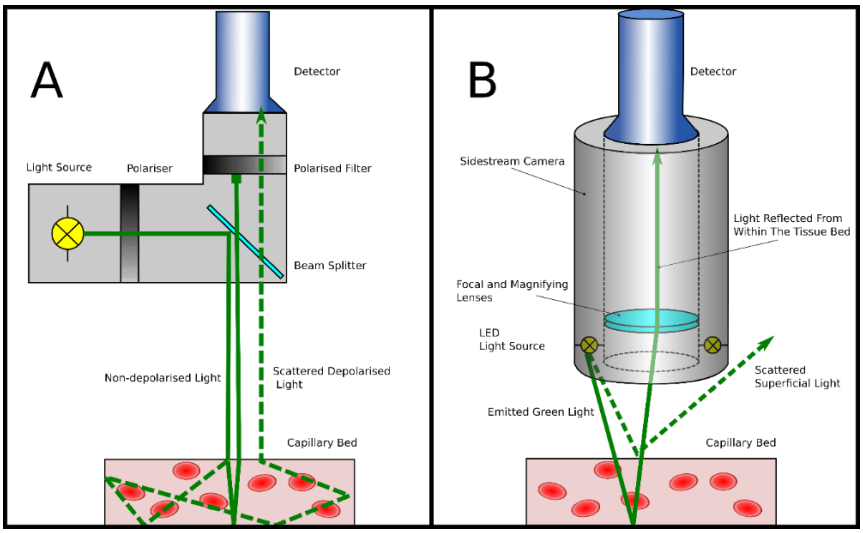

Figure 15 Schematic of handheld video microscopy. A) orthogonal polarisation spectroscopy (OPS): green light is emitted, polarised and reflected to pass through the tissue bed, light which remains polarised is stopped by a filter, whilst scattered light, depolarised as it passes through RBCs may pass through into the detector. B) Sidestream dark field (SDF) microscopy emits green light in close proximity to the camera. Only incident light from sufficient depth passes through the lenses for detection.

The emitted light with a wavelength of 530nm is absorbed and depolarised by both deoxygenated and oxygenated haemoglobin but only a few other significant chromophores, enabling selective imaging of red blood cells. However, selectively imaging haemoglobin makes the vessel edges imperceptible and empty vessels invisible. In addition, free haemoglobin and red cells are visible and bleeding mucosa may obstruct the field of view, a common problem when repeatedly imaging friable membranes in shocked patients. HVM cameras are poorly penetrant of adult skin and are only capable of imaging areas covered in a thin epithelium such as mucus membranes. The sublingual membrane has been selected for study in the majority of HVM literature; it is readily accessible and considered a central circulatory bed, less complicated by changes in temperature and vasoactive agents. The microcirculation is imaged directly and the site of substrate exchange (vessels <20µm) can be specified, an advantage over other methods of microcirculatory analysis.

Assessed variables relate to the number, density and velocity of RBCs within the microcirculation.

2.4.2.2 Image Acquisition

The CytoCam (Braedius Medical, The Netherlands) is the most recently developed device and is the only device to use IDF technology, it is the device used in this thesis. 12 short-pulsed LEDs illuminate the subject area and are coupled to a short-pulsed, high-pixel density image sensor. The light source and sensor alternate in a synchronized fashion in 2msec cycles, producing uncompressed image sequences. Output is via high-definition multimedia interface (HMDI) to the PC interface. Focus is achieved by an in-built stepper-motor. CytoCam Tools is the associated software package which controls all the features of the camera, with no direct controls on the device. Video can be assessed using CytoCam Tools, but typically is exported to the industry standard software AVA 3.1(Automated Vascular Analysis, Microvision Medical, The Netherlands). Despite the wider field of view, files exported to AVA 3.1 are cropped by approximately one third and the additional data is lost. Comparative studies have shown greater capillary detection, contrast and focus of the CytoCam IDF camera in comparison to older devices[324,326,327]. AVA 3.1 is used as the reference method of analysing HVM in this thesis.

Acquiring an image

Following suctioning of the oropharynx, a gauze swab or further gentle suctioning is applied to gently remove saliva from the mucosal surface. The camera probe is placed on the

sublingual area and care taken to exclude areas of the buccal microcirculation with large numbers of looped vessels. Focus is adjusted until individual erythrocytes and plasma gaps are visualized within capillaries and brightness and contrast are adjusted until acceptable. Pressure artefact needs to be scrupulously avoided by applying only the minimal amount of pressure necessary to obtain an image. Three to five video images of the sublingual microcirculation are taken from different regions of the sublingual capillary bed and each clip should consist of at least 100 video frames at a frame rate of 20 per second[328].

To improve comparison, consistency and promote high quality data acquisition and analysis, two round-table summits have provided standardization for HVM. A summary of the key points from the most recent conference is given below [328,329]:

- Vessels of ≤20μm form the microcirculation and only these should be analysed.
- Only vessels where individual RBCs are clearly seen should be assessed.
- Vessels should be evenly illuminated, with good contrast and free of pressure artefact. To this end, an image quality score should be reported.
- The minimum capture duration of motion-free imaging should be 4 seconds and ≥100 frames.
- 3-5 sampling regions should be sought with ≥4 individual videos.
- Hyperdynamic flow should not be routinely reported.
- Looped capillary segments should be avoided. Areas studied should be selected based on a good distribution of both large and small vessels and have less than 30% looped capillaries.
- The capillary bed is a three-dimensional structure and imaging methods with a greater

depth of focus generally produce higher density scores. Differences of vessel density may be up to 30% depending on the imaging system and this should be reported in the study.

- Analysis may be by real-time visual estimation, off-line manual or software enabled analysis or fully automated analysis. The chosen method should be stated.
- Reported variables should include measures of capillary density, RBC flow and heterogeneity.
- Visual estimation may be done by grid or “eyeballing” methods.
- User training should be reported with the results.

Limitations

Limitations of acquisition

Stability

The view of the capillary bed needs to be motion free for the duration of the imaging clip and microscopy in sedated patients can be hampered by movement. Instability may be due to user movement but from experience, is more frequently due to the stimulation of the patient’s tongue by the probe. Interacting with the probe is less problematic with patients who are either deeply sedated or fully compliant. Lesser sedated patients frequently move in response to the probe or have limited mouth opening which cannot be overcome with gentle pressure on the chin and sedation boluses may alter haemodynamics and microcirculatory flow confounding measurements. Analysis software provides motion correction for lateral movement but certain movements distorting the three-dimensional structure of the tissue planes are not correctable. Software motion-stabilisation is achieved by tracking capillaries across the screen during the clip and cropping the final video to those

visible throughout, removing data in the process, therefore stable video clips are highly desirable.

Pressure

In health standardised capillary pressures range from 10-22mmHg [330]. External pressure from the camera, perpendicular to the driving flow will impede flow within the microvessels and if great enough will cause occlusion. The CytoCam has a probe tip diameter of approximately 10mm, an area of 80mm^2, a weight of 120g will exert a pressure by gravity alone of 110mmHg. A tilted probe exerts a pressure over one edge and therefore the edges of images are at increased risk of pressure artefact, however the entire image must be analysed and edges cannot be excluded. In shock, capillary pressure is likely to be less than in the example above and the potential for pressure artefact increases, which is unfortunate as it is shocked patients where microcirculatory analysis is informative. Patients who are severely shocked are likely to be identifiable with clinical measures and HVM will be of limited additional benefit. The middle group of patients, with lesser degrees of shock may be where HVM is most beneficial, but pressure artefact may alter subtle findings. Excessive pressure can be identified by assessing the larger vessels in the image as vessels >20µm usually maintain continual forward flow even in the presence of profound microcirculatory dysfunction [328]. If larger vessels demonstrate flow abnormalities then significant pressure artefact is likely to be present; flow reversal is pathognomic of pressure artefact. Large vessels maintain flow more readily than capillaries and therefore lesser degrees of pressure may still be present but undetectable. Pressure artefact may be reduced by operator training, but no technological solution such as an integrated pressure monitor is available. Such a device could also be used to measure the microcirculatory occlusion pressure and

form the basis of further research.

Image selection

The buccal circulation lies near the sublingual circulation but is tightly looped and has historically been excluded, deemed to be of lower quality, lying outside of the sublingual bed and with less evidence supporting its analysis. The buccal circulation but may be the preponderant circulation beneath the tongue however and requires careful avoidance by the operator. The image can also be spoiled by overlying debris including mucus and blood.

2.4.2.3 Handheld Video Microscopy Analysis

In this thesis HVM was analysed by visual estimation, manual and semi-automated analysis. Manual analysis is accurate but is off-line, slow and unsuitable for clinical application. Automated techniques are unreliable although recent improvements in software are promising.

Quadrant Microcirculatory Flow Index Score (MFIq)

Confusingly two variations of MFI exist, the quadrant MFI score (MFIq) and MFI vessel-by-vessel (MFIv) calculated using manual analysis, described below. MFIq, the score which features most in the literature, uses a grid system to divide the image into quadrants. Each quadrant is given a predominate flow score (0, no flow; 1, intermittent flow; 2, sluggish flow and 3, normal) and the MFIq is the mean value of the quadrant scores, Figure 16 provides an example. MFIq describes flow. It has been validated in clinical studies showing good intra and inter-user reliability[331,332]. Studies investigating the precision of MFIq have been mixed, Arnold reported good agreement with quantitative assessment by Bland Altmann analysis

(mean difference of -0.031, SD = 0.198)[300], but Pozo showed limited correlation with quantitative RBC velocity (RBCv) (R^2=0.54), although RBCv is not a routinely reported variable[333].

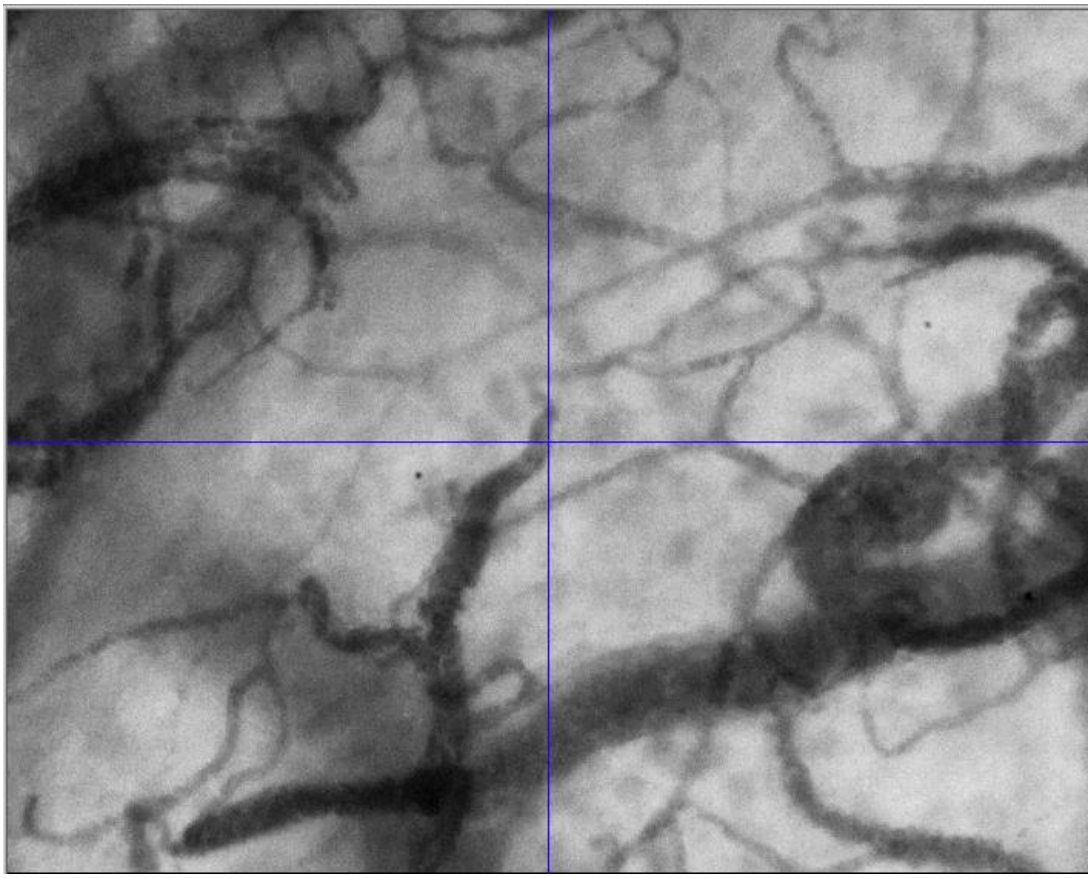

Figure 16 Determination of Microvascular Flow Index quadrant score. The image is divided into four quadrants and the predominant flow type for each quadrant is given a value between 0 for no flow and 3 for normal flow. MFIv is the mean value of the quadrant scores

Semi-automated analysis and manual analysis

Semi-automated and manual analyses are similar, only differing with the mechanism used to identify blood vessels; the reported variables are the same. Once exported to AVA 3.1 motion-stabilisation and vessel identification are undertaken. For manual analysis the centrelines of vessels <20µm are traced by the operator, Figure 17B refers. Semi-

automation relies on the computer selecting the vessel segments and the operator editing the selection until reflective of the capillary bed. Figure 17C demonstrates the issue of automated identification, multiple short snippets of vessels are identified instead of continues lengths. After manual vessel identification, each segment has a velocity score manually applied (normal: 3, sluggish: 2, intermittent: 1, absent: 0) as shown in Figure 17D[334]. A vessel segment may display a number of velocity states within the 4 second clip, allowing a degree of subjectivity. Only RBCs can be visualised, so flow must occur within the 4-5 second window to be captured. After velocity scoring, AVA 3.1 summates the velocity scores and vessel sizes to provide the variables recommended by consensus opinion[329,335].

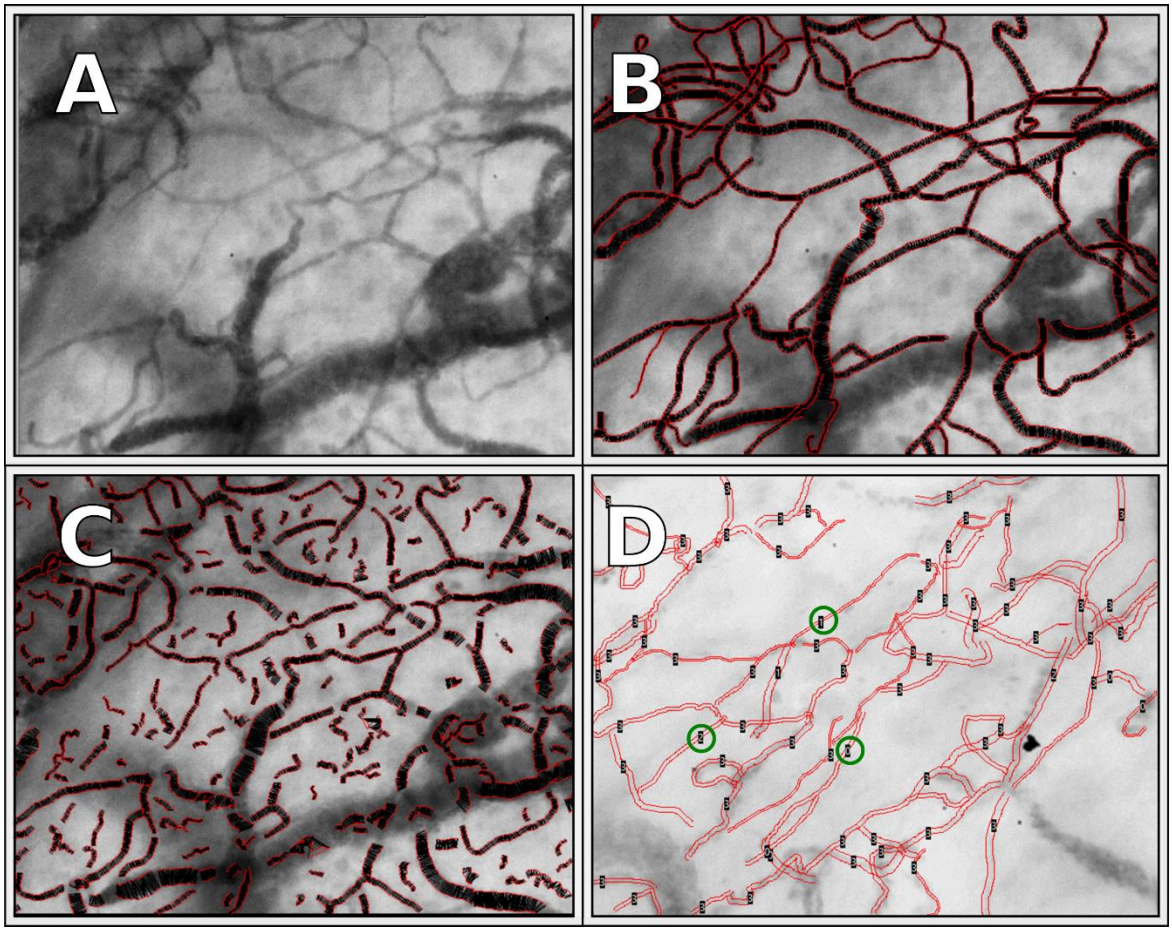

Figure 17; (A) example of an HVM video image, before analysis. (B) after manual vessel identification. The large vessel in the bottom right of the image has been excluded, being too large for analysis (>20µm). (C) The same video image as shown

in A after automatic vessel detection by AVA3.1. Short fragments are identified rather than the continuous vascular segments visible in B. (D), manual vessel scoring of a different still image. Vessels are given a score between 0 and 3 depending on the flow characteristics of the vessel for the MFIv score (see text). Examples of segments with abnormal flow are identified by green circles

2.4.2.4 Microcirculatory Parameters

The flow, density and heterogeneity of perfusion are described in the following variables[328]:

Total Vessel Density (TVD) (mm/mm^2) describes the vascular density of the image, regardless of whether vessels are perfused. Aykut et al reported normal TVD values of 21.6±4.3mm/mm^2 using the CytoCam [324]

$$TVD = \frac{total\ length\ of\ blood\ vessels}{area\ of\ image}$$

Perfused Vessel Density (PVD) (mm/mm^2): The total length of vessels with velocity scores of 2 (sluggish) or greater, relative to the area imaged. Normal PVD values are 21.5±4.38 mm/mm^2, TVD and PVD should be equal in health[324].

$$PVD = \frac{total\ length\ of\ blood\ vessels\ with\ velocity\ score\ \geq 2}{area\ of\ image}$$

Proportion of Perfused Vessels (PPV): the ratio of PVD to TVD, expressed as a percentage.

The normal value is 100%.

$$PPV = 100 \times \left(\frac{PVD}{TVD}\right)$$

Microvascular Flow Index, Quadrant (MFIq): MFIq is a visual estimation score, already described, but is also a reported component of quantitative analysis. The flow in each quadrant is scored from 0 to 3 and the average quadrant score is reported. The value in health is 3.0.

$$MFIq = \frac{Q_1 + Q_2 + Q_3 + Q_4}{4}$$

Microvascular Flow Index, Velocity (MFIv): Describes the flow characteristics of the clip. The percentage of vessels with normal velocity (V_n) are multiplied by 3, sluggish velocity (V_s) by 2, intermittent velocity (V_i) by 1 and no flow by 0 (V_0). The sum of these values is divided by 100. The value in health is 3.0.

$$MFIv = \frac{(3V_n + 2V_s + 1V_i + 0V_0)}{100}$$

Microcirculation Heterogeneity Index (MHI): describes the heterogeneity of flow in an individual patient's microcirculation. As such it is derived from all the video clips, unlike the

other variables which are derived from single videos. The maximum, minimum and mean MFIq recorded in all the videos are required. The value in health is 0.

$$MHI = \frac{MFIq\ max - MFIq\ min}{MFIq\ mean}$$

A large observational study of 252 patients identified PPV as the microcirculatory variable which best predicted patient outcome (AUROC 0.818), demonstrating superiority over conventional haemodynamic markers; MFI was also informative[305]. PPV and MFI correlating closely with outcome in patients with septic shock was also demonstrated in a smaller study published the year before[302]. Both studies demonstrate that despite normalisation of macro-haemodynamic variables, patients with persistent microcirculatory abnormalities had an increased risk of death, not reflected by standard haemodynamic assessment[295,302,305,336].

Summary of introduction and basis for studies

Sepsis presents a massive disease burden and septic shock, the most severe form of sepsis is predominately a condition managed in higher and middle-income countries, where effective organ support allows survival to a point where the manifestations of organ failure become apparent. Despite refinement of the definitions and diagnostic criteria, which make temporal and geographical comparison more difficult, the overall mortality rate and incidence is thought to be gradually decreasing.

Patients with chronic kidney disease are more at risk of AKI and have worse outcomes from AKI when compared to those with normal renal function at the time of injury. The incidence of severe AKI is increasing but the mortality rate appears to be gradually reducing. It is becoming increasingly clear that AKI is a harbinger for major adverse cardiac events in the longer term. Patients with AKI, particularly that which persists, are also at far greater risk of CKD than that suggested by the post-injury creatinine, a crude and ineffective indicator of renal health. Renal injury is an independent predictor of short-term mortality and has an associated risk far greater than that expected from a pure loss of function.

Sepsis accounts for a significant proportion of acute kidney injury in higher and middle-income countries and the aeitology is not entirely understood. There are scant other causes of renal injury that result in such profound loss of function, where at least partial recovery is expected and histological changes are few. Animal data differs significantly depending on the model, but large animal data thought more reflective of humans, suggests an increase in whole-organ blood flow with intra-renal haemodynamic alterations. Certainly the

microcirculation in all studied tissue beds is highly interactive undergoing multiple alterations in sepsis. The same would not be unexpected in the kidney, but additionally the kidney has a unique microcirculatory anatomy and the possibilities of intrarenal alterations to blood flow are multiple but difficult to demonstrate in clinical studies where techniques are limited and the changes highly complex.

Hypotheses examined in this thesis

1. Renal perfusion can be reliably assessed in controls using dynamic renal contrast ultrasound.
2. Alterations in intrarenal blood flow are a central feature of sepsis associated AKI and can be identified by dynamic contrast enhanced ultrasound.
3. Renal microcirculatory alterations will be distinct from renal macrocirculatory alterations due to dynamic intrarenal mechanisms.
4. Renal microcirculatory alterations are unique and cannot be predicted by the assessment of systemic perfusion.
5. Patients with different septic AKI subphenotypes will display different patterns of renal microcirculatory alterations.
6. Dynamic contrast ultrasound assessment can be used to predict patients who will develop severe AKI in sepsis.
7. Renal microcirculatory alterations may not be exclusive to sepsis and exist in other cohorts of critically ill patients. These can also be detected by DCE-US.

3 Development of a dynamic contrast enhanced ultrasound technique suitable for intensive care and its validation in healthy controls

3.1 Introduction

As described in General Methods, dynamic contrast enhanced ultrasound (DCE-US) is an established technique in assessing solid organ perfusion but is yet to be fully explored in the unique environment of critical care renal imaging. Critically ill patients are inherently unstable, harder to reposition and transfer off the ICU for imaging is difficult. DCE-US provides a potential method of assessing renal perfusion at the bedside but requires further development and validation prior to increased use as a research or clinical tool.

Contrast may be given by bolus or infusion. Bolus-transit kinetics are likely to be confounded by cardiac output in the critically ill population, generating indicator-dilution curves within the kidney. Bolus-transit is used predominately in oncological imaging where tissue types can be compared within the same image, however it does not lend itself as neatly to the study of single tissue beds such as the renal cortex. Destruction-replenishment kinetics are likely to be less confounded by cardiac output, but are largely untested in shocked patients.

This study measured normal renal perfusion in controls, developed a predominately outpatient radiology-based technique to a method which would be suitable for use in critically

ill patients, enabled me to gain familiarity with the acquisition, analysis and veracity of the data and to assess reliability of the analysis phase.

3.2 Method

Overview

A single centre prospective observational control study of healthy volunteers was undertaken at King's College Hospital in March 2019. The primary objective of this study was to measure normal cortical perfusion values using DCE-US thus providing previously unreported reference data for the clinical study described in later chapters. Additional objectives were to adapt the technique, making it suitable for use in critically ill patients. The test protocol for the present study ran contrast continually for four minutes, a far shorter period than typically used in outpatients. An oscillatory pump is used for prolonged imaging periods, for example cardiac contrast imaging may take up to half an hour, but for the ICU bedspace would prove cumbersome, only compatible with proprietary equipment and was also not currently manufactured. Therefore an assessment of contrast settling needed to be made if contrast were to be given by a standard syringe driver. Proprietary equipment uses 5mL of neat contrast but needed to be diluted in saline to 20mL permit the recommended rate to be infused; such a dilution has previously demonstrated by Chan and colleagues to be effective, but it was necessary to be sure and familiar of this method prior to adoption[108]. This study enabled me to gain familiarity with the technique, assess the quality of the replenishment destruction cycles, assess the reliability of analysis, both intra- and inter-user and to determine if different size regions of interest (ROIs) produced variation in the data analysis. Optimal patient positioning, breath-holds and ultrasound windows could also be determined. An additional purpose of this study was to measurement renal blood flow which is difficult in

clinical studies, the renal artery is hard to see with B-mode ultrasound and colour doppler aliases outside the vessel wall making measurements difficult [337]. This study looked to develop a technique using contrast to measure vessel diameter before using doppler to calculate flow.

Study Participants

Healthy volunteers between 18 and 40 years of age were recruited and enrolled between February and March 2019. Volunteers were screened prior to attending by electronic questionnaire to ensure no history of renal disease, medication or comorbidity that could reasonably be considered to have a renal interaction. On attending, baseline creatinine was checked and a renal ultrasound performed to define the size and appearance of both kidneys and the ease of which each kidney could be imaged. A urine dipstick and a pregnancy test were performed and a baseline echocardiogram to ensure the absence of structural disease and cardiac output calculated. DCE-US requires the probe to be motionless for up to five minutes and an easily imaged kidney is preferential. The resistive index was measured.

The study was performed under a major amendment to the permission granted by Yorkshire and the Humber, Leeds West Research Ethics Committee (18/YH/0371). It was conducted in accordance with the Declaration of Helsinki and Good Clinical Practice guidelines. All participants gave written informed consent.

Test protocol

Both kidneys were imaged during screening and the most accessible selected for contrast infusion imaging, the right kidney was used if both had adequate views. The volunteer rolled away from the side of the kidney being imaged, remaining in the supine position they were propped with a pillow under the thorax and another under the pelvis, leaving the renal angle exposed. 4.8mL of neat SonoVue contrast was diluted in an additional 15.2mL of saline generating 20mL of solution in a standard Luer lock syringe and giving set. Each volunteer was cannulated with an 18g cannula placed in a large vein of the upper limb. Using manufacturer recommended flow rates of 1mL / min of neat contrast, diluted contrast was infused at 240mL an hour, giving an identical flow rate of contrast to the undiluted method. Gain selection was set to provide a black image in contrast mode, which became bright on the arrival of bubbles, but not excessively, so as the calyces remained dark. The focal point was set just beneath the kidney as recommended by the Dr Huang, the radiology expert who provided prior training. Image capture was commenced in dual mode (contrast and grey-scale) with time zero set to commencement of the infusion. Typically, the first ultrasound bubbles appear from 45 seconds and steady state is achieved by approximately one minute in health. Destruction replenishment cycles were undertaken from two minutes, every 30 seconds until four minutes, generating five cycles per contrast run. One contrast run was performed per volunteer. All volunteers had basic monitoring applied throughout the imaging protocol. There were no adverse events.

Following completion of the DCE-US protocol, the contrast infusion rate was halved to 0.5ml/min to provide more time and reduced intensity to image the renal artery. The diameter of the renal artery was measured on contrast-enhanced zoom mode imaging. Pulsed wave Doppler was aligned within the RA and the time-averaged mean frequency was

measured as described by Blanco[62]. Quantification of renal blood flow was calculated using the following equation:

$$\boldsymbol{RBF = \pi renal\ artery\ radius^2 \times TAMV \times HR \times 2}$$

RBF: renal blood flow; πr^2 provides the area of the renal artery. TAMV: time averaged mean velocity within the renal artery; HR: heart rate; 2: assuming 50% RBF per kidney

Analysis protocol

DICOM clips were exported via USB device to VueBox analysis software and images were analysed in GI-Perfusion mode. Regions of interest (ROIs) were selected within the renal cortex, identified as the area peripheral to the renal calyces, but beneath the capsule. All ROIs were selected in well visualised cortex and were screened to ensure no large vessels were present throughout the analysis period. The remainder of the DICOM clip was deselected from analysis and destruction-replenishment curves were automatically drawn by the VueBox software. Each DICOM clip was then refined to ensure sufficient time had passed to reach steady state after destruction, identified as the plateau phase of the reperfusion curve. Provided plateau was reached the remainder of the clip was deselected to prevent renal respiratory motion artefact from a vessel moving into the ROI. The use of multiple ROIs helped identify any aberrant curves, affected by the movement of the undetected vessel. If an outlying result was identified at this stage, the ROI was redrawn to avoid the blood vessel. Once three similar reperfusion curves were drawn, median values were taken. This process was repeated for all five destruction replenishment cycles and median values taken from each patient.

The assessment of ROIs is also necessary to assess for selection bias by the operator. The first analysis was undertaken by myself. The second analysis was a blinded repeat of the first analysis, assessing intra-user correlation and test reliability. The third analysis was again a repeat of the process by a second blinded user to assess inter-user reliability. The second blinded user, with no prior experience had an hour of prior training by myself at a later time, after I had undertaken approximately 1000 destruction replenishment cycles.

A fourth analysis assessed whether the size of ROIs influenced the results. Two smaller sampling regions of approximately 0.4cm^2 were averaged and compared to larger regions mapped to the entirety of the well visualised cortex and the correlation between these small and large ROIs were compared; Figure 18 provides an example of this comparison.

The fifth analysis assessed whether degradation of the contrast occurred from settling by not using the oscillatory pump. To assess the effect of settling, the first destruction-replenishment cycle was compared with the last cycle with the assumption that the signal at two minutes would be different to that at four minutes if the contrast degraded.

Statistics

Descriptive data are presented as median (Q1-Q3) or mean (±SD) depending on the distribution after assessment by Shapiro-Wilk test for normalcy. Agreement is presented by Bland-Altman plot and correlation by Pearson's correlation coefficient. First and last destruction replenishment cycles are compared by Wilcoxon Rank Sum test and paired T-test

depending on data distribution and type. Statistical analysis was performed in R. P values <0.05 were considered significant.

A power calculation was not undertaken as no prior data were available on which to base it.

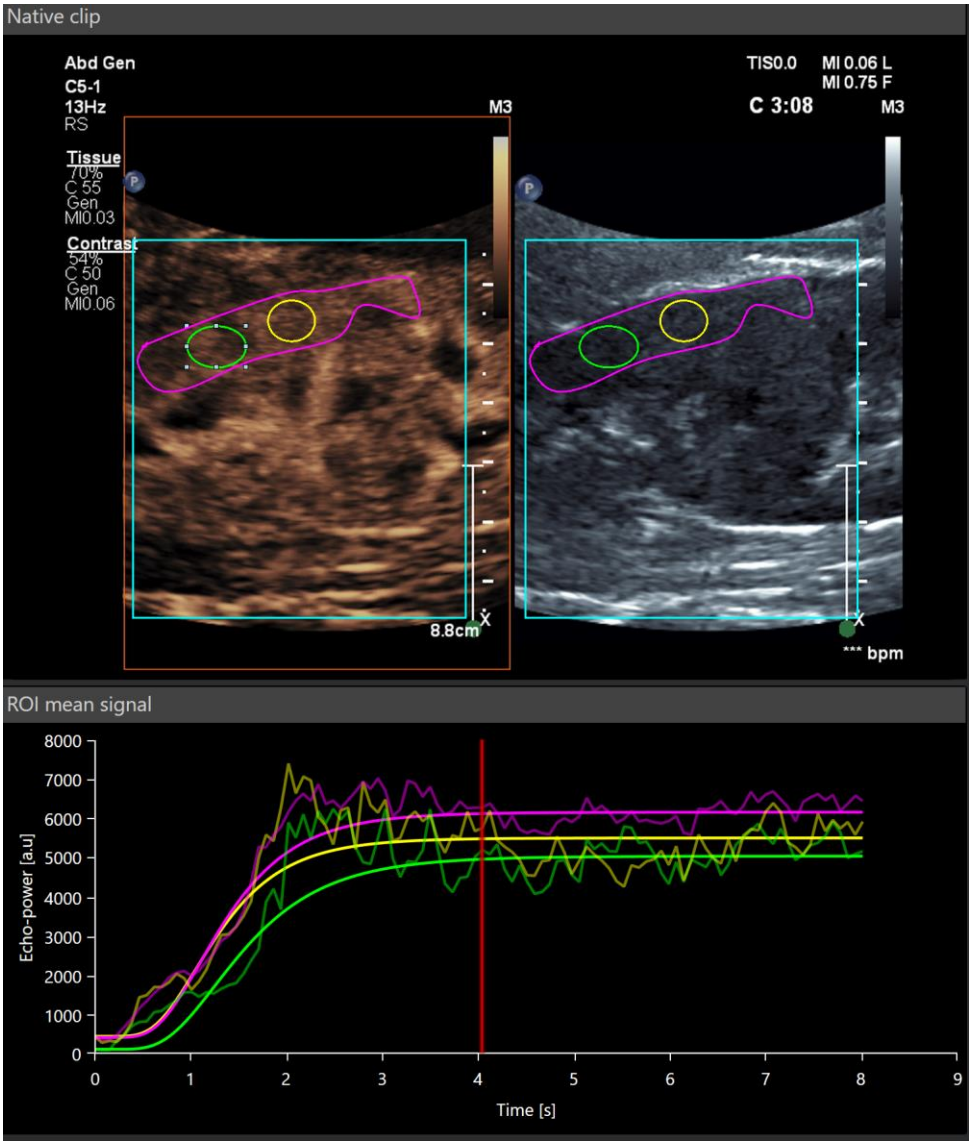

Figure 18 Upper image - Comparison between the signal from the well visualised cortex (purple region) and arbitrarily selected smaller sampling volumes (green and yellow regions) – ensuring large vessels are avoided and the ROI is well visualised throughout the replenishment process. Destruction replenishment curves are demonstrated in the lower half of the figure.

3.3 Results

12 healthy controls were enrolled and successfully underwent renal DCE-US imaging. The mean age was 33 (range 26-40) and 7 were female. One participant was of Chinese origin and the rest were Caucasian British. Average GFR was 114(±9)ml/min and BMI 23(±3). Average values for the four DCE-US variables are presented in Table 2. The average renal resistive index was 0.60±0.06.

Cortical perfusion values from healthy controls are presented in Table 2 along with the inter-user correlation, intra-user correlation and the correlation between larger and smaller ROIs. The median sampling size for the small regions of interest was 0.4(0.36-0.48)cm^2 and the large ROI 3.8(3.49-4.09)cm^2. Bland Altman analysis of the inter-user agreement for the four variables are presented in Figure 19. Graphical data of the small vs large ROI comparison are presented in Figure 20.

Variable	Assessor 1 absolute value	Assessor 2 absolute value	Inter-user correlation	Intra-user correlation	Large vs small ROI correlation
Cortical relative blood volume (a.u.)	5608±869	5553±2283	0.52	0.88	0.96
Cortical mean transit time (sec)	1.84(1.66-2.13)	1.81(1.63-2.12)	0.65	0.77	0.87
Cortical wash-in rate (a.u.)	1979±372	1943±490	0.67	0.9	0.96
Cortical Perfusion Index (a.u.)	2740(2570-3070)	2673(2284-2983)	0.74	0.9	0.98

Table 2 Average values of normal renal cortical perfusion in healthy controls when assessed by DCE-US by two blinded assessors, Assessor 1 and Assessor 2. Inter-user, intra-user and ROI size comparisons are presented (Pearson's correlation coefficient).

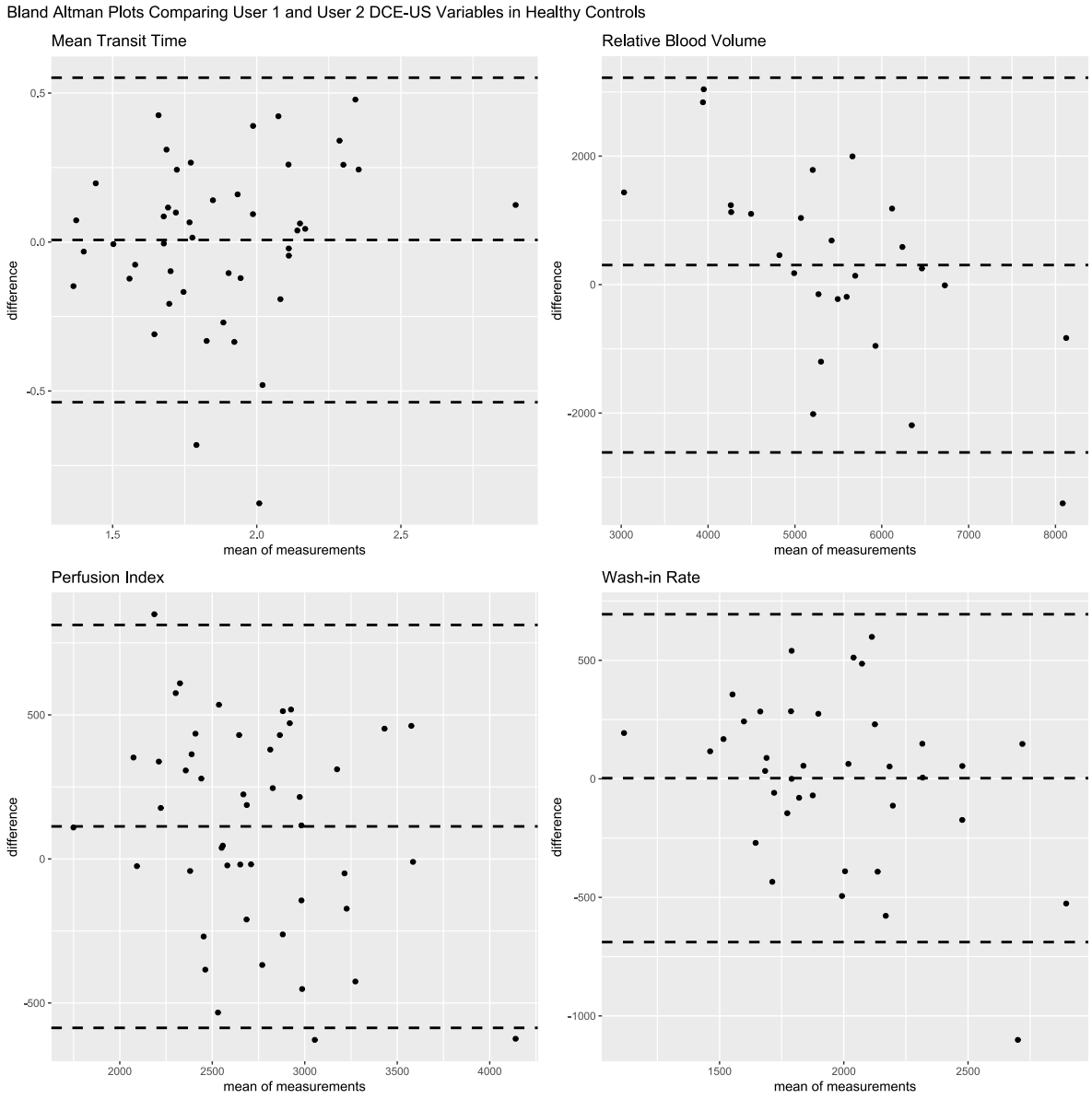

Figure 19 Bland Altman analysis of the four DCE-US variables assessed in the renal cortex by two blinded assessors, the inter-user agreement.

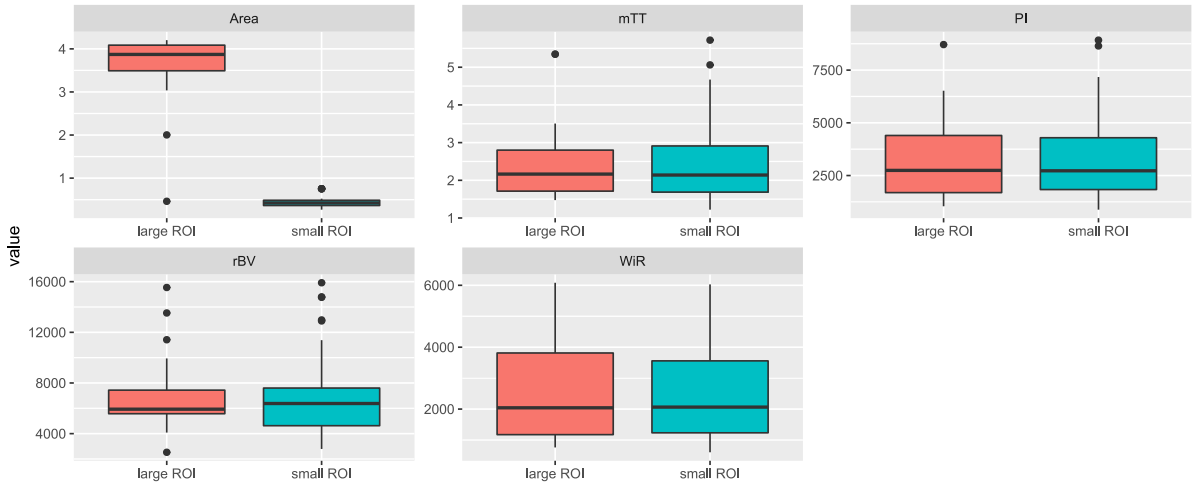

Figure 20 Boxplots demonstrating the variation between ROI area and DCE-US variables between larger and smaller ROIs. Units: Area cm2; mean transit time (mTT) sec; perfusion index (PI) a.u.; relative blood volume (rBV) a.u.; wash-in rate (WiR) a.u. Clear separation is demonstrated in the area of the ROI but no difference in measured variable was identified (all values p>0.05)

Table 3 provides the comparative data from the variables of the destruction-replenishment kinetics at two minutes and the final destruction replenishment kinetics at four minutes. No differences were demonstrated between the compared kinetics.

variable	Destruction-replenishment cycle one (two min)	Destruction-replenishment cycle five (four min)	P value
Mean transit time (sec)	1.91(1.78-2.06)	1.75(1.63-2.03)	0.501
Perfusion index (a.u.)	2760(2575-3110)	2845(2657-3481)	0.801
Relative blood vol (a.u.)	5704+-949	5756±959	0.9
Wash-in rate (a.u.)	1880(1735-2280)	2130(1867-2446)	0.455

Table 3 A comparison of dynamic contrast ultrasound variables at two minutes (destruction replenishment cycle one) and at four minutes (destruction replenishment cycle five) using a non-oscillatory syringe driver.

Renal artery diameters measured using CEUS were 7.6±0.08mm. Velocity time integrals measured using time averaged mean frequency were 21.2±5.3cm making crude flow values of 1.4±0.53/min, which were then corrected to normal RBF (1.2l/min) using a correction factor (k) of 0.85 which was used in later patient studies.

3.4 Discussion

The present study demonstrates the development and validation of a renal perfusion imaging technique that may be used at the bedside of critically ill patients. The principal results are the presentation of DCE-US renal perfusion values in healthy controls which are previously unpublished.

Development of a DCE-US technique

Dilution of contrast with saline has previously been described by Chan et al[108] and was easily achievable in the present study by backfilling a 20mL syringe with the 4.8ml of neat contrast. This approach allowed contrast to be delivered by a standard syringe driver as the small syringe of neat contrast is incompatible. Flow rates to deliver a comparative 1mL/min of neat contrast were reliable on a standard syringe driver and delivered through an 18g peripheral cannula. Whilst this may seem trivial, it is a deviation from outpatient practice, therefore to ensure it was feasible was a necessary step. There was no difference between the first and last destruction replenishment cycle to suggest settling of contrast which may occur after prolonged use. Direct comparison directly with the oscillatory syringe driver would have provided a higher standard of evidence, but the current comparison is pragmatic and at the time of writing, the oscillatory pump was not being manufactured. The use of a standard syringe driver also further simplifies the technique, making it more suitable for wider research adoption.

Small regions of interest were compared with larger regions and provided the cortex was well visualised, small sampling volumes had an excellent correlation with larger regions, meaning small or large regions could be used in the patient study. This corroborates with the findings

of two previous groups who demonstrated that provided regions of interest were within well-visualised tissue, the exact shape, size or location of the ROI made little difference to the reproducibility[117,118].

A correction factor (k) was subsequently applied to the RBF calculation; k was calculated from calibration of the mean RBF measurement (1.4l/min) to an assumed normal RBF value of 1.2 l/min. An over-estimation may have resulted from non-laminar flow within the renal artery. Whilst Doppler RBF assessment has previously been shown to have reduced sensitivity, the combination of contrast assessment of renal artery diameter, the use of time averaged mean velocity rather than peak velocity – as described by Blanco[62] and calibration using controls are hoped to improve the accuracy in patients.

Reliability

This study also assessed the reliability of DCE-US analysis, although it does not assess the reliability of image acquisition. Blinded intra-user agreement was reassuringly excellent. Inter-user correlation between an experienced and naïve user was moderate to good, depending on the variable. This increased variation is probably expected and the reasons multiple. Firstly the difference in experience between the two users points to a skill which needs development. Sufficient training in both acquisition and analysis would be necessary beyond the hour provided for this study if the technique were to see wider adoption. This is not unique, such a learning curve is true for many imaging methods and analyses, particularly so with ultrasound where the image acquisition is user dependent. Established ultrasound techniques have an accepted inter-user variability in analysis[338], more so than cross-sectional imaging, although variation still exists here[339]. An additional reason for the variation seen in

the present study is specific to DCE-US. Cortical areas with suboptimal visualisation have reduce perfusion variables, an issue with the image rather than a true reflection of function. This may occur because of rib shadows but signal also attenuates towards the poles and renal pelvis, the signal being scattered by other bubbles as described by Sidhu and colleagues[116]. Respiratory motion of the kidney may cause areas of high perfusion, such as larger vessels to inadvertently drift into the field of view, or areas with reduced perfusion, such as calyces. As such a breath hold is helpful and screening of the generated sequence prior to analysis is essential, reperfusion curves generated by VueBox should be scrutinised for blips in the signal and redrawn if necessary. This limited inter-user correlation should be considered in context, the study only considered healthy control data, where all observations would be expectedly similar. Because the dataset featured only healthy controls, with minimal dispersion between the observations, any variation between users will be more obvious. If the dataset featured a range of perfusion from poor to good, the correlation may be less problematic. For example, 95% of MTT values were within 0.5sec in the present study and inter-user means varied by 0.03sec. The natural variation in the patient dataset presented in chapter 7 demonstrated a standard deviation of 14.5sec in those with AKI. This makes the observer variation less of an issue. As the true variation is much wider, small differences between the users' observations may be less noticeable.

As discussed in General Methods, both Hudson and Averkiou demonstrated DCE-US to be reliable[112,126] and both groups found time dependent variables to be more reliable than intensity-based variables. As shown in the present study, relative blood volume was less reliable than the other variables. This variability is also recognised by the European Committee in contrast ultrasound, EFSUMB in their 2012 recommendations on bolus-transit

kinetics[120]. Intensity parameters such as relative blood volume can vary even within the same model, as both signal saturation from dynamic range settings, microbubble concentration, depth and acoustic shadowing from both microbubbles and native structures can affect them[118].

Limitations

These results are taken from a majority female cohort who are healthy, in the third decade of life and have normal renal function. As such, the comparison to an older, predominately male cohort of the patient chapters, who may have stage three chronic kidney disease needs to be considered. As this is a novel technique in this setting, it is important to define normal values which provide a reference. The predominate comparison in the future chapters is between patients with and without severe AKI, the data from this chapter informs that comparison. Regardless, a second control group of ICU patients without AKI may have provided additional information as previously provided by Harrois et al in their pilot study[82]. The average mTT in their control group with traumatic brain injury was 2.9(2.6-3.1) sec, whereas in the healthy controls of the present study was 1.8(1.6-2.1) sec. Why this difference exists is unclear if both cohorts had normal kidneys and would need further study, subclinical AKI in the ICU control cohort is a possibility. Physiological differences between the healthy controls of this study and the predominately male control cohort with a mean age of 50 in the Harrois study is another possibility. Differences in acquisition and analysis is a third potential.

It would have been useful to undertake further training with the second operator to see if reliability could be improved, but the improvement between the inter- and intra-user variability points to this. Assessing reliability of the various stages of the technique,

particularly image acquisition would have provided greater insight. A direct comparison against the oscillatory syringe driver would have added to the comparison; a future study could combine these points. Finally a repeat-measures observational study comparing destruction-replenishment and bolus-transit kinetics in a group where cardiac output is varied may prove to be a useful analysis, I would hypothesise that bolus kinetics are confounded by cardiac output whereas destruction replenishment is not, but there is no evidence to support this.

Conclusion

This study provides normal values for renal perfusion in healthy controls and informs the clinical study presented in later chapters. It demonstrates that DCE-US analysis is a skill which requires training and development to produce meaningful data. It demonstrates development of the technique, enabling an infusion of dilute contrast run on a standard syringe driver with non-proprietary equipment making it pragmatic for the bedspace of critically ill patients.

4 Introduction and methods of the MICROSHOCK RENAL study: Macro and micro haemodynamic responses to septic shock in the renal and systemic circulations.

4.1 Introduction

Septic shock is one of the commonest causes of AKI in critically ill patients and is associated with a mortality of approximately 50%[2,25]. It presents a unique pathophysiology; the result of multiple factors including inflammation, alterations in renal perfusion and changes in cellular bioenergetics [340–342]. Interest in the perturbations of renal blood flow and microvascular perfusion have sparked multiple experiments and studies, but the data is unclear. Renal blood flow is likely conserved in hyperdynamic shock experimental models whilst microcirculatory flow is subject to multiple inducible shunting mechanisms. Some preclinical data shows preservation of cortical perfusion, but others have demonstrated the opposite[343–347]. Medullary perfusion is technically more difficult to study but detailed large-animal studies suggest severe impairment, potentially because of cortical bypassing of the medullary circulation[348]. The pathogenesis in humans remains elusive and difficult to study in critical illness.

Dynamic contrast-enhanced ultrasound (DCE-US) is an emerging imaging technique in the field of critical illness using highly echogenic but inert microbubbles to delineate areas of microvessel perfusion within organs. Both experimental data[323] and clinical studies[82,163,349] using DCE-US have suggested renal cortical perfusion is impaired in sepsis associated AKI. Ultrasound contrast agents (UCAs) are widely used in other fields, they are licensed

pharmaceutical agents with rarely reported adverse events.

4.2 Overall Method For the Microshock Renal Study

4.2.1.1 Study design:

A single-centre prospective longitudinal observational study. Serial assessments were undertaken using the methods in the two-by-two grid in Figure 21. Demographic variables, arterial and venous blood gases and blood results were recorded from the electronic ICU database. Serum, plasma and urine were stored for subsequent assessment. Clinical care, resuscitation protocols including fluid type, volume and selection of vasoactive agents remained at the discretion of the treating clinician, these were recorded but not controlled.

	Microcirculation	*Macrocirculation*
Renal	Dynamic contrast enhanced ultrasound	Contrast enhanced renal artery quantification and Doppler
Systemic	Incident dark-field handheld video-microscopy	Echocardiography

Figure 21 principal methods of assessing the systemic and renal macro- and microvasculature

4.2.1.2 Grouping Variables

All patients presenting to the Critical Care Units of King's College Hospital, London, UK were screened for inclusion between October 2018 and June 2021. Two grouping variables were applied retrospectively:

1. Sequential patients who present with septic shock were assigned retrospectively to either severe AKI, classified as KDIGO stage 3 (severe group), or patients with less severe or no AKI (non-severe group).

2. The same patient population was also grouped according to whether they had above or below average renal perfusion based on median perfusion index and mean transit time providing two groups, the detail is explained in 5.2.2.

4.2.1.3 Sample Size:

The sample size was derived from a power calculation using a previous study assessing cortical perfusion in septic shock with DCE-US[82]. Based on an estimated difference in perfusion index of 1000 au between groups (severe vs non-severe) and on a SD of 1000 au and assuming a power of 90% and alpha of 0.05 22 patients in each group (n=44) were required to detect a difference in perfusion index, assuming approximately 50% of patients with septic shock developed severe AKI[28]. To address potential for missing data, unequal groupings or refusal of retrospective consent, 50 patients were planned for recruitment.

4.2.1.4 Inclusion Criteria:

The septic shock defining criteria from SEPSIS-3 were used, in part, as inclusion criteria[5]:

- Over 18 years old

- ≤ 24 hours since ICU admission
- Evidence of suspected or confirmed infection
- Serial Organ Failure Assessment (SOFA) score increase of 2 or greater
- Requiring vasopressor support to maintain mean arterial blood pressure > 65mmHg
- Arterial blood lactate > 2.0mmol/l after initial fluid resuscitation

4.2.1.5 Exclusion Criteria:

- CKD stage 4 or worse
- Renal transplantation
- Severe obesity as adequate renal ultrasound images were unlikely
- Known intolerance to Sonovue ultrasound contrast agent
- Contraindications listed by the contrast manufacturer:
  . Established acute respiratory distress syndrome
  . Pregnancy
  . Breast feeding
  . Severe pulmonary hypertension (pulmonary artery systolic pressure >90mmHg) measured by transthoracic echocardiography
- Co-administration of dobutamine
- Patients in whom the initial treatment was palliative

4.2.1.6 Time points and techniques for data collection:

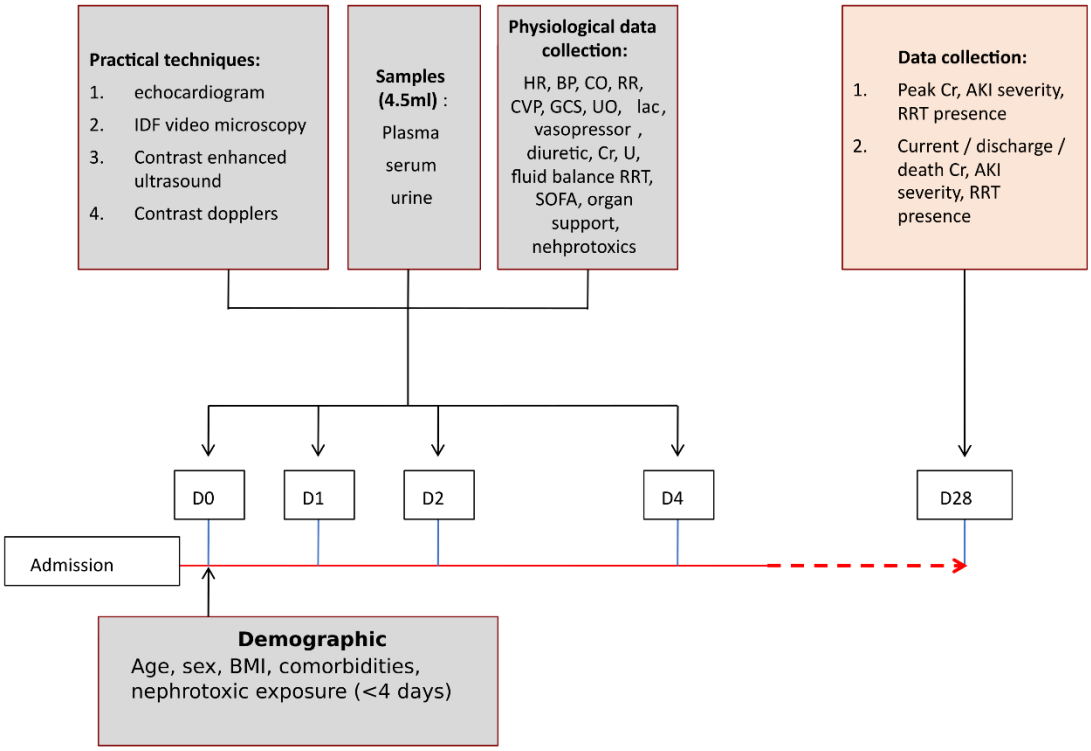

Figure 22 Investigation timeline for a single patient enrolled in the MICROSHOCK RENAL study. HR (heart rate), BP (blood pressure), CO (cardiac output), RR (respiratory rate), CVP (central venous pressure), UO (hourly urine output for last 6 hours and 24hr urine output, lac (arterial blood lactate), vasopressor (current vasopressor types and dosage), diuretic (presence and dose of diuretic use in past 24 hours), Cr (creatinine), U (urea), fluid balance (past 24 hours and duration of admission), RRT (presence or absence of renal replacement therapy), organ support (tidal volume, PEEP, peak pressure, arterial and venous blood gases), nephrotoxic exposure (within past 24 hours or prior to ICU admission). Admission (D0), after 24 h (D1), 48 h (D2) and 96 h (D4).

Figure 22 describes the data collected at the various time points, initial observations were undertaken within 24 hours of admission to ICU with subsequent studies after one and two days. A later day four time point was also added hoping to capture patients with established AKI requiring RRT but before recovery occurred. Due to cost considerations, biomarkers were not analysed at the D1 timepoint.

4.2.1.7 Baseline creatinine:

Patients with stage 4 CKD or worse were excluded to avoid chronic kidney disease confounding acute changes in cortical perfusion. To determine CKD severity, baseline renal function was assessed from available creatinine measurements within the 24 months prior to ICU admission. If no suitable result was available, the patient was enrolled and baseline creatinine was assumed from the creatinine measurements following ICU discharge, assuming post-discharge creatinine would not be lower than the admission level. If no pre or post discharge creatinine levels were available, the lowest creatinine during admission was used in the absence of RRT, and failing that, the baseline function was marked as unknown.

4.2.1.8 Assessment of the renal microcirculation:

Renal ultrasound was performed using a Philips Affiniti ultrasound system (Philips, UK). Conventional grayscale US imaging was performed, image optimised and both kidneys visualized and length measured. Any patient with ultrasonographic evidence of CKD (bright or shrunken kidneys) was excluded and the most accessible kidney chosen to perform the study, provided both kidneys were sonographically normal. Baseline grayscale and colour Doppler sonographic images were acquired and the renal resistive index measured.

A low–mechanical index (MI) technique (range: 0.04 – 0.1) was utilised for DCE-US with MI set at or below 0.10. A dilute infusion of 20mL with 4.8mL of SonoVue^{TM} (Bracco SpA, Milan, Italy) contrast agent, was administered at 240mL/hr.

Images of the entire examination were digitally recorded. By 2min steady state was reliably

achieved and 5 high frequency pulses subsequently delivered, one every 30 sec until 4min.

Destruction-replenishment kinetics were quantified by post-processing, performed offline using VueBox™ (Bracco Diagnostic Imaging, Switzerland). Cortical regions lying in proximity to the probe with good views and reliably visible reperfusion were identified as regions of interest, the cortical mean transit time (CMTT), perfusion index (CPI), wash-in rate (CWIR) and relative blood volume (CRBV) were calculated. I collected all the data myself having received approximately 8 hours of further training in DCE-US acquisition and analysis from Dr Dean Huang an expert from within our Radiology department, I was already proficient in renal ultrasound prior to the study. The first patient enrolled in the study was undertaken jointly with Dr Huang. Further detail on the ultrasound technique and its development are described in the previous chapter.

4.2.1.9 Assessment of the systemic microcirculation:

Videos of the sublingual microcirculation were acquired using an Incident Dark Field video-microscope (Cytocam, Braedius Medical, Huizen, The Netherlands) using the technique described in General Methods. Images were blinded to the investigator, deidentified and batch-analysed offline using Automated Vascular Analysis software, (AVA) v 3.02 (Microvision Medical, Amsterdam, The Netherlands) as described in 2.4.2.3. Data collection and analysis was undertaken by myself and the Total Vessel density (TVD), Perfused Vessel Density (PVD), Microvascular Flow Index (MFI) and Microvascular Heterogeneity Index (MHI) were calculated. Data were extracted from the.txt output files produced by AVA into an excel

database using a program I created in Python.

4.2.1.10 Renal artery ultrasonography

Measurement of renal blood flow was made using the technique described in the technique development chapter, section 3.2.

4.2.1.11 Echocardiography:

Echocardiography was performed to quantify global haemodynamic status and a comprehensive echocardiogram undertaken to gather the minimum dataset required by the British Society of Echocardiography[350]. I am BSE certified in TTE. The echocardiogram along with vital signs and standard ICU monitoring was used to quantify macrocirculatory changes, cardiac output, cardiac index and calculated pulmonary artery pressures.

4.2.1.12 Blood and urine samples:

Biochemical analysis was undertaken at each time point. This included urine output and creatinine to quantify the stage of AKI using the KDIGO classification[351], laboratory variables were recorded to calculate a SOFA score and blood gas data for the assessment of tissue perfusion (ScvO2, SaO2, PaCO2, PvCO2, lactate etc). Plasma, serum and urine were centrifuged for 15 minutes at 4500rpm and stored at -80c for subsequent batch analysis by enzyme-linked immunosorbent assay. Urinary cell-cycle arrest regulatory proteins (tissue inhibitor of metalloproteinases-2 (TIMP2) and insulin like growth factor binding protein – 7 (IGFBP7)) were quantified. Urinary neutrophil gelatinase associated lipocalin (uNGAL) levels were quantified was was urinary albumin (uAlb). The data from these were analysed together and in isolation. TIMP2*IGFBP7 and uNGAL*uAlb were used to quantify tubular injury.

Proenkephalin-A (PENK) was used as an additional marker of filtration. Chemokine ligand-14 which may predict long term renal injury was also measured. For more detail on the specific biomarkers see section 2.2. These biomarkers were selected after taking advice from Dr Nick Selby (Derby, UK) and Dr Kate Bramham (KCL/KCH, London, UK).

Vascular inflammatory profiles were quantified by assessing syndecan-1 and AKI subphenotypes were identified using a triple analysis of angiopoietin 2 to 1 (ang2to1) ratio, interleukin-8 (IL8) and soluble tumour necrosis factor alpha (TNFR) levels as previously described by Bhatraju and colleagues[234].

The urinary creatinine level was measured and both normalised (biomarker divided by urinary creatinine) and non-normalised values reported. Biomarkers were measured at admission, after 48 hours and 96 hours. Biomarkers were omitted from the day one (24hr) timepoint after cost considerations.

4.2.1.13 Patient and Public Involvement:

The research questions and aims are developed from published research priorities by relevant charities and national organisations. The question was advanced and consulted with the Kings College Hospital Renal Patient and Public Involvement Engagement group who highlighted the perceived need for the study and found it to be important and interesting. They found the risk profile to patients to be acceptable and were supportive of its undertaking. Changes were made to the protocol and patient facing documentation based on the feedback we

received from this group.

4.2.1.14 Patient identification capacity and consent:

A process of personal consultee was used in patients without capacity and personal consent was sought retrospectively.

4.2.1.15 Confidentiality, data storage and security:

The studied complied with the principles of the Data Protection Act, 2018. All retained data were de-identified and all physical data, such as Clinical Report Forms & Consent Forms securely stored in a locked research office. All electronic data was maintained on a secure electronic database accessible only by members of the research team.

4.2.1.16 Ethical approval:

Research Ethics Committee (REC) approval was granted by Yorkshire and the Humber, Leeds West Research Ethics Committee (18/YH/0371).

4.2.1.17 Statistical analysis:

Continuous data were examined for normality using the Shapiro Wilk test and parametric data reported as mean ± 1 standard deviation and compared using non-paired t-tests. Non-parametric data is reported as median and inter-quartile range and compared using the Wilcoxon rank-sum test. Ordinal data was reported as number and percentage and compared using the Chi-squared test. Longitudinal data was compared between individual days using regression analysis, Pearson's correlation coefficient and significance. Data was normalised

by log transformation, square root or Cox-Box transformation where log-transform was unsuccessful. All data was assessed using R version 4.0.3 with appropriately installed packages. R was used to generate all graphical data, receiver operator curves and survival probability plots. All p-values were two-sided and considered significant at <0.05.

5 Time-based variables appear superior to intensity-based variables: a comparison using patient data

5.1 Introduction and method

The four DCE-US variables generated from destruction replenishment kinetics describe both the rate of reperfusion and the maximal signal generated following reperfusion. MTT is a time-based variable – half the time to maximal signal return, RBV provides the maximal signal, WIR the gradient and PI the RBV/MTT. It is unclear how these variables relate to each other in practice and which variables are most representative of perfusion. Correlations were therefore sought between the individual variables to assess this interrelationship. As a gold standard comparator was not available, values and distributions were compared to controls, who were assumed to have normal perfusion.

To fully describe the dataset in subsequent chapters, comparisons directly with perfusion are necessary, rather than with AKI. The study population was therefore regrouped to those with better or worse renal perfusion, the generation of this new grouping variable is described in the second part of this chapter. The use of two grouping variables – AKI and perfusion allow a greater comparison and understanding of the data in subsequent analyses. Those changes associated with AKI in its broader form could therefore be compared to those more specifically related to renal hypoperfusion.

5.2 Results

5.2.1 Correlation between individual variables

Correlation coefficients for the four DCE-US variables taken from all observations in the study (n=190) are presented in Figure 23.

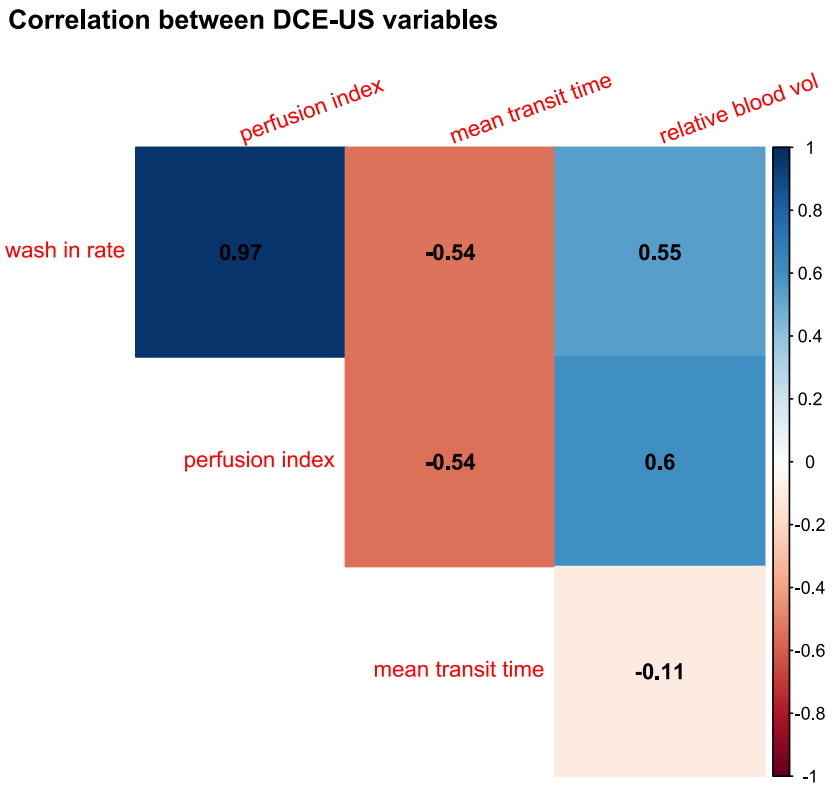

Figure 23 Correlation coefficients of the DCE-US parameters.

Comparisons of the DCE-US variables between the patient population and controls are provided in Figure 24. Density plots display the shape of the distribution similar to a histogram.

MTT is highly skewed in patients, but control values had a normal distribution, lower than patients. The opposite is true of RBV where both patients and controls are parametric and median control data overlaps closely with median patient data. PI and WIR are both positively

skewed and median values lower in patients than controls.

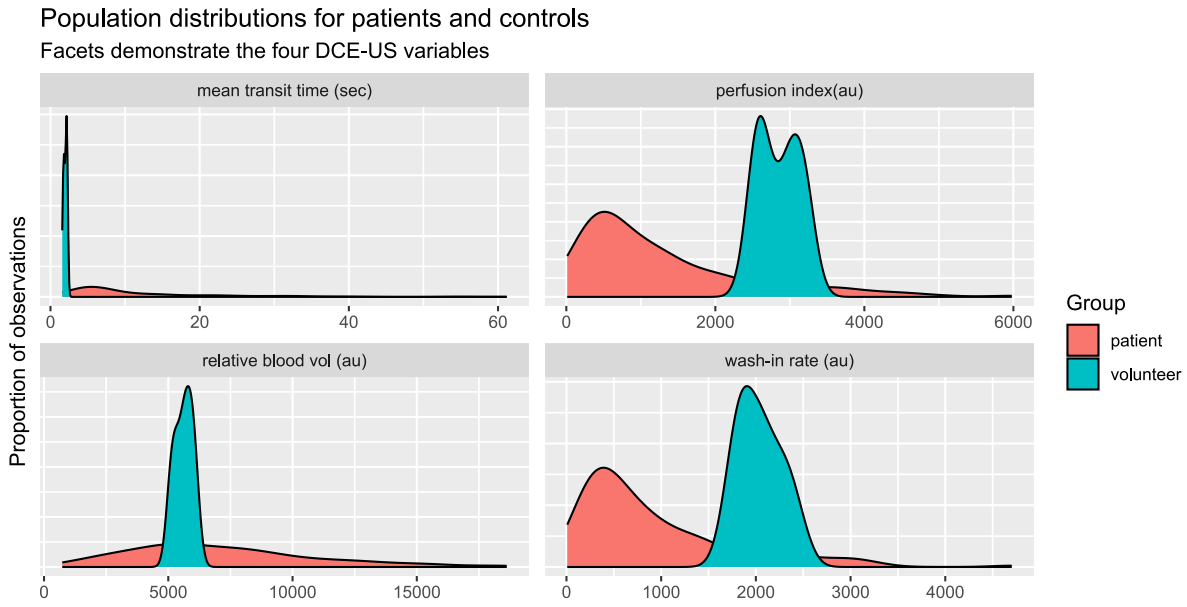

Figure 24 population distributions for patients (red) and controls (blue) for variables generated by DCE-US

5.2.2 Generating a new grouping variable: High and low perfusors

To dichotomise the patients into perfusion groups, a combination of perfusion index and mean transit time were selected as WIR and PI were near identical (correlation coefficient 0.97 – see above) and RBV appeared less robust, with significant overlap between patients and controls in Figure 24.

Cut-off thresholds were assigned using the day zero median perfusion index and mean transit time (perfusion index >713 & mean transit time <7.25s assigned as “high perfusors”, else “low perfusors”), to generate two equal size perfusion groups and the control data (high perfusion group n=24, low perfusion group n=25). Figure 25 and Figure 26 demonstrate these groupings.

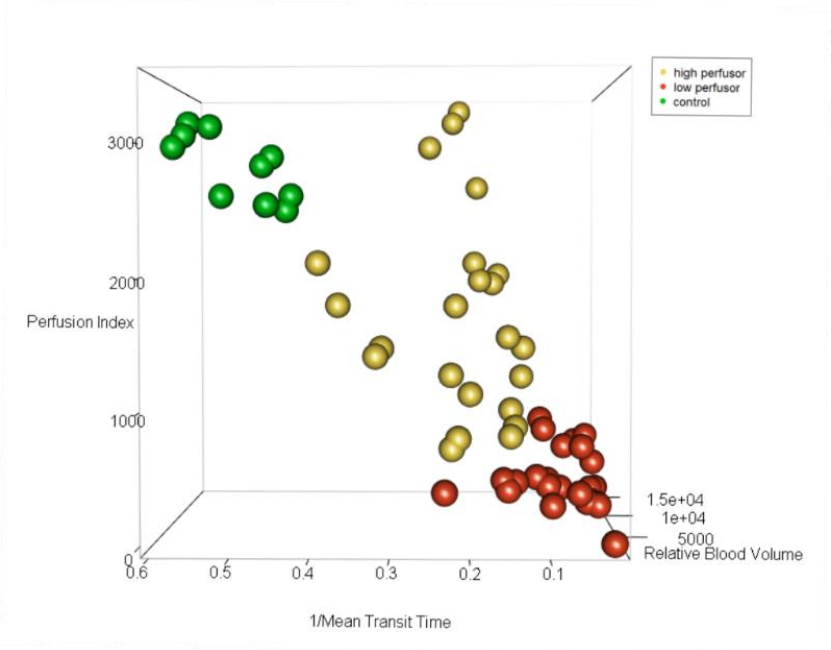

Figure 25 3D correlation plot of day 0 observations, perfusion index, 1/mean transit time, relative blood volume. Colour groupings: green = controls, yellow = high perfusors, red = low perfusors

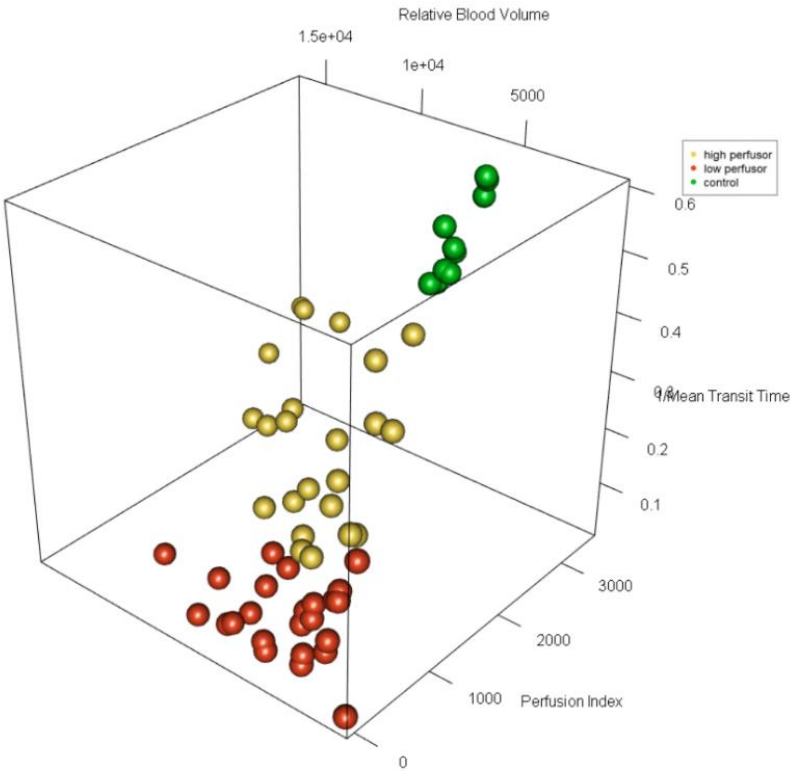

Figure 26 3D correlation plot, rotated from Figure 25

5.3 Discussion

The role of DCE-US in critical illness is novel, the control data from chapter 3 helped provide a reference from which the abnormal could be assessed and provided baseline values from which the four DCE-US variables could be compared, aiding an understanding of their individual characteristics. The addition of patient data from the Microshock Renal study to controls provided additional datapoints. Perfusion index and wash-in rate demonstrate extreme collinearity (R=0.97). RBV represents the maximum signal after reperfusion and is used to calculate WIR and PI, as such a correlation of 0.55 and 0.6 respectively exists between these three variables. mTT reflects half the time to maximum signal and demonstrates no significant relationship to RBV, it does demonstrate a reasonable correlation with WIR and PI.

The intensity based variable RBV appeared to be inferior to the other variables and has previously performed poorly in reliability studies, with significant intra and inter-individual variability[112], these are discussed further in General Methods. In the present study, RBV was the only one to demonstrate a parametric distribution, a different distribution to the remaining variables. It was the only variable where healthy control data centred closely to the mean patient value, and if controls are assumed to have better perfusion than patients, which the other variables suggest, then RBV is largely non-discriminatory. It is also concerning that RBV and MTT were not correlated, although strictly RBV represents red cell density whilst MTT provides a measure of velocity[120]. It is possible that RBV represents a measurement comparable to that of total vessel density measured with handheld video microscopy – described in 2.4.2.4. TVD is a measure of red cell density within a tissue bed, proportional to the capillary density and analogous to the bubble concentration quantified by RBV. As TVD in health represents the anatomical density of vessels within a tissue bed[328], only after sufficient

reduction in capillary segment flow does it become abnormal, or in the case of DCE-US, those with more severe reductions in renal perfusion.

Perfusion index and wash-in rate demonstrate extreme collinearity and one variable would therefore suffice in future studies as they are essentially the same, the calculation of PI is made by the RBV (maximum signal) divided by the mean transit time (half time to max signal) – two components necessary to describe a gradient, whilst WIR measures the actual gradient[114].

Mean transit time is less dependent on factors such as organ depth and gain settings, as demonstrated in a laboratory model by Averkiou et al[112]. In the present study, MTT values were lowest in healthy controls where values were tightly grouped, whereas patients had much greater dispersion and positive skewness.

Unfortunately there is no gold standard comparator to which these variables can be compared in clinical studies. This would have provided greater insight and only limited conclusions can be reached about which values best represent blood flow within the microvasculature of the renal cortex. Comparison with controls informs this assessment but remains inferior to a theoretical gold-standard comparator.

6 Patients with severe AKI have higher vasopressor requirements and a higher burden of organ failure: Descriptive and Demographic Results of the Microshock Renal Study

6.1 Introduction

The extremes of age are particularly vulnerable to AKI and are also more susceptible to infectious disease and sepsis. CKD reveals a close linear correlation with risk of AKI, AKI non-recovery and mortality[352]. Pre-existing proteinuric patients are more at risk of AKI and new proteinuria can be used as a potential biomarker for AKI[218]. Other non-modifiable risk factors include being male, of black race, hypertension, diabetes, malignancy and other chronic organ impairments including disease of the cardiac, hepatic, pulmonary and vascular systems[12].

This chapter examines the baseline demographic data between those who developed AKI and those who did not, to identify if any baseline differences in such risk factors existed between the two patient cohorts. The severe AKI group was also subdivided into those with CKD stage 2 or greater and those without and their admission renal perfusion values were compared (CKD stage 4 or greater were excluded). If differences in renal perfusion were detected during the study it was important to determine if these changes were acute or confounded by pre-existing CKD.

6.2 Results

52 patients were recruited during the period between November 2018 and July 2021. The recruitment window was extended due to the COVID-19 pandemic and the associated

difficulties in undertaking clinical research. The initial patient was later excluded as the images were of insufficient quality. Of the remaining 51, one further patient withheld retrospective consent.

37 (74%) patients developed stage 3 AKI, all of which were defined by the commencement of RRT. There were no patients with stage 3 AKI who did not receive RRT in this study of sequential patients. The decision to deliver RRT was independent of the study and remained the responsibility of the clinical team.

There was no difference in preadmission baseline creatinine values between patients who developed and did not develop severe AKI (67.4umol/L±22.1 vs 62.5umol/L ±17, P=0.42).

Admission urinary albumin values were significantly higher within 24 hours of admission in those with severe AKI (119(59-391)mg/dl vs 50(28-134)mg/dl; $p<0.05$).

38% of the severe group were female and 39% of the non-severe group. By comparison 58% of healthy controls described in Chapter 3 were female although not significantly different to the patient groups (p=0.56). The mean age of patients was 61 years but 33 in controls ($p<0.0001$). The mean age of patients with severe AKI was 60±17, and 66±8 in the non-severe group (p=0.11). As presented in Figure 27, there was no difference between the causative organism, the site of infection or comorbidities between the two patient groups (p=0.34, p= 0.28, p=0.31 respectively). 23% of the AKI group were black but none of those without severe AKI (p=0.26).

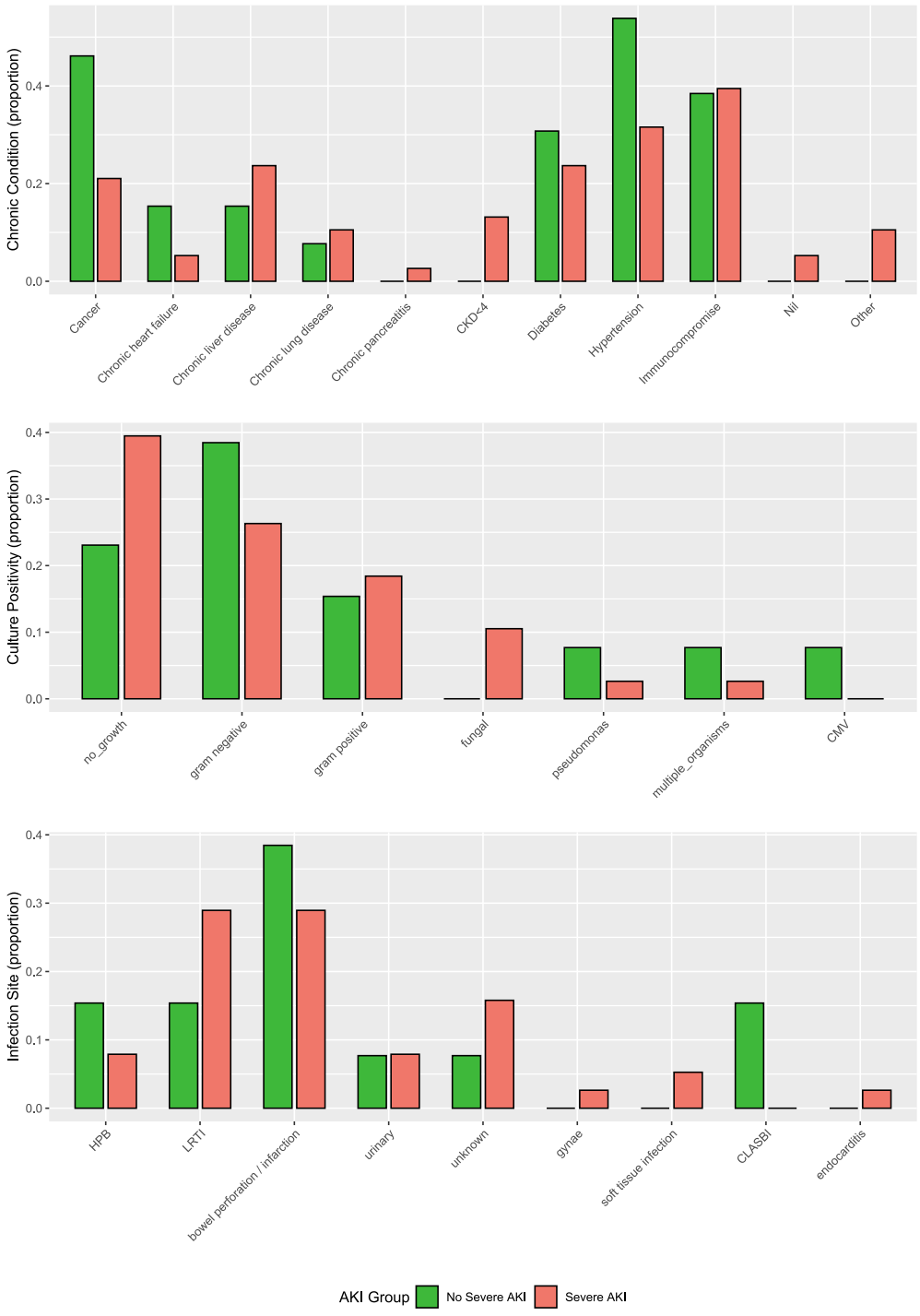

Figure 27: Descriptive data for the Severe and Non-severe AKI groups. Top graph provides proportions for comorbidities; middle graph provides proportions for microbiology culture positivity and bottom the infection site, again as a proportion of the sample size

After adjustment for renal injury, the SOFA score was higher on admission in patients with severe AKI (11.3±3.28 vs 9.3±1.9, $p<0.05$). Patients with severe AKI had higher noradrenaline doses and were on a second inotrope more frequently, see Table 4, this finding is more closely

examined in chapter 8.

Day	Severe AKI noradrenaline dose (mcg/kg/min)	No severe AKI noradrenaline dose (mcg/kg/min)	Significance (p)	Severe AKI on second inotrope (%)	No-severe AKI on second inotrope (%)	Significance (p)
0	0.35(0.26-0.51)	0.21(0.14-0.3)	<0.001	50	8	<0.05
1	0.24(0.08-0.43)	0.06(0-0.11)	<0.001	34	0	<0.05
2	0.11(0.01-0.26)	0(0-0.05)	<0.001	26	0	0.09
4	0(0-0.06)	0	<0.05	8	0	0.68

Table 4 Noradrenaline doses and presence of a second inotrope, by day and between groups

In the severe AKI group admission CEUS variables were not significantly different between those with and without CKD, see Figure 28. Baseline creatinine values were used to calculate eGFR prior to admission using the CKD-EPI equation[353]. Normal or stage 1 CKD (n=20) and CKD2 or greater (n=15), baseline creatinine values were not available for 2 patients.

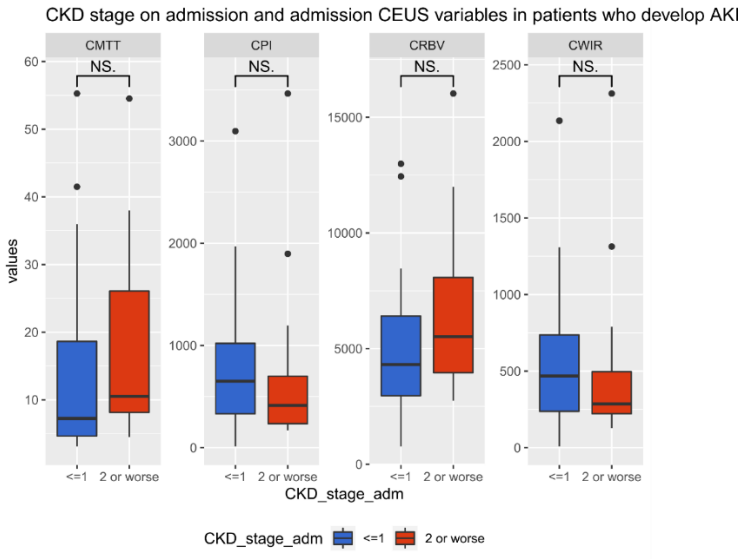

Figure 28 CKD stage on admission and admission DCE-US variables. Cortical mean transit time (CMTT), cortical perfusion index (CPI), cortical relative blood volume (CRBV), cortical wash-in rate (CWIR).

6.3 Discussion

The two most striking differences between the cohorts were sickness severity and higher inotrope requirements in the severe AKI group. The presence of an additional vasopressor was also more common. Noradrenaline has direct renal interactions, increasing renovascular resistance through alpha-1 mediated vasoconstriction. Noradrenaline also increases perfusion pressure by increasing the systemic blood pressure, but due to renal autoregulation the renovascular bed increases resistance through a myogenically triggered vasoconstrictor response, maintaining flow within a set range[354]. The interaction between these two factors depends on sickness severity, becoming more linearised in sepsis and also the previous set autoregulatory range from chronic changes in blood pressure[162], chronic hypertension rates were similar between groups. Higher use of noradrenaline in patients with AKI in this study likely demonstrates the association with sickness severity, but being vasoactive may alter renal perfusion directly and may confound the later analysis, this is described further in chapter 8. Previous concerns regarding the use of noradrenaline and its association with AKI are considered unfounded [355].

There were no discernible differences in causative organism, site of infection, or pre-existing CKD. Patients with pre-existing chronic disease are frequently exposed to multiple modifiable risk factors, such as antibiotics and contrast agents, dehydration and major surgery and have a greater risk of sepsis[25], but there was no difference in these cohorts, although the cohorts are relatively small and accepting this was not designed to be an epidemiological study. The risks of AKI are compounded by chronic risk factors; modifiable factors such as these become risk-multipliers in already at-risk groups[21].

There were no differences in age between the two groups, which is important as age-related nephron loss reduces the resilience of the elderly kidney to injury by lowering the renal reserve[356].

Proteinuria is a marker of ineffective filtration due to GBM disruption and a marker of proximal tubular dysfunction, unable to retain this 70kDa anion. Proteinuria is an independent risk factor, regardless of baseline GFR and can be used as a predictive factor to highlight at risk groups prior to a known insult such as surgery, iodinated contrast or chemotherapy[218,352,357]. The patients who developed severe AKI had a higher degree of proteinuria within 24 hours of admission than those who did not, although this could well be due to the presence of severe AKI alone. Preadmission values would be advantageous, although impossible to achieve in sepsis studies.

In summary, the patient cohorts were similar, but notable exceptions include higher inotrope doses and a greater degree of multiorgan impairment in the severe AKI group.

7 Patients with more severe cortical hypoperfusion have more severe AKI: Alterations in the renal *micro*vasculature in sepsis associated AKI

7.1 Introduction

The kidney has a unique vascular structure with multiple connections for homeostatic effector loops to interact, maintaining adequate tissue oxygenation despite alterations in RBF. This also permits the opposite effect however, maintenance of RBF despite alterations in cortical perfusion. Indeed there is experimental data to suggest such changes are fundamental to AKI development in sepsis but much of this data is conflicting[342], with large animal and small animal studies demonstrating opposite results and even within large animal studies the evidence is mixed. Alterations in microvascular perfusion in humans with septic shock is largely inferred from experimental data and to what degree any changes contribute to the development of AKI is unknown. In a small pilot study using CEUS in human septic shock, cortical hypoperfusion occurred early and improved over time[82]. No other clinical study has attempted to assess renal tissue perfusion in sepsis including a detailed MRI study in humans by Prowle and Bellomo in 2012 which assessed RBF[358].

This chapter examines the primary outcome of the main study, whether alterations in renal cortical perfusion occur as a component of AKI development in humans who develop septic shock.

7.2 Results

As presented in Figure 29, cortical perfusion was reduced on admission in patients who developed severe AKI. Mean transit time was signficantly prolonged – longer mTTs being reflective of worse perfusion (severe 10.2(6.5-23)sec vs non-severe 5.5(4.6-6.5)sec, $p<0.005$), whilst the perfusion index, wash-in rate and relative blood volume were reduced, again indicative of worse perfusion: PI severe: 485 (302-829)au vs non-severe: 1757 (1126-2100)au, $p<0.0005$; WiR severe: 408(238-606)au vs non-severe: 1203(790-1489)au, $p<0.005$; RBV severe: 5123(3604-7209)au vs non-severe: 8538(5659-11030)au, $p<0.05$.

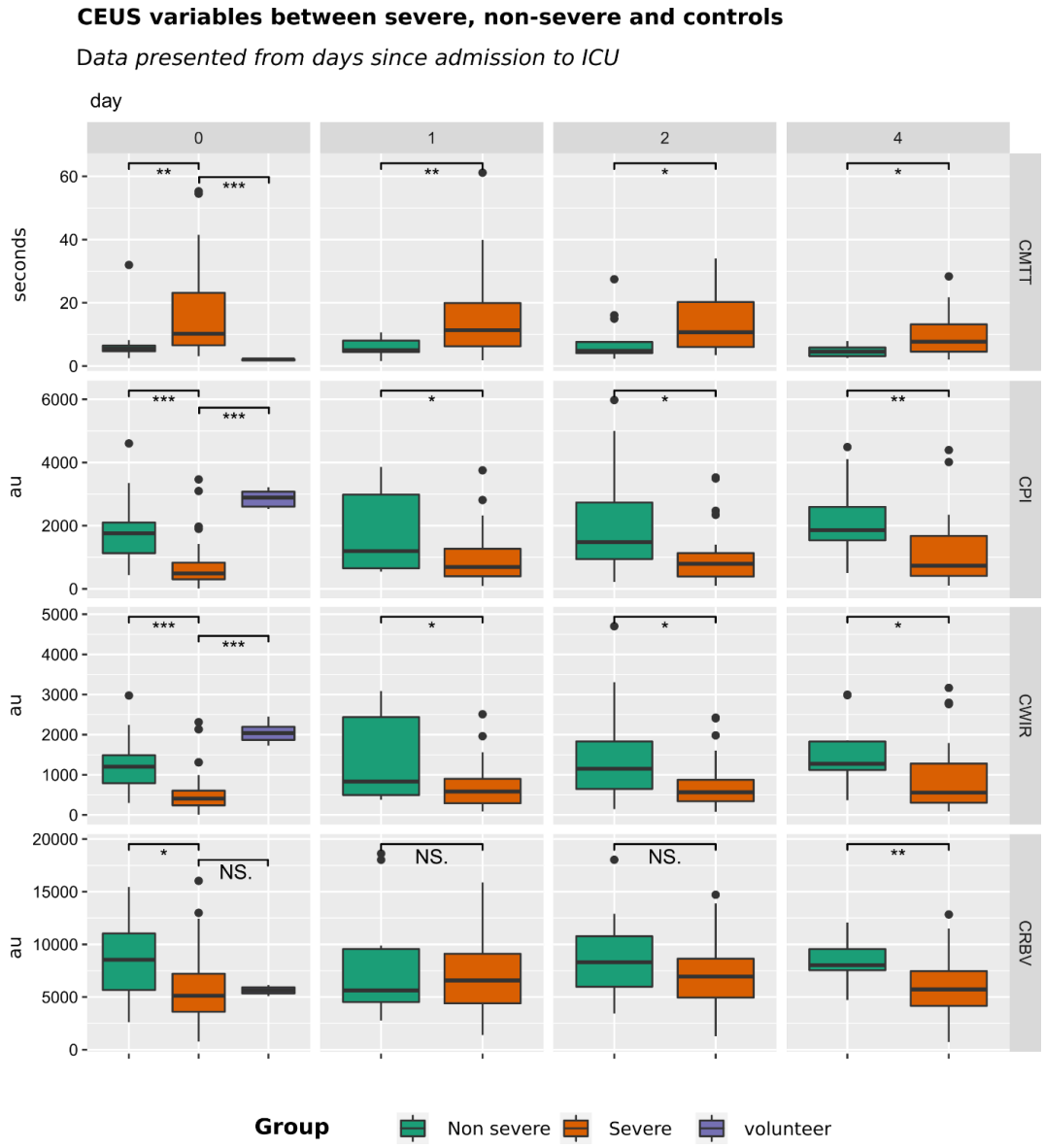

Figure 29 Differences in renal perfusion variables between severe, non-severe and control groups over time. (CMTT: cortical mean transit time; CPI: cortical perfusion index; CRBV: cortical relative blood volume; CWIR: cortical wash-in rate). Significant perfusion differences are demonstrated between controls and patients and between patient groups over time.

Table 5 demonstrate how this reduced perfusion persisted for the the majority of the study duration. Using a mixed effects logistic regression to assess changes over time, a slight improvement in the mean transit time and wash-in rate were demonstrated by day 4 in the severe AKI group, suggesting that hypoperfusion occurs early and is slow to improve.

	Day 0	Day 1	Day 2	Day 4	P value
	5.5(4.7-6.5)	5.0(4.4-8.1)	4.8(4.1-7.6)	4.6(3.1-5.9)	0.2

Mean transit time (sec)	10.2(6.5-23.2)	11.3(6.24-19.9)	10.7(6.0-20.2)	7.7(4.5-13.2)	**<0.05**
Perfusion index (a.u.)	1758(1126-2100)	1193(649-2983)	1479(942-2743)	1856(1538-2595)	0.6
	485(302-829)	690(396-1266)	791(390-1130)	732(410-1676)	0.07
RBV (a.u.)	8538(5659-11030)	5630(4523-9558)	8308(5978-10770)	8025(7549-9553)	0.7
	5123(3604-7209)	6572(4397-9102)	6940(4950-8642)	5722(4155-7463)	0.9
Wash-in rate(a.u.)	1203(790-1489)	833(496-2438)	1152(649-1830)	1274(1119-1829)	0.5
	409(238-606)	583(291-899)	565(342-876)	558(304-1278)	**<0.05**

Table 5 Longitudinal perfusion data from day 1 through day 4. Severe AKI group is presented in orange and non-severe in green. Changes over time are assessed by mixed effects logistic regression and significance reported in the right-hand column. Improvement is seen in the mean transit time and wash-in rate of the severe group.

7.2.1 Differences between individual stages of AKI

Figure 30 provides an analysis of the most severe AKI stage which developed following admission and the DCE-US perfusion assessment on day 0. Individual cohort population sizes are small and under-powered; it may however provide useful pilot data for future studies.

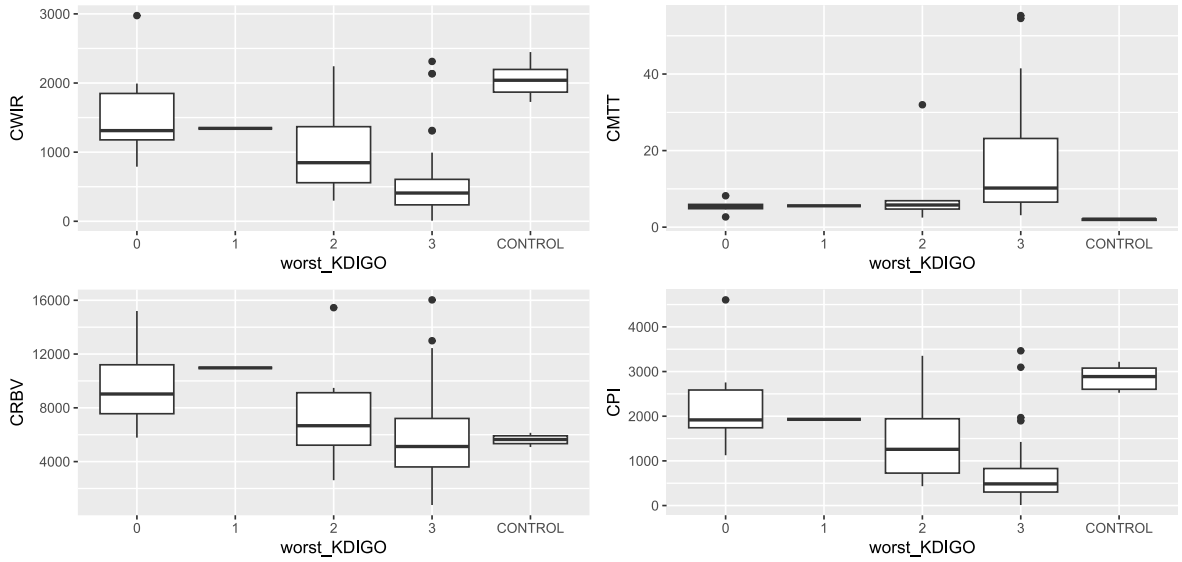

Figure 30 Perfusion variables on admission and the most severe stage of AKI that developed during ICU stay (worst KDIGO). CWIR: cortical wash-in rate; CMTT: cortical mean transit time; CRBV: cortical relative blood volume; CPI: cortical perfusion index. (n=6 stage-0, 1 stage-1, 6 stage-2, 38 stage-3, 12 controls).

7.3 Discussion

The principal finding of both this chapter and this study is that patients who develop severe AKI have significantly reduced renal perfusion on admission, but more surprising is that all patients with septic shock demonstrate some degree of cortical hypoperfusion when compared to controls regardless of whether they develop AKI or not and this is a new finding.

It also appears to be proportional to the severity of injury with a stepwise reduction in perfusion between AKI severity stages. This reduced perfusion is immediate and persistent; indeed it is more persistent than global perfusion abnormalities – described in chapter 9. Importantly perfusion abnormalities were identified in all, only to a greater degree in those with stage 3 AKI.

Blood is distributed through the segmental, lobular and arcuate vascular network to supply the cortex. Medullary supply is post-glomerular from some but not all efferent arterioles, taking only 20% of total flow in healthy conditions but an increasing proportion in pre-renal azotaemia[359]. Multiple previous experimental studies concur with the present study demonstrating a rapid reduction in cortical perfusion in sepsis with an increase in heterogeneity of the cortical microcirculation[323,360,361]. Not all studies support this concept however, Calzavacca et al implanted combined laser-doppler flowmetry and tissue oxygenation probes in sheep, both in the cortex and medulla and infused *Escherichia coli* over 24 hours. RBF increased significantly on induction of sepsis and slowly reduced again with treatment as did renal vascular resistance. Cortical tissue perfusion was maintained in this model, whereas medullary perfusion and oxygenation decreased rapidly[348]. Laser doppler flowmetry is unable to select the microvasculature and therefore may have been unable to identify certain changes[362], but generally the methodology was sound. Although the preservation of perfusion in the sheep cortex conflicts with the findings in humans presented here, both demonstrate a redistribution of intrarenal blood flow under septic conditions. Cavelcazza's findings are not definitive however as several other animal models have shown different responses in renal perfusion, many in support of cortical hypoperfusion[47,323,347,363,364]. A limitation of CEUS is that it is unable to quantify medullary

perfusion because of the complex vascular arrangement, further work is necessary to determine if this is possible after development of the technique.

Flow redistribution is made possible by peri-glomerular shunts between interlobular vessels demonstrated by Schurek et al in the rat cortex[365], see Figure 31. Such shunts would allow RBF to be maintained whilst reducing GFR, cortical and medullary perfusion. The recruitment of shunts particularly during injury and repair would reduce TEC exposure to reactive oxygen species and active sodium transport necessary for filtrate reabsorption at a time of stress[366367]. Non-anatomical shunts have also been suggested as potential mechanisms for changes in oxygenation. The proximity and parallel nature of arterioles to venules within the medulla may permit a diffusive shunt from one to the other, reducing the capillary pO2 in the process. Such a diffusive shunt is unlikely to be wholly accountable for such changes however, as in the present study bubble concentration is reduced which is reliably reflective of RBC density and flow[120] and demonstrates a true reduction in blood volume within the tissue rather than oxygenation alone. The heterogeneity of microcirculatory flow common to capillary beds is a further type of shunt, capillaries with normal flow, allow capillaries with reduced flow to be bypassed, allowing heterogenous regions of perfusion to coexist, hypoperfusion alongside normal flow, this remains a possibility based on the present data. Lastly an oxygen off-loading shunt has been suggested where oxyhaemaglobin is unable to release its oxygen molecule[48] but there is a lack of evidence to support this as hypoxic acidotic environments typically increase oxygen dissociation and blood flow is reduced on DCE-US assessment. In essence, if shunting is the cause of the observed changes, the data presented here makes an anatomical shunt by far

the most likely of the mechanisms suggested.

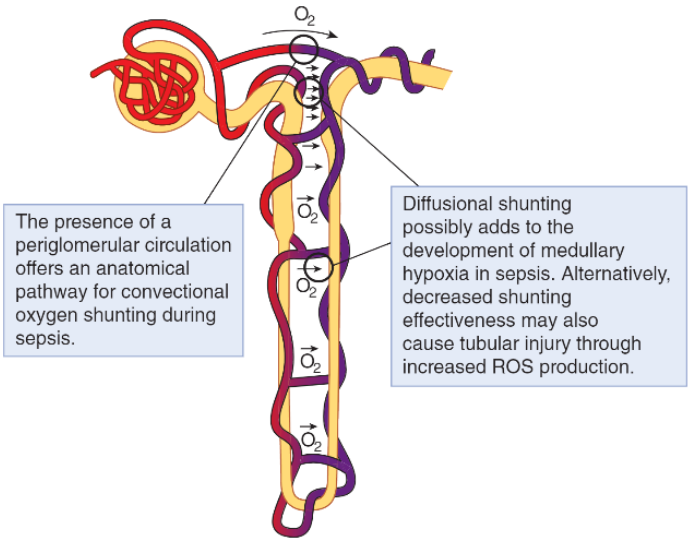

Figure 31 taken from Post et al. [340]. Diagram illustrating the presence of peritubular arterio-venous shunts which may facilitate the maintenance of normal RBF whilst permitting a reduction in GFR.

Individual microcirculatory alterations were heterogenous in the present study; patients with sepsis associated AKI did not follow a distinct perfusion pattern from injury through to recovery as may be expected with a single insult. Some demonstrated improved perfusion whilst others the converse, with significant inter-individual variation and the inter- and intraindividual biomarker values were also variable over time – described in chapter 12. Such variation has previously been suggested in animal models[323,361]. Human septic shock is more protracted and convoluted than experimental, patients do not follow a distinct pathway and potentially it is the variation from clinical instability that accounts for this heterogeneity. An alternative but speculative explanation for this inter-individual variation within the same phenotype is epigenetic and genetic factors, certainly there is emerging evidence for these factors in the broader context of AKI development, where given the same insult, there is a

variation in response across the population in question[368–370].

The individual perfusion variables had different responses to AKI development. MTT values were lowest in healthy controls, elevated in patients who did not develop severe AKI and most elevated in those who did. In the analysis of DCE-US variables by individual AKI stages, it was not until stage 3 AKI that MTT got much longer. This contrasts with the other variables which showed a stepwise reduction in perfusion with each AKI stage. These stage-by-stage observations are underpowered however and more data is needed to confirm this. Another observation is that non-severe patients demonstrated limited data dispersion for MTT, but the variation within the severe group was far more apparent, the IQR for stage 3 being seven times larger than the other stages. Such a range of MTT values in this group could be because hypoperfusion and AKI severity do not have a linear correlation, or because within stage 3 there is still a wide-ranging severity of pathophysiological change masked by using discrete groupings. Afterall, the staging system of AKI has no biological basis, but divides up a continuum of severity based on phenotypes. It is a clinical construct rather than a pathological one.

The principal findings of this chapter are that renal hypoperfusion occurs immediately in all patients who develop septic shock and are proportional to the clinical AKI severity, including noticeable reductions in perfusion in those without clinical AKI. Hypoperfusion is persistent, with only mild improvement by day 4 in those with severe AKI. Such changes are possible due to the unique microvasculature of the kidney and this data supports the hypothesis of

recruitable shunting mechanisms which may underlie the adaptive response.

7.3.1 Nitric oxide and its role in regulation of perfusion

A description of the microcirculatory alterations would not be comprehensive without a discussion on the mechanisms of regulation. Nitric oxide (NO) dysregulation is a key feature of the endothelial and microcirculatory dysfunction of sepsis associated AKI. The powerful locally-acting vasodilator NO is produced by endothelial nitric oxide synthase, and the inducible isoform (iNOS). iNOS in contradiction to its name, is constitutively expressed in proximal tubular cells but upregulates rapidly following cytokine activation[371]. NO causes systemic vasodilatation with subsequent sympathetic activation and angiotensin mediated intrarenal vasoconstriction reducing GFR[372]. Renal iNOS is produced predominately by TECs and vascular endothelium[373–375]. The NO produced has multiple actions in the maintenance of the microcirculation, including regulating vascular tone and permeability, leucocyte adhesion, platelet aggregation and microthrombi formation[376]. Multiple studies in the 1990s demonstrated that non-selective NOS blockade was harmful to perfusion and increased leucocyte adhesion and platelet activation[363,377–380]. Attempts to administer exogenous NO were subsequently made noting an improvement in these parameters[381–383].

NO has a feedback inhibitory effect on eNOS but not iNOS and as a result iNOS expression paradoxically results in eNOS suppression, removing the feedback to endogenous vasoconstrictor inhibition, making vessels less able to dilate and more susceptible to shear stress[384]. Increased iNOS expression correlates with regions of tubular injury and apoptosis and selective inhibition of iNOS reduces the injury, suggesting a fundamental role in the

microcirculatory impairment of sepsis associated AKI[385]. iNOS expression is heterogenous within the kidney and may contribute to the heterogeneity of perfusion seen in tissue beds and the focal histological lesions identified[376]. Together these findings led to the hypothesis that background NO is beneficial for the kidney, but the excessive levels produced by iNOS may account for alterations in perfusion. Whilst non-selective NOS blockade was harmful, selective iNOS blockade has demonstrated improvements in GFR and RBF in multiple animal studies[386–390]. The differential expression of iNOS, present in the cortex but less so in the medulla, may permit preferential cortical shunting, favouring vasodilated cortical flow over the resistance of medullary capillaries[42].

8 Cortical hypoperfusion is not associated with cardiac output, renal blood flow or markers of venous hypertension: Alterations in the renal and systemic *macro*vasculature

8.1 Introduction

"For the development of the science of circulation it was fateful that it is comparatively so awkward to measure flow, yet so easy to measure pressure: this is why the blood pressure manometer gained almost fascinating influence, while most organs do not require pressure, but flow volume"[391]

A. Jarisch 1928

Sepsis associated AKI was once considered a result of hypotension, reduced cardiac output, renal hypoperfusion and ischaemic tubular injury but has been challenged through a body of recent evidence. Whilst septic shock does present with features of circulatory failure, early restoration of blood pressure does not prevent severe AKI or multiorgan failure. Likewise, patients who are not septic but present in cardiac arrest infrequently develop severe or protracted AKI and therefore sepsis delivers an additional insult, beyond that of reduced flow[37].

That is not to diminish the role of adequate perfusion pressure and flow but to note an additional contribution, observational data suggest that sepsis coupled with hypotension is a precipitant of AKI, but it is not the entire picture. Mean arterial pressures maintained

consistently above 70-72mmHg are most protective, with no additional benefit >80mmHg[392–394]. Manipulation of blood pressure to mean targets of 80-85mmHg reduced the incidence of chronic hypertensives requiring RRT in comparison to MAP targets of 60mmHg[395], although MAP targets of 60 and 65mmHg produce equivalent renal outcomes in older patients[396].

Pressure and flow are not synonymous as resistance needs to be considered. In septic conditions whole-organ renal blood flow is controversial according to multiple authors who have spent many years developing animal models to study it[340]. Ovine models have previously demonstrated increased, decreased and unaltered renal perfusion in response to sepsis, however the later models have tended toward an increase[343,344,346,397,398]. Studies in sheep and pigs have shown intrarenal vasoconstriction and flow redistribution to other organs[399]. In humans with sepsis, a condition characterised by distributive abnormalities and vasoplegia, autoregulation is impaired and the pressure-flow relationship becomes more linearised[400]. Redfors invasively demonstrated a reduction in autoregulatory mechanisms in post operative patients and below a mean arterial pressure of 75mmHg autoregulation was lost[162], although no human data in sepsis exists.

This section examines renal blood flow and cortical perfusion to investigate whether renal hypoperfusion is secondary, captive to alterations in systemic flow. The systemic data is divided into observations of left heart function and cardiac output, whilst the right heart function is considered along with venous pressures and congestion assessment. Renal

macrovascular data is assessed later in the chapter.

8.2 Results

8.2.1 Right heart function and venous congestion

8.2.1.1 AKI groups

Table 6 demonstrates that in severe AKI central venous pressures tended to be higher and BNP levels were higher throughout. Pulmonary artery pressures were higher in severe AKI, likely secondary to more difficult ventilation in this group, but there was no reduction in right ventricular function, with no difference between both right ventricular S prime velocity and TAPSE.

Variable	Day	No severe AKI	Severe AKI	Significance (p)
Fluid balance				
24 hr fluid balance (ml)	0	3200(1500-4300)	1900(1500-3500)	0.58
	1	1000(210-1800)	1000(420-2600)	0.6
	2	200(-450-1300)	870(380-2400)	0.086
	4	300+-1300	450-1326	0.5
Fluid balance from admission (ml)	0	3200(1500-4900)	2200(1500-4000)	0.71
	1	3400(2200-5700)	4600(2200-6800)	0.5
	2	4900+-2900	6400+-5100	0.21
	4	6000+-4000	6100+-4900	0.98
Right atrium pressure assessment				
Right atrial pressure (echo) (mmH2O)	0	12(7.5-18)	12(12-12)	0.86
	1	12(12-20)	12(12-12)	0.44
	2	12(8.8-12)	12(12-18)	0.31
	4	12(2.5-12)	12(12-12)	0.072
CVP (mmH2O)	0	10+-4.3	13+-5.6	0.1
	1	11+-5.9	12+-4.8	0.73
	2	8.9+-4.6	13+-5.4	**<0.05**
	4	8.7+-3.1	13+-4.8	**<0.05**
BNP (ng/ml)	0	4700(1100-6900)	7900(3400-26000)	**<0.05**
	2	2000(1300-3900)	8900(3200-21000)	**<0.05**
	4	2400(1100-3000)	5700(2800-14000)	**<0.05**
Pulmonary pressure				
Pulmonary artery systolic pressure	0	36(28-41)	36(28-48)	0.5
	1	32(28-38)	38(32-46)	0.085
	2	34+-6.8	40+-16	0.18
	4	32+-10	41+-15	0.067
Pulmonary acceleration time (msec)	0	100+-29	110+-25	0.28
	1	120+-37	120+-30	0.81
	2	120+-33	120+-24	0.74
	4	130+-22	120+-36	0.35
Right heart function				
RV s' (cm/sec)	0	18+-9.8	17+-5.7	0.7
	1	15(14-17)	16(13-20)	0.5
	2	13+-4.6	17+-4.7	0.057
	4	15+-3.9	17+-4.4	0.13
TAPSE (cm)	0	2+-0.33	1.9+-0.6	0.53
	1	2.4+-0.5	2.2+-0.55	0.26
	2	2.1(1.8-2.4)	2.4(1.9-2.7)	0.26
	4	2.2+-0.41	2.2+-0.47	0.91

Table 6 Assessments of right heart function and venous congestion. Fluid balance, atrial pressure, ventilatory pressures, pulmonary pressures and right heart function are given individual sections. Data are presented by AKI group and by day

8.2.1.2 Perfusion groups

Table 7 demonstrates that in cortical hypoperfusion a more positive fluid balance was associated, particularly toward later study days. Central venous pressures and BNP levels were now no different between groups in contrast to those with AKI. The hypoperfusion group had higher pulmonary pressures in the latter half of the study, which likely reflected the patients with hypoperfusion remaining intubated.

Variable	Day	High perfusion	Low perfusion	Significance (p)
Fluid balance				
24 hr fluid balance (ml)	0	2600(800-4200)	1600(1400-3700)	0.83
	1	1000(-400-2800)	1100(780-2900)	0.11
	2	700+-500	1400+-1900	0.28
	4	22+-1200	130+-1400	0.81
Fluid balance for admission (ml)	0	2700+-1700	2000+-600	0.52
	1	3600+-3000	5300+-1200	0.057
	2	4000+-3200	8100+-4900	**<0.05**
	4	3900+-3300	9300+-4700	**<0.05**
Right atrial pressure and venous congestion				
Right atrial pressure (echo) (mmHg)	0	12(12-22)	12(2.5-12)	**<0.05**
	1	12(12-22)	12(12-12)	0.25
	2	12(12-12)	12(8.8-22)	0.68
	4	12(10-12)	12(12-12)	0.27
CVP (mmHg)	0	12+-5.4	13+-5.5	0.7
	1	12+-5.8	11+-4.5	0.77
	2	11+-4.6	13+-6	0.12
	4	11+-4.5	13+-5	0.29
BNP (ng/ml)	0	6900(3900-16000)	7500(2600-20000)	0.94
	2	3900(2000-11000)	4100(1400-16000)	0.96
	4	3400(1700-11000)	3400(2000-5900)	0.94
Pulmonary Pressures				
Pulmonary acceleration time (sec)	0	110+-21	110+-31	0.44
	1	120+-34	120+-30	0.96
	2	110+-23	130+-28	0.25
	4	120+-29	110+-40	0.53
Pulmonary artery pressure (mmHg)	0	37(26-44)	34(28-48)	0.7
	1	37(25-48)	36(32-44)	0.48
	2	33+-9.1	42+-17	**<0.05**
	4	36+-14	44+-13	0.087
Right heart function				
RV s' (cm/s)	0	18+-7.2	16+-6.4	0.43
	1	14+-2.0	17+-4.3	0.1
	2	14+-3.8	17+-5.3	0.084
	4	16+-4.2	16+-4.9	0.97
TAPSE (cm)	0	2.1+-0.59	1.8+-0.45	**<0.05**
	1	2.1+-0.54	2.3+-0.55	0.43
	2	2.2+-0.42	2.2+-0.45	0.74
	4	2.2+-0.48	2.1+-0.39	0.72

Table 7 Assessments of right heart function and venous congestion. Fluid balance, atrial pressure, ventilatory pressures, pulmonary pressures and right heart function are given individual sections. Data are presented by perfusion group and by day

8.2.2 Left heart function and afterload

8.2.2.1 AKI groups

Table 8 demonstrates the higher noradrenaline doses in those who developed severe AKI and a higher proportion received a second inotrope, but cardiac output, and cardiac function were no different. Troponin tended to be higher in the AKI group but failed to meet significance. Blood pressure was no different in the first half of the study and differences may represent the proportion extubated – reported in Table 9.

Variable	Day	No severe AKI	Severe AKI	Significance (p)
Proportion of patients on a second inotrope (terlipressin)	0	8%	50%	**<0.05**
	1	0%	34%	**<0.05**
	2	0%	26%	0.09
	4	0%	8%	0.68
Noradrenaline dose (mcg/kg/min)	0	0.21(0.14-0.3)	0.34(0.26-0.51)	**<0.05**
	1	0.06(0-0.11)	0.24(0.08-0.46)	**<0.05**
	2	0(0-0.048)	0.16(0.044-0.27)	**<0.05**
	4	0(0-0)	0.02(0-0.074)	0.06
Heart rate (bpm)	0	92+-16	100+-18	0.063
	1	88+-20	95+-22	0.37
	2	80+-12	92+-20	**<0.05**
	4	83+-16	92+-21	0.17
Mean arterial blood pressure (mmHg)	0	70+-5.2	69+-8.7	0.63
	1	73+-8.4	70+-7.1	0.26
	2	80(73-86)	70(64-78)	**<0.05**
	4	87+-17	80+-14	0.26
Cardiac index (l/min/1.73m2)	0	3.2+-1.2	3.3+-1.2	0.8
	1	3.1(2.8-3.7)	3.2(2.7-3.6)	0.95
	2	3.1+-0.52	3.3+-1.1	0.49
	4	3.3+-0.65	3.4+-0.9	0.57
Ejection fraction (%)	0	62+-12	57+-20	0.31
	1	67+-15	63+-16	0.52
	2	62+-16	63+-15	0.97
	4	67(63-72)	72(59-76)	0.49
Troponin (ng/ml)	0	84(21-390)	180(88-900)	0.068
	2	58(35-280)	200(28-600)	0.29
	4	36(6.4-120)	72(39-380)	0.082

Table 8: Indicators of left ventricular function, cardiac output and afterload

Day	Proportion intubated (%)	
	Severe AKI	Non-severe AKI
0	87	61
1	84	53
2	78	46
4	63	28

Table 9 Proportion of patients with severe AKI intubated per day

8.2.2.2 Perfusion Groups

In the perfusion groups noradrenaline doses were similar on admission, unlike those who developed AKI where the differences were more striking, but inotrope doses were higher on later days. Lower blood pressures were seen in the hypoperfusion group toward the end of the study. Both findings are likely a reflection of ongoing sedation and ventilation in this group (proportion still intubated by day 4 low-group 93% vs high-group 54%). Cardiac function was the same. Numeric data is presented in Table 10.

Variable	Day	High perfusion	Low perfusion	Significance (p)
Noradrenaline dose (mcg/kg/min)	0	0.32(0.19-0.41)	0.3(0.24-0.46)	0.73
	1	0.11(0-0.3)	0.16(0.072-0.43)	0.28
	2	0.048(0-0.13)	0.15(0.023-0.34)	0.088
	4	0(0-0)	0.074(0.029-0.2)	**<0.05**
Receiving terlipressin (%)	0	25	56	0.05
	2	12.5	32	0.22
	4	0	20	0.09
Heart rate (bpm)	0	99+-16	99+-20	0.98
	1	91+-26	95+-18	0.56
	2	89+-18	88+-20	0.86
	4	91+-21	86+-17	0.45
MAP (mmHg)	0	70+-8.1	68+-7.6	0.92
	1	71+-6.9	72+-8	0.73
	2	71+-5	75+-10	0.64
	4	88+-15	72+-9	**<0.05**
Cardiac index (l/min/1.73m2)	0	3.4±1.1	3.1+-1.2	0.16
	1	3.3+-0.82	3.2±1.0	0.95
	2	3.2+-0.73	3.3+-1.2	0.88
	4	3.5+-0.81	3.2+-0.87	0.29
Ejection fraction (%)	0	57+-17	59+-21	0.71
	1	59+-19	68+-11	0.08
	2	63+-18	63+-13	0.99
	4	68(59-75)	72(63-76)	0.85
Troponin (ng/ml)	0	150(83-620)	190(63-1200)	0.79
	2	130(31-400)	230(35-1400)	0.36
	4	56(26-200)	150(37-410)	0.34

Table 10 Indicators of left ventricular function, cardiac output and afterload in patients with high and low renal perfusion

8.2.3 Changes in renal blood flow

8.2.3.1 AKI groups

These data compare changes in the renal vasculature, there were no real differences between patient groups but comparison to controls demonstrated significant differences, particularly in resistive index (non-severe AKI 0.80±0.08, severe AKI 0.80±0.07, controls 0.60±0.06, p<0.05 vs controls. Renal artery VTI non-severe AKI 29cm±11, severe AKI 27±12, control 36±9, p=0.09 vs control).

Variable	Day	No severe AKI	Severe AKI	Significance (p)
Renal artery VTI	0	29+-12	28+-12	0.71
	1	29±4	25±9	0.43
	2	26+-13	25+-8.6	0.84
	4	31±5	24±6	**<0.05**
RBF/BSA	0	0.88+-0.38	0.86+-0.45	0.84
	1	0.83+-0.31	0.8+-0.4	0.8
	2	0.51(0.44-0.87)	0.66(0.49-0.79)	0.45
	4	0.75(0.62-1)	0.63(0.46-0.89)	0.33
Resistive Index	0	0.8+-0.078	0.81+-0.067	0.66
	1	0.78+-0.053	0.8+-0.071	0.3
	2	0.8(0.76-0.84)	0.81(0.74-0.87)	0.66
	4	0.78+-0.069	0.77+-0.099	0.9

Table 11: Renovascular variables, flow within the renal artery (renal artery volume time integral (VTI) (cm), indexed renal blood flow to body surface area (l/min/1.73m2), renal resistive index)

8.2.3.2 Perfusion Groups

Table 12 demonstrate the same variables between the perfusion groups. Control data were significantly different again, particularly resistive index, otherwise there are no real differences in this section.

Variable	Day	High perfusion	Low perfusion	Significance (p)
Renal artery VTI	0	29+-11	28+-12	0.7
	1	25+-7	29+-10	0.15
	2	23+-7.2	27+-12	0.26
	4	25+-6	28+-11	0.93
RBF/BSA	0	1.6+-0.31	1.4+-0.76	0.2
	1	1.5+-0.73	1.5+-0.69	1
	2	1.2+-0.64	1.2+-0.4	0.83
	4	1.2+-0.21	1.4+-0.65	0.94
Resistive Index	0	0.8+-0.072	0.82+-0.066	0.22
	1	0.78+-0.07	0.8+-0.064	0.35
	2	0.81+-0.04	0.8+-0.095	0.91
	4	0.78+-0.092	0.77+-0.093	0.92

Table 12 Renovascular variables, flow within the renal artery (renal artery volume time integral (VTI) (cm), indexed renal blood flow to body surface area (l/min/1.73m2), renal resistive index) when compared between perfusion groups

8.3 Discussion

8.3.1 Key findings

This chapter demonstrates that perfusion alterations occur independently of supply. Renal artery blood flow was unchanged in septic shock, with similar values between patient groups and controls, both in those who develop severe AKI and those with cortical hypoperfusion. This assessment was enabled through contrast enhanced measurements of the renal artery diameter in combination with renal artery dopplers, a method not previously described and these findings agree with previous data from multiple large animal studies demonstrating maintained RBF in septic shock[345,346,397]. This suggests a disconnect between hypoperfusion of the microcirculation and large vessel flow.

8.3.2 RBF in sepsis associated AKI

Accurate measurement of RBF in clinical studies is difficult. In 1990 Brenner and colleagues placed renal vein catheters fluoroscopically in 8 patients within 18 hours of admission with septic shock and documented RBFs ranging between 112ml/min and 1767ml/min (mean 690ml/min±179ml/min), after 24 hours RBF increased (mean 737ml/min±168ml/min, $p<0.05$). Renal vascular resistance was unaltered and GFR was unrelated to RBF [401] as was demonstrated in the current data where no differences existed between RBF and AKI development. In 1959 Bergström published values from healthy volunteers using the same technique of 616ml/min to 2190ml/min, depending on patient size[402]. The current data found RBF to be 1440±720ml/min in patients and 1200±450ml/min in controls. A meta-analysis on RBF in sepsis reports the Brenner study and two other studies from the 1970s' but describes them as using techniques which are inaccurate and not reproducible,

although the reasons for exclusion are not fully explained[345]. Prowle reported variability in RBF in septic shock using phase-contrast MRI, from low to supra-normal, although the mean time between admission and investigation was 3.5 days[358].

Animal studies targeting RBF and renal tissue perfusion are numerous. A group from Melbourne, Australia have published widely using an ovine septic model[403]. By cannulating the sheep's renal vasculature with flow and tissue oxygenation probes they have been able to test a variety of hypotheses and interventions aimed at improving renal outcomes. They demonstrated that medullary hypoxia can be transiently improved by a single fluid bolus, but repeat boluses have no further benefit[404]. Increasing haemaglobin from 7 to 9g/dL through blood transfusion also has no benefit to medullary tissue oxygenation[405]. Furosemide administration improves medullary oxygenation with no effect on RBF or medullary perfusion, likely an effect of reduced oxygen consumption from inhibition of active sodium transport[406]. They have recently demonstrated by invasive measurement that medullary pO_2 correlates with urinary pO_2, when measured using a modified bladder catheter, potentially providing an opportunity for real-time clinical measurement (r^2=0.49-0.63) [344,407].

8.3.3 Cardiac function

Cardiac function and cardiac output were similar between those with severe and non-severe AKI and those with high and low perfusion, suggesting that neither are driven by poor cardiac output and impaired delivery, once considered the predominant cause for AKI in sepsis. Troponin values tended to be higher in patients with severe AKI, but troponin is non-specific in this situation, more reflective of illness severity than cardiac injury[408].

8.3.4 Venous assessment and right heart

Data from assessment of the right heart and the venous system demonstrated significant alterations in those who develop severe AKI. They had elevated atrial stretch noted by higher BNP values, higher central venous pressures and worse ventilatory pressures. Venous congestion is thought to reduce renal perfusion pressure and elevations in central venous pressure and peripheral oedema are associated with an increased risk of AKI[409]. Interestingly these differences were not present in renal perfusion groups in the current data, suggesting that whilst these factors are potential culprits in AKI development, the data presented here does not support venous congestion as the mediator of hypoperfusion. This conclusion cannot be drawn definitively as a more detailed examination of the venous system would be needed such as the Renal Venous Stasis Index (RVSI) [410] and the venous excess ultrasound system (VExUS)[411]. These new scoring systems are used to assess the inverse association between the proportion of time spent in forward flow and AKI risk, unfortunately they were not described at the onset of the current study. More studies are needed in addition to the perfusion data presented here to confirm and explain why venous congestion was associated with AKI development if it did not affect renal perfusion in some way.

8.3.5 Fluid balance and volume administration

Careful volume resuscitation is necessary to maintain adequate perfusion pressure in septic shock, however intravenous fluid may also have deleterious effects on renal function. Synthetic colloid use has decreased significantly over the past decade, due to an increased risk of AKI and mortality in the resuscitation of septic patients[412–414] with mechanistic studies revealing a variety of renal injuries[415]. Chloride-rich solutions cause vasoconstriction of the

afferent arteriole and reduced RBF[416] and clinical trials have recently identified increased renal injury in acute patients[417,418]. The volume of administered fluid and a positive balance increase AKI risk, although it is difficult to determine the confounding effects of illness severity in such studies[419,420]. There was a significant difference in fluid balance between perfusion groups in the present data which may point to either the effects of chloride on the microcirculation or another previously postulated mechanism for renal hypoperfusion[421] – that of renal interstitial oedema. A positive fluid balance resulting in swelling of the kidney, an encapsulated organ with an inability to distend, demonstrating a non-linear pressure-volume relationship following induced renal oedema[422]. This increases renal vascular resistance, reduces perfusion and is not identified through venous pressure monitoring. This iatrogenic effect would be compounded by increased vascular permeability in the severe AKI and hypoperfusion groups – as demonstrated by the elevation in syndecan-1 and angiopoietin ratios in these patients which is described in chapter 10.

8.3.6 The renal effects of select inotropes and vasopressors

Severe AKI patients had higher inotrope requirements, being on higher doses of noradrenaline and requiring a second inotrope typically vasopressin, more frequently. This association between inotrope use and acute kidney injury is significant. One explanation of this association could be renovascular haemodynamic effects of these drugs, both macro- and microcirculatory. Both drugs have intra-renal receptors and their effects are not completely understood. Lankadeva demonstrated that noradrenaline in a septic ovine model restored blood pressure at the expense of medullary oxygenation, although cortical oxygenation was preserved[344]. Interestingly in the data presented here, the differences were less apparent when compared between perfusion groups than AKI groups. This closer association with AKI

severity than perfusion fits with Lankadeva's findings of noradrenaline having a more minor effect on cortical oxygenation than medullary. An alternative explanation for these findings with vasopressors is the presence of a third factor, such as sickness severity, being causative for both inotrope dose and AKI.

Multiple vasopressor studies have reported that noradrenaline administration worsens medullary hypoxia[344] but co-administration with dexmedetomidine may reduce this[423]. Cortical perfusion following noradrenaline administration is variable in a clinical study using CEUS, with some patients showing improvement but others hypoperfusion[424]. In sheep, adrenaline has no effect on RBF but transiently decreases creatinine clearance in sepsis, returning to baseline within a few hours[425]. Dopamine may increase RBF in the healthy state but has either has no effect in septic conditions[425], or may improve flow[426] depending on the study. The dopamine agonist fenoldopam had no effect on RBF and at high dose was detrimental[427]. Attempts to selectively block the renal vasodilatation of sepsis and its resultant increase in RBF using nitric oxide synthase inhibition had no effect on GFR[428,429]. Vasopressin does not appear to cause medullary hypoxia to the same extent as noradrenaline [430,431] and its analogue terlipressin increases renovascular resistance and creatinine clearance with no change in RBF[432]. The mechanism is potentially through activation of the selectively expressed V1 receptors on glomerular efferent arterioles[433] and vasodilatation of afferent arterioles[434,435]. Administration of angiotensin II (AgII) has striking effects on renal haemodynamics, reducing renal blood flow by 22%, at the same time increasing renovascular resistance, creatine clearance and urine output 7-fold, which like vasopressin, may be mediated through selective vasoconstriction of efferent arterioles[436]. Whilst selective vasoconstriction of the efferent arteriole will logically produce these

outcomes, potentially a downstream detrimental effect on medullary perfusion may occur. Again, the Melbourne ovine model was used to examine this issue but found no difference in medullary oxygenation when AgII was administered in comparison to controls[407]. In clinical studies post-hoc analyses of two large, randomised control trials suggested vasopressin may improve renal outcomes in comparison to noradrenaline, although the evidence is unclear. A post-hoc analysis of the initial VASST study demonstrated reduced progression of AKI and a lower rate of renal replacement, but the follow up study VANISH failed to find a reduction in AKI free days[434,437,438].

9 Cortical hypoperfusion is not associated with systemic shock: A comparison with traditional markers

9.1 Introduction

"First of all the doctor should look at the patient's face […], the following are bad signs […] hollow eyes, cold ears, dry skin on the forehead, strange face colour such as green, black, red or lead"[7].

Hippocrates – The Hippocratic Collection

The microcirculation is the vascular network responsible for substrate exchange; vessels under 20µm. The microvascular unit comprises the terminal arteriole, 15-20 capillaries and the collecting venule[9]. The terminal arteriole and collecting venule are generally between 20-100µm and are involved in the regulation of flow.

A reduction in microcirculatory flow is common early in the admission of a shocked patient, with the degree of shock correlating with the severity of the reduction. Generally, impaired tissue perfusion early in the admission highlights the presence of shock but it is the persisting impairment following initial resuscitation efforts that portends surgical complications, morbidity and death, as evidenced in multiple longitudinal studies[298,302,307,311]. Conversely an improvement in microcirculatory parameters precedes

clinical improvement in a variety of conditions[295,310].

A wide number of techniques for assessing perfusion are described, which provide either an average estimate of global perfusion or rely on a specific region or window to reflect the global state, noting that variability within different tissue beds is common. Any such technique therefore has the potential to under- or over-estimate global perfusion. Whilst perfusion assessment methods may be classified as global or local, such methods may also be classified as clinical, biochemical or using a bedside device.

This section contrasts organ specific perfusion – that of the renal cortex with systemic tissue perfusion assessed using a variety of techniques, including sublingual incident dark-field microscopy, lactate clearance, carbon dioxide gap and central venous oxygen saturations; a description of these methods is given in section 2.4. Further mechanistic data are presented from markers of endothelial and glycocalyx injury. The aim of this section is to understand the relationships of renal hypoperfusion, whether alterations are unique to the kidney or are features of a wider shock-state and whether impairment of one microcirculatory bed predicts impairment of another.

A description of the techniques used, the rationale and the method is provided in 2.4. Grouping variables are those of previous chapters.

9.2 Results:

9.2.1 Sublingual microcirculation

9.2.1.1 AKI groups

There were no significant differences in the sublingual microcirculation between those who developed severe AKI on any day of admission presented in Figure 32.

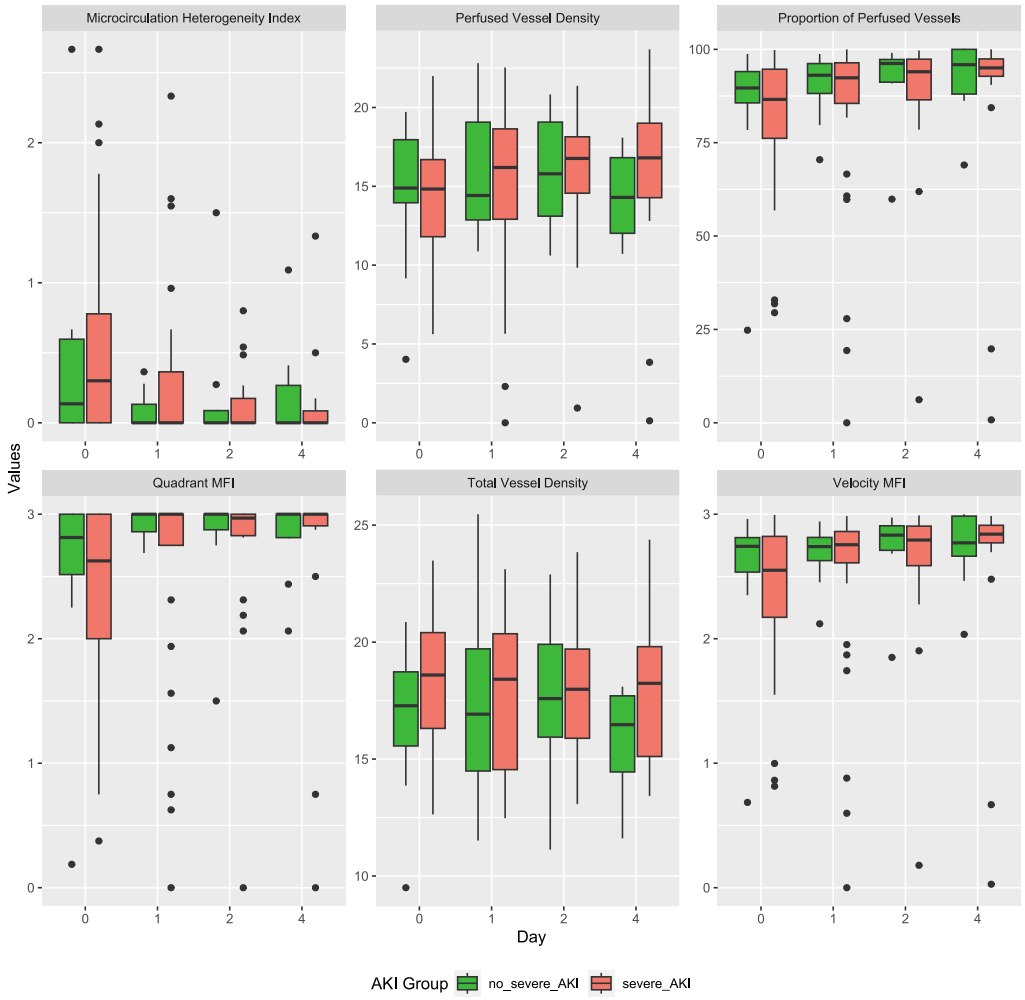

Figure 32 Boxplots of alterations in sublingual perfusion between those who developed severe AKI and those who did not.

9.2.1.2 Renal perfusion groups

Sublingual microcirculatory analysis between those with above and below average renal perfusion is presented in Figure 33. The greatest difference in sublingual perfusion is seen on admission where MFIq is reduced (high perfusors 2.9(2.6-3) vs low perfusors 2.4(1.8-3) $p<0.05$) and MFIv (high 2.7(2.5-2.8) vs low 2.4(2-2.8) $p=0.095$), PPv (high 90(84-94) vs low 81(71-95) $p=0.11$) and MHI (high 0.085(0-

0.6) vs low0.63(0-1.2) p=0.068) tended to be lower. By the later stages, rapid improvement in sublingual perfusion in the renal hypoperfusion group eliminate these early differences. This normalization by day 4 was the result of both recovery and patient death removing the most severe from the sample population, see Table 13.

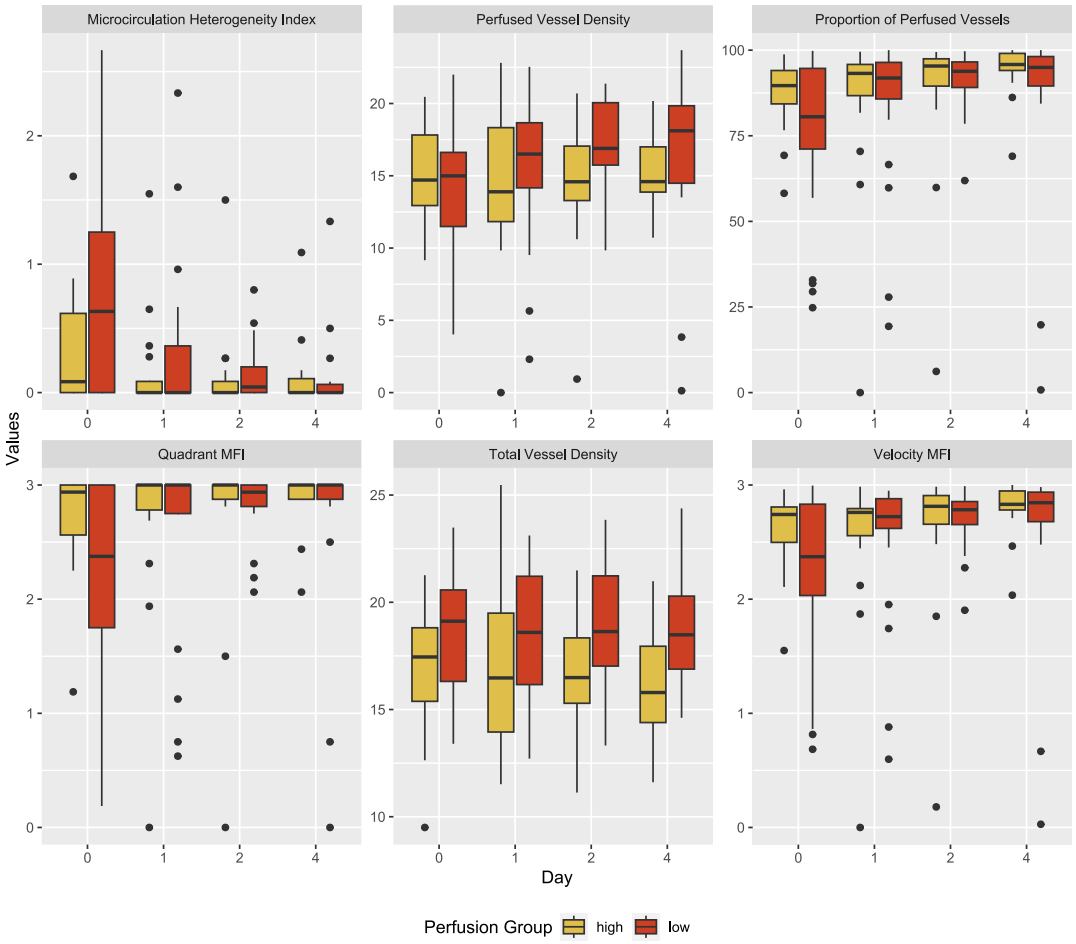

Figure 33 Handheld video microscopy findings in the sublingual mucosa between those with above and below average renal perfusion on admission

Day	High perfusors alive (%)	Low perfusors alive (%)
0	100	100
1	96	88
2	92	88
4	92	60

Table 13 Number of patients alive by day

9.2.2 Alterations in biomarkers

9.2.2.1 AKI Groups

In patients who developed severe AKI, higher values (more endothelial damage) were seen throughout the study period in angiopoietin ratios ($p<0.05$ all days) Figure 34 refers. The same was true of syndecan-1 – an endothelial sheddase indicative of endothelial injury ($p<0.05$ all days). Arterial blood lactate was also higher throughout the study period in the severe AKI group (D0, 1, 2 $p<0.05$, day 4 $p=0.13$).

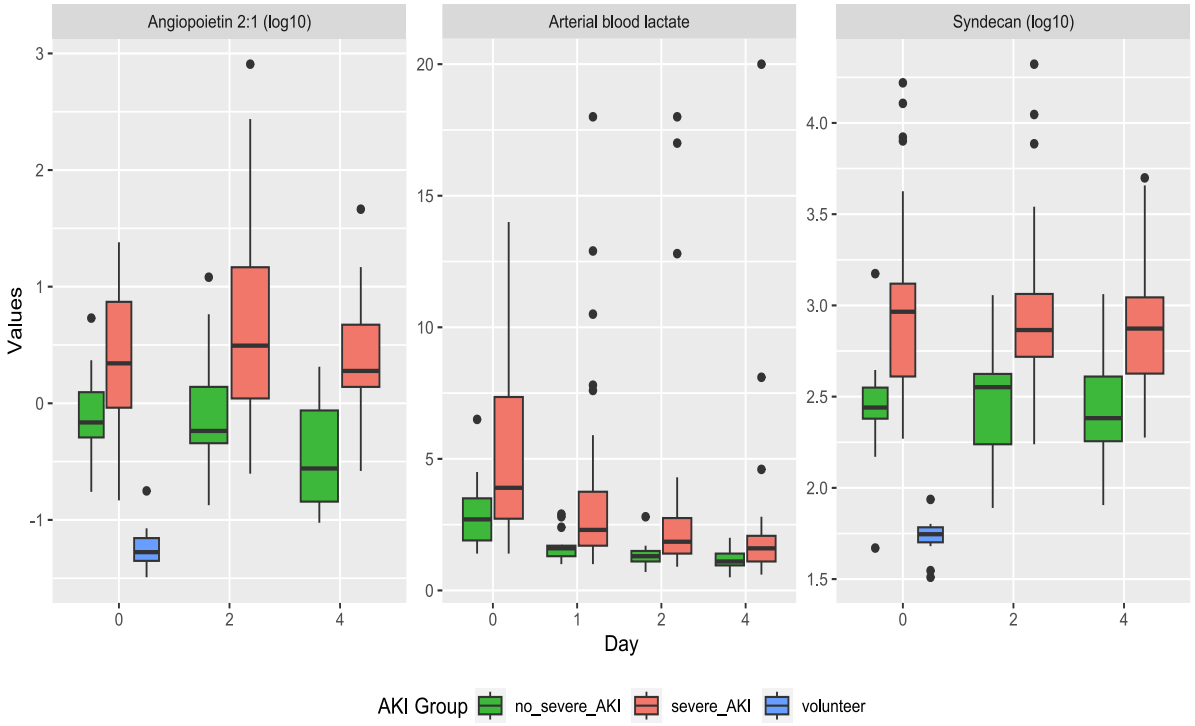

Figure 34 shock biomarkers between those with severe and non severe AKI. Healthy control values are demonstrated in blue on day 0. Angiopoetin ratios and syndecan scaled to log10 on Y axis. Lactate values mmol/l, syndecan log10(ng/ml).

9.2.2.2 Renal perfusion Groups

Lactate tended to be higher in the renal hypoperfusion group but did not reach significance on any study day (D0 $p=0.3$, D1 $p=0.28$, D2 $p=0.055$, D4 $p=0.07$), angiopoietin ratios improved more rapidly in those with above average renal perfusion but persisted in those with hypoperfusion generating a

difference by day 4 ($p<0.05$). Syndecan levels were higher in the renal hypoperfusion group on admission (low 350(260-1000)ng/ml vs high 800(430-1500)ng/ml $p<0.05$) but were no different by day 4 (low 450(220-920)ng/ml vs high 560(400-1100)ng/ml $p=0.54$). Figure 35 refers. Due to extreme outliers syndecan and angiopoietin ratios are scaled logarithmically on the y axis, which may reduce visual appearances.

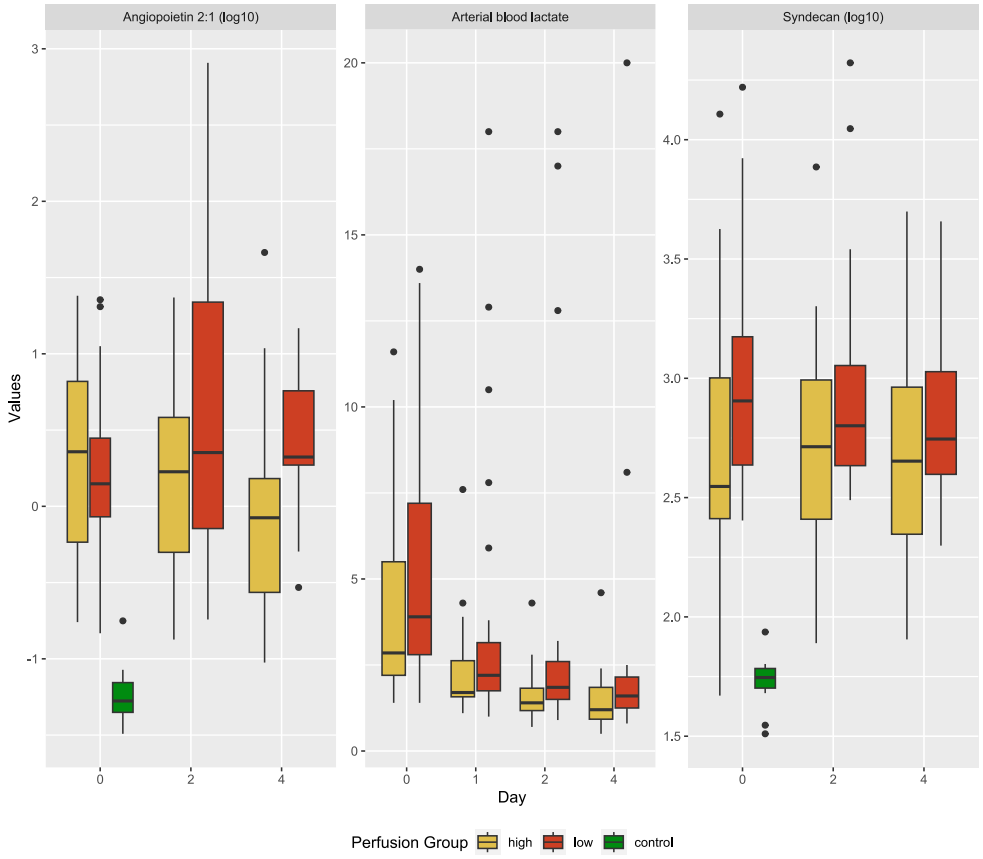

Figure 35 boxplots of angiopoietin ratio, arterial blood lactate and syndecan between those with above and below average renal perfusion on admission. Angiopoetin ratios and syndecan scaled to log10 on Y axis. Lactate values mmol/l, syndecan log10(ng/ml).

9.2.3 Analysis of supply adequacy and oxygen consumption by blood gases

9.2.3.1 AKI Groups

Variables which represent the severity of shock and oxygen delivery calculated from blood gas analysis are presented in Table 14. Oxygen consumption was generally higher in the non-severe group than the severe group, but otherwise there were minimal differences. The description and calculation of these variables are provided in general methods (2.4.1.1 onwards).

Variable	Day	Severe AKI	No Severe AKI	Significance (p)
Arterial oxygen saturations (%)	0	95+-2	97+-1.1	**<0.05**
	1	96+-2	97+-2	0.2
	2	95+-2.5	96+-1.6	0.14
	4	97+-1.5	97+-0.75	0.42
Central venous saturations (%)	0	71+-3	70+-6.8	0.94
	1	71+-8	70+-6.8	0.65
	2	72+-6.9	69+-7.4	0.29
	4	69+-8.3	64+-8.4	0.2
Carriage of oxygen l/min	0	7.8+-3	8.2+-1.1	0.38
	1	7.3+-2.3	8+-2.3	0.38
	2	6.9+-2.5	7+-1.5	0.8
	4	6.3+-1.7	6.9+-1.3	0.87
Oxygen consumption (CaO2-CvO2) l/min	0	3±1.0	3.8+-0.82	0.061
	1	2.9+-1.2	3.4+-0.92	0.17
	2	2.6+-0.75	3.2+-0.77	**<0.05**
	4	3+-0.88	4+-1.2	0.059
CO2 gap (kPa)	0	0.84±0.3	0.88±0.12	0.55
	1	0.76+-0.33	0.81+-0.28	0.62
	2	0.66+-0.24	0.76+-0.16	0.093
	4	0.83+-0.29	0.75+-0.32	0.55
Delta delta ΔpCO_2/ $C_{a\text{-}v}O_2$ (kPa/l/min)	0	0.38(0.24-0.72)	0.42(0.35-0.46)	0.8
	1	0.37(0.32-0.55)	0.43 (0.2-0.55)	0.84
	2	0.38(0.29-0.52)	0.43 (0.39-0.57)	0.77
	4	0.48(0.21-0.6)	0.35(0.28-0.62)	0.13

Table 14 Blood gas analysis values for those with severe and non-severe AKI.

9.2.3.2 Perfusion Groups

Indices calculated from blood gases are presented in Table 15 for perfusion groups. Those who had impaired renal perfusion on admission had reduced venous oxygen saturations but with a concomitant reduction in arterial oxygen saturations. Oxygen consumption was lower in the hypoperfusion group on D2. No other significant differences are demonstrated.

Variable	Day	High perfusors	Low perfusors	Significance (p)
Arterial oxygen saturations (%)	0	97(95-98)	96(94-97)	**<0.05**
	1	96(93-98)	95(92-97)	0.25
	2	95(92-97)	96(94-97)	0.62
	4	97(96-98)	96(94-98)	0.48
Central venous oxygen saturations (%)	0	73+-6.4	66+-12	**<0.05**
	1	69+-7.6	73+-7.5	0.16
	2	71+-6.8	71+-7.5	0.72
	4	66+-9.4	70+-6.5	0.17
Carriage of oxygen (l/min)	0	8.8+-2.7	7.3+-3	0.062
	1	8.1+-2.2	7.1+-2.2	0.12
	2	7+-1.9	6.8+-2.6	0.73
	4	7.1(5.9-8.4)	6.6(4.8-7.1)	0.18
Oxygen consumption (CaO2-CvO2)(l/min)	0	2(1.7-2.2)	2.1(1-3.2)	0.62
	1	2.2(1.7-2.4)	1.5(0.9-2.1)	**<0.05**
	2	1.7+-0.62	1.6+-0.68	0.68
	4	2.2+-0.48	1.8+-0.68	0.083
CO2 gap(kPa)	0	0.81+-0.35	1.1+-0.2	0.062
	1	0.84+-0.34	0.72+-0.29	0.21
	2	0.67+-0.24	0.7+-0.21	0.64
	4	0.85+-0.32	0.74+-0.24	0.29
Delta delta $\Delta pCO_2 / C_{a-v}O_2$ (kPa/l/min)	0	0.38(0.28-0.46)	0.45(0.3-0.98)	0.16
	1	0.38(0.27-0.49)	0.37(0.33-0.6)	0.32
	2	0.37(0.31-0.47)	0.42(0.3-0.56)	0.57
	4	0.4+-0.16	0.52+-0.26	0.21

Table 15 biochemical measures of shock severity in patients with above and below average renal perfusion on admission.

9.2.4 Correlation between shock indices

The correlation between the shock based indices and cardiac output are provided in Figure 36. Lactate demonstrated only weak correlations with other shock-based indices and no correlation with cardiac output. Blood gas based indices had modest associations with cardiac output, other than the delta-delta (ΔpCO_2/ $C_{a\text{-}v}O_2$) which correlated closely (R=-0.73). PPV was selected as one of the most robust sublingual indices for the comparison[439] and it demonstrated modest association with other markers of shock severity (R values between 0.14 and 0.31).

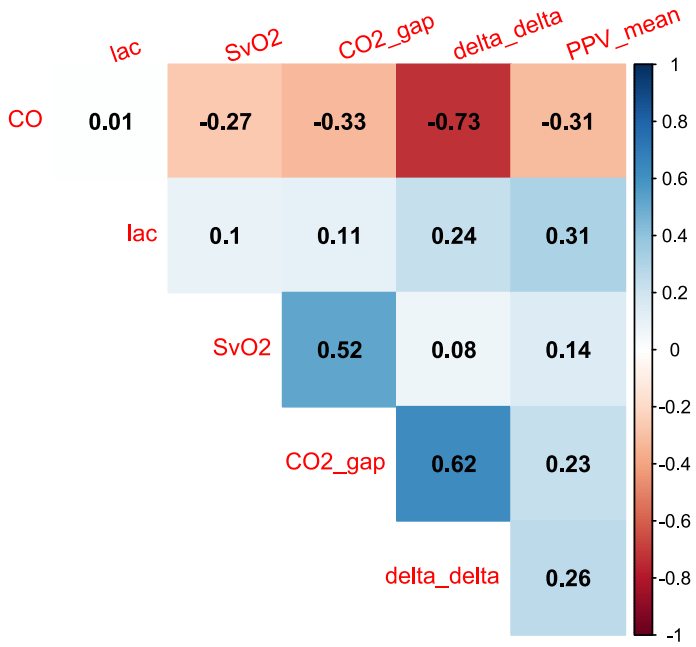

Figure 36 Correlation between individual perfusion variables and cardiac output. Correlation coefficient reported. Darker red points to a stronger negative correlation, darker blue a stronger positive correlation (scale on right refers). CO= cardiac output, lac=arterial lactate, SvO2 central venous oxygen saturations, CO2_gap carbon dioxide gap, delta_delta the Mekonsto-Dessap gap (CO2 gap/venous oxygen consumption), PPV_mean proportion of perfused vessels.

9.3 Discussion

Impairment of the microcirculation has been demonstrated in septic[294–302], cardiogenic[303–305] and haemorrhagic shock[306,307], patients on ECMO[308–310], after major surgery[311] and in general critical illness[301,312]. Perfusion impairment has been demonstrated not just in the sublingual circulation but in other tissue beds such as stomas[314] and operative observations of the brain[315], serosa[316], peritoneum[317] and liver[318].

In animal shock models abnormalities have been identified in two separate tissue beds, but the degree of correlation is often limited. Changes in gut perfusion reflected sublingual measurements in two studies[319,320] but not in another[321]; whereas renal and sublingual perfusion barely correlated in one study[322] but did in another[323]. In the present study patients with renal hypoperfusion had worse sublingual perfusion, however the differences were limited and confined to admission. This has not been demonstrated clinically before as previous studies have tended to observe one or other microcirculatory bed. Lima et al demonstrated a very close association between the renal and sublingual beds in pigs, but this study was far shorter than the four-day observations presented here [323]. Another study by Sui et al induced intra-abdominal hypertension in pigs and assessed renal perfusion with CEUS and applied IDF directly to the surface of the kidney and mouth, finding a close correlation between renal IDF and renal CEUS, but no correlation with sublingual IDF, perhaps not unexpected given the mechanism used[322]. Neither of these experimental studies concur completely with the clinical data presented here which identified a limited and transient association, nor is it entirely conflicting either. The data from the present study support two hypotheses, firstly systemic hypoperfusion either rapidly improves or if persistent leads to death. The improvement of sublingual hypoperfusion seen by day one

and near-normalisation by day two supports this. This is also seen in the higher fatality rate of the renal hypoperfusion group. Multiple previous studies using longitudinal observations have reached the same conclusion, that of persistent hypoperfusion portending a poor outcome[298,302,307,311]. The second hypothesis supported by the IDF data is that microcirculatory flow is unique in individual tissue beds, the renal microcirculation differs from sublingual as improvement is more gradual with only mild improvement by day four, although impairment is immediate in both. Renal hypoperfusion cannot therefore be predicted by systemic parameters of shock. DCE-US enables such observation within the kidney, providing a new window through which the previously unknown renal perfusion alterations may be viewed.

The blood gas analysis data presented were not particularly informative, the renal hypoperfusion group tended to have higher CO2 gaps earlier in the admission. CO2 gap correlated negatively with cardiac output, and the correlation was stronger than with ScvO2 which agrees with previous descriptions in the literature[282]. Central venous oxygen saturations were lower, but had lower arterial saturations. The so-called delta-delta [289], (ΔpCO_2/ $C_{a\text{-}v}O_2$) did not relate to renal hypoperfusion, AKI development, lactate or other markers of shock. It provided no further insight than other biochemical parameters. It did show a strong negative correlation with cardiac output, but as explained in Methods, was described as a method of identifying tissue hypoxia rather than impaired cardiac function.

Patients with severe AKI had higher levels of arterial lactate, but despite this no differences in sublingual perfusion values were identified, nor were there any differences in blood gas analysis of shock severity. This begs the question of where lactate is generated in such

circumstances. Whether these patients were truly below the critical delivery threshold is difficult to know as the data are conflicting, proponents of anaerobic lactate production would suggest the lactate demonstrates global hypoperfusion, but multiple biochemical and sublingual assessments did not. It may be argued that lactate is more sensitive than other parameters in identifying tissue hypoperfusion – identifying the occult hypoperfusion not demonstrated by other methods. If undetectable solid organ hypoperfusion were responsible for hyperlactataemia in this cohort of shocked patients, renal hypoperfusion or sublingual hypoperfusion might be expected to demonstrate a clear association, but the lactate data in the renal hypoperfusion group was not convincing, tending towards higher values but not the clear group separation one might expect if occult hypoperfusion were causative.

An alternative explanation is that increased lactate and pyruvate production results from enhanced aerobic glycolysis, rather than anaerobic production. This aerobic glycolysis results from increased Na^+K^+ATPase activity, under catecholamine control, as was demonstrated in a series of well conducted experiments by Levy et al. demonstrating that inhibition of muscle Na^+K^+ATPase stopped the over production of lactate and pyruvate and concluding that elevated lactate levels act as an important metabolic stress signal rather than a marker of oxygen debt[440]. They went on describe how septic patients have significantly more pyruvate and lactate in the muscle than artery. Those with the greatest levels of muscle lactate and pyruvate progressed to septic shock and there was a close correlation between plasma adrenaline level, muscle lactate production and the severity of illness[441].

In summary, this section demonstrates that cortical hypoperfusion is unique to the kidney and does not particularly reflect any systemic measure of global perfusion. There is a limited

association with sublingual hypoperfusion on day 0, but this resolved by day 1, systemic hypoperfusors either improved or died, whilst renal hypoperfusion persists in AKI. Various methods of assessing systemic hypoperfusion are described, but none demonstrated strong correlations with each other or cardiac output. There were minimal differences between renal perfusion and lactate, which would have helped support the hypothesis of lactate generation through occult solid organ hypoperfusion.

10 The relationship between inflammation, renal perfusion and AKI development

10.1 Introduction

Blood flow to the kidneys is approximately 1.25l/min at rest and roughly 1/10th of this is filtered. Once in the nephron or peritubular capillaries, pattern associated molecular patterns and damage associated molecular patterns present to toll-like receptor (TLR)-2 and 4 expressed on the luminal and basal surface of tubular epithelial cells (TECs) and cause a double hit from both circulating and filtered molecules, with subsequent release of cytokines and an auto-upregulation in TLR-4 expression[442–444]. TECs with repeated endotoxin exposure become hyperresponsive[445], they have recently been shown as having immunological memory and are actively involved in inflammation[446].

The activation of TLR-4 results in degradation of tight junctions permitting paracellular fluid leakage in the proximal tubule and hampering fluid resuscitation. The interstitial oedema can be significant enough to obstruct the tubular lumen in some models but these regions of interstitial oedema are not co-localised with regions of microcirculatory impairment[447–449].

TNF-α stimulates the innate immune system[48,444], although the role of a cellular immune response and the presence of apoptosis has limited evidence early in sepsis associated AKI. Despite the apparent absence of cellular infiltrates, a wide body of evidence supports a significant component of AKI mediated by inflammatory processes. Inflammation appears

fundamental in the development of perfusion abnormalities within the kidney. An association would therefore be expected between inflammation, endothelial activation, glycocalyceal injury and renal perfusion.

TNF-α and IL-8 have been identified in multiple studies as important in AKI development secondary to sepsis. TNF-α is associated with iNOS upregulation[450], endothelial injury[451] and is a key mediator of damage to the glomerular glycocalyx[452]. Disruption of the glomerular glycocalyx both reduces microcirculatory flow and enables the filtration of larger molecules[453], giving albuminuria a role as a potential biomarker of AKI[454]. IL8 is independently associated with AKI development after adjustment for clinical factors[249]. Elevated levels correlate with ischaemia-reperfusion injury of allografts[250], prediction of AKI in sepsis[251] and demonstrate higher levels in non-survivors of septic shock[252]. Both cytokines along with angiopoietin ratios are group defining in a recent description of AKI subphenotypes; see chapter 11.

This chapter compares longitudinal measurements of inflammatory cytokines with renal perfusion.

10.2 Results

10.2.1 AKI groups

Patients who had severe AKI had elevated cytokines in comparison to those who did not ($p<0.05$), as presented in Figure 37. This was seen on all days of the study and was more apparent in AKI than in renal hypoperfusion data (non-linear Y axis scaling is used for displaying angiopoietin ratios and syndecan due to extreme outliers).

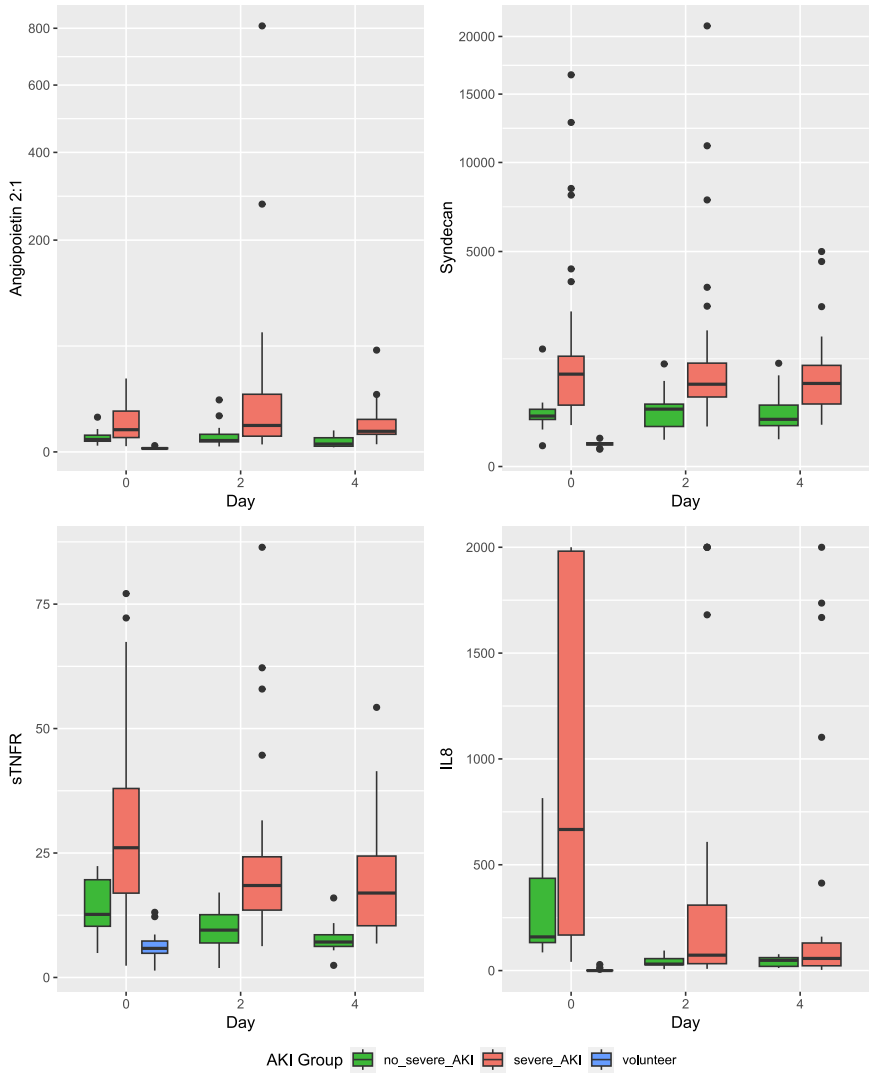

Figure 37 Inflammatory cytokine levels in patients with and without severe AKI (units syndecan ug/ml, sTFNR ug/ml, IL8 ng/ml).

10.2.2 Perfusion groups

Inflammatory profiles between renal perfusion groups are presented in Figure 38. Differences were only apparent in later days of the study, in comparison to patients with above average perfusion, those with below average perfusion had higher IL-8 values (32(15-62)ng/ml vs 69(45-154) ng/ml, p<0.05) and angiopoietin ratios by day 4 (0.88(0.27-1.53) vs 2.11(1.86-5.82), p <0.05), but early in the study there was no difference between groups. sTNFR showed no difference (D0 p=0.28, D2 p=0.26, D4 p=0.2). Syndecan was higher on admission in renal hypoperfusors (D0 p<0.05, D2 p=0.12, D4 p=0.54).

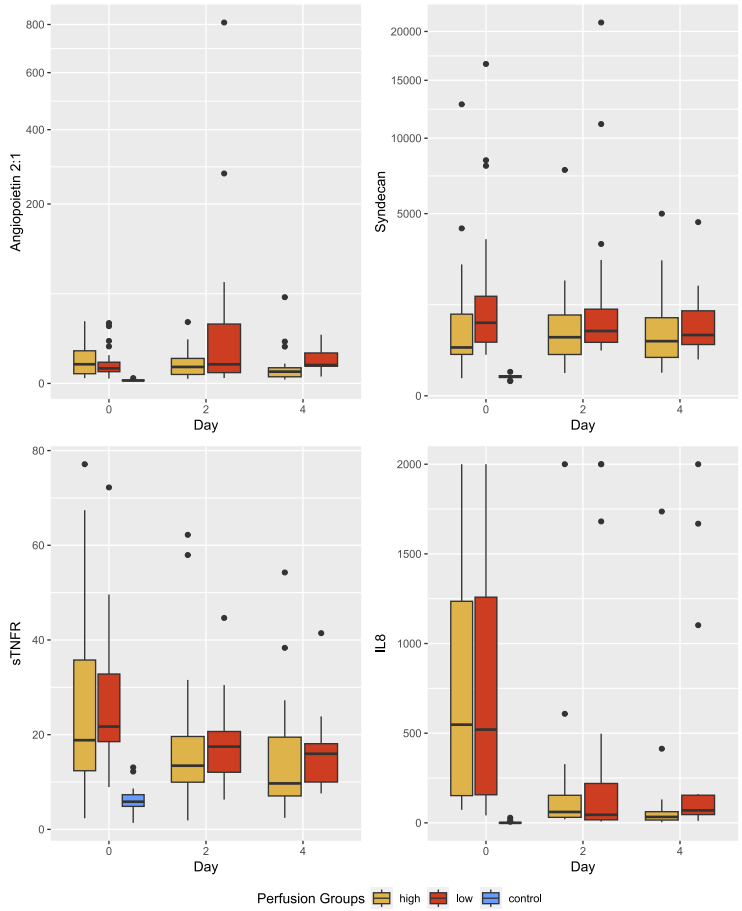

Figure 38: Boxplots demonstrating differences between inflammatory cytokine profiles (angiopoietin 2:1 ratio, syndecan, soluble tumour necrosis factor receptor (sTNFR) and interleukin 8 (IL8). Control data is provided in the day 0 column in blue. Angiopoietin ratios and syndecan are scaled on the y axis using a square-root transformation for ease of plotting extreme outliers.

10.3 Discussion

10.3.1 Key findings

Expectedly all patients in the study mounted an early cytokine response, having presented in septic shock with peaks in sTNFR and IL8 on day 0. These peaks were similar between perfusion groups early on, but by day four those with hypoperfusion had persistent levels of inflammatory cytokines, whilst those with preserved renal perfusion had a waning inflammatory response. The greatest association between perfusion and inflammation was seen later in the admission. There was however a far closer association between AKI and inflammation, with clear group separation in cytokine levels throughout.

The weaker association between inflammation and perfusion may be partly accounted for by the series of studies presented by Nakano and colleagues[447–449], demonstrating that the resultant oedema from breakdown in paracellular tight junctions inhibits tubular flow but is distal to, and has a limited effect on capillary flow. Indeed in these small animal studies, regions of hypoperfusion and paracellular leakage were random and not collocated. The hypoperfusion may provide only a part of the picture in AKI development, one of the three interlinked contributors along with inflammation and metabolic alterations.

10.3.2 The interaction between TECs and the immune system

As mentioned in the introduction, emerging evidence suggests the interaction between the immune response and TECs to be fundamental in AKI development. Following activation, paracrine signalling downregulates adjacent segments, as noted by the increase in cell cycle arrest proteins detectable in the urine. In the proximal segment (S1) of the proximal tubule, TECs are thought to act as sepsis sensors, taking in filtered endotoxin via TLR-4 and releasing

cytokines for uptake by TECs in the S2 segments. This results in significant injury to S2 TECs but surprisingly S1 TECs escape relatively unscathed despite the uptake of endotoxin[455,456].

Whilst inflammation has a key role in the pathogenesis of AKI, it is also implicated in its persistence. Hyperinflammatory responses from TECs may be seen on re-exposure to stressors, due to immunological memory, accounting for an exaggerated response if cytokine exposure does not resolve [457,458]. As seen in the data presented early on inflammatory profiles were not different between those with more severe hypoperfusion and those without, but later differences can be seen with persistent elevation of inflammatory cytokines in these patients.

10.3.3 The emerging interaction of immunological resistance and tolerance mechanisms

The confrontation of microbial invasion and resistance mechanisms results in collateral damage to the host, an under-damped response with immunosuppressive failure results in immune cell death, an over-damped response leads to an increased mortality. The early metabolic responses of cells are thought to determine the balance between resistance and tolerance processes[459]. Early metabolic reprogramming allows cells to respond to pathogens through resistance mechanisms. Tolerance mechanisms may determine repair, fibrosis and progression to CKD[457]. Pathogenic tolerance refers to a spectrum of recently described host factors which limit the collateral injury from inflammation. The evidence for such processes remain within experimental study, but involve haem, haemopexin and the stimulation of specific energy regulatory pathways[460–463]. They are also likely to alter depending on genetic differences between individuals[464].

This tolerance-resistance balance may contribute to the stronger late-stage association between hypoperfusion and inflammation identified in the present data. If resistance mechanisms predominate later in the disease process inflammatory profiles are likely to be higher with concomitant damage and alterations in cortical blood flow, whereas if tolerance predominates the opposite may be expected due to the higher energy requirements from healing and repair, potentially leading to earlier resolution of AKI and restoration of perfusion. A limitation of the current dataset is that we did not measure cytokines associated with immunological tolerance and repair mechanisms which may have proved insightful.

10.3.4 Endothelial and glycocalyx involvement in AKI development

The data presented in this chapter also supports endothelial and glycocalyx disruption in AKI and hypoperfusion development, with higher angiopoietin ratios later on and syndecan values higher on admission in these groups. Xu et al demonstrated a TNF mediated glomerular endothelial injury in sepsis associated AKI[452] and in the present study syndecan-1 levels were elevated in hypoperfusors on day 0, suggesting the glycocalyx damage occurs early and may account for the elevation in albuminuria described in chapter 12, whereas angiopoietin ratios reflective of endothelial activation had later differences, mirroring the association with inflammatory cytokines.

10.3.5 Cellular immune response in AKI

The role of leukocytes is unclear in sepsis associated AKI and is inferenced from experimental study of ischaemia-reperfusion injury (IRI). Neutrophils[465], macrophages[466], NK cells[467] and dendritic cells[468] have been demonstrated, but a recent large-animal study designed to examine the early pathogenic changes failed to demonstrate cellular

recruitment[343]. A human post-mortem human study reported the limited presence of repair-type M2 macrophages and neutrophils in glomeruli and neutrophils alone in peritubular capillaries; lymphocytes were absent from all regions[44]. Aslan et al reported a significantly higher number of proliferating glomerular cells and TECs, which is likely during the healing phase of the disease process given the cell-cycle arrest with early sepsis associated AKI[21].

The contribution of cell death to the pathogenesis of AKI is controversial, necrosis is not a feature, but low-grade apoptosis appears in several human and experimental studies[43,44,469,470]. Aslan found virtually no apoptotic glomerular cells, but tubulointerstitial cells were apoptotic to a low degree (1-10%) in most patients. Other human studies have reported a surprising absence[471]. In the review literature several authors support apoptosis as a potentially important mechanism in the pathogenesis of AKI[48,469], whereas others suggest the sparsity of human apoptotic features portends a discretely functional cause[41,472]. The most recent human tissue study which demonstrated low grade apoptosis drew no firm conclusion and recommended further research[44].

10.3.6 Bioenergetic Adaption and mitochondrial function

Early in the septic episode TECs are fuelled by aerobic glycolysis, so called Warburg metabolism with a later switch to the catabolic process of oxidative phosphorylation of fatty acids[444,459]. During Warburg metabolism, the typical anaerobic pathway of converting pyruvate to lactate occurs under aerobic conditions. Whilst not generating large quantities of ATP it allows for the creation of intermediate substrates for onward anabolism, allowing the intermediates to be readily utilized, including fatty acids, amino acids and nucleotides,

essential for repair[473]. It was first identified in tumorigenesis but later recognised to be a process of immune cells[474]. The evidence for Warburg metabolism in renal TECs is not conclusive but is building. Recent evidence has shown a reduction in total ATP levels in TECs in septic models and an increase in cortical glycolysis[475,476]. Metabolomics have demonstrated early suppression of oxidative phosphorylation and an increase in glycolytic intermediates[47,477]. The initial switch to Warburg metabolism may avoid build-up of potentially harmful oxygen free radicals from oxidative phosphorylation. Switching to Warburg metabolism is through activation of HIF-1α, the master regulator of the cell's hypoxic response. This transcription factor has a host of intracellular actions from which the glycolytic pathway is slowed further increasing the availability of intermediates for cellular proliferation[478]. Together these alterations in metabolic mechanics slow energy production but with the benefit of producing a wealth of intermediates for cell division. If the host survives the initial insult, a further switch back to oxidative phosphorylation occurs and inhibitors of Warburg metabolism are detectable[479]. Persistent inflammation results in fibrosis and CKD progression, an association is demonstrated in the current dataset and described later. The ability to deescalate inflammatory processes are fundamental to organ recovery and an inability to switch back from Warburg metabolism to oxidative phosphorylation results in worse organ injury[480].

TEC mitochondrial injury occurs early in sepsis[481]. TECs are capable of engulfing mitochondrial debris through autophagy and impaired autophagy is associated with TEC death and proximal tubular dysfunction[482]. This may act to remove ROS producing units which are harmful if left unchecked[462]. Repair mechanisms include the synthesis of new

mitochondrial units[481].

In summary, early metabolic switching may prevent cellular injury from damaged mitochondria, an example of tolerance and provides a wealth of useful intermediate metabolites. Later biogenesis restores sufficient functional mitochondria, biogenesis is an ATP requiring process via oxidative phosphorylation and therefore requires another metabolic switch, this time away from Warburg metabolism[459]. The parallels with perfusion here are key, early in the process there is a significant reduction in energy consumption during Warburg metabolism which would require less blood flow, whilst recovery and biogenesis are likely to have greater oxygen demands and necessitate increased perfusion.

11 AKI subphenotypes: A reassessment using data from the Microshock Renal study

11.1 Introduction

The reasons for a lack of progress in AKI studies are suggested to be multifactorial, ranging from comparison with flawed gold standards to reliance on outdated classification systems such as pre-renal, renal and obstructive[483,484]. [485]To better describe AKI, exploration of subphenotypes may identify common modifiable biological mechanisms, differences in treatment responses and enable targeted interventions for high risk patients, similar to advances in rheumatoid arthritis and asthma[170].

A clinical study by Bhatraju and colleagues used latent class analysis (LCA) to identify two distinct subgroups in hospital admissions with AKI, predominately sepsis, termed AKI-SP1 and AKI-SP2, where AKI-SP1 had lower levels of endothelial injury and inflammation. This study demonstrated a lower mortality and better recovery of renal function by 28 days in AKI-SP1[234]. The three-phased study found AKI-SP1 had better outcomes from the preferential use of vasopressin compared to noradrenaline, but not in AKI-SP2. The study considered clinical parameters, laboratory variables and biomarker levels after controlling for the severity of illness. Subphenotypes were best defined using a three-variable model of angiopoietin 1 and 2 ratio (Ang1:Ang2), soluble tumour necrosis factor-1 (sTNFR-1) and urinary interleukin-8 (IL8). Urinary biomarkers were not included in the study.

Due to the association between inflammation and renal hypoperfusion presented in chapter 10 and the differential response to vasopressors presented in the reference study, this

chapter looks for an association in the present dataset. The hypothesis examined is that different degrees of perfusion would be detectable between these subphenotypes.

11.2 Methods

To replicate the subphenotypes, admission levels of IL-8, sTNFR and angiopoietin ratios were compared with those previously published and are presented in Table 16. Cytokine levels were notably different between the two studies however. All patients in the present study had IL8 levels beyond those of either subphenotype described by Bhatraju. The lowest recorded IL-8 value was well above the range of the severe subphenotype in the reference study. Therefore in 50 sequentially admitted patients with septic shock, regardless of the presence of AKI, we were unable to detect any patients who could be classified as subphenotype-1 using admission values.

Variable	Bhatraju study populations						Microshock-Renal	
	SP	Discovery median (range)		Replication median (range)		VAAST median (range)	Severe AKI median (range)	Non-severe AKI median (range)
IL8 (ng/ml)	*SP1*	10.0	(5-21)	16.0	(10-26)	23.0 (13-47)	666 (167-1981)	159 (132-435)
	SP2	22.0	(12-55)	60.0	(28-149)	106 (49-345)		
ang 2:1	*SP1*	1.4	(0.7-3.2)	9.4	(3.3-25.5)	2.0 (0.7-2.8)	2.2 (0.92-7.5)	0.7 (0.5-1.2)
	SP2	18.1	(8.2-53.9)	87.1	(35.7-226)	10 (7-16)		
sTNFR (ng/ml)	*SP1*	6.8	(4.7-10.1)	10.6	(6.8-15.7)		26.0 (16.9-38.0)	12.7 (10.3-19)
	SP2	18.8	(12.7-30.9)	25.8	(16.1-36.2)			
SOFA	*SP1*	3		8			15	9
	SP2	7		11				

Table 16 Comparative data between the study populations of Bhatraju et al and the present study. Data is presented by variable and across study populations as median values. Subphenotypes are separated and data from the present study is presented on the right, by stage-3 AKI group and non-stage-3 AKI group. Variable (vars), subphenotype (SP), SOFA score (SOFA).

The severe AKI cohort was divided into equal size groups, those with more modest elevation

in inflammatory cytokine profiles as mild group (n=19) and the remainder as high group (n=18). Different thresholds to define the groupings were obviously needed but relied on the assumption that higher values in one study reflected higher values in the other. A cluster-graphic is presented in Figure 39.

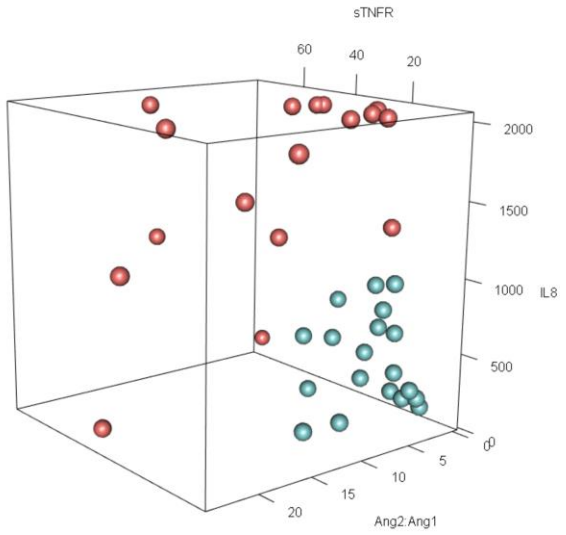

Figure 39 3D clustering of inflammatory groups. The mild inflammatory group (blue) clusters toward lower values and high inflammatory group (red) is more dispersed. Units (ng/ml).

11.3 Results

Table 17 demonstrates the lack of differences in cortical perfusion during early septic shock on days 0 and 1 but later group separation is seen. This is similar to the findings described in chapter 10 of inflammation and hypoperfusion later in the disease process, a finding which is not present on admission.

Variable	Day	High inflammatory group	Low inflammatory group	Significance (p)
Mean transit time (s)	0	8.3(4.8-17.9)	6.8(5.4-13.3)	0.506
	1	7.2(4.7-13.4)	8.1(5.1-13.1)	0.761
	2	6.9(5.5-17.8)	8.7(4.1-15.5)	0.437
	4	8.02(4.1-15.8)	5.06(3.9-7.3)	0.114
Perfusion index (au)	0	713(334-1374)	719(402-1792)	0.445
	1	642(397-1603)	891(618-1237)	0.486
	2	728.(375-1061)	1130(782-1844)	**<0.05**
	4	596(397-1500)	1716(847-2307)	**<0.05**
Relative blood vol (au)	0	5290(4067.5-7170)	5782(3621-10227)	0.668
	1	5946(3664-10369)	7352(5146-8902)	0.663
	2	5779(4937-8259)	8391(6222-10372)	**<0.05**
	4	5671(2982-6460)	8025(6696-9724)	**<0.05**
Wash-in rate (au)	0	494(258-989)	535(275-1230)	0.572
	1	432(299-1120)	639(479-849)	0.433
	2	522(336-717)	817(547-1322)	**<0.05**
	4	417(296-1185)	1225(636-1524)	**<0.05**

Table 17 Differences in cortical perfusion between high and low inflammatory groups

Macrovascular data demonstrated no difference in the cardiac output between patients with high and mild inflammatory profiles on any day of the study. Renal blood flow tended to be higher in the high inflammatory subgroup than the lower inflammatory subgroup – see Table

18.

Variable	Day	High inflammatory group	Mild inflammatory group	Significance(p)
CO	0	6±2.5	6.3±1.9	0.59
	1	6.7±2.0	5.9±1.4	0.16
	2	6.5±2.4	5.7±1.5	0.18
	4	6.1±1.8	6.4±1.7	0.69
Longitudinal trend (R) and significance (p)		0.01(0.9)	0.02(0.8)	
RBF (l/min)	0	0.9±0.5	0.8±0.4	0.39
	1	0.9±0.4	0.7±0.3	**<0.05**
	2	0.8±0.4	0.6±0.3	0.06
	4	0.8±0.4	0.7±0.4	0.76
Longitudinal trend (R) and significance (p)		-0.16(0.18)	-0.09(0.42)	

Table 18 Trends in haemodynamic variables in low and high inflammatory subgroups. No significant differences occurred over time or between groups.

11.4 Discussion

Subdividing patients into the pre-published subphenotypes was not possible using admission cytokine levels as they were far higher than the group defining values published by the reference paper[234]. The reason cytokine levels, particularly IL8 and TNFR were far higher in the present study population was probably due to the rapid fall from peak values seen after the day of admission. It is not clear how far into the Bhatraju study such values were measured, one of the reference study's cohorts describes admission values but no other temporal data is reported. Our data demonstrates the importance of timing such measurements, for example, day 2 IL8 values had dropped by 90% from the admission value and by a further 50% by day 4. TNFR dropped by approximately 50% between day 0 and day 4. Without temporal data it is impossible to replicate their findings. A clarification email was sent to the reference study author without reply.

Being unable to reproduce the pre-published subphenotypes, we explored the association between inflammation and cortical perfusion using thresholds specific to this study, assuming those with higher values would be reflective of higher values in the reference study. Renal perfusion values were similar between the two subphenotypes early on, but by day 2 and 4 the high inflammatory group demonstrated worse renal perfusion. Cytokine values between perfusion groups only differed later in the time course of AKI. To define subphenotypes using day 4 cytokine values would be most discriminatory, but clinically to wait until later in an admission to identify such patients would reduce the value of such a finding.

Much work has gone into describing subphenotypes in AKI, particularly following the widespread adoption of machine learning, looking for signals in large datasets. Experimental

data has demonstrated the upregulation of thousands of different genes but in two distinct profiles and with little overlap when comparing hypovolaemic and intrinsic AKI, with distinct biomarker profiles detectable in plasma and urine demonstrating a dissimilar pathogenesis[486].

A study published after the Bhatraju paper but from the same group identified a protective polymorphism of Ang2, suggesting a genetic predisposition to the hypo-inflammatory subphenotype[487]. Machine learning processes were applied to 29 biomarkers from 769 patients from the ASSESS-AKI study[488] and best identified the same two subphenotypes, AKI-SP1 with an increased incidence of cardiac failure and a favourable biomarker profile, whilst AKI-SP2 had increased endothelial injury, inflammation and elevated urinary biomarkers of tubular damage. AKI-SP2 demonstrated worse renal outcomes at 5 years. This is the first study to incorporate renal biomarkers in subphenotype assignment, demonstrating uNGAL, sTNFR-1 and urinary IL-18 amongst the most predictive[489].

A post-hoc analysis by a separate group also used latent class analysis across a greater number of biomarkers although in a relatively small population, finding biomarkers assessing endothelial injury and inflammation best identified subphenotypes[490]. A two-group model proved the best fit. Again, patients in a hyperinflammatory state with increased vascular permeability had an increased mortality and reduced renal recovery in comparison to those in a quiescent state. Further studies utilised data from electronic health records and unsupervised machine learning identifying two distinct clusters from 58 clinical variables in 1865 patients[491] and another identified three distinct clusters in 4001 patients using 2546 combined features[492]. Whilst the variables used to define the subpopulations were unique to each study, what is common to all these studies is the presence of lower levels of

inflammation and better renal outcomes in one subphenotypes compared to the other.

The more favourable biomarker profile, with less inflammation and relatively preserved perfusion may enable better renal outcomes in some patients with personalised treatment in AKI through selective vasopressor use. Bhatraju et al suggest this in the reference paper where vasopressin had a selective response in the mild inflammatory group. More work is required however to determine if renal perfusion assessment with DCE-US can add insight into the identification or treatment of such groups.

12 Biomarker Profiles and Renal Perfusion

12.1 Introduction

Clinical studies of AKI frequently yield disappointing results for a variety of reasons, but the limitations of traditional markers are partly responsible. Another reason for this disappointment is in treating AKI as a distinct disease, rather than a syndrome with multiple causes such as sepsis, hypovolaemia and ischaemia-reperfusion injury, but current markers are unable to differentiate. The early diagnosis of AKI, especially of a severity necessitating renal replacement therapy, progression to CKD and a higher risk of poor outcomes is important, but it is also difficult to identify. Moreover, the management involves early intervention which is also important as usual measures such as creatinine have a lag between injury and detection, hampering successful strategies. Much work has gone into describing novel biomarkers with better sensitivity and specificity for AKI and with earlier detection than creatinine. Individual markers are generated from different regions of the nephron as described in section 2.2 and can be largely categorised as enzymes, proinflammatory mediators, structural proteins, markers of filtration, hormones and tubular proteins[493]. Profiling multiple markers may help identify the site and mechanism of injury.

DCE-US has the potential to work as a functional assessment and predictor of AKI, much as the newer biomarkers do, but would require further work in assessing perfusion across the spectra of AKI causes. There is scant data in sepsis comparing renal perfusion to biomarkers as perfusion assessment in clinical study has previously not been practicable. This chapter aims to compare the two, looking for associations between specific markers and hypoperfusion, which may inform where the site of vascular alterations occurs, or at least

relevant associations. This chapter also explores the predictive power of DCE-US to determine those who go on to develop severe AKI.

To gain an understanding of the pathophysiological changes that occur with renal hypoperfusion, comparisons against multiple biomarkers are made, including markers of overall function (urine output), filtration (albuminuria, creatinine and PENK) and tubular injury (IGFBP7*TIMP2 and NGAL). These are assessed longitudinally as the pathogenesis of the condition is likely to demonstrate different phases, as described with the inflammatory and metabolic components of AKI in chapter 10. Correlations are sought between perfusion and biomarkers using perfusion index and day 0 results. The ability of perfusion variables to predict stage 3 AKI are assessed using ROCs and compared with biomarkers. PENK is analysed separately as the results were unexpected.

12.2 Results

Comparison of biomarkers with perfusion groups are provided in Figure 40. Patients were grouped according to perfusion status as described in section 5.2.2. Control data are provided alongside day 0 values for reference.

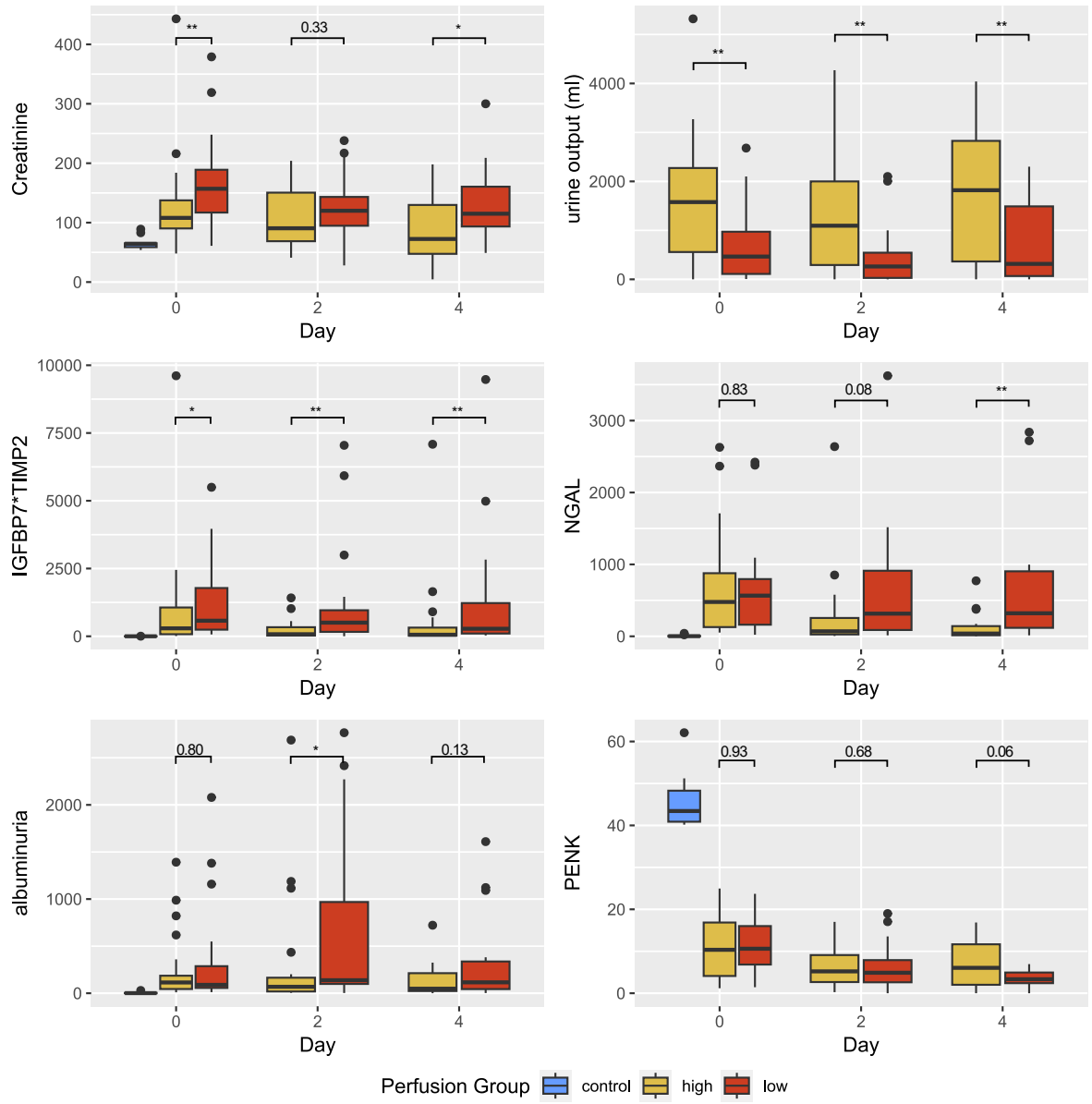

*Figure 40: Data comparing patients with higher and lower than average renal perfusion on admission to ICU. Boxplots demonstrate changes in levels over time. Serum creatinine levels (umol/l), 24hr urine output (ml), IGFBP7*TIMP2 (extreme outliers cropped), urinary NGAL ng/ml (extreme outliers cropped), urine albumin (mg/dl) and Proenkephalin A levels (ng/ml).*

The high perfusion group had significantly less tubular hibernation with lower IGFBP7*TIMP2 throughout the study and the strongest correlation with perfusion index, see Table 19. NGAL levels differed from day 2 onwards. Albuminuria tended to be higher in the low perfusion group with a significant spike by day 2. Creatinine was higher in hypoperfusors. PENK seemed non-discriminatory.

12.2.1 Correlation between DCE-US variables and biomarkers

Following normalisation, correlation coefficients are provided in Table 19 for the admission biomarker values. Perfusion index was used for the comparison, being one of the best performing DCE-US variables, mean transit time correlations were similar.

Biomarker	Correlation coefficient	Significance (p)
Creatinine	-0.34	<0.05
IGFBP7*TIMP2	-0.54	<0.05
uNGAL	-0.47	<0.05
Urinary albumin	-0.35	<0.05
Urine output	0.38	<0.05
PENK	0.31	<0.05

Table 19 correlation between biomarker and perfusion index on day 0

12.2.2 Prediction of AKI using DCE-US

The ability to predict severe AKI using DCE-US was assessed using receiver operator curves and compared to biomarkers. All four variables were assessed and curves are provided in Figure 41. AUROC was greatest for perfusion index (0.84, CI 0.73-0.96) and relative blood volume was least predictive (AUROC 0.73 CI 0.56-0.90). A two-factor multiple regression model was no more predictive than perfusion index or wash-in rate. Further factors did not

increase the predictive power of the model.

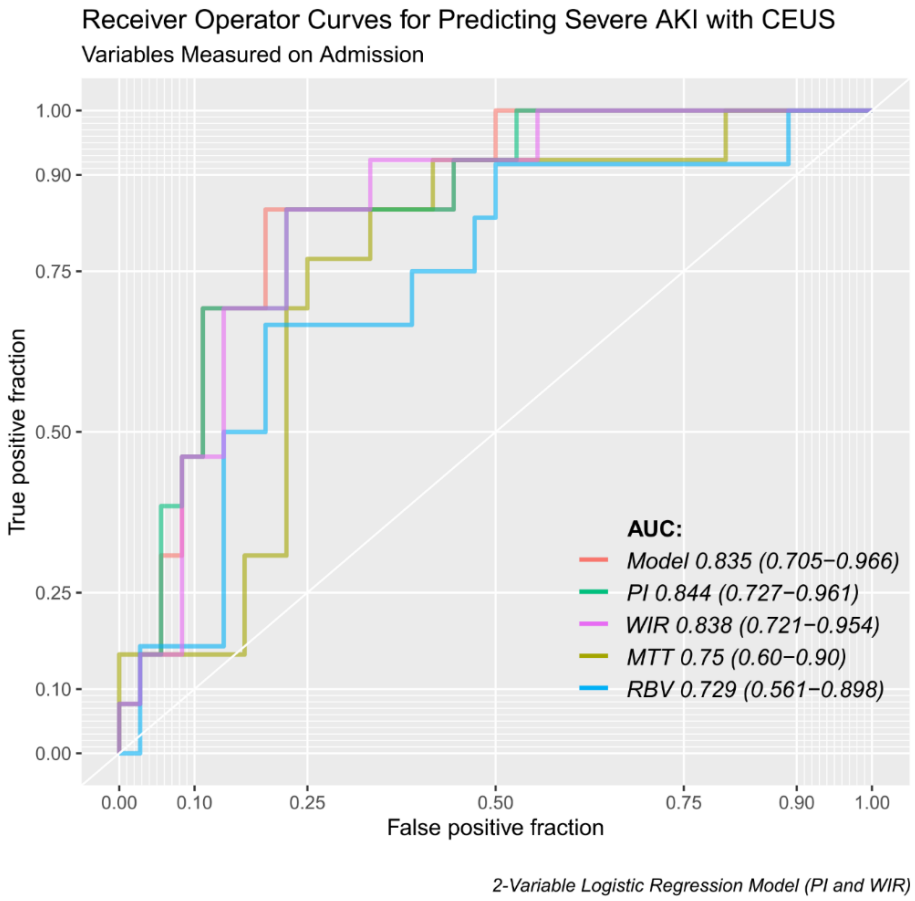

Figure 41 ROC analysis for DCE-US (CEUS) variables in the prediction of severe AKI. A linear model demonstrated no greater predictive power than single variables alone.

Existing biomarkers were used as comparitors for the DCE-US model. Both actual values and those normalised to urinary creatinine are reported in Figure 42. NGAL is reported in combination with urinary albumin and without. Urinary biomarkers normalised to urinary creatinine were consistently more powerful than non-normalised biomarkers. Admission normalised TIMP2*IGFBP7 demonstrated the greatest ability to predict stage-3 AKI (AUROC 0.959, CI 0.90-1.0).

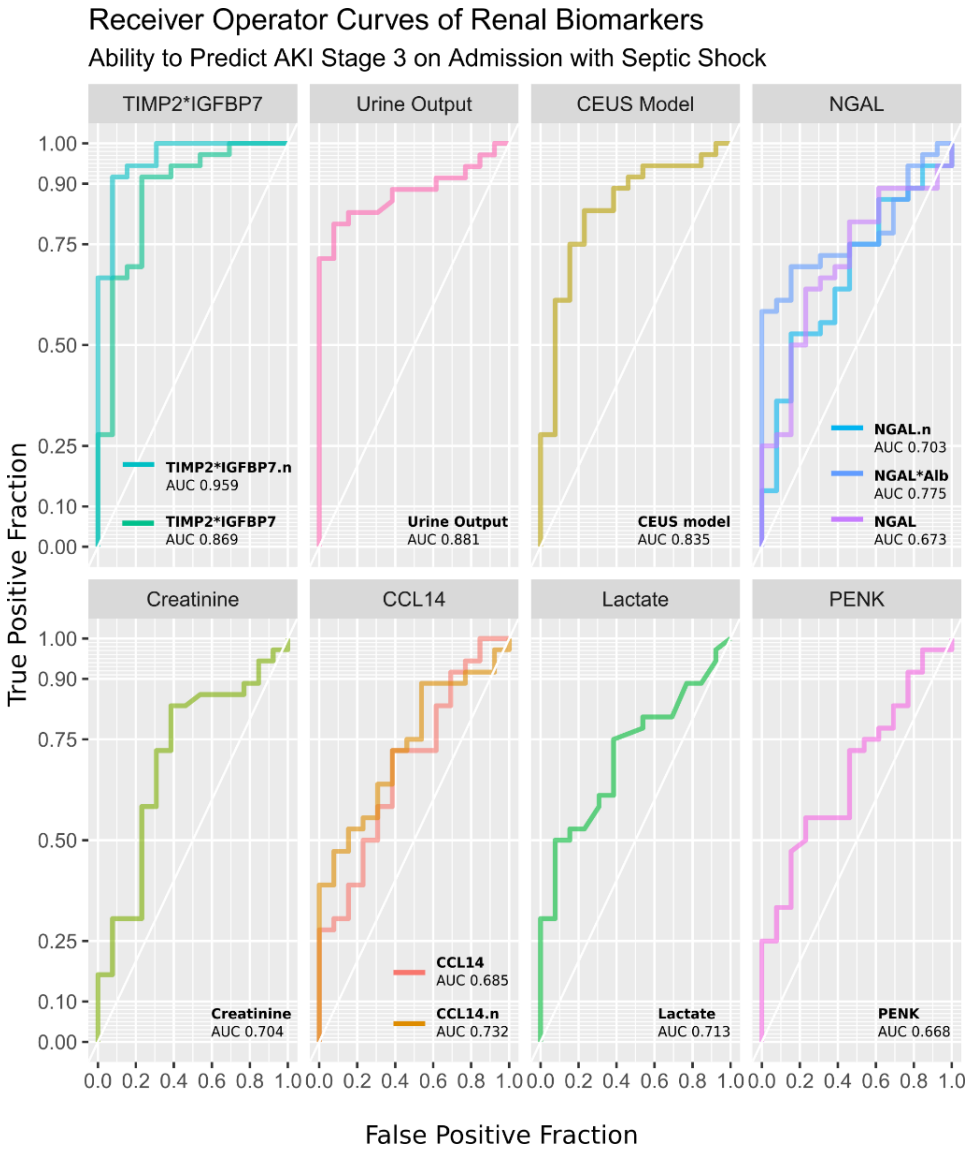

Figure 42 ROC charts of predictive power of admission biomarker levels to detect severe AKI in septic shock. Contrast ultrasound (CEUS) model is presented alongside conventional and novel biomarkers.

12.2.3 Proenkephalin A

PENK, a recently described biomarker of filtration has been shown in multiple studies to have a close inverse correlation with GFR, with lower values representing higher filtration rates[201–203]. However observations in this study failed to replicate these findings. Although no gold standard for filtration was used, this study identified higher values in healthy controls and patients without severe AKI which is contrary to what was expected. It correlated poorly with creatinine although both reflect filtration and showed a positive correlation with urine output. Levels did not correlate with markers of tubular injury or duration of RRT but had unexpected correlations with haemaglobin and platelet levels, see the mixed graphic in Figure 43 which presents the salient data.

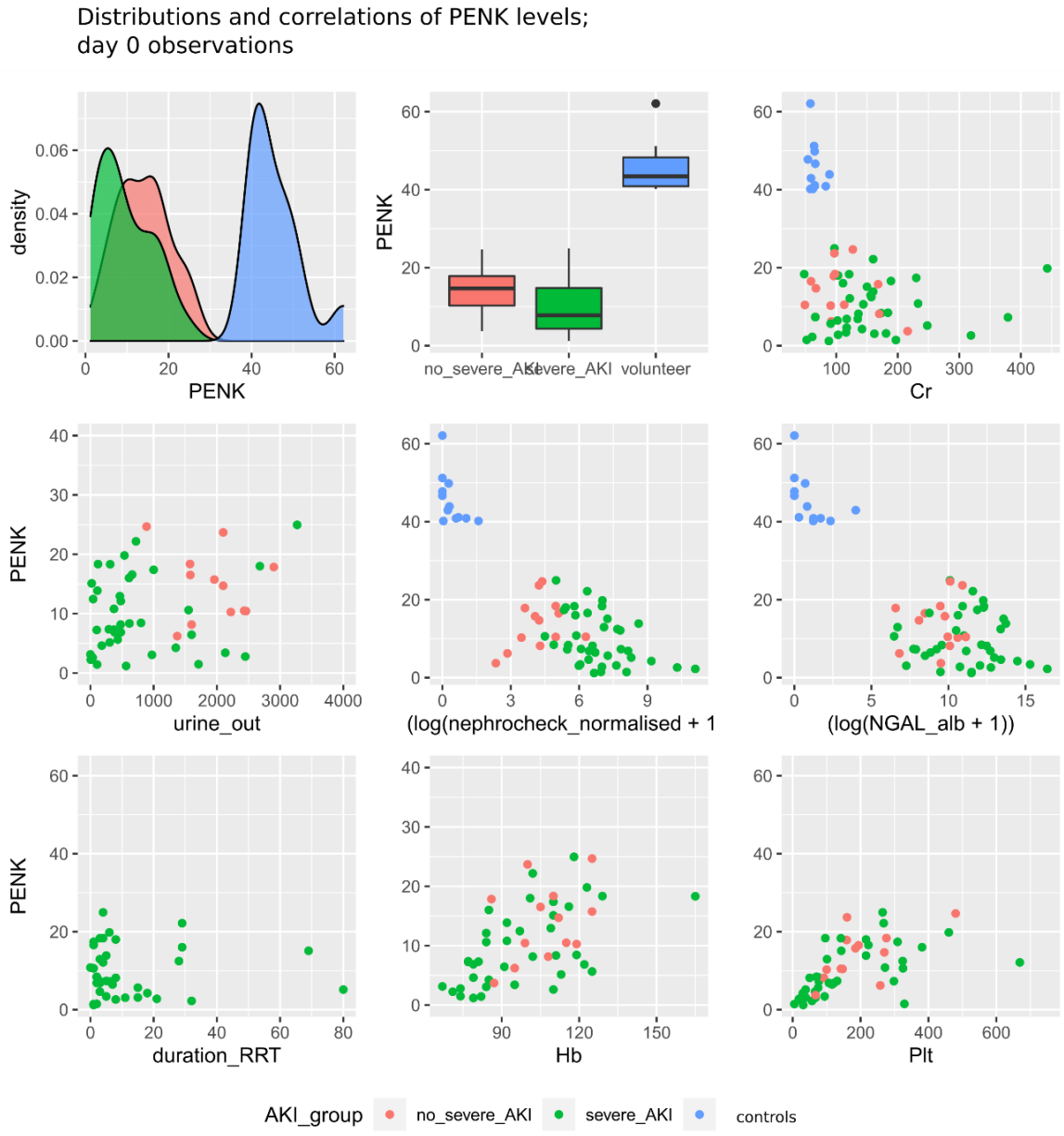

*Figure 43 Mixed graphic summarising the key findings of proenkephalin-A (PENK) values. Observations from day 0. Density and boxplots demonstrate data distribution between groups with higher values in volunteers and little separation between patient cohorts. No correlation exists with urine output, creatinine, markers of tubular injury or duration of RRT. However correlations were seen with haemgolobin and platelet levels. Creatinine (cr); 24 hour urine output (urine_out); log-transformed TIMP2*IGFBP7/uCr (log(nephrocheck_normalised+1)); log-transformed uNGAL*uAlb (log(NGAL_alb+1)); duration of RRT in days (duration_RRT).*

12.3 Discussion

Patients with cortical hypoperfusion had impaired renal function immediately on admission to ICU, demonstrated by higher creatinine values and lower urine output on day 0. Tubular alterations were detectable in all, but values were higher from admission in those with hypoperfusion.

By day 2 creatinine was no different between groups likely due to the frequent use of RRT in the low perfusion group reducing plasma values. Urine output remained significantly lower in this group and tubular cell cycle arrest was greater. NGAL values had decreased significantly in those with preserved perfusion, but persisted in those with hypoperfusion, suggestive of an ongoing tubular injury in the hypoperfused group which had largely resolved in the others. Albuminuria levels rose in the hypoperfusion group between day 0 and day 2. Albuminuria is largely reflective of the glomerular basement membrane and the adequacy of its permselective function[494,495]. Glomerular function appears to be disrupted by day 2 in those with hypoperfusion, a finding which is further supported by the early increase in syndecan in these patients described in chapter 10. Syndecan elevation is indicative of glycocalyx injury and injury to the glomerular glycocalyx permits albumin to pass through[453,454]. This has previously been shown to have an association with hypoperfusion in experimental study[453].

By day 4 overall function remained worse in the hypoperfusion group with lower urine output and higher creatinine values. Tubular injury persisted with greater cell cycle arrest and injury markers. Albuminuria levels had decreased by day 4 in the hypoperfusion group and was no

longer significant between the two groups.

As was the case with the persistence of hypoperfusion, tubular biomarkers remained elevated for the duration of the 4-day study period in patients with severe AKI, whereas those without severe AKI saw an early peak but a more rapid improvement in both biomarkers and perfusion. Renal alterations in sepsis are therefore immediate, but continue in those who manifest severe AKI, whilst those who do not get severe AKI also have an early peak but then see these biomarkers fall, much as they do in AKI following cardiac surgery[496]. This persistence of alterations in both perfusion, tubular inactivity and injury points to an ongoing process in sepsis associated AKI. This is coupled with a late association with inflammation in such patients as described in chapter 10.

12.3.1 Predicting AKI

At present biomarkers cannot be used to guide renal interventions, such as volume administration or removal, or selectively use vasoactive drugs. Functional imaging therefore has a potential role in both early detection of AKI and to guide management strategies. Ultrasound lends itself to this, being a standard of care in AKI investigations, cheap and commonplace at the bedside. One commonly used ultrasound measure, resistive index, presented in chapter 8 did not differ between patient groups in this dataset, which agrees with other studies which found it largely unhelpful in differentiating outcomes [79,80]. The ability of DCE-US to predict severe AKI was assessed in the current study. RBV was inferior to the other DCE-US values, whilst perfusion index was most predictive (AUROC 0.84). Although outperformed by TIMP2*IGFBP7, DCE-US was more predictive than the remaining biomarkers, both standard and novel.

DCE-US prediction is imperfect however, the potential reasons for which are multiple. It could be that some patients with normal perfusion still develop AKI, or the commencement of some patients who did not get severe AKI being started on RRT diminished the outcome measure. Another possibility is that the technique itself needs refinement with intra-user variability; some patients would therefore have been assessed as impaired, where perfusion was maintained and vice versa. If this is the case, further development of the technique would help improve its predictive performance.

12.3.2 Normalisation to urinary creatinine

In this study urine output ranged from oligo-anuria to polyuria despite stage 3 AKI and it was logical to report both referenced and crude values. We observed extreme elevation of biomarkers in patients with severe AKI however, making the referencing argument partly academic; essentially if these values rise, they seem to rise by a magnitude that normalisation to urinary creatinine may not be necessary.

12.3.3 PENK

PENK performed poorly in the present study, providing conflicting results. Measurement of filtration in AKI is difficult because RRT removes plasma biomarkers. PENK has previously demonstrated a close inverse correlation with gold-standard GFR measurements and thought superior to creatinine in reflecting measured GFR[202]. We measured PENK values in this study to gauge the association between filtration and perfusion but values were significantly higher in controls and a positive correlation was demonstrated with urine output which was

unexpected. PENK demonstrated weak negative correlations with markers of tubular injury and an unexpectedly strong positive correlation with haemaglobin and platelet values. As a result, we failed to replicate the findings of studies from the group who initially described it[202,203]. It is not clear why PENK performed poorly and it warrants repeat in other before conclusions are drawn.

13 Renal hypoperfusion is associated with an increased risk of death and a prolonged duration of RRT

13.1 Introduction

There is a clear association between severity of AKI and mortality regardless of the pathogenesis in multiple retrospective studies[25,497–500] and recently confirmed in a large prospective study, ASSESS-AKI [501]. Odds ratio for in-hospital mortality are 1.7-2.5 for mild, 2.9-5.4 for moderate and 6.9-10.1 for severe[28,498]. Following survival to discharge, mortality risk remains longer-term[502], mainly dying from cancer and cardiovascular disease[503]. If fully recovered and without proteinuria at three-month follow-up mortality risk returns to normal however[501], particularly in those who recover rapidly[504]. 50% of patients with severe AKI will completely recover and 13% will partially recover[40].

Relapsing AKI is common, especially within 72 hours of recovery and increases the risk of death 5-fold[208]. AKI non-recovery and CKD are a risk in all AKI episodes, but the risk increases in those with more severe AKI, older patients, those with CKD and more episodes of AKI[505–508]. Those who do not recover have an increased risk of death. Figure 44 presents data from an observational study by Wang et al in 20,000 patients, demonstrating the highest risk of death in patients requiring RRT[509]. Whether timing of RRT makes a difference to chronicity is controversial, but on balance probably makes no difference[510–513].

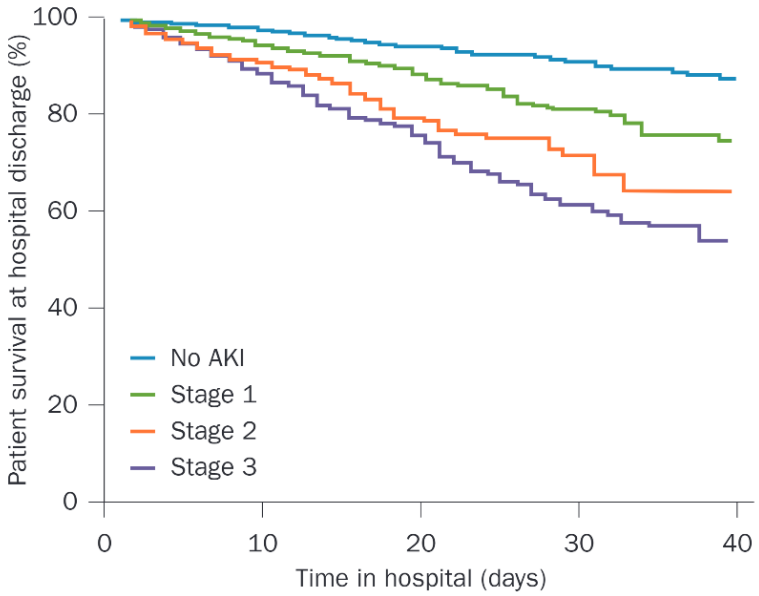

Figure 44 Kaplan-Meier graph for hospital survival by KDIGO AKI stage. Taken from Wang et al.[12,509]

Patients with a greater reduction in renal perfusion seem to have persistent renal injury, data presented thus far demonstrates an association with both an inflammatory signal beyond 48 hours and persistent and greater elevation in damage markers. Experimental studies point to the interrelationship between hypoperfusion and AKI development and severity[323,360,361,514,515]. To assess this association parameters were compared with outcome data from ICU including the duration of RRT, change in GFR after ICU discharge and chemokine (C-C motif) ligand-14 (CCL14). As described in General Methods, CCL14 is a small cytokine predictive of persistent AKI.

13.2 Results

Differences in admission values of CCL-14, perfusion indices and IGFBP7*TIMP2 were used to assess those who would have a persistent RRT requirement, this data is presented in Figure 45. Patients who never received RRT were classified in the <7 days group, whereas those who died were classified in the ≥7 days group (<7 days n=25, ≥7 days n=25). CCL-14 tended to be higher in the ≥7 days group but did not reach significance (p= 0.097), both perfusion variables and cell cycle arrest markers were significant (p<0.05). Note log transforms on y axis for biomarkers. A similar analysis generated from receiver operator characteristics is presented in Table 20.

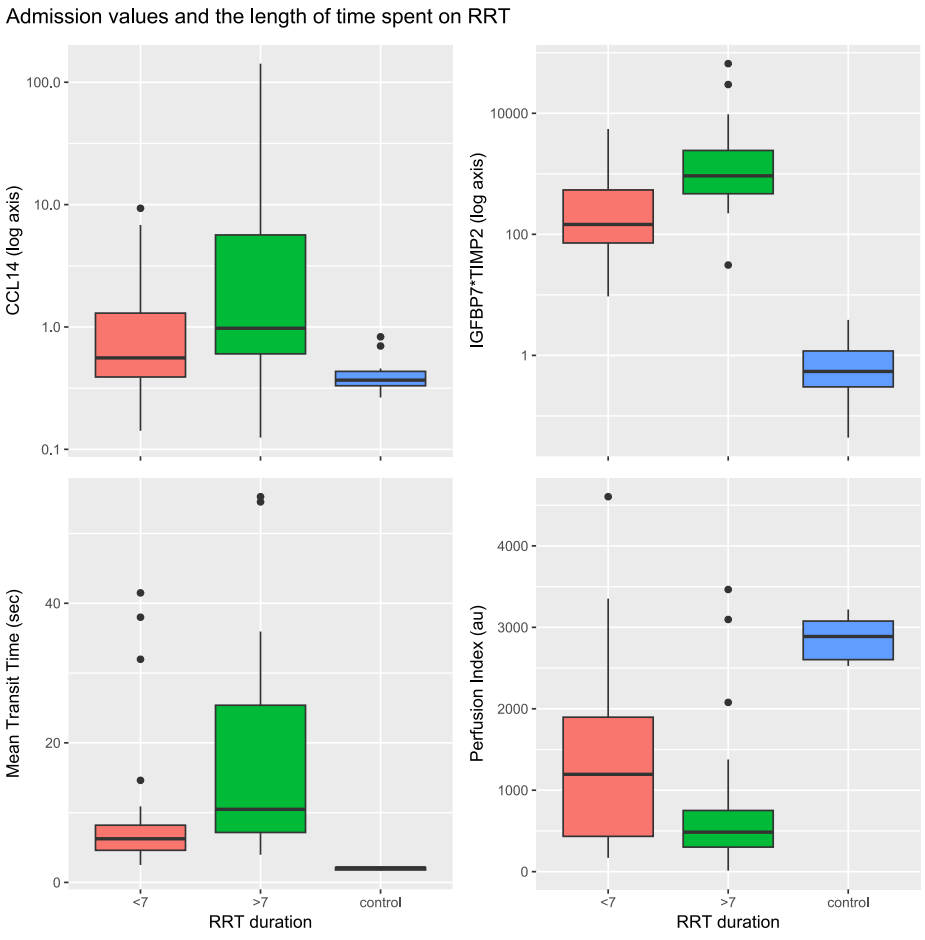

*Figure 45 Ability of admission biomarkers to predict RRT requirement for greater than or equal to 7 days (green), les than 7 days (red) and controls (blue). Note logarithmic y axis scales for CCL14 and IGFBP7*TIMP2 for ease of plotting extreme outliers*

Variable	AUROC (95% CI)
Mean transit time	0.73(0.57-0.87)
Perfusion index	0.69(0.54-0.85)
IGFBP7*TIMP2	0.79(0.67-0.93)
CCL14	0.61(0.45-0.77)

*Table 20 Ability of admission MTT, PI, IGFBP7*TIMP2 and CCL14 values to predict an RRT requirement beyond 7 days*

13.2.1 Alterations in baseline function

To assess long term functional impairment, baseline creatinine values before admission and after discharge from ICU were used to define those with worse function (n=15) and those who were not worse (n=16). 7 patients lacked a pre- or post-discharge creatinine and 12 died. Neither the two biomarkers (CCL14 p=0.24, IGFBP7*TIMP2 p=0.67) or perfusion based variables (MTT p=0.32, PI p=0.45) were able to predict patients who would go on to have impaired function after discharge, Figure 46 refers.

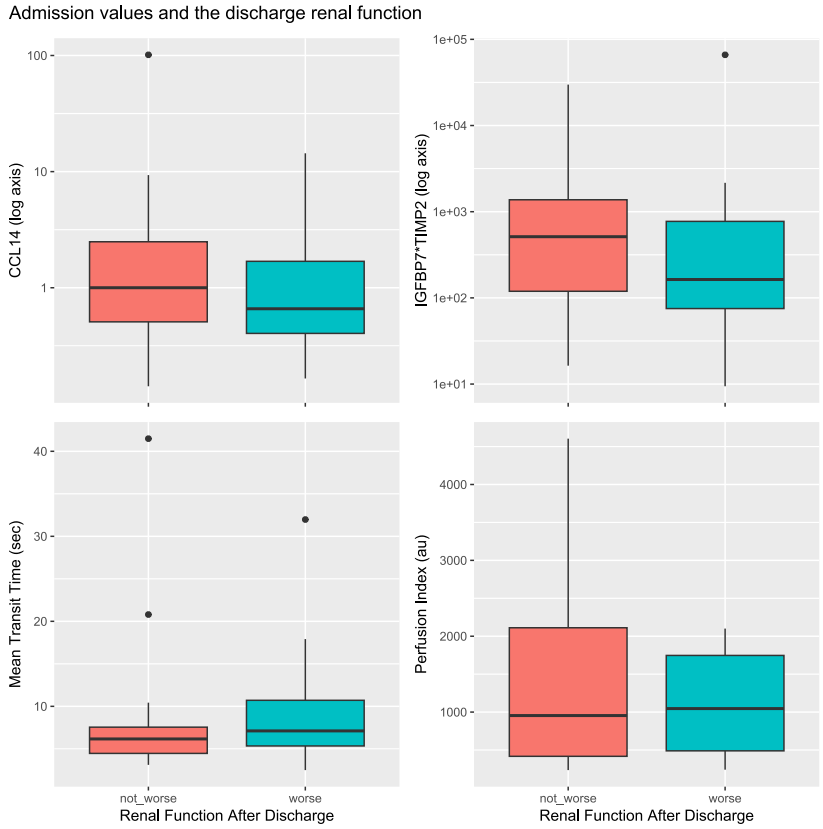

*Figure 46 Admission IGFBP7*TIMP2, CCL14, PI and MTT values and the ability to predict patients who would have higher creatinines after discharge.*

13.2.2 Outcome data for patients with better or worse renal perfusion

Survival and freedom from RRT plots were drawn for those with above and below average renal perfusion and are presented Figure 47. Patients with above average renal perfusion on admission were more likely to survive ($p<0.001$). 11 patients with maintained perfusion required RRT (46%), vs 23 lower perfusors (92%), $p<0.01$. Patients who required RRT required it for a longer if renal perfusion was poor on admission ($p<0.05$).

We also noted similar outcome data for extreme TIMP2*IGFBP7 values. Of the five patients with the greatest values by day two, only one survived to day four.

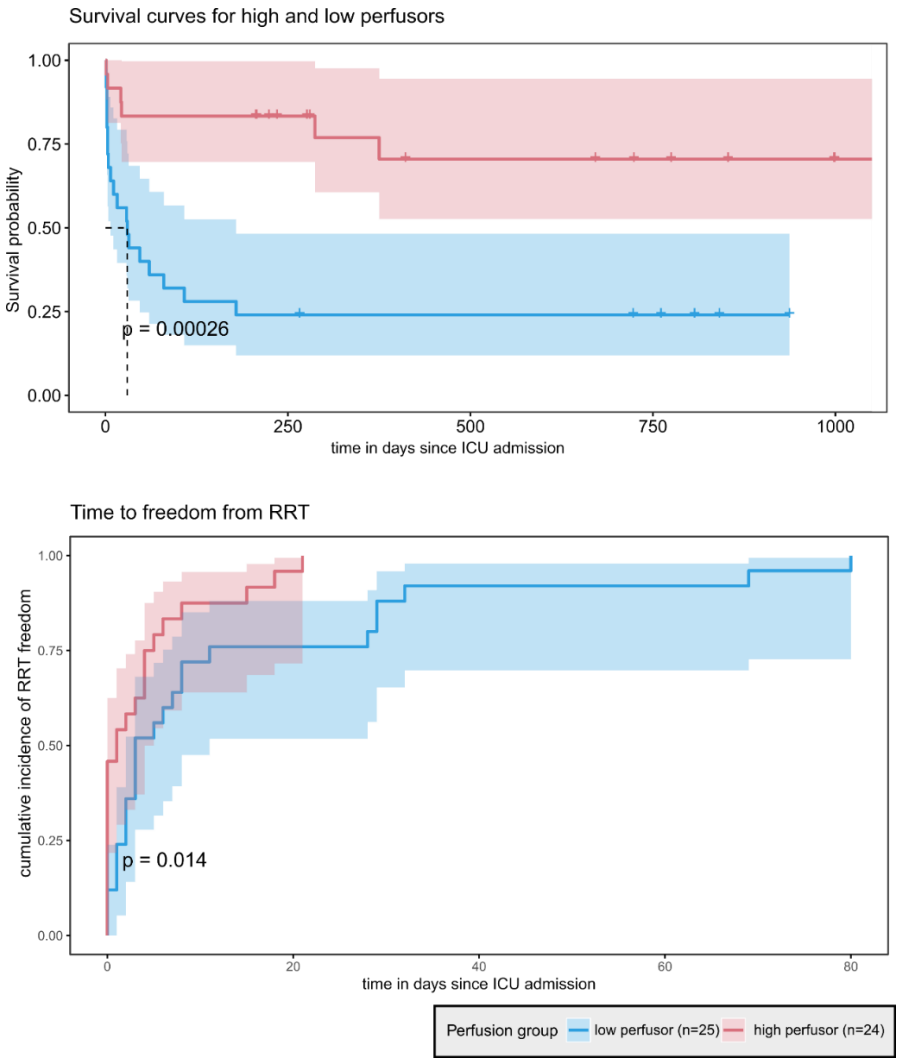

Figure 47 Kaplan-Meir curves for high and low perfusion groups, probability of survival (top); cumulative incidence of freedom from RRT (bottom).

13.3 Discussion

To determine whether severe impairment in cortical perfusion increased the chances of long-term injury, admission renal perfusion values were compared to the length of time spent on RRT and the delta between the pre-admission and post-discharge creatinine values. Levels of TIMP2*IGFBP7 and CCL14 were used as comparators to the assessment of perfusion; CCL14 predicts persistent injury[170,210–212] and TIMP2*IGFBP7 being one of the best performing biomarker available for predicting AKI[493]. An RRT requirement beyond 7 days provided an endpoint at which the risk of progression to CKD increases, hence the requirement for the newly adopted term acute kidney disease (AKD)[209], it also fortunately provided equal group sizes in the present study. Patients who never received RRT were included in the <7 day group, as all patients in our study had some degree of renal injury, even if it was subclinical.

Admission perfusion values, TIMP2*IGFBP7 and CCL14 were predictive of AKD. The same findings were demonstrated in the survivability plots, where patients with renal hypoperfusion were more likely to require RRT and if needed, were more likely to require it for longer. Such patients are therefore at an increased risk of AKD and by inference CKD[209]. Patients with hypoperfusion were also more likely to die acutely and this finding was again true of cell cycle arrest markers with only 20% survivability for those with the highest values in the current data. This finding of cell cycle arrest markers with not only AKI but death echoes previously published findings[195].

Following AKI, the likelihood of CKD increases up to 30-fold[48], the increasing risk dependent on factors related to the acute injury such as severity, although the mechanisms dictating severity are unclear. Duration also has a clear association with progression, prompting the

adoption of the AKD term to signify this[240]. Non-modifiable risk factors for progression include underlying pathology, gender, race and age, as pre-existing disease and age-related nephron loss are common[516]. In addition, older patients have a greater proportion of senescent immune cells secreting cytokines which promote a chronic inflammatory state[517] and chemokines associated with fibrosis, potentially contributing to the abnormal repair mechanisms of the aged kidney and increasing the likelihood of CKD[518,519].

Recovery from tubular injury is dependent on regeneration of TECs, either from multipotent cells scattered along the nephron[520] or from mature TEC dedifferentiation, replication and redifferentiation[521]. If renal injury is severe enough progenitors are lost, irreversible nephron damage ensues and as a result, the mass of lost nephrons is proportional to the severity of CKD[522]. Maladaptive repair may occur from tubular cells remaining dedifferentiated and producing profibrotic factors[523]. In addition to TECs, M2 phenotype macrophages are frequently identified in injured peritubular and glomerular capillaries, responsible for removing cellular debris, providing support to epithelial cell proliferation and promoting healing. M1 macrophages have been demonstrated to switch to an M2 phenotype during recovery[466] whilst TLR-4, the pro-inflammatory PRR in early AKI interestingly switches to promote repair in the later stages[524]. CCL14 is involved in macrophage recruitment, activation and maladaptive repair, probably why it is a useful marker of progression[211]. Its function in the kidney is not fully elucidated, it is not expressed in rodents preventing experimental study, but higher values demonstrate increased macrophage signalling. Its association with persistent AKI was demonstrated in the RUBY study and a post-hoc analysis of the Sapphire study[210,211]. We were unable to replicate the strength of the association in these studies, which demonstrated AUROC of 0.83 and 0.81

respectively for predicting persistence of 7 days or beyond. Admittedly these studies used larger datasets, although the frequency of persistent AKI was much lower, 50% in the present study vs 33% and 15% respectively.

The comparison between baseline renal function before and after ICU discharge showed no difference, as is often the case in such an assessment. It points to one of the limitations of renal assessments using current clinical methods. Despite the true loss of functioning nephrons, clinically assessed renal function frequently recovers in the short to medium term. TECs hypertrophy in unaffected nephrons, increasing their functional capacity, a process known as polyploidization[522]. In addition, hyperfiltration by remaining nephrons, recruitment of the renal reserve and the inadequacy of creatinine to detect subtle functional loss at high GFRs account for some of this. The loss of muscle mass following critical illness provides a non-renal cause for a lack of signal in this analysis. Longer term data, over months to years, formal assessment of GFR or proteinuria quantification after discharge would be helpful in future studies if long term outcomes in hypoperfusion were examined again.

14 Patients with COVID-19 associated acute kidney injury have reduced renal perfusion and reduced renal blood flow despite preserved cardiac output. A case-control study

14.1 Introduction

Alpha variant COVID-19 swept through the United Kingdom in early 2020, causing pressures on hospitals not known in modern times. In those who developed critical illness, acute kidney Injury (AKI) complicated a substantial proportion. Data from Wuhan, China reported the AKI prevalence to be between 5% and 29% in intensive care[525,526], however, Western data suggested AKI complicated a greater proportion, approximately 27-40% of COVID-19 ICU admissions[527,528].

AKI regardless of severity is an independent risk factor for death in critical illness from multiple causes, including COVID-19, with greater mortality associated with more severe kidney damage[525,527]. The AKI which developed because of COVID-19 occurred predominately at the onset of ventilation[529], with an increased risk in men, the elderly and with greater acuity of illness[530]; the use of catecholamines was associated with an odds ratio of 19.4 for AKI in one study[531]. Researchers have sought a specific renal injury or glomerulopathy as a result of SARS-CoV2 but no clear evidence has been corroborated. Early post-mortem data reported the presence of viral inclusion bodies within tubular epithelial cells[532], although a later report demonstrated these findings to be non-specific components of the endosomal pathway[533]. Acute tubular injury, micro-infarctions and focal segmental glomerulosclerosis have all been identified, but such findings have been demonstrated in other viral illnesses including HIV,

HTLV-1 and EBV[534–536].

As the pandemic continued it became evident that pre-renal injury may have been contributing to the renal damage, Hirsch et al demonstrated urine sodium <35mmol/L in 66% of patients with AKI, supportive of this hypothesis[537]. Thus, a vascular aetiology from hypovolaemia, haemodynamic compromise, venous hypertension from ventilatory pressures and endotheliitis were likely candidates rather than a novel pathogenesis[538].

The aim of the current study was to measure RBF and renal cortical microcirculatory perfusion in patients with COVID-19 and established AKI. These could then be used as a patient comparator group to those in the Microshock Renal study, both groups having established AKI and being critically ill, but from different aetiology, to understand whether alterations in renal haemodynamics and perfusion were unique to either process.

14.2 Materials and Methods

14.2.1.1 Study design

A prospective observational case-control study utilising renal ultrasound, DCE-US and trans-thoracic echocardiography performed at a single time point in critically ill patients with COVID-19 and KDIGO stage 3 AKI, patients with sepsis associated AKI and healthy controls were used as comparators. This study was undertaken in April 2020 when alpha-variant SARS-CoV2 was the dominant strain in the UK.

14.2.1.2 Ethical Approval

Approval for this study was obtained from the Yorkshire and Humber (Leeds East) Research Ethics committee (18/YH/0371); deferred patient consent for data usage was sought on recovery with an emergency waiver of consent at the time of study.

14.2.1.3 Patient selection

- COVID 19 group: Adult patients admitted to ICU with confirmed positive SARS-COV-2 infection and KDIGO stage 3 AKI treated on one of the intensive care units of King's College Hospital, London. This was an opportunistic study undertaken at the height of the pandemic. As result all patients were recruited and studied on the same day, selecting as many eligible patients as possible.
- Septic shock group: Adult patients with suspected or confirmed infection, a requirement for vasopressor therapy and a lactate > 2 mmol/L after fluid resuscitation and stage 3 AKI. All patients in this cohort had been admitted to the ICU for four days

with the data taken from the Microshock-Renal study described in chapter 4.

- Healthy controls

14.2.1.4 Exclusion criteria

Patients were excluded if they had a body mass index greater than 40kg/m^2 due to the likelihood of poor ultrasound image quality, other exclusion criteria included known chronic kidney disease (CKD) stage 4 or worse or renal transplantation, ultrasonographic appearances of CKD (bright, shrunken kidneys (<8cm length)), severe pulmonary hypertension (>90mmHg) or an intolerance to SonoVue contrast agent.

14.2.1.5 Sample Size

This study was exploratory and undertaken during a pandemic with no prior data from which to predict appropriate sample sizes. A convenience sampling method was used based on what was achievable in the given period.

14.2.1.6 Renal Dynamic Contrast Enhanced Ultrasound (DCE-US) and measurement of RBF

The acquisition and analysis process were identical to that described in Microshock Renal, see section 4.2

14.2.1.7 Transthoracic echocardiography

Contemporaneous transthoracic echocardiography measurements were made alongside renal ultrasound and DCE-US assessments. Assessments of biventricular and valvular function

was necessary to ensure confounding from severe cardiac disease did not occur. Indices including pulmonary artery systolic pressure, right ventricular s prime velocity, TAPSE and cardiac index were used to inform the comparison. The method was identical to the Microshock Renal Study.

14.2.1.8 Outcome Measures

The primary outcome measure was a difference in DCE-US variables between patients with COVID-19 and septic shock, secondary differences in cardiac output, renal blood flow, resistive index and other macrohaemodynamic variables were assessed.

14.2.1.9 Statistical analysis

Distribution of data was assessed using the Shapiro-Wilk normality test. Parametric data is reported as mean±SD and non-parametric as median (Q1-Q3). Differences between 3 or more groups were assessed using Kruskal-Wallis test or analysis of variance. Statistical analysis and graphical data was generated using R version 4.0.3. P values of <0.05 were taken to indicate significance.

14.3 Results

14.3.1.1 Patient Characteristics

Characteristics of patients at the time of study enrolment are shown below in Table 21.

	COVID-19 (n=10)	*Septic Shock (n=13)*	*Control (n=12)*	*p value*
Age	60±7	56±18	32±3.9	<0.01 vs control Pts p=0.43
Gender	7 Male (70%)	10 Male (77%)	5 Male (42%)	0.14
Co Morbid (DM)	4 (40%)	4 (30%)		0.68
Co Morbid (BP)	7 (70%)	6 (46%)		0.40
Co Morbid (CVS)	3 (30%)	0 (0%)		0.17
Co Morbid (Resp)	2 (20%)	2 (15%)		0.41
Co Morbid (any)	10 (100%)	11 (84%)		0.48
Documented CKD stage 3	1 (10%)	3 (23%)		0.60
Baseline Creatinine(μmol /l)	89±5	74±6	65±10.8	0.02 COVID vs control
Baseline GFR (ml/min)	73±4	76±4		0.58
Days since symptoms	23±8	NR		NA
ICU day	10 (7-16)	4 (4)		<0.0001
Duration of RRT	6 (2-9)	4 (3-4)		0.10
SOFA score	16±2	14±4		0.02
HR (beats/min)	88±11	86±16		0.72
MAP (mmHg)	80 (74-88)	76 (69-83)		0.25
CVP (mmHg)	13.1±4.9	12.3±4.5		0.68
Norepinephrine dose (mcg/kg/min)	0 (0-0.07)	0.02 (0-0.2)		0.47
Other inotropes	0 (0%)	4 (30%)		0.10
Lactate (mmol/l)	1.0 (0.9-1.4)	1.6 (1.1-1.9)		0.07
WCC x 10^9 /L	17.8 (11.9-26.3)	16.9 (10.5-26.7)		0.72
CRP (mg/L)	207±136	164±107		0.38

Table 21 ***Demographic and baseline patient characteristics at time of study enrolment.*** *Co-Morbidities: CVS: Ischaemic heart disease, chronic heart failure, chronic dysrhythmia; BP: hypertension; DM: diabetes mellitus type 1 or 2; Respiratory: asthma, chronic airways disease; any: all recorded co-morbidity including those listed above. CKD chronic kidney disease, GFR glomerular filtration rate, SOFA Sequential Organ Failure Assessment, HR heart rate, MAP mean arterial pressure, CVP central venous pressure, WCC White Cell Count, CRP C-Reactive Protein, RRT renal replacement therapy. Values expressed as mean±SD or median(Q1-Q3)*

12 patients with COVID-19 were recruited but DCE-US image quality was poor in 2 who were

not analysed. Patients with COVID-19 had a greater burden of organ dysfunction and had been in the ICU longer than those with septic shock. The patient groups were otherwise similar, including baseline renal function. All patients had stage 3 AKI and were dependent on CRRT, there was no difference in the duration of RRT. Patients in the septic group had a higher urine output in the preceding 24 hours than COVID-19 patients (706±716 v 155±199ml, p 0.01). The fluid balance for the preceding 24hrs before measurements was more negative in the septic group (-597±750 v 1493±1583 ml, p <0.05) but the overall balance was no different (covid 5.7l±5.0 v septic 8.9l±4.8, p 0.12).

14.3.1.2 DCE-US Derived Renal Perfusion Variables

DCE-US derived perfusion parameters are shown in Figure 48. Other than the relative blood volume, all measures of cortical perfusion were reduced compared to controls in both patient groups and values were lower in the covid group than those with sepsis, but this did not reach significance. Data dispersion appeared greater in the septic group.

14.3.1.3 Macrovascular indices

Cardiac output was higher in patient groups than controls (covid 3.58(3.38-3.83)l/min vs septic 3.56(2.53-3.94)l/min vs controls 2.73(2.25-2.87)l/min; covid v control p<0.05, septic v control p= 0.05) but no different between patient groups. RBF was not different between the three groups. Resistive Index (RI) was different between all three groups, highest in covid, then sepsis then controls. Figure 48 refers.

14.3.1.4 Right heart and venous assessment

Values are presented in Figure 48. Right heart pressure were higher in patients, likely due to the presence of positive pressure ventilation in these groups, but function was not impaired and if anything the right ventricle was hyperdynamic based on RV s prime values in the patient groups (covid 19.8(15.5-21.4)cm/s, septic 16.6(14.1-20.4)cm/s, normal range minimum = 10cm/s).

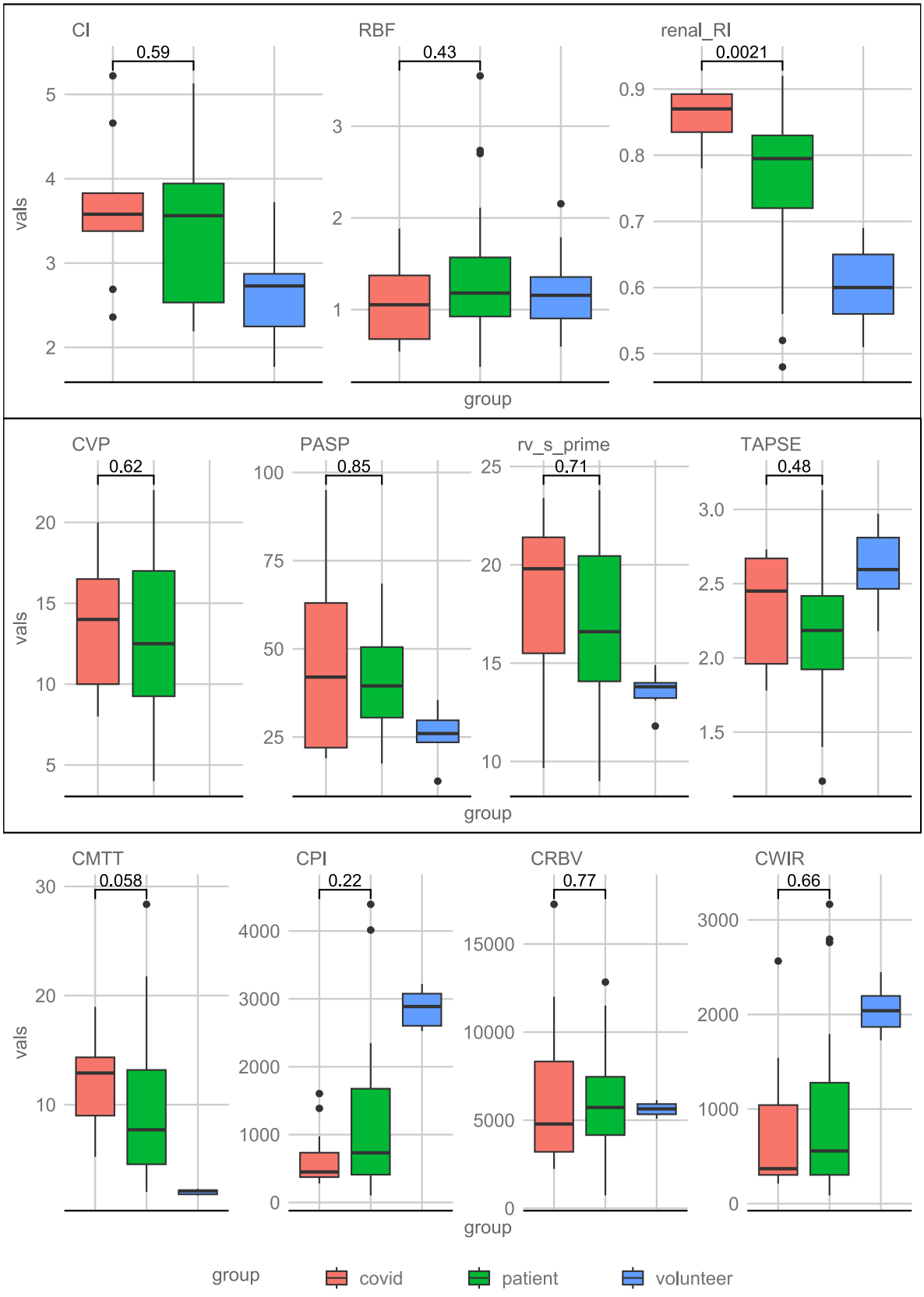

Figure 48 boxplots comparing patients with sepsis, covid and controls. Upper box cardiac index (CI), renal blood flow (RBF), resistive index (renal_RI). Middle box: central venous pressure (CVP), pulmonary artery systolic pressure (PASP), right ventricular s prime velocity (rv_s_prime), TAPSE. Lower box mean transit time (CMTT), perfusion index (CPI), relative blood volume (CRBV), wash-in rate (CWIR). P values are provided in the figure between patient groups. Controls are in blue providing reference data.

14.3.1.5 Long term outcomes

Mortality in the sample cohort was 60% for COVID-19, vs 26% for patients with septic shock (p=0.4). Of the surviving patients, the median time to recover renal function for COVID-19 was 54 (19-65) days vs 7(6-15) days for septic shock (p<0.05). The median ICU stay for survivors with COVID-19 was 52 (49-56) days vs septic shock 14(11-46) days (p<0.05).

14.4 Discussion

There is a significant reduction in renal perfusion in COVID-19 like the alterations seen in sepsis associated AKI, although marginally worse. The sepsis patients had a more negative fluid balance on the day of assessment, perhaps from their higher urine output than the covid patients, they took less time to recover renal function than the covid patients. These differences existed despite any difference in macrovascular parameter including RBF.

At the onset of the pandemic intensive care units were experiencing a high burden of AKI due to COVID-19. The development of COVID-19 related AKI during the alpha-variant wave appeared to be more frequent, of increased severity and slower to recover than other causes of AKI in critically ill patients, such as sepsis[539] and whilst there is similarity in the phenotype of AKI caused by these two diseases, the pathophysiology is likely to be distinct. A meta-analysis of 26,000 patients reported the overall incidence of AKI in COVID-19 to be 15%, albeit with significant variation between individual studies and far higher rates in critical illness[540]. Much has been described since the time of this study in April 2020, but the mechanisms for the AKI are still not entirely understood. Both right heart failure and venous congestion or left heart failure with hypoperfusion have been touted as potential mechanisms[541]. Management

of COVID-19 respiratory failure as acute respiratory distress syndrome may have been contributory in some, with unavoidably high positive end expiratory pressures (PEEP) and very negative fluid balance targets, both of which may be detrimental to renal function. Indeed, one study demonstrated a five-fold increase in the odds ratio of developing AKI with average PEEP values of 14.7cmH_2O vs 9.6 cmH_2O[542].

No hallmark tissue finding has been described in COVID-19 associated AKI. ACE2 receptors are widely expressed on renal endothelial cells, the binding site for SARS-CoV2, and the viral nucleocapsid has been identified in tissue[543], but the proportion of patients in whom this is detected varies from 6% on admission[544] to 60% at post-mortem[545] and although present in some, does not confirm causality. Other non-specific findings include organ specific endotheliitis, glomerular tuft collapse and interstitial oedema but again are not thought to be pathognomic features[532,542]. Microvascular obstruction from erythrocyte deposition and fibrin thrombi may cause glomerular infarction and necrosis in one post-mortem study but these findings were not commonly identified[532].

The results of the current study demonstrate significantly reduced cortical replenishment kinetics between patient groups and healthy controls. A reduction in time-based variables is evident, with reductions in WiR, mTT and PI, however the intensity based variable RBV remained unchanged between patient groups and controls and is largely non-discriminatory as described earlier in the thesis.

The septic group demonstrate a greater data dispersion of renal perfusion than the COVID-19

group, this may be explained by a more severe injury within stage 3 AKI in the covid group. This is demonstrated by their reduced urine output and the fact they took 54 days to regain independent renal function rather than the 7 days of septic shock. Perfusion assessment therefore shows promise in providing greater detail in the severity of injury and prognosis than current clinical assessment. It would have been particularly useful to measure novel biomarkers in the covid cohort, to see if these could provide further detail to the severity of renal injury.

The significant increase in resistive index in the COVID-19 group provides evidence of a vascular phenomenon and an impairment to forward flow within the renal vasculature. RI has multiple patient-related limitations and is non-specific, as explored in 2.1.2.3, but the two patient groups had similar characteristics, which should allow many of the causes related to age and comorbidity which exist when compared to controls, to be discounted when the patient groups are compared. If flow through the capillary bed is reduced due to higher resistance from whatever mechanism one would expect an increase in RI.

There was no difference in the right heart indices between patient groups and therefore venous congestion from ventilation or fluid overload may remain a feature in covid associated AKI, but no more of a feature than in sepsis.

Another potential explanation for the reduction in perfusion demonstrated in COVID-19 associated AKI would be the same mechanisms as those postulated for sepsis associated AKI, an adaptive response by tubular cells to avoid oxidative stress and inflammation, reduce

energy consumption, downregulated metabolism and tubular cell cycle arrest[41].

This study has several limitations. Firstly, it is a small case-control series conducted in a single centre and the results require confirmation by other investigators and in larger numbers of patients. The challenging nature of conducting clinical research during a pandemic meant that I was unable to recruit a larger cohort. I only assessed patients with severe AKI and exploration in earlier stages of AKI or COVID-19 with normal function would have been important to establish the temporal relationship between vascular changes and AKI onset. Covid patients were unmatched for the duration of admission, although the duration of RRT was no different. Novel biomarkers would have provided greater insight into the mechanism of injury in the covid cohort.

14.5 Conclusion

Renal perfusion is significantly reduced in patients with COVID associated AKI, independent of macrovascular alterations and RBF. Perfusion tended to be worse in covid than in sepsis and these patients had lower urine output and required RRT far longer than the septic cohort. This suggests perfusion assessment can predict the severity and duration of acute kidney injury in AKI that does not have a septic aetiology.

15 Final Discussion and Conclusion

Progress in reducing the morbidity of sepsis associated AKI is hampered by definitions, diagnostics and a limited understanding of the pathogenesis. The often rapid and profound loss of renal function is not explicable through histopathological features and functional alterations are predominant[43]. Whilst the existing paradigm describes shock causing reduced global flow, ischaemia-reperfusion and cell death, it is now clear that these processes are not primary in its development and widespread damage is largely absent[43,343,470]. Experimental studies have shown that alterations in the microcirculation are one of several cornerstones in the development of sepsis associated AKI, but difficulties remain in confirming such findings in patients[340]. Using contrast ultrasound amongst other techniques, this thesis provides new insight into the renal microcirculation, hypoperfusion and its involvement in human AKI development from sepsis.

Accurate *in vivo* measurement of renal perfusion is challenging in critical illness; patients are inherently unstable, non-compliant and often position dependent, reducing the possibility of functional cross-sectional imaging, or even repositioning within the bedspace. Invasive measurements of renal blood flow are not practicable in clinical research. DCE-US is a relatively novel technique in this context but has the potential to selectively monitor organ perfusion in such patients and has shown potential as an imaging modality in pilot studies, being safe, feasible and reproducible in both cardiac surgery and septic shock[161,424].

For DCE-US imaging to be applicable at the bedside the technique required further development from its radiology-predominant base. The initial chapter describes this

development making it more practical and easier to perform. It demonstrates a degree of inter-user variability with the analysis phase, but possibly minor in comparison to the relative changes seen between patient groups. It demonstrates the intra-user variability of someone with sufficient training is low and region selection is largely reliable. This chapter also develops a pragmatic method of measuring RBF at the bedside, noting prior criticisms of Doppler based quantification[64], but using CEUS to enhance the renal artery diameter, time averaged mean velocities for flow waveform analysis and referencing the technique in healthy controls all helped refine the method. Importantly this chapter defined normal values for renal perfusion and provided a reference for the patient studies.

The bulk of work in this thesis is dedicated to the Microshock Renal study; a relatively complex prospective, longitudinal observational study of the renal microcirculation in sepsis associated AKI. By comparing it to multiple other factors and variables, it enables a better understanding of the role of perfusion in AKI development and persistence. The key observation is that renal microcirculatory alterations are universal in patients with septic shock, but only those with the more severe alterations manifest an AKI phenotype. This was demonstrated with DCE-US and the same findings were true of cell-cycle arrest and tubular injury, where the minimum TIMP2*IGFBP7 admission value for all patients was more than three times greater than controls and the average MTT even in those who do not have severe AKI was 2.5 times greater. Put another way, current clinical measures on which the AKI staging system depend only identify a proportion, the remainder are not unaffected, but remain subclinical. Whilst this “tip of the iceberg” observation is not new[369] the perfusion data presented is, and adds further evidence and a new perspective to this argument. By analysing the data, not just by the development of severe AKI but by perfusion alterations further

insights are made.

The unique architecture of the renal microvasculature, with afferent and efferent arterioles and tightly looped vasa recta means the possibilities for vascular interactions are high, indeed the microvasculature is more of a meshed network of parallel circuits than a continuum of inert vessels in series[546]. Periglomerular shunts have been suggested to permit movement of blood directly into the venous system, bypassing much of the cortical and medullary circulation and could potentially account for these findings.

How the renal microcirculation interacts to recruit shunts and drive hypoperfusion has been suggested by experiments. The cytokine load, PAMPs and DAMPs present to tubular epithelial cells both through filtrate and capillaries, leading to immunological interaction and upregulation of TECs[171,446,457]. TECs demonstrate paracrine signalling and downregulating adjacent segments [455,456]. After TEC activation tight junctions become degraded and the subsequent oedema impairs tubular flow[453]. TECs are therefore seemingly active in their own regulation. Another key component of TEC adaptation to sepsis is an alteration in cellular metabolism. There is now reasonable evidence to support TECs switching to aerobic glycolysis early in the septic episode, such pathways result in much lower energy expenditure and generate multiple biochemical intermediaries for future synthesis and repair[444]. During the initial phase TECs enter cell cycle arrest, which again is energy conserving. Both mechanisms would have less demand and hypoperfusion would be a natural homeostatic response to match supply. The mechanism of this interaction is not entirely clear, but nitric oxide production in TECs plays a role, the interaction between eNOS and iNOS, becomes

unbalanced, increasing iNOS expression and resulting in hypoperfusion[373–375].

Why hypoperfusion would be advantageous has multiple explanations. TECs may produce these interactions to prevent exposure to cytokine signals, endotoxin and reactive oxygen species all of which are potentially harmful[472]. Following TEC downregulation, cessation of active sodium transport would reduce cellular demands and therefore reducing exposure to filtrate by decreasing GFR would be advantageous. As filtration is passive, alterations in the vasculature are necessary to induce downstream changes. Another beneficial reason for hypoperfusion is that cells under stress, such as the conditions created by septic shock, have increased mitochondrial injury[46,459,482] and this injury is likely to be potentiated if the cellular workload demands are high. Mitochondrial injury is not benign with the release of multiple free radicals within the cell. Furthermore, certain regions of the tubule are at an increased risk of ischaemia due to their anatomical position and relative hypoxia within the kidney[449]. Reduced perfusion to match these cellular adaptations would be appropriate and its persistence for as long as cytokine or endotoxin stimulation exists would also be advantageous. On recovery, when cellular anabolic demands are high and metabolism has switched back to oxidative phosphorylation, increased perfusion would be necessary to help restore cellular and whole-organ function. The findings presented in this thesis are congruent with this evidence. The point on this severity spectrum at which physiological adaptation becomes pathological is therefore ill-defined. Indeed it could be argued that this process is not pathological, AKI in such conditions could represent a protective adaptation to the shocked state, just given the term `acute kidney injury` by clinicians. It more likely reflects

tubular epithelial cells prioritizing survival at the expense of organ function[472].

There is good evidence however that persistent AKI increases the risk of chronicity, fibrosis and non-recoverable function[523], whereas AKI which fully resolves within a few days has minimally increased risk after resolution[501]. The risks of progression increase with severity and duration so whilst these mechanisms may be protective at the cellular level, there is associated harm. The data presented in this thesis demonstrates that a greater degree of tubular downregulation has a concurrently greater degree of hypoperfusion and if these changes persist beyond 48 hours higher levels of inflammation, endothelial activation and glycocalyx disruption are evident. There was an initial spike in cytokines levels in all patients, but these persisted in those with more severe renal injury and hypoperfusion, whilst resolving in those without. These patients were also sicker, with a greater burden of organ failure which again points to an inflammatory component to AKI persistence. Such longitudinal trends are seldom borne out in experimental study as they are often terminated earlier and use a single initial septic insult whereas human sepsis is more complex[323]. The present data demonstrates how patients with severe hypoperfusion on admission are more likely to have persistent injury and require RRT for longer. It is reasonable to infer that the risk of CKD increases in such patients as the risk of CKD development is proportional to the duration of AKI. Patients with hypoperfusion are also more likely to die.

Whilst no differences in RBF could be detected, other macrovascular variables were different in those who developed severe AKI. They had higher venous pressures and atrial stretch. They were on higher doses of inotropes and vasopressors and were on a second vasopressor more frequently. All these factors are known to be associated with AKI development[344,409] but

interestingly the association was seen more in AKI than in hypoperfusion per se, again suggestive that these macrovascular factors are related to disease severity and the severity of shock and sepsis, but it is the intrinsic factors which are more determinative of hypoperfusion, whilst these factors do have renal interactions they may not underpin alterations in perfusion.

Another key finding is that renal hypoperfusion follows a unique time course and has only a limited association with systemic measures of shock, be it biochemical or through direct assessment of the tissue bed. Immediate changes occur in both the sublingual and renal microcirculations but those in the kidney persist whilst systemic measures resolve rapidly or lead to death. There is little prior evidence demonstrating this in solid organ perfusion[319,547] and none comparing the renal microcirculation in a clinical study. Shock related variables also demonstrates little association between arterial blood lactate and solid organ hypoperfusion, a long-held opinion for lactate generation in such circumstances[548].

Examination of large datasets, across a broad array of variables and without the inherent biases of investigators has become possible due to the widespread adoption of machine learning and artificial intelligence. These methods have identified in multiple studies distinct subphenotypes within AKI, one related to heart failure and fluid overload and the other a hyperinflammatory state[234,248,487,488,549]. We set to identify these groups within the current dataset and discovered that a high inflammatory subphenotype had distinct differences in renal perfusion after 48-96 hours from the onset of septic shock. The prior studies suggest a preferential response to vasopressin in the lower inflammatory subphenotype and the present study therefore adds further information, that such a finding may be due relatively

maintained cortical perfusion in this group, as opposed to the hyperinflammatory group who had more severe and persistent hypoperfusion.

Sepsis causes multiple alterations along the nephron[449]. Those of tubular downregulation and injury are described above and were associated with hypoperfusion. Assessment of filtration in this study is limited, both by available biomarkers and the widespread use of RRT in the study population, but notably albuminuria increased between day 0 and day 2, which largely reflects filtration[495]. This rise may be due to proximal tubular dysfunction as it is responsible for albumin reabsorption, or it may be because glomerular alterations occur during hypoperfusion which are associated with degradation of the glomerular glycocalyx[454].

DCE-US had a similar ability to predict severe AKI as novel and conventional biomarkers but was imperfect (AUROC 0.84). Potentially some patients develop AKI with preserved perfusion, or the use of RRT for non-standard reasons diminished the outcome measure. Alternatively it points to a limitation of the technique and the requirement for further refinement if imaging is to find a place alongside biomarkers in this setting.

DCE-US requires a contrast capable ultrasound platform, analysis software and a trained operator. As renal perfusion assessments are not a routine part of practice, developing the technique outside of a research environment was difficult. Ultrasound is an increasingly ubiquitous tool in ICUs, but contrast capability is not common and further equipment and training would be necessary if this technique were to be more broadly adopted into clinical research. Novel biomarkers also require specialist equipment and either laboratory support

or a dedicated device. The two methods should not be considered exclusive however as both provide valuable information to the status of the injured kidney. DCE-US has distinct advantages, providing a real-time functional assessment and repeatability. Biomarkers remain elevated for several days and as yet they cannot be used monitor fluid or vasopressor use, nor can DCE-US, but it has potential. DCE-US provides a new window and permits targeted renal resuscitation to be observed.

A cohort of patients with COVID-19 associated AKI is lastly presented, demonstrating hypoperfusion and again preservation of macrovascular flow. This chapter demonstrates that hypoperfusion is not unique to sepsis associated AKI, but also points to the utility of the technique in assessing critically ill patients with kidney injury from other causes. All the patients in this study had stage 3 AKI, but the covid group had lower urine output and took a far longer period until free from RRT. Therefore the COVID-19 group probably had a more severe injury and it is interesting that their perfusion values were uniform and slightly worse those with sepsis, the lack of significance possibly relating to the small cohort size in the covid group and warrants repeat in other studies with other causes of AKI.

15.1 Limitations

Components of the design, operation and analysis of this study have been complex. Firstly, it is not possible to determine a gold-standard measurement of cortical perfusion in clinical studies preventing a comparative analysis. The same is true for the measurement of RBF. A perfect standard for diagnosing AKI is also lacking; novel biomarkers are predominately research tools and have individual limitations, whereas clinical indicators such as creatinine have multiple flaws. AKI staging reduces a continuum of disease severity into a small number

of ordinal outcomes and stage 3 is in part, based on whether the clinician commences RRT. A proportion of the patients in this study were commenced on RRT who had not met the now clinically accepted indications[511,512] which diminished the outcome measure. By analysing the data according to whether renal perfusion was above or below average was ultimately key as perfusion was the principal focus of this thesis and provided additional insight.

The use of ultrasound to assess blood flow within the renal artery has previously been criticised. There is no reliable quantification method for the assessment of RBF in clinical studies of critical illness. We sought to overcome some of these limitations by combining Doppler assessment with contrast derived measurements of the renal artery diameter and calibrating this technique to normal RBF using a healthy control cohort. The use of time averaged mean velocities was also considered more reliable. It is pragmatic but needs to be validated against a gold standard in a further study.

There is a risk of bias in these studies, they are single-centre and single operator dependent. From acquisition through to analysis there are multiple steps where bias could occur. It is reassuring that the findings reflect the literature and the pilot study[82], but that in itself could represent confirmation bias. A more thorough reliability assessment would be beneficial, particularly in image acquisition. Given further time and funding it would be insightful to compare DCE-US based quantification to fMRI. Alternatively an ex vivo model could be used such as a large animal kidney on machine perfusion, as is used in transplantation, where exact RBF and invasive measures of cortical perfusion could be compared to DCE-US. It would a

lso be insightful to study medullary perfusion and attempt to develop a quantitative

assessment tool with ultrasound.

Finally this is a relatively small, single-centre, single-operator study. However, I feel we have provided a wealth of hypothesis-generating data and would hope this study could inform future, larger, confirmatory studies with less intense study protocols but with equal ambition to develop effective personalised management of acute kidney injury.

15.2 Conclusion and suggestions for further work

Renal alterations including TEC downregulation and hypoperfusion are present in all patients with septic shock but more so in patients who go on to develop the AKI clinical phenotype. Despite this reduction in cortical perfusion large vessel supply is preserved. This renal hypoperfusion bears limited association and persists far longer than systemic perfusion abnormalities in shocked patients. Prolonged hypoperfusion is associated with increased inflammation and could partly explain recently described subphenotypes. Differences in venous congestion and inotrope dose were more associated with wider AKI development than hypoperfusion per se. Intrarenal shunting mechanisms are likely, permitting large vessel flow but reducing small vessel perfusion. The reduction in perfusion is likely to be orchestrated by TECs, providing them with multiple survival advantages during sepsis. Indeed, such changes may well be protective of organ survival despite the temporary loss of function.

DCE-US can accurately predict AKI in septic shock and performs comparably to recently described novel renal biomarkers. The additional advantage of repeated examination makes it a promising tool to guide future studies.

Such future studies should aim to maximise the potential of DCE-US guided perfusion assessment and its distinct advantages. This includes investigating the potential for individualised renal-centred care, such as the perfusion alterations induced by different inotropes and fluid therapy, determining if perfusion can be altered and if it is beneficial or harmful. Additional work should also further examine the reliability of DCE-US. The acquisition phase could be compared between users and compared to a gold-standard such as functional MRI. Invasive measures of RBF could be compared to the method used in this thesis. Finally, there is hidden information within the medulla which is difficult to extract. If the technique could examine this region, it would certainly provide important data.

16 References

1. Rudd KE, Johnson SC, Agesa KM, Shackelford KA, Tsoi D, Kievlan DR, et al. Global, regional, and national sepsis incidence and mortality, 1990–2017: analysis for the Global Burden of Disease Study. Lancet. 2020;395(10219):200–11.

2. Vincent JL, Rello J, Marshall J, Silva E, Anzueto A, Martin CD, et al. International Study of the Prevalence and Outcomes of Infection in Intensive Care Units. Jama. 2009;302(21):2323–9.

3. Levy MM, Fink MP, Marshall JC, Abraham E, Angus D, Cook D, et al. 2001 SCCM/ESICM/ACCP/ATS/SIS International Sepsis Definitions Conference. Intens Care Med. 2003;29(4):530–8.

4. Subgroup* TSSCGC including TP, Dellinger RP, Levy MM, Rhodes A, Annane D, Gerlach H, et al. Surviving Sepsis Campaign: International Guidelines for Management of Severe Sepsis and Septic Shock, 2012. Intens Care Med. 2013;39(2):165–228.

5. Singer M, Deutschman CS, Seymour CW, Shankar-Hari M, Annane D, Bauer M, et al. The Third International Consensus Definitions for Sepsis and Septic Shock (Sepsis-3). In 2016. p. 801–10. (JAMA; vol. 315).

6. Vincent JL, Jones G, David S, Olariu E, Cadwell KK. Frequency and mortality of septic shock in Europe and North America: a systematic review and meta-analysis. Crit Care. 2019;23(1):196.

7. Chadwick, Mann J, Lonie WN; Hippocratic Writings. Penguin, editor. 1978.

8. Millham FH. A brief history of shock. Surgery. 2010;148(5):1026–37.

9. Bateman RM, Sharpe MD, Ellis CG. Bench-to-bedside review: Microvascular dysfunction in sepsis –hemodynamics, oxygen transport, and nitric oxide. Crit Care. 2003;7(5):359–73.

10. Ait-Oufella H, Maury E, Lehoux S, Guidet B, Offenstadt G. The endothelium: physiological functions and role in microcirculatory failure during severe sepsis. Intens Care Med. 2010;36(8):1286–98.

11. SEGAL SS. Regulation of Blood Flow in the Microcirculation. Microcirculation. 2005;12(1):33–45.

12. Rewa O, Bagshaw SM. Acute kidney injury—epidemiology, outcomes and economics. Nat Rev Nephrol. 2014;10(4):193–207.

13. Kellum JA, Levin N, Bouman C, Lameire N. Developing a consensus classification system for acute renal failure. Curr Opin Crit Care. 2002;8(6):509–14.

14. Bellomo R, Ronco C, Kellum JA, Mehta RL, Palevsky P, workgroup ADQI. Acute renal failure – definition, outcome measures, animal models, fluid therapy and information

technology needs: the Second International Consensus Conference of the Acute Dialysis Quality Initiative (ADQI) Group. Crit Care. 2004;8(4):R204–12.

15. Mehta RL, Kellum JA, Shah SV, Molitoris BA, Ronco C, Warnock DG, et al. Acute Kidney Injury Network: report of an initiative to improve outcomes in acute kidney injury. Crit Care. 2007;11(2):R31–R31.

16. Lopes JA, Jorge S. The RIFLE and AKIN classifications for acute kidney injury: a critical and comprehensive review. Clin Kidney J. 2013;6(1):8–14.

17. Kellum J, Lameire N. KDIGO clinical practice guideline for AKI. Kidney Int Suppl. 2012 Feb 7;2(1):1.

18. Makris K, Spanou L. Acute Kidney Injury: Definition, Pathophysiology and Clinical Phenotypes. Clin Biochem Rev. 2016;37(2):85–98.

19. Cerdá J, Bagga A, Kher V, Chakravarthi RM. The contrasting characteristics of acute kidney injury in developed and developing countries. Nat Clin Pract Nephr. 2008;4(3):138–53.

20. Susantitaphong P, Cruz DN, Cerda J, Abulfaraj M, Alqahtani F, Koulouridis I, et al. World Incidence of AKI: A Meta-Analysis. Clin J Am Soc Nephro. 2013;8(9):1482–93.

21. Kellum JA, Romagnani P, Ashuntantang G, Ronco C, Zarbock A, Anders HJ. Acute kidney injury. Nat Rev Dis Primers. 2021;7(1):52.

22. Hsu RK, McCulloch CE, Dudley RA, Lo LJ, Hsu C yuan. Temporal Changes in Incidence of Dialysis-Requiring AKI. J Am Soc Nephrol. 2013;24(1):37–42.

23. Siddiqui NF, Coca SG, Devereaux PJ, Jain AK, Li L, Luo J, et al. Secular trends in acute dialysis after elective major surgery — 1995 to 2009. Can Med Assoc J. 2012;184(11):1237–45.

24. Holmes J, Rainer T, Geen J, Roberts G, May K, Wilson N, et al. Acute Kidney Injury in the Era of the AKI E-Alert. Clin J Am Soc Nephro. 2016;11(12):2123–31.

25. Uchino S, Kellum JA, Bellomo R, Doig GS, Morimatsu H, Morgera S, et al. Acute Renal Failure in Critically Ill Patients: A Multinational, Multicenter Study. Jama. 2005 Aug 17;294(7):813–8.

26. Group TFS, Nisula S, Kaukonen KM, Vaara ST, Korhonen AM, Poukkanen M, et al. Incidence, risk factors and 90-day mortality of patients with acute kidney injury in Finnish intensive care units: the FINNAKI study. Intens Care Med. 2013;39(3):420–8.

27. Vaara ST, Pettilä V, Reinikainen M, Kaukonen KM, Consortium FIC. Population-based incidence, mortality and quality of life in critically ill patients treated with renal replacement therapy: a nationwide retrospective cohort study in finnish intensive care units. Crit Care. 2012;16(1):R13–R13.

28. Hoste EAJ, Bagshaw SM, Bellomo R, Cely CM, Colman R, Cruz DN, et al. Epidemiology of acute kidney injury in critically ill patients: the multinational AKI-EPI study. Intens Care Med. 2015 Aug;41(8):1411–23.

29. Bagshaw SM, George C, Bellomo R, Committee ADM. Changes in the incidence and outcome for early acute kidney injury in a cohort of Australian intensive care units. Crit Care. 2007;11(3):R68–R68.

30. Krishnamurthy S, Mondal N, Narayanan P, Biswal N, Srinivasan S, Soundravally R. Incidence and Etiology of Acute Kidney Injury in Southern India. Indian J Pediatrics. 2013;80(3):183–9.

31. Ahmed Z, Gilibert S, Krevolin L. Cost analysis of continuous renal replacement and extended hemodialysis. Dialysis Transplant. 2009;38(12):500–3.

32. Singh A, Hussain S, Kher V, Palmer AJ, Jose M, Antony B. A systematic review of cost-effectiveness analyses of continuous versus intermittent renal replacement therapy in acute kidney injury. Expert Rev Pharm Out. 2021;1–9.

33. Srisawat N, Lawsin L, Uchino S, Bellomo R, Kellum JA, Investigators BK. Cost of acute renal replacement therapy in the intensive care unit: results from The Beginning and Ending Supportive Therapy for the Kidney (BEST Kidney) Study. Crit Care. 2010;14(2):R46–R46.

34. Ostermann M, Bellomo R, Burdmann EA, Doi K, Endre ZH, Goldstein SL, et al. Controversies in Acute Kidney Injury: Conclusions from a Kidney Disease Improving Global Outcomes (KDIGO) Conference. Kidney Int. 2020;98(2):294–309.

35. Schneider AG, Bellomo R, Bagshaw SM, Glassford NJ, Lo S, Jun M, et al. Choice of renal replacement therapy modality and dialysis dependence after acute kidney injury: a systematic review and meta-analysis. Intens Care Med. 2013;39(6):987–97.

36. Xu X, Nie S, Liu Z, Chen C, Xu G, Zha Y, et al. Epidemiology and Clinical Correlates of AKI in Chinese Hospitalized Adults. Clin J Am Soc Nephro. 2015;10(9):1510–8.

37. Vincent JL, Sakr Y, Sprung CL, Ranieri VM, Reinhart K, Gerlach H, et al. Sepsis in European intensive care units: Results of the SOAP study* Crit Care Med. 2006;34(2):344–53.

38. Padkin A, Goldfrad C, Brady AR, Young D, Black N, Rowan K. Epidemiology of severe sepsis occurring in the first 24 hrs in intensive care units in England, Wales, and Northern Ireland. Crit Care Med. 2003;31(9):2332–8.

39. Brun-Buisson C, Meshaka P, Pinton P, Vallet B, Group ES. EPISEPSIS: a reappraisal of the epidemiology and outcome of severe sepsis in French intensive care units. Intens Care Med. 2004;30(4):580–8.

40. Kellum JA, Chawla LS, Keener C, Singbartl K, Palevsky PM, Pike FL, et al. The Effects of Alternative Resuscitation Strategies on Acute Kidney Injury in Patients with Septic Shock. Am J Resp Crit Care. 2016;193(3):281–7.

41. Gomez H, Ince C, Backer DD, Pickkers P, Payen D, Hotchkiss J, et al. A Unified Theory of Sepsis-Induced Acute Kidney Injury. Shock [Internet]. 2014 Jan;41(1):3–11. Available from: https://www.ncbi.nlm.nih.gov/pmc/articles/PMC3918942/pdf/nihms542926.pdf

42. Langenberg C, Gobe G, Hood S, May CN, Bellomo R. Renal Histopathology During Experimental Septic Acute Kidney Injury and Recovery* Crit Care Med. 2014 Jan;42(1):e58–67.

43. Takasu O, Gaut JP, Watanabe E, To K, Fagley RE, Sato B, et al. Mechanisms of Cardiac and Renal Dysfunction in Patients Dying of Sepsis. American journal of respiratory and critical care medicine. 2013 Mar 1;187(5):509–17.

44. Aslan A, Heuvel MC van den, Stegeman CA, Popa ER, Leliveld AM, Molema G, et al. Kidney histopathology in lethal human sepsis. Crit Care. 2018;22(1):359.

45. Lerolle N, Nochy D, Guérot E, Bruneval P, Fagon JY, Diehl JL, et al. Histopathology of septic shock induced acute kidney injury: apoptosis and leukocytic infiltration. Intens Care Med. 2010 Mar;36(3):471–8.

46. Kosaka J, Lankadeva YR, May CN, Bellomo R. Histopathology of Septic Acute Kidney Injury. Crit Care Med. 2016;44(9):e897–903.

47. Tran M, Tam D, Bardia A, Bhasin M, Rowe GC, Kher A, et al. PGC-1α promotes recovery after acute kidney injury during systemic inflammation in mice. J Clin Invest. 2011;121(10):4003–14.

48. Fani F, Regolisti G, Delsante M, Cantaluppi V, Castellano G, Gesualdo L, et al. Recent advances in the pathogenetic mechanisms of sepsis-associated acute kidney injury. J Nephrol. 2018;31(3):351–9.

49. Challiner R, Ritchie JP, Fullwood C, Loughnan P, Hutchison AJ. Incidence and consequence of acute kidney injury in unselected emergency admissions to a large acute UK hospital trust. Bmc Nephrol. 2014;15(1):84.

50. Endo Y. Renal Ultrasonography in the Evaluation of Acute Kidney Injury. Ultrasound Q. 2011;27(2):116–7.

51. Katagiri D, Wang F, Gore JC, Harris RC, Takahashi T. Clinical and experimental approaches for imaging of acute kidney injury. Clin Exp Nephrol. 2021;25(7):685–99.

52. Moroz J, Reinsberg SA. Preclinical MRI, Methods and Protocols. Methods Mol Biology. 2018;1718:71–87.

53. Zhou HY, Chen TW, Zhang XM. Functional Magnetic Resonance Imaging in Acute Kidney Injury: Present Status. Biomed Res Int. 2016;2016:1–7.

54. Goldstein A, Powis RL. 2 Medical Ultrasonic Diagnostics. Phys Acoustics. 1999;23:43–195.

55. Saha A, Mathur M. Ultrasound Fundamentals, An Evidence-Based Guide for Medical Practitioners. 2021;3–16.

56. Azhari H. Basics of Biomedical Ultrasound for Engineers.

57. Hangiandreou NJ. AAPM/RSNA Physics Tutorial for Residents: Topics in US. Radiographics. 2003;23(4):1019–33.

58. Szabo TL. Diagnostic Ultrasound Imaging: Inside Out (Second Edition). 2014;(IEEE Engineering in Medicine and Biology MagazineSeptember2004):605–51.

59. Dietrich C, Averkiou M, Nielsen M, Barr R, Burns P, Calliada F, et al. How to perform Contrast-Enhanced Ultrasound (CEUS). Ultrasound Int Open. 2018;04(01):E2–15.

60. Williams R, Hudson JM, Lloyd BA, Sureshkumar AR, Lueck G, Milot L, et al. Dynamic Microbubble Contrast-enhanced US to Measure Tumor Response to Targeted Therapy: A Proposed Clinical Protocol with Results from Renal Cell Carcinoma Patients Receiving Antiangiogenic Therapy. Radiology. 2011;260(2):581–90.

61. Çınar C, Türkvatan A. Prevalence of renal vascular variations: Evaluation with MDCT angiography. Diagn Interv Imag. 2016;97(9):891–7.

62. Blanco P. Volumetric blood flow measurement using Doppler ultrasound: concerns about the technique. J Ultrasound. 2015 Jun;18(2):201–4.

63. Li S, Hoskins PR, Anderson T, McDicken WN. Measurement of mean velocity during pulsatile flow using time-averaged maximum frequency of doppler ultrasound waveforms. Ultrasound Medicine Biology. 1993;19(2):105–13.

64. Wan L, Yang N, Hiew CY, Schelleman A, Johnson L, May C, et al. An assessment of the accuracy of renal blood flow estimation by Doppler ultrasound. Intens Care Med. 2008 Aug;34(8):1503–10.

65. Avasthi PS, Greene ER, Voyles WF, Eldridge MW. A comparison of echo-Doppler and electromagnetic renal blood flow measurements. J Ultras Med. 1984;3(5):213–8.

66. Jury D, Shaw A. Utility of bedside ultrasound derived hepatic and renal parenchymal flow patterns to guide management of acute kidney injury. Curr Opin Crit Care. 2021;

67. O'Neill WC. Renal resistive index: a case of mistaken identity. Hypertension (Dallas, Tex : 1979). 2014 Nov;64(5):915–7.

68. Saade A, Bourmaud A, Schnell D, Darmon M, Group RS. Performance of Doppler-Based Resistive Index and Semiquantitative Renal Perfusion in Predicting Persistent Acute Kidney Injury According to Operator Experience: Post Hoc Analysis of a Prospective Multicenter Study. Crit Care Med. 2021;Publish Ahead of Print.

69. Sugiura T, Wada A. Resistive index predicts renal prognosis in chronic kidney disease: results of a 4-year follow-up. Clin Exp Nephrol. 2011;15(1):114–20.

70. Adibi A, Ramezani M, Mortazavi M, Taheri S. Color Doppler indexes in early phase after kidney transplantation and their association with kidney function on six month follow up. Adv Biomed Res. 2012;1(1):62.

71. Schwenger V, Hankel V, Seckinger J, Macher-Göppinger S, Morath C, Zeisbrich M, et al. Contrast-Enhanced Ultrasonography in the Early Period After Kidney Transplantation Predicts Long-Term Allograft Function. Transplant P. 2014;46(10):3352–7.

72. Lerolle N, Guérot E, Faisy C, Bornstain C, Diehl JL, Fagon JY. Renal failure in septic shock: predictive value of Doppler-based renal arterial resistive index. Intens Care Med. 2006;32(10):1553–9.

73. Zhi HJ, Zhao J, Nie S, Ma YJ, Cui XY, Zhang M, et al. Semiquantitative Power Doppler Ultrasound Score to Predict Acute Kidney Injury in Patients With Sepsis or Cardiac Failure: A Prospective Observational Study. J Intensive Care Med. 2019;36(1):115–22.

74. Mulier JLGH, Rozemeijer S, Röttgering JG, Man AMES de, Elbers PWG, Tuinman PR, et al. Renal resistive index as an early predictor and discriminator of acute kidney injury in critically ill patients; A prospective observational cohort study. Plos One. 2018;13(6):e0197967.

75. Dewitte A, Coquin J, Meyssignac B, Joannès-Boyau O, Fleureau C, Roze H, et al. Doppler resistive index to reflect regulation of renal vascular tone during sepsis and acute kidney injury. Crit Care. 2012;16(5):R165–R165.

76. Deruddre S, Cheisson G, Mazoit JX, Vicaut E, Benhamou D, Duranteau J. Renal arterial resistance in septic shock: effects of increasing mean arterial pressure with norepinephrine on the renal resistive index assessed with Doppler ultrasonography. Intens Care Med [Internet]. 2007 May 8;33(9):1557–62. Available from: https://link.springer.com/content/pdf/10.1007%2Fs00134-007-0665-4.pdf

77. Bossard G, Bourgoin P, Corbeau JJ, Huntzinger J, Beydon L. Early detection of postoperative acute kidney injury by Doppler renal resistive index in cardiac surgery with cardiopulmonary bypass. Bja Br J Anaesth. 2011;107(6):891–8.

78. Schnell D, Deruddre S, Harrois A, Pottecher J, Cosson C, Adoui N, et al. Renal Resistive Index Better Predicts the Occurrence of Acute Kidney Injury Than Cystatin C. Shock. 2012;38(6):592–7.

79. Darmon M, Schortgen F, Vargas F, Liazydi A, Schlemmer B, Brun-Buisson C, et al. Diagnostic accuracy of Doppler renal resistive index for reversibility of acute kidney injury in critically ill patients. Intens Care Med. 2011;37(1):68–76.

80. Darmon M, Bourmaud A, Reynaud M, Rouleau S, Meziani F, Boivin A, et al. Performance of Doppler-based resistive index and semi-quantitative renal perfusion in predicting persistent AKI: results of a prospective multicenter study. Intens Care Med. 2018;44(11):1904–13.

81. Ninet S, Schnell D, Dewitte A, Zeni F, Meziani F, Darmon M. Doppler-based renal resistive index for prediction of renal dysfunction reversibility: A systematic review and meta-analysis. J Crit Care. 2015;30(3):629–35.

82. Harrois A, Grillot N, Figueiredo S, Duranteau J. Acute kidney injury is associated with a decrease in cortical renal perfusion during septic shock. Crit Care. 2018 Jun 15;22(1):161.

83. Calabia J, Torguet P, Garcia I, Martin N, Mate G, Marin A, et al. The Relationship Between Renal Resistive Index, Arterial Stiffness, and Atherosclerotic Burden: The Link Between Macrocirculation and Microcirculation. J Clin Hypertens. 2014;16(3):186–91.

84. Naesens M, Heylen L, Lerut E, Claes K, Wever LD, Claus F, et al. Intrarenal Resistive Index after Renal Transplantation. New Engl J Medicine. 2013 Nov 7;369(19):1797–806.

85. Schnell D, Darmon M. Bedside Doppler ultrasound for the assessment of renal perfusion in the ICU: advantages and limitations of the available techniques. Critical Ultrasound J. 2015;7(1):8.

86. Boddi M, Natucci F, Ciani E. The internist and the renal resistive index: truths and doubts. Intern Emerg Med. 2015;10(8):893–905.

87. Gramiak R, Shah PM, Kramer DH. Ultrasound Cardiography: Contrast Studies in Anatomy and Function. Radiology. 1969;92(5):939–48.

88. Keller MW, Segal SS, Kaul S, Duling B. The behavior of sonicated albumin microbubbles within the microcirculation: a basis for their use during myocardial contrast echocardiography. Circ Res. 1989;65(2):458–67.

89. Lindner JR, Wei K. Contrast echocardiography. Curr Prob Cardiology. 2002;27(11):454–519.

90. Klibanov AL. Ultrasound Contrast: Gas Microbubbles in the Vasculature. Invest Radiol. 2021;56(1):50–61.

91. Helfield BL, Chen X, Qin B, Watkins SC, Villanueva FS. Mechanistic Insight into Sonoporation with Ultrasound-Stimulated Polymer Microbubbles. Ultrasound Medicine Biology. 2017;43(11):2678–89.

92. MATTREY RF, WRIGLEY R, STEINBACH GC, SCHUTT EG, EVITTS DP. Gas Emulsions as Ultrasound Contrast Agents Preliminary Results in Rabbits and Dogs. Invest Radiol. 1994;29:S139–41.

93. Bracco. SonoVue Product Monograph. Dynamic Contrast Enhancement in Real Time [Internet]. Bracco; [cited 2021 Jun 23]. Available from: https://imaging.bracco.com/sites/braccoimaging.com/files/technica_sheet_pdf/se-en-2016-04-30-monograph-sonovue.pdf

94. Hyvelin JM, Tardy I, Arbogast C, Costa M, Emmel P, Helbert A, et al. Use of Ultrasound Contrast Agent Microbubbles in Preclinical Research. Invest Radiol. 2013;48(8):570–83.

95. MOREL DR, SCHWIEGER I, HOHN L, TERRETTAZ J, LLULL JB, CORNIOLEY YA, et al. Human Pharmacokinetics and Safety Evaluation of SonoVue™, a New Contrast Agent for Ultrasound Imaging. Invest Radiol. 2000;35(1):80.

96. Sun T, Zhang Y, Power C, Alexander PM, Sutton JT, Aryal M, et al. Closed-loop control of targeted ultrasound drug delivery across the blood–brain/tumor barriers in a rat glioma model. Proc National Acad Sci. 2017;114(48):E10281–90.

97. Mead BP, Mastorakos P, Suk JS, Klibanov AL, Hanes J, Price RJ. Targeted gene transfer to the brain via the delivery of brain-penetrating DNA nanoparticles with focused ultrasound. J Control Release. 2016;223:109–17.

98. Klibanov AL. Preparation of targeted microbubbles: ultrasound contrast agents for molecular imaging. Med Biol Eng Comput. 2009;47(8):875–82.

99. Schneider M. Bubbles in echocardiography: climbing the learning curve. Eur Heart J Suppl. 2002;4(suppl_C):C3–7.

100. Muskula PR, Main ML. Safety With Echocardiographic Contrast Agents. Circulation Cardiovasc Imaging. 2018;10(4):e005459.

101. Wei K, Main ML, Lang RM, Klein A, Angeli S, Panetta C, et al. The Effect of Definity on Systemic and Pulmonary Hemodynamics in Patients. J Am Soc Echocardiog. 2012;25(5):584–8.

102. Wever-Pinzon O, Suma V, Ahuja A, Romero J, Sareen N, Henry SA, et al. Safety of echocardiographic contrast in hospitalized patients with pulmonary hypertension: a multi-center study. European Hear J - Cardiovasc Imaging. 2012;13(10):857–62.

103. Abdelmoneim SS, Bernier M, Scott CG, Dhoble A, Ness SAC, Hagen ME, et al. Safety of Contrast Agent Use During Stress Echocardiography in Patients With Elevated Right Ventricular Systolic Pressure. Circulation Cardiovasc Imaging. 2010;3(3):240–8.

104. Main ML, Grayburn PA, Lang RM, Goldman JH, Gibson CM, Sherwin P, et al. Effect of Optison on Pulmonary Artery Systolic Pressure and Pulmonary Vascular Resistance. Am J Cardiol. 2013;112(10):1657–61.

105. Kummer T, Oh L, Phelan MB, Huang RD, Nomura JT, Adhikari SR. Emergency and critical care applications for contrast-enhanced ultrasound. Am J Emerg Medicine. 2018 Jul;36(7):1287–94.

106. Selby NM, Williams JP, Phillips BE. Application of dynamic contrast enhanced ultrasound in the assessment of kidney diseases. Curr Opin Nephrol Hypertens. 2021;30(1):138–43.

107. Eichhorn ME, Klotz LV, Luedemann S, Strieth S, Kleespies A, Preissler G, et al. Vascular targeting tumor therapy: Non-invasive contrast enhanced ultrasound for quantitative assessment of tumor microcirculation. Cancer Biol Ther. 2010;9(10):794–802.

108. Chan A, Barrett EJ, Anderson SM, Kovatchev BP, Breton MD. Muscle microvascular recruitment predicts insulin sensitivity in middle-aged patients with type 1 diabetes mellitus. Diabetologia. 2012;55(3):729–36.

109. Wang Y, Li N, Tian X, Lin L, Liang S, Zhao P, et al. Evaluation of Renal Microperfusion in Diabetic Patients With Kidney Injury by Contrast-Enhanced Ultrasound. J Ultras Med. 2020;

110. Kersting S, Konopke R, Kersting F, Volk A, Distler M, Bergert H, et al. Quantitative Perfusion Analysis of Transabdominal Contrast-Enhanced Ultrasonography of Pancreatic Masses and Carcinomas. Gastroenterology. 2009;137(6):1903–11.

111. Prada F, Gennari AG, Linville IM, Mutersbaugh ME, Chen Z, Sheybani N, et al. Quantitative analysis of in-vivo microbubble distribution in the human brain. Sci Rep-uk. 2021;11(1):11797.

112. Averkiou MA, Juang EK, Gallagher MK, Cuevas MA, Wilson SR, Barr RG, et al. Evaluation of the Reproducibility of Bolus Transit Quantification With Contrast-Enhanced Ultrasound Across Multiple Scanners and Analysis Software Packages—A Quantitative Imaging Biomarker Alliance Study. Invest Radiol. 2020;55(10):643–56.

113. Quaia E. Assessment of tissue perfusion by contrast-enhanced ultrasound. Eur Radiol. 2011;21(3):604–15.

114. VueBox Quantification Toolbox, Instructions For Use. Bracco Suisse SA; 2019.

115. Goetti R, Reiner CS, Knuth A, Klotz E, Stenner F, Samaras P, et al. Quantitative Perfusion Analysis of Malignant Liver Tumors. Invest Radiol. 2012;47(1):18–24.

116. Sidhu P, Cantisani V, Dietrich C, Gilja O, Saftoiu A, Bartels E, et al. The EFSUMB Guidelines and Recommendations for the Clinical Practice of Contrast-Enhanced Ultrasound (CEUS) in Non-Hepatic Applications: Update 2017 (Long Version). Ultraschall Der Medizin - European J Ultrasound. 2018;39(02):e2–44.

117. Macrì F, Pietro SD, Liotta L, Piccionello AP, Pugliese M, Majo MD. Effects of size and location of regions of interest examined by use of contrast-enhanced ultrasonography on renal perfusion variables of dogs. Am J Vet Res. 2016;77(8):869–76.

118. Ignee A, Jedrejczyk M, Schuessler G, Jakubowski W, Dietrich CF. Quantitative contrast enhanced ultrasound of the liver for time intensity curves—Reliability and potential sources of errors. Eur J Radiol. 2010;73(1):153–8.

119. Sidhu P, Cantisani V, Dietrich C, Gilja O, Saftoiu A, Bartels E, et al. The EFSUMB Guidelines and Recommendations for the Clinical Practice of Contrast-Enhanced Ultrasound (CEUS) in Non-Hepatic Applications: Update 2017 (Short Version). Ultraschall Der Medizin - European J Ultrasound. 2018;39(02):154–80.

120. Dietrich C, Averkiou M, Correas JM, Lassau N, Leen E, Piscaglia F. An EFSUMB Introduction into Dynamic Contrast-Enhanced Ultrasound (DCE-US) for Quantification of Tumour Perfusion. Ultraschall Med. 2012;33(4):344–51.

121. Lucidarme O, Franchi-Abella S, Correas JM, Bridal SL, Kurtisovski E, Berger G. Blood Flow Quantification with Contrast-enhanced US: “Entrance in the Section” Phenomenon—Phantom and Rabbit Study. Radiology. 2003;228(2):473–9.

122. Wei K, Jayaweera AR, Firoozan S, Linka A, Skyba DM, Kaul S. Quantification of Myocardial Blood Flow With Ultrasound-Induced Destruction of Microbubbles Administered as a Constant Venous Infusion. Circulation. 1998;97(5):473–83.

123. Wei K, Le E, Bin JP, Coggins M, Thorpe J, Kaul S. Quantification of renal blood flow with contrast-enhanced ultrasound. J Am Coll Cardiol. 2001;37(4):1135–40.

124. Krix M, Kiessling F, Farhan N, Schmidt K, Hoffend J, Delorme S. A multivessel model describing replenishment kinetics of ultrasound contrast agent for quantification of tissue perfusion. Ultrasound Medicine Biology. 2003;29(10):1421–30.

125. Arditi M, Frinking PJA, Zhou X, Rognin NG. A New Formalism for the Quantification of Tissue Perfusion by the Destruction-Replenishment Method in Contrast Ultrasound Imaging. Ieee Transactions Ultrasonics Ferroelectr Freq Control. 2006;53(6):1118–29.

126. Hudson JM, Karshafian R, Burns PN. Quantification of Flow Using Ultrasound and Microbubbles: A Disruption Replenishment Model Based on Physical Principles. Ultrasound Medicine Biology. 2009;35(12):2007–20.

127. QIAN H, BASSINGTHWAIGHTE JB. A Class of Flow Bifurcation Models with Lognormal Distribution and Fractal Dispersion. J Theor Biol. 2000;205(2):261–8.

128. Hudson JM, Williams R, Lloyd B, Atri M, Kim TK, Bjarnason G, et al. Improved Flow Measurement Using Microbubble Contrast Agents and Disruption-Replenishment: Clinical Application to Tumour Monitoring. Ultrasound Medicine Biology. 2011;37(8):1210–21.

129. Hudson JM, Leung K, Burns PN. The Lognormal Perfusion Model for Disruption Replenishment Measurements of Blood Flow: In Vivo Validation. Ultrasound Medicine Biology. 2011;37(10):1571–8.

130. Metoki R, Moriyasu F, Kamiyama N, Sugimoto K, Iijima H, Xu H xiong, et al. Quantification of hepatic parenchymal blood flow by contrast ultrasonography with flash-replenishment imaging. Ultrasound Medicine Biology. 2006;32(10):1459–66.

131. Cang?r1 H, Meyer-Wiethe1 K, Seidel1 G. Comparison of Flow Parameters to Analyse Bolus Kinetics of Ultrasound Contrast Enhancement in a Capillary Flow Model. Ultraschall Med. 2004;25(06):418–21.

132. Gauthier M, Leguerney I, Thalmensi J, Chebil M, Parisot S, Peronneau P, et al. Estimation of intra-operator variability in perfusion parameter measurements using DCE-US. World J Radiology. 2011;3(3):70–81.

133. Tang MX, Mulvana H, Gauthier T, Lim AKP, Cosgrove DO, Eckersley RJ, et al. Quantitative contrast-enhanced ultrasound imaging: a review of sources of variability. Interface Focus. 2011;1(4):520–39.

134. Greis C. Quantitative evaluation of microvascular blood flow by contrast-enhanced ultrasound (CEUS). Clin Hemorheol Micro. 2011;49(1–4):137–49.

135. Li PC, Yeh CK, Wang SW. Time-intensity-based volumetric flow measurements: an in vitro study. Ultrasound Medicine Biology. 2002;28(3):349–58.

136. Averkiou M, Lampaskis M, Kyriakopoulou K, Skarlos D, Klouvas G, Strouthos C, et al. Quantification of Tumor Microvascularity with Respiratory Gated Contrast Enhanced Ultrasound for Monitoring Therapy. Ultrasound Medicine Biology. 2010;36(1):68–77.

137. Rognin NG, Frinking P, Costa M, Arditi M. In-vivo Perfusion Quantification by Contrast Ultrasound: Validation of the Use of Linearized Video Data vs. Raw RF Data. 2008 Ieee Ultrasonics Symposium. 2008;1690–3.

138. Lassau N, Koscielny S, Lacroix J, Cuinet M, Aziza R, Taieb S, et al. Final results of a French multicentric prospective study of dynamic contrast-enhanced ultrasound (DCE-US) for the evaluation of antiangiogenic treatments in 537 patients. J Clin Oncol. 2011;29(15_suppl):e13500–e13500.

139. Peronneau1 P, Lassau1 N, Leguerney2 I, Roche1 A, Cosgrove3 D. Contrast Ultrasonography: Necessity of Linear Data?Processing for the Quantification of Tumor Vascularization. Ultraschall Med. 2010;31(04):370–8.

140. Fröhlich E, Muller R, Cui XW, Schreiber-Dietrich D, Dietrich CF. Dynamic Contrast-Enhanced Ultrasound for Quantification of Tissue Perfusion. J Ultras Med. 2015;34(2):179–96.

141. Zhang Y, Zhang X, Li J, Cai Q, Qiao Z, Luo Y kun. Contrast-enhanced ultrasound: a valuable modality for extracapsular extension assessment in papillary thyroid cancer. Eur Radiol. 2021;31(7):4568–75.

142. Pinto SPS, Huang DDY, Dinesh AA, Sidhu PPS, Ahmed MK. A systematic review on the use of qualitative and quantitative contrast-enhanced ultrasound in diagnosing testicular abnormalities. Urology. 2021;

143. Ma F, Cang Y, Zhao B, Liu Y, Wang C, Liu B, et al. Contrast-enhanced ultrasound with SonoVue could accurately assess the renal microvascular perfusion in diabetic kidney damage. Nephrol Dial Transpl. 2012;27(7):2891–8.

144. Ma F, Yadav GP, Cang Y, Dang Y, Wang C, Liu B, et al. Contrast-enhanced ultrasonography is a valid technique for the assessment of renal microvascular perfusion dysfunction in diabetic Goto-Kakizaki rats. Nephrology. 2013;18(12):750–60.

145. Grzelak P, Szymczyk K, Strzelczyk J, Kurnatowska I, Sapieha M, Nowicki M, et al. Perfusion of kidney graft pyramids and cortex in contrast-enhanced ultrasonography in the determination of the cause of delayed graft function. Ann Transpl. 2011;16(1):48–53.

146. Erlichman DB, Weiss A, Koenigsberg M, Stein MW. Contrast enhanced ultrasound: A review of radiology applications. Clin Imag. 2019;60(2):209–15.

147. Rodríguez SÁ, Palacios VH, Mayayo ES, Santos VGD, Nicolás VD, Gallego MDS, et al. The Usefulness of Contrast-Enhanced Ultrasound in the Assessment of Early Kidney Transplant Function and Complications. Diagnostics. 2017;7(3):53.

148. Dong Y, Wang W p, Cao J, Fan P, Lin X. Early assessment of chronic kidney dysfunction using contrast-enhanced ultrasound: a pilot study. Br J Radiology. 2014;87(1042):20140350.

149. Buchanan CE, Mahmoud H, Cox EF, McCulloch T, Prestwich BL, Taal MW, et al. Quantitative assessment of renal structural and functional changes in chronic kidney disease using multi-parametric magnetic resonance imaging. Nephrol Dial Transpl. 2019;35(6):955–64.

150. Kogan P, Johnson KA, Feingold S, Garrett N, Guracar I, Arendshorst WJ, et al. Validation of Dynamic Contrast-Enhanced Ultrasound in Rodent Kidneys as an Absolute Quantitative Method for Measuring Blood Perfusion. Ultrasound Medicine Biology. 2011;37(6):900–8.

151. Selkurt EE. RENAL BLOOD FLOW AND RENAL CLEARANCE DURING HEMORRHAGIC SHOCK. Am J Physiology-legacy Content. 1946;145(5):699–709.

152. HOSOTANI Y, TAKAHASHI N, KIYOMOTO H, OHMORI K, HITOMI H, FUJIOKA H, et al. A New Method for Evaluation of Split Renal Cortical Blood Flow with Contrast Echography. Hypertens Res. 2002;25(1):77–83.

153. Muskiet MHA, Emanuel AL, Smits MM, Tonneijck L, Meijer RI, Joles JA, et al. Assessment of real-time and quantitative changes in renal hemodynamics in healthy overweight males: Contrast-enhanced ultrasonography vs para-aminohippuric acid clearance. Microcirculation. 2019;26(7).

154. Kishimoto N, Mori Y, Nishiue T, Shibasaki Y, Iba O, Nose A, et al. Renal blood flow measurement with contrast-enhanced harmonic ultrasonography: evaluation of dopamine-induced changes in renal cortical perfusion in humans. Clin Nephrol. 2003;59(06):423–8.

155. KISHIMOTO N, MORI Y, NISHIUE T, NOSE A, KIJIMA Y, TOKORO T, et al. Ultrasound Evaluation of Valsartan Therapy for Renal Cortical Perfusion. Hypertens Res. 2004 May;27(5):345–9.

156. Kalantarinia K, Belcik JT, Patrie JT, Wei K. Real-time measurement of renal blood flow in healthy subjects using contrast-enhanced ultrasound. Am J Physiol-renal. 2009 Oct;297(4):F1129–34.

157. Schneider AG, Hofmann L, Wuerzner G, Glatz N, Maillard M, Meuwly JY, et al. Renal perfusion evaluation with contrast-enhanced ultrasonography. Nephrol Dial Transpl. 2012 Feb;27(2):674–81.

158. Schneider AG, Calzavacca P, Schelleman A, Huynh T, Bailey M, May C, et al. Contrast-enhanced ultrasound evaluation of renal microcirculation in sheep. Intensive Care Medicine Exp. 2014 Dec;2(1):33.

159. Schneider AG, Schelleman A, Goodwin MD, Bailey M, Eastwood GM, Bellomo R. Contrast-enhanced ultrasound evaluation of the renal microcirculation response to

terlipressin in hepato-renal syndrome: a preliminary report. Renal Failure. 2014;37(1):175–9.

160. Schneider A, Johnson L, Goodwin M, Schelleman A, Bellomo R. Bench-to-bedside review: contrast enhanced ultrasonography--a promising technique to assess renal perfusion in the ICU. Critical care (London, England). 2011;15(3):157.

161. Schneider AG, Goodwin MD, Schelleman A, Bailey M, Johnson L, Bellomo R. Contrast-enhanced ultrasonography to evaluate changes in renal cortical microcirculation induced by noradrenaline: a pilot study. Crit Care. 2014 Dec 2;18(6):653.

162. Redfors B, Bragadottir G, Sellgren J, Swärd K, Ricksten SE. Effects of norepinephrine on renal perfusion, filtration and oxygenation in vasodilatory shock and acute kidney injury. Intens Care Med. 2011;37(1):60–7.

163. Wang XY, Pang YP, Jiang T, Wang S, Li JT, Shi BM, et al. Value of early diagnosis of sepsis complicated with acute kidney injury by renal contrast-enhanced ultrasound. World J Clin Cases. 2019;7(23):3934–44.

164. Johnson RJ, Feehally J, Floege J. Comprehensive Clinical Nephrology. fifth. Elsevier Saunders; 2015. 66–68 p.

165. Waikar SS, Bonventre JV. Creatinine Kinetics and the Definition of Acute Kidney Injury. J Am Soc Nephrol. 2009;20(3):672–9.

166. Waikar SS, Betensky RA, Emerson SC, Bonventre JV. Imperfect Gold Standards for Kidney Injury Biomarker Evaluation. J Am Soc Nephrol. 2012;23(1):13–21.

167. Macedo E, Malhotra R, Bouchard J, Wynn SK, Mehta RL. Oliguria is an early predictor of higher mortality in critically ill patients. Kidney Int. 2011;80(7):760–7.

168. Legrand M, Payen D. Understanding urine output in critically ill patients. Ann Intensive Care. 2011;1(1):13.

169. Ostermann M, Philips BJ, Forni LG. Clinical review: Biomarkers of acute kidney injury: where are we now? Crit Care. 2012;16(5):233.

170. Pickkers P, Darmon M, Hoste E, Joannidis M, Legrand M, Ostermann M, et al. Acute kidney injury in the critically ill: an updated review on pathophysiology and management. Intens Care Med. 2021;47(8):835–50.

171. Vaidya VS, Ozer JS, Dieterle F, Collings FB, Ramirez V, Troth S, et al. Kidney injury molecule-1 outperforms traditional biomarkers of kidney injury in preclinical biomarker qualification studies. Nat Biotechnol. 2010;28(5):478–85.

172. Endre ZH, Pickering JW, Walker RJ, Devarajan P, Edelstein CL, Bonventre JV, et al. Improved performance of urinary biomarkers of acute kidney injury in the critically ill by stratification for injury duration and baseline renal function. Kidney Int. 2011;79(10):1119–30.

173. Malyszko J, Lukaszyk E, Glowinska I, Durlik M. Biomarkers of delayed graft function as a form of acute kidney injury in kidney transplantation. Sci Rep-uk. 2015;5(1):11684.

174. Murray PT, Mehta RL, Shaw A, Ronco C, Endre Z, Kellum JA, et al. Potential use of biomarkers in acute kidney injury: report and summary of recommendations from the 10th Acute Dialysis Quality Initiative consensus conference. Kidney Int. 2014;85(3):513–21.

175. Nickolas TL, Schmidt-Ott KM, Canetta P, Forster C, Singer E, Sise M, et al. Diagnostic and Prognostic Stratification in the Emergency Department Using Urinary Biomarkers of Nephron Damage A Multicenter Prospective Cohort Study. J Am Coll Cardiol. 2012;59(3):246–55.

176. Coca SG, Parikh CR. Urinary Biomarkers for Acute Kidney Injury: Perspectives on Translation. Clin J Am Soc Nephro. 2008;3(2):481–90.

177. Ostermann M, Zarbock A, Goldstein S, Kashani K, Macedo E, Murugan R, et al. Recommendations on Acute Kidney Injury Biomarkers From the Acute Disease Quality Initiative Consensus Conference. Jama Netw Open. 2020;3(10):e2019209.

178. Mishra J, Ma Q, Prada A, Mitsnefes M, Zahedi K, Yang J, et al. Identification of Neutrophil Gelatinase-Associated Lipocalin as a Novel Early Urinary Biomarker for Ischemic Renal Injury. J Am Soc Nephrol. 2003;14(10):2534–43.

179. Kjeldsen L, Johnsen AH, Sengeløv H, Borregaard N. Isolation and primary structure of NGAL, a novel protein associated with human neutrophil gelatinase. J Biol Chem. 1993;268(14):10425–32.

180. Cowland JB, Borregaard N. Molecular Characterization and Pattern of Tissue Expression of the Gene for Neutrophil Gelatinase-Associated Lipocalin from Humans. Genomics. 1997;45(1):17–23.

181. Devarajan P. Neutrophil gelatinase-associated lipocalin—an emerging troponin for kidney injury. Nephrol Dial Transpl. 2008;23(12):3737–43.

182. Mishra J, Dent C, Tarabishi R, Mitsnefes MM, Ma Q, Kelly C, et al. Neutrophil gelatinase-associated lipocalin (NGAL) as a biomarker for acute renal injury after cardiac surgery. Lancet. 2005;365(9466):1231–8.

183. Geus HRH de, Bakker J, Lesaffre EMEH, Noble JLML le. Neutrophil Gelatinase-associated Lipocalin at ICU Admission Predicts for Acute Kidney Injury in Adult Patients. Am J Resp Crit Care. 2011;183(7):907–14.

184. Bachorzewska-Gajewska H, Malyszko J, Sitniewska E, Malyszko JS, Dobrzycki S. Neutrophil-Gelatinase-Associated Lipocalin and Renal Function after Percutaneous Coronary Interventions. Am J Nephrol. 2006;26(3):287–92.

185. Mishra J, Ma Q, Kelly C, Mitsnefes M, Mori K, Barasch J, et al. Kidney NGAL is a novel early marker of acute injury following transplantation. Pediatr Nephrol. 2006;21(6):856–63.

186. Geus HRH de, Woo JG, Wang Y, Devarajan P, Betjes MG, Noble JLML le, et al. Urinary Neutrophil Gelatinase-Associated Lipocalin Measured on Admission to the Intensive Care Unit Accurately Discriminates between Sustained and Transient Acute Kidney Injury in Adult Critically Ill Patients. Nephron Extra. 2011;1(1):9–23.

187. Zhang A, Cai Y, Wang PF, Qu JN, Luo ZC, Chen XD, et al. Diagnosis and prognosis of neutrophil gelatinase-associated lipocalin for acute kidney injury with sepsis: a systematic review and meta-analysis. Crit Care. 2016;20(1):41.

188. Parikh CR, Coca SG, Thiessen-Philbrook H, Shlipak MG, Koyner JL, Wang Z, et al. Postoperative Biomarkers Predict Acute Kidney Injury and Poor Outcomes after Adult Cardiac Surgery. J Am Soc Nephrol. 2011;22(9):1748–57.

189. Siew ED, Ware LB, Gebretsadik T, Shintani A, Moons KGM, Wickersham N, et al. Urine Neutrophil Gelatinase-Associated Lipocalin Moderately Predicts Acute Kidney Injury in Critically Ill Adults. J Am Soc Nephrol. 2009;20(8):1823–32.

190. Kashani K, Al-Khafaji A, Ardiles T, Artigas A, Bagshaw SM, Bell M, et al. Discovery and validation of cell cycle arrest biomarkers in human acute kidney injury. Crit Care. 2013 Feb 6;17(1):R25.

191. Bihorac A, Chawla LS, Shaw AD, Al-Khafaji A, Davison DL, DeMuth GE, et al. Validation of Cell-Cycle Arrest Biomarkers for Acute Kidney Injury Using Clinical Adjudication. Am J Resp Crit Care. 2014;189(8):932–9.

192. El-Khoury JM. Nephrocheck®: Checkmate or reality check? Ann Clin Biochem. 2021;58(1):3–5.

193. Bell M, Larsson A, Venge P, Bellomo R, Mårtensson J. Assessment of Cell-Cycle Arrest Biomarkers to Predict Early and Delayed Acute Kidney Injury. Dis Markers. 2015;2015:1–9.

194. Chindarkar NS, Chawla LS, Straseski JA, Jortani SA, Uettwiller-Geiger D, Orr RR, et al. Reference intervals of urinary acute kidney injury (AKI) markers [IGFBP7]·[TIMP2] in apparently healthy subjects and chronic comorbid subjects without AKI. Clin Chim Acta. 2016;452:32–7.

195. Koyner JL, Shaw AD, Chawla LS, Hoste EAJ, Bihorac A, Kashani K, et al. Tissue Inhibitor Metalloproteinase-2 (TIMP-2)·IGF-Binding Protein-7 (IGFBP7) Levels Are Associated with Adverse Long-Term Outcomes in Patients with AKI. J Am Soc Nephrol. 2015;26(7):1747–54.

196. Klein SJ, Brandtner AK, Lehner GF, Ulmer H, Bagshaw SM, Wiedermann CJ, et al. Biomarkers for prediction of renal replacement therapy in acute kidney injury: a systematic review and meta-analysis. Intens Care Med. 2018 Mar;44(3):323–36.

197. Zarbock A, Brendolan A, Martino F, Samoni S, Marchionna N, fan W, et al. TIMP-2*IGFBP7 as an auxiliary identification of successful discontinuation CRRT and prediction of renal recovery in critically ill patients: a case control study. 2020;

198. Peerapornratana S, Priyanka P, Wang S, Smith A, Singbartl K, Palevsky PM, et al. Sepsis-Associated Acute Kidney Disease. Kidney Int Reports. 2020;5(6):839–50.

199. Jia L, Sheng X, Zamperetti A, Xie Y, Corradi V, Chandel S, et al. Combination of biomarker with clinical risk factors for prediction of severe acute kidney injury in critically ill patients. Bmc Nephrol. 2020;21(1):540.

200. Sezen SF, Kenigs VA, Kapusta DR. Renal excretory responses produced by the delta opioid agonist, BW373U86, in conscious rats. J Pharmacol Exp Ther. 1998;287(1):238–45.

201. Donato LJ, Meeusen JW, Lieske JC, Bergmann D, Sparwaßer A, Jaffe AS. Analytical performance of an immunoassay to measure proenkephalin. Clin Biochem. 2018;58:72–7.

202. Khorashadi M, Beunders R, Pickkers P, Legrand M. Proenkephalin: A New Biomarker for Glomerular Filtration Rate and Acute Kidney Injury. Nephron. 2020;144(12):655–61.

203. Beunders R, Groenendael R van, Leijte GP, Kox M, Pickkers P. Proenkephalin Compared to Conventional Methods to Assess Kidney Function in Critically Ill Sepsis Patients. Shock. 2020;54(3):308–14.

204. Matsue Y, Maaten JM ter, Struck J, Metra M, O'Connor CM, Ponikowski P, et al. Clinical Correlates and Prognostic Value of Proenkephalin in Acute and Chronic Heart Failure. J Card Fail. 2017;23(3):231–9.

205. Marino R, Struck J, Hartmann O, Maisel AS, Rehfeldt M, Magrini L, et al. Diagnostic and short-term prognostic utility of plasma pro-enkephalin (pro-ENK) for acute kidney injury in patients admitted with sepsis in the emergency department. J Nephrol. 2015;28(6):717–24.

206. Caironi P, Latini R, Struck J, Hartmann O, Bergmann A, Bellato V, et al. Circulating Proenkephalin, Acute Kidney Injury, and Its Improvement in Patients with Severe Sepsis or Shock. Clin Chem. 2018;64(9):1361–9.

207. Gayat E, Touchard C, Hollinger A, Vieillard-Baron A, Mebazaa A, Legrand M, et al. Back-to-back comparison of penKID with NephroCheck® to predict acute kidney injury at admission in intensive care unit: a brief report. Crit Care. 2018;22(1):24.

208. Kellum JA, Sileanu FE, Bihorac A, Hoste EAJ, Chawla LS. Recovery after Acute Kidney Injury. Am J Resp Crit Care. 2016;195(6):784–91.

209. Chawla LS, Bellomo R, Bihorac A, Goldstein SL, Siew ED, Bagshaw SM, et al. Acute kidney disease and renal recovery: consensus report of the Acute Disease Quality Initiative (ADQI) 16 Workgroup. Nat Rev Nephrol. 2017;13(4):241–57.

210. Hoste E, Bihorac A, Al-Khafaji A, Ortega LM, Ostermann M, Haase M, et al. Identification and validation of biomarkers of persistent acute kidney injury: the RUBY study. Intens Care Med. 2020;46(5):943–53.

211. Bagshaw SM, Al-Khafaji A, Artigas A, Davison D, Haase M, Lissauer M, et al. External validation of urinary C–C motif chemokine ligand 14 (CCL14) for prediction of persistent acute kidney injury. Crit Care. 2021;25(1):185.

212. Massoth C, Küllmar M, Enders D, Kellum JA, Forni LG, Meersch M, et al. Comparison of C-C motif chemokine ligand 14 to other biomarkers for adverse kidney events after cardiac surgery. J Thorac Cardiovasc Surg. 2021;

213. MacKinnon KL, Molnar Z, Lowe D, Watson ID, Shearer E. Use of microalbuminuria as a predictor of outcome in critically ill patients. Bja Br J Anaesth. 2000;84(2):239–41.

214. Ralib AM, Pickering JW, Shaw GM, Than MP, George PM, Endre ZH. The clinical utility window for acute kidney injury biomarkers in the critically ill. Crit Care. 2014;18(6):601.

215. Faubel S. SuPAR: a potential predictive biomarker for acute kidney injury. Nat Rev Nephrol. 2020;16(7):375–6.

216. Zewinger S, Rauen T, Rudnicki M, Federico G, Wagner M, Triem S, et al. Dickkopf-3 (DKK3) in Urine Identifies Patients with Short-Term Risk of eGFR Loss. J Am Soc Nephrol. 2018 Nov;29(11):ASN.2018040405.

217. Coca SG, Garg AX, Thiessen-Philbrook H, Koyner JL, Patel UD, Krumholz HM, et al. Urinary Biomarkers of AKI and Mortality 3 Years after Cardiac Surgery. J Am Soc Nephrol. 2014;25(5):1063–71.

218. Coca SG, Jammalamadaka D, Sint K, Philbrook HT, Shlipak MG, Zappitelli M, et al. Preoperative proteinuria predicts acute kidney injury in patients undergoing cardiac surgery. J Thorac Cardiovasc Surg. 2012;143(2):495–502.

219. Goldstein SL. Urinary kidney injury biomarkers and urine creatinine normalization: a false premise or not? Kidney Int. 2010;78(5):433–5.

220. Waikar SS, Sabbisetti VS, Bonventre JV. Normalization of urinary biomarkers to creatinine during changes in glomerular filtration rate. Kidney Int. 2010;78(5):486–94.

221. Miftode RS, Şerban IL, Timpau AS, Miftode IL, Ion A, Buburuz AM, et al. Syndecan-1: A Review on Its Role in Heart Failure and Chronic Liver Disease Patients' Assessment. Cardiol Res Pract. 2019;2019:1–7.

222. Götte M. Syndecans in inflammation. Faseb J. 2003;17(6):575–91.

223. Stepp MA, Pal-Ghosh S, Tadvalkar G, Pajoohesh-Ganji A. Syndecan-1 and Its Expanding List of Contacts. Adv Wound Care. 2015;4(4):235–49.

224. Becker BF, Jacob M, Leipert S, Salmon AHJ, Chappell D. Degradation of the endothelial glycocalyx in clinical settings: searching for the sheddases. Brit J Clin Pharmaco. 2015;80(3):389–402.

225. Ogawa F, Oi Y, Nakajima K, Matsumura R, Nakagawa T, Miyagawa T, et al. Temporal change in Syndecan-1 as a therapeutic target and a biomarker for the severity classification of COVID-19. Thrombosis J. 2021;19(1):55.

226. Padberg JS, Wiesinger A, Marco GS di, Reuter S, Grabner A, Kentrup D, et al. Damage of the endothelial glycocalyx in chronic kidney disease. Atherosclerosis. 2014;234(2):335–43.

227. Wang J bo, Guan J, Shen J, Zhou L, Zhang Y jun, Si Y fang, et al. Insulin increases shedding of syndecan-1 in the serum of patients with type 2 diabetes mellitus. Diabetes Res Clin Pr. 2009;86(2):83–8.

228. Suzuki K, Okada H, Sumi K, Tomita H, Kobayashi R, Ishihara T, et al. Serum Syndecan-1 Reflects Organ Dysfunction in Critically Ill Patients. 2020;

229. Nelson A, Johansson J, Tydén J, Bodelsson M. Circulating syndecans during critical illness. Apmis. 2017;125(5):468–75.

230. Puskarich MA, Cornelius DC, Tharp J, Nandi U, Jones AE. Plasma syndecan-1 levels identify a cohort of patients with severe sepsis at high risk for intubation after large-volume intravenous fluid resuscitation. J Crit Care. 2016;36:125–9.

231. SALLISALMI M, TENHUNEN J, YANG R, OKSALA N, PETTILÄ V. Vascular adhesion protein-1 and syndecan-1 in septic shock. Acta Anaesth Scand. 2012;56(3):316–22.

232. Anand D, Ray S, Srivastava LM, Bhargava S. Evolution of serum hyaluronan and syndecan levels in prognosis of sepsis patients. Clin Biochem. 2016;49(10–11):768–76.

233. Cavalcante CT de MB, Branco KMC, Júnior VCP, Meneses GC, Neves FM de O, Souza NMG de, et al. Syndecan-1 improves severe acute kidney injury prediction after pediatric cardiac surgery. J Thorac Cardiovasc Surg. 2016;152(1):178-186.e2.

234. Bhatraju PK, Zelnick LR, Herting J, Katz R, Mikacenic C, Kosamo S, et al. Identification of Acute Kidney Injury Subphenotypes with Differing Molecular Signatures and Responses to Vasopressin Therapy. Am J Resp Crit Care. 2018;199(7):863–72.

235. Hahn RG, Patel V, Dull RO. Human glycocalyx shedding: Systematic review and critical appraisal. Acta Anaesth Scand. 2021;65(5):590–606.

236. Fiusa MML, Costa-Lima C, Souza GR, Vigorito AC, Aranha FJP, Lorand-Metze I, et al. A High Angiopoietin-2/Angiopoietin-1 Ratio Independently Predicts Septic Shock Development in Patients with Chemotherapy-Associated Febrile Neutropenia and Hematological Malignancies. Blood. 2012;120(21):2154–2154.

237. Ricciuto DR, Santos CC dos, Hawkes M, Toltl LJ, Conroy AL, Rajwans N, et al. Angiopoietin-1 and angiopoietin-2 as clinically informative prognostic biomarkers of morbidity and mortality in severe sepsis* Crit Care Med. 2011;39(4):702–10.

238. Parikh SM, Mammoto T, Schultz A, Yuan HT, Christiani D, Karumanchi SA, et al. Excess Circulating Angiopoietin-2 May Contribute to Pulmonary Vascular Leak in Sepsis in Humans. Plos Med. 2006;3(3):e46.

239. Binkowska A, Michalak G, Kopacz M, Słotwiński R. Soluble tumour necrosis factor receptor I is a promising early indicator of complicated clinical outcome in patients following severe trauma. Cent Eur J Immunol. 2019;44(4):423–32.

240. Bhatraju PK, Zelnick LR, Chinchilli VM, Moledina DG, Coca SG, Parikh CR, et al. Association Between Early Recovery of Kidney Function After Acute Kidney Injury and Long-term Clinical Outcomes. Jama Netw Open. 2020;3(4):e202682.

241. Bhatraju PK, Zelnick LR, Katz R, Mikacenic C, Kosamo S, Hahn WO, et al. A Prediction Model for Severe AKI in Critically Ill Adults That Incorporates Clinical and Biomarker Data. Clin J Am Soc Nephro. 2019;14(4):CJN.04100318.

242. Klimiuk PA, Sierakowski S, Domyslawska I, Chwiecko J. Serum chemokines in patients with rheumatoid arthritis treated with etanercept. Rheumatol Int. 2011;31(4):457–61.

243. Chang LH, Hwu CM, Lin YC, Huang CC, Won JGS, Chen HS, et al. SOLUBLE TUMOR NECROSIS FACTOR RECEPTOR TYPE 1 LEVELS EXHIBIT THE BETTER ASSOCIATION WITH RENAL OUTCOMES THAN TRADITIONAL RISK FACTORS IN CHINESE SUBJECTS WITH TYPE 2 DIABETES MELLITUS. Endocr Pract. 2020;26(10):1115–24.

244. Mikacenic C, Price BL, Harju-Baker S, O'Mahony DS, Robinson-Cohen C, Radella F, et al. A Two-Biomarker Model Predicts Mortality in the Critically Ill with Sepsis. Am J Resp Crit Care. 2017;196(8):1004–11.

245. Iglesias J, Marik PE, Levine JS. Elevated serum levels of the type I and type II receptors for tumor necrosis factor-α as predictive factors for ARF in patients with septic shock. Am J Kidney Dis. 2003;41(1):62–75.

246. Murugan R, Wen X, Shah N, Lee M, Kong L, Pike F, et al. Plasma inflammatory and apoptosis markers are associated with dialysis dependence and death among critically ill patients receiving renal replacement therapy. Nephrol Dial Transpl. 2014;29(10):1854–64.

247. Pike F, Murugan R, Keener C, Palevsky PM, Vijayan A, Unruh M, et al. Biomarker Enhanced Risk Prediction for Adverse Outcomes in Critically Ill Patients Receiving RRT. Clin J Am Soc Nephro. 2015;10(8):1332–9.

248. Bhatraju PK, Zelnick LR, Shlipak M, Katz R, Kestenbaum B. Association of Soluble TNFR-1 Concentrations with Long-Term Decline in Kidney Function: The Multi-Ethnic Study of Atherosclerosis. J Am Soc Nephrol. 2018;29(11):2713–21.

249. Liangos O, Kolyada A, Tighiouart H, Perianayagam MC, Wald R, Jaber BL. Interleukin-8 and Acute Kidney Injury following Cardiopulmonary Bypass: A Prospective Cohort Study. Nephron Clin Pract. 2009;113(3):c148–54.

250. Kwon O, Molitoris BA, Pescovitz M, Kelly KJ. Urinary actin, interleukin-6, and interleukin-8 may predict sustained arf after ischemic injury in renal allografts. Am J Kidney Dis. 2003;41(5):1074–87.

251. Åhlström A, Hynninen M, Tallgren M, Kuusela P, Valtonen M, Orko R, et al. Predictive value of interleukins 6, 8 and 10, and low HLA-DR expression in acute renal failure. Clin Nephrol. 2004;61(02):103–10.

252. Simmons EM, Himmelfarb J, Sezer MT, Chertow GM, Mehta RL, Paganini EP, et al. Plasma cytokine levels predict mortality in patients with acute renal failure. Kidney Int. 2004;65(4):1357–65.

253. Nelson DP, Beyer C, Samsel RW, Wood LD, Schumacker PT. Pathological supply dependence of O2 uptake during bacteremia in dogs. J Appl Physiol. 1987;63(4):1487–92.

254. Ronco JJ, Fenwick JC, Tweeddale MG, Wiggs BR, Phang PT, Cooper DJ, et al. Identification of the Critical Oxygen Delivery for Anaerobic Metabolism in Critically Ill Septic and Nonseptic Humans. Jama. 1993;270(14):1724–30.

255. Hemodynamic Monitoring. Lessons Icu. 2019;

256. Janotka M, Ostadal P. Biochemical markers for clinical monitoring of tissue perfusion. Mol Cell Biochem. 2021;476(3):1313–26.

257. Rivers E, Nguyen B, Havstad S, Ressler J, Muzzin A, Knoblich B, et al. Early Goal-Directed Therapy in the Treatment of Severe Sepsis and Septic Shock. New Engl J Medicine. 2001 Nov 8;345(19):1368–77.

258. Walley KR. Use of central venous oxygen saturation to guide therapy. American journal of respiratory and critical care medicine. 2011 Sep 1;184(5):514–20.

259. Gutierrez G. Central and Mixed Venous O2 Saturation. Turkish journal of anaesthesiology and reanimation. 2020 Feb;48(1):2–10.

260. Investigators A, Group ACT, Peake SL, Delaney A, Bailey M, Bellomo R, et al. Goal-Directed Resuscitation for Patients with Early Septic Shock. New Engl J Medicine. 2014 Oct 16;371(16):1496–506.

261. Investigators P, Yealy DM, Kellum JA, Huang DT, Barnato AE, Weissfeld LA, et al. A Randomized Trial of Protocol-Based Care for Early Septic Shock. New Engl J Medicine. 2014 May 1;370(18):1683–93.

262. Mouncey PR, Osborn TM, Power GS, Harrison DA, Sadique MZ, Grieve RD, et al. Trial of Early, Goal-Directed Resuscitation for Septic Shock. New Engl J Medicine. 2015 Apr 2;372(14):1301–11.

263. Arnold RC, Shapiro NI, Jones AE, Schorr C, Pope J, Casner E, et al. Multicenter study of early lactate clearance as a determinant of survival in patients with presumed sepsis. Shock. 2009 Jul;32(1):35–9.

264. Perz S, Uhlig T, Kohl M, Bredle DL, Reinhart K, Bauer M, et al. Low and “supranormal” central venous oxygen saturation and markers of tissue hypoxia in cardiac surgery patients: a prospective observational study. Intens Care Med. 2011 Jan;37(1):52–9.

265. Bracht H, Hänggi M, Jeker B, Wegmüller N, Porta F, Tüller D, et al. Incidence of low central venous oxygen saturation during unplanned admissions in a multidisciplinary intensive care unit: an observational study. Crit Care. 2007;11(1):R2.

266. Ince C, Sinaasappel M. Microcirculatory oxygenation and shunting in sepsis and shock. Crit Care Med. 1999;27(7):1369-1377.

267. Alegría L, Vera M, Dreyse J, Castro R, Carpio D, Henriquez C, et al. A hypoperfusion context may aid to interpret hyperlactatemia in sepsis-3 septic shock patients: a proof-of-concept study. Ann Intensive Care. 2017;7(1):29.

268. Wittayachamnankul B, Apaijai N, Sutham K, Chenthanakij B, Liwsrisakun C, Jaiwongkam T, et al. High central venous oxygen saturation is associated with mitochondrial dysfunction in septic shock: A prospective observational study. J Cell Mol Med. 2020;24(11):6485–94.

269. Beest P van, Wietasch G, Scheeren T, Spronk P, Kuiper M. Clinical review: use of venous oxygen saturations as a goal - a yet unfinished puzzle. Crit Care. 2011;15(5):232.

270. Puskarich MA, Trzeciak S, Shapiro NI, Arnold RC, Heffner AC, Kline JA, et al. Prognostic value and agreement of achieving lactate clearance or central venous oxygen saturation goals during early sepsis resuscitation. Academic emergency medicine : official journal of the Society for Academic Emergency Medicine. 2012 Mar;19(3):252–8.

271. Teboul JL, Mercat A, Lenique F, Berton C, Richard C. Value of the venous-arterial PCO2 gradient to reflect the oxygen supply to demand in humans: effects of dobutamine. Critical Care Medicine. 1998 Jun;26(6):1007–10.

272. Bakker J, Vincent JL, Gris P, Leon M, Coffernils M, Kahn RJ. Veno-arterial carbon dioxide gradient in human septic shock. CHEST. 1992 Feb;101(2):509–15.

273. Mecher CE, Rackow EC, Astiz ME, Weil MH. Venous hypercarbia associated with severe sepsis and systemic hypoperfusion. Critical Care Medicine. 1990 Jun;18(6):585–9.

274. Zhang H, Spapen H, Manikis P, Backer DD, Vincent J. ARTERIOVENOUS DIFFERENCES IN PCO2 AND pH ARE RELIABLE INDICATORS OF CRITICAL HYPOPERFUSION IN SEPTIC SHOCK. Shock. 1994;2(Supplement):18.

275. Vallée F, Vallet B, Mathe O, Parraguette J, Mari A, Silva S, et al. Central venous-to-arterial carbon dioxide difference: an additional target for goal-directed therapy in septic shock? Intens Care Med. 2008 Dec;34(12):2218.

276. Dres M, Monnet X, Teboul JL. Hemodynamic management of cardiovascular failure by using PCO2 venous-arterial difference. J Clin Monitor Comp. 2012 Oct;26(5):367–74.

277. Randall HM, Cohen JJ. Anaerobic CO2 production by dog kidney in vitro. The American journal of physiology. 1966 Aug;211(2):493–505.

278. Jensen FB. Red blood cell pH, the Bohr effect, and other oxygenation-linked phenomena in blood O2 and CO2 transport. Acta Physiol Scand. 2004;182(3):215–27.

279. Groeneveld ABJ. Interpreting the venous-arterial PCO2 difference. Crit Care Med. 1998;26(6):979-980.

280. Nevière R, Chagnon JL, Teboul JL, Vallet B, Wattel F. Small intestine intramucosal PCO(2) and microvascular blood flow during hypoxic and ischemic hypoxia. Critical Care Medicine. 2002 Feb;30(2):379–84.

281. Groeneveld ABJ, Vermeij CG, Thijs LG. Arterial and Mixed Venous Blood Acid-Base Balance During Hypoperfusion With Incremental Positive End-Expiratory Pressure in the Pig. Anesthesia Analgesia. 1991;73(5):576.

282. Cuschieri J, Rivers EP, Donnino MW, Katilius M, Jacobsen G, Nguyen HB, et al. Central venous-arterial carbon dioxide difference as an indicator of cardiac index. Intens Care Med. 2005;31(6):818–22.

283. Gavelli F, Teboul JL, Monnet X. How can CO 2 -derived indices guide resuscitation in critically ill patients? J Thorac Dis. 2019 Jul;1(1):S1528–37.

284. Monnet X, Julien F, Ait-Hamou N, Lequoy M, Gosset C, Jozwiak M, et al. Lactate and Venoarterial Carbon Dioxide Difference/Arterial-Venous Oxygen Difference Ratio, but Not Central Venous Oxygen Saturation, Predict Increase in Oxygen Consumption in Fluid Responders* Crit Care Med. 2013 Jun;41(6):1412–20.

285. Futier E, Robin E, Jabaudon M, Guerin R, Petit A, Bazin JE, et al. Central venous O2 saturation and venous-to-arterial CO2 difference as complementary tools for goal-directed therapy during high-risk surgery. Crit Care. 2010;14(5):R193.

286. Robin E, Futier E, Pires O, Fleyfel M, Tavernier B, Lebuffe G, et al. Central venous-to-arterial carbon dioxide difference as a prognostic tool in high-risk surgical patients. Crit Care. 2015;19(1):227.

287. Guinot PG, Badoux L, Bernard E, Abou-Arab O, Lorne E, Dupont H. Central Venous-to-Arterial Carbon Dioxide Partial Pressure Difference in Patients Undergoing Cardiac Surgery is Not Related to Postoperative Outcomes. J Cardiothor Vasc An. 2017;31(4):1190–6.

288. Beest PA van, Lont MC, Holman ND, Loef B, Kuiper MA, Boerma EC. Central venous-arterial pCO2 difference as a tool in resuscitation of septic patients. Intens Care Med. 2013;39(6):1034–9.

289. Mekontso-Dessap A, Castelain V, Anguel N, Bahloul M, Schauvliege F, Richard C, et al. Combination of venoarterial PCO2 difference with arteriovenous O2 content difference to detect anaerobic metabolism in patients. Intens Care Med. 2002 Mar;28(3):272–7.

290. Mesquida J, Saludes P, Gruartmoner G, Espinal C, Torrents E, Baigorri F, et al. Central venous-to-arterial carbon dioxide difference combined with arterial-to-venous oxygen content difference is associated with lactate evolution in the hemodynamic resuscitation process in early septic shock. Crit Care. 2015 Mar 28;19(1):126.

291. He H wu, Liu D wei, Long Y, Wang X ting. High central venous-to-arterial CO2 difference/arterial-central venous O2 difference ratio is associated with poor lactate clearance in septic patients after resuscitation. J Crit Care. 2016;31(1):76–81.

292. Kolsi H, Jawadi W, Chaabouni A, Fki M, Walha K, Karoui A. THE ABILITY OF CARBON DIOXYDE-DERIVED INDICES TO PREDICT ADVERSE OUTCOME AFTER CARDIAC SURGERY. J Cardiothor Vasc An. 2021;

293. Pavez N, Kattan E, Vera M, Ferri G, Valenzuela ED, Alegría L, et al. Hypoxia-related parameters during septic shock resuscitation: Pathophysiological determinants and potential clinical implications. Ann Transl Medicine. 2020;8(12):784.

294. Backer DD, Creteur J, Preiser JC, Dubois MJ, Vincent JL. Microvascular Blood Flow Is Altered in Patients with Sepsis. Am J Resp Crit Care. 2002 Jul;166(1):98–104.

295. Sakr Y, Dubois MJ, Backer DD, Creteur J, Vincent JL. Persistent microcirculatory alterations are associated with organ failure and death in patients with septic shock* Crit Care Med. 2004 Sep;32(9):1825–31.

296. Sakr Y, Chierego M, Piagnerelli M, Verdant C, Dubois MJ, Koch M, et al. Microvascular response to red blood cell transfusion in patients with severe sepsis* Crit Care Med. 2007 Jul;35(7):1639–44.

297. Sakr Y, Gath V, Oishi J, Klinzing S, Simon TP, Reinhart K, et al. Characterization of buccal microvascular response in patients with septic shock. European journal of anaesthesiology. 2010 Apr;27(4):388–94.

298. Trzeciak S, McCoy JV, Dellinger RP, Arnold RC, Rizzuto M, Abate NL, et al. Early increases in microcirculatory perfusion during protocol-directed resuscitation are associated with reduced multi-organ failure at 24 h in patients with sepsis. Intens Care Med. 2008 Dec;34(12):2210–7.

299. Massey MJ, Hou PC, Filbin M, Wang H, Ngo L, Huang DT, et al. Microcirculatory perfusion disturbances in septic shock: results from the ProCESS trial. Crit Care. 2018 Nov 20;22(1):308.

300. Arnold RC, Parrillo JE, Dellinger RP, Chansky ME, Shapiro NI, Lundy DJ, et al. Point-of-care assessment of microvascular blood flow in critically ill patients. Intens Care Med. 2009 Jun 24;35(10):1761–6.

301. Scorcella C, Damiani E, Domizi R, Pierantozzi S, Tondi S, Carsetti A, et al. MicroDAIMON study: Microcirculatory DAIly MONitoring in critically ill patients: a prospective observational study. Ann Intensive Care. 2018 May 15;8(1):64.

302. Edul VSK, Enrico C, Laviolle B, Vazquez AR, Ince C, Dubin A. Quantitative assessment of the microcirculation in healthy volunteers and in patients with septic shock. Critical Care Medicine. 2012 May;40(5):1443–8.

303. Uil CA den, Lagrand WK, Ent M van der, Nieman K, Struijs A, Jewbali LSD, et al. Conventional Hemodynamic Resuscitation May Fail to Optimize Tissue Perfusion: An Observational Study on the Effects of Dobutamine, Enoximone, and Norepinephrine in Patients with Acute Myocardial Infarction Complicated by Cardiogenic Shock. Merx MW, editor. Plos One. 2014;9(8):e103978.

304. Uil CA den, Lagrand WK, Ent M van der, Jewbali LSD, Cheng JM, Spronk PE, et al. Impaired microcirculation predicts poor outcome of patients with acute myocardial infarction complicated by cardiogenic shock. Eur Heart J. 2010 Dec;31(24):3032–9.

305. Backer DD, Donadello K, Sakr Y, Ospina-Tascon G, Salgado D, Scolletta S, et al. Microcirculatory Alterations in Patients With Severe Sepsis. Crit Care Med. 2013 Mar;41(3):791–9.

306. Tachon G, Harrois A, Tanaka S, Kato H, Huet O, Pottecher J, et al. Microcirculatory Alterations in Traumatic Hemorrhagic Shock* Crit Care Med. 2014 Jun;42(6):1433–41.

307. Hutchings SD, Naumann DN, Hopkins P, Mellis C, Riozzi P, Sartini S, et al. Microcirculatory Impairment Is Associated With Multiple Organ Dysfunction Following Traumatic Hemorrhagic Shock. Crit Care Med. 2018 Sep;46(9):e889–96.

308. Top APC, Ince C, Dijk M van, Tibboel D. Changes in buccal microcirculation following extracorporeal membrane oxygenation in term neonates with severe respiratory failure. Critical Care Medicine. 2009 Mar;37(3):1121–4.

309. Kara A, Akin S, Miranda D dos R, Struijs A, Caliskan K, Thiel RJ van, et al. Microcirculatory assessment of patients under VA-ECMO. Crit Care. 2016 Oct 25;20(1):344.

310. Akin S, Miranda D dos R, Caliskan K, Soliman OI, Guven G, Struijs A, et al. Functional evaluation of sublingual microcirculation indicates successful weaning from VA-ECMO in cardiogenic shock. Crit Care. 2017;21(1):265.

311. Jhanji S, Lee C, Watson D, Hinds C, Pearse RM. Microvascular flow and tissue oxygenation after major abdominal surgery: association with post-operative complications. Intens Care Med. 2009 Apr;35(4):671–7.

312. Pranskunas A, Tamosuitis T, Balciuniene N, Damanskyte D, Sneider E, Vitkauskiene A, et al. Alterations of conjunctival glycocalyx and microcirculation in non-septic critically ill patients. Microvasc Res. 2018;118:44–8.

313. Shih CC, Liu CM, Chao A, Lee CT, Hsu YC, Yeh YC. Matched Comparison of Microcirculation Between Healthy Volunteers and Patients with Sepsis. Asian J Anesthesiol. 2018;56(1):14–22.

314. Boerma C, Voort PHJ van der, Spronk PE, Ince C. Relationship between sublingual and intestinal microcirculatory perfusion in patients with abdominal sepsis. Critical Care Medicine. 2007 Apr;35(4):1055–60.

315. Mathura KR, Bouma GJ, Ince C. Abnormal microcirculation in brain tumours during surgery. Lancet. 2001;358(9294):1698–9.

316. Tavy ALM, Bruin AFJ de, Sloot K van der, Boerma EC, Ince C, Noordzij PG, et al. Effects of Thoracic Epidural Anaesthesia on the Serosal Microcirculation of the Human Small Intestine. World J Surg. 2018;42(12):3911–7.

317. Uz Z, Kastelein AW, Milstein DMJ, Liu D, Rassam F, Veelo DP, et al. Intraoperative Incident Dark Field Imaging of the Human Peritoneal Microcirculation. J Vasc Res. 2018;55(3):136–43.

318. Uz Z, Ince C, Rassam F, Ergin B, Lienden KP van, Gulik TM van. Assessment of hepatic microvascular flow and density in patients undergoing preoperative portal vein embolization. Hpb. 2019;21(2):187–94.

319. Verdant CL, Backer DD, Bruhn A, Clausi CM, Su F, Wang Z, et al. Evaluation of sublingual and gut mucosal microcirculation in sepsis: a quantitative analysis. Critical Care Medicine. 2009 Nov;37(11):2875–81.

320. Ferrara G, Edul VSK, Canales HS, Martins E, Canullán C, Murias G, et al. Systemic and microcirculatory effects of blood transfusion in experimental hemorrhagic shock. Intensive Care Medicine Exp. 2017;5(1):24.

321. Jacquet-Lagrèze M, Allaouchiche B, Restagno D, Paquet C, Ayoub JY, Etienne J, et al. Gut and sublingual microvascular effect of esmolol during septic shock in a porcine model. Crit Care. 2015;19(1):241.

322. Sui F, Zheng Y, Li WX, Zhou JL. Renal circulation and microcirculation during intra-abdominal hypertension in a porcine model. Eur Rev Med Pharmaco. 2016;20(3):452–61.

323. Lima A, Rooij T van, Ergin B, Sorelli M, Ince Y, Specht PAC, et al. Dynamic Contrast-Enhanced Ultrasound Identifies Microcirculatory Alterations in Sepsis-Induced Acute Kidney Injury. Crit Care Med [Internet]. 2018 Aug;46(8):1284–92. Available from: message:%3C2CFF0F1E-0136-429D-9138-4B030C74BED1@nhs.net%3E

324. Aykut G, Veenstra G, Scorcella C, Ince C, Boerma C. Cytocam-IDF (incident dark field illumination) imaging for bedside monitoring of the microcirculation. Intensive Care Medicine Exp. 2015 Dec;3(1):4.

325. Sherman H, Klausner S, Cook WA. Incident dark-field illumination: a new method for microcirculatory study. Angiology. 1971 May;22(5):295–303.

326. Elteren HA van, Ince C, Tibboel D, Reiss IKM, Jonge RCJ de. Cutaneous microcirculation in preterm neonates: comparison between sidestream dark field (SDF) and incident dark field (IDF) imaging. J Clin Monitor Comp. 2015 Oct;29(5):543–8.

327. Hutchings S, Watts S, Kirkman E. The Cytocam video microscope. A new method for visualising the microcirculation using Incident Dark Field technology. Clinical hemorheology and microcirculation. 2016;62(3):261–71.

328. ESICM O behalf of the CDS of the, Ince C, Boerma EC, Cecconi M, Backer DD, Shapiro NI, et al. Second consensus on the assessment of sublingual microcirculation in critically ill patients: results from a task force of the European Society of Intensive Care Medicine. Intens Care Med. 2018 Mar;44(3):281–99.

329. Backer DD, Hollenberg S, Boerma C, Goedhart P, Büchele G, Ospina-Tascon G, et al. How to evaluate the microcirculation: report of a round table conference. Crit Care. 2007 Oct 5;11(5):R101.

330. Shore AC. Capillaroscopy and the measurement of capillary pressure. British journal of clinical pharmacology. 2000 Dec;50(6):501–13.

331. Boerma EC, Mathura KR, Voort PH van der, Spronk PE, Ince C. Quantifying bedside-derived imaging of microcirculatory abnormalities in septic patients: a prospective validation study. Crit Care. 2005;9(6):R601.

332. Tanaka S, Harrois A, Nicolaï C, Flores M, Hamada S, Vicaut E, et al. Qualitative real-time analysis by nurses of sublingual microcirculation in intensive care unit: the MICRONURSE study. Crit Care. 2015 Nov 2;19(1):388.

333. Pozo MO, Edul VSK, Ince C, Dubin A. Comparison of Different Methods for the Calculation of the Microvascular Flow Index. Critical Care Res Pract. 2012;2012(5):102483.

334. Spronk PE, Ince C, Gardien MJ, Mathura KR, Straaten HMO van, Zandstra DF. Nitroglycerin in septic shock after intravascular volume resuscitation. Lancet. 2002 Nov 2;360(9343):1395–6.

335. Donati A, Domizi R, Damiani E, Adrario E, Pelaia P, Ince C. From Macrohemodynamic to the Microcirculation. Critical Care Res Pract. 2013;2013(9):892710.

336. Arnold RC, Dellinger RP, Parrillo JE, Chansky ME, Lotano VE, McCoy JV, et al. Discordance between microcirculatory alterations and arterial pressure in patients with hemodynamic instability. Journal of Critical Care. 2012 Oct;27(5):531.e1-7.

337. Johnson C, Grant R, Dansie B, Taylor J, Spyropolous P. Measurement of blood flow in the vertebral artery using colour duplex Doppler ultrasound: establishment of the reliability of selected parameters. Man Ther. 2000;5(1):21–9.

338. Bunting KV, Steeds RP, Slater LT, Rogers JK, Gkoutos GV, Kotecha D. A Practical Guide to Assess the Reproducibility of Echocardiographic Measurements. J Am Soc Echocardiog. 2019;32(12):1505–15.

339. Benchoufi M, Matzner-Lober E, Molinari N, Jannot AS, Soyer P. Interobserver agreement issues in radiology. Diagn Interv Imag. 2020;101(10):639–41.

340. Post EH, Kellum JA, Bellomo R, Vincent JL. Renal perfusion in sepsis: from macro- to microcirculation. Kidney Int. 2017 Jan 1;91(1):45–60.

341. Benes J, Chvojka J, Sykora R, Radej J, Krouzecky A, Novak I, et al. Searching for mechanisms that matter in early septic acute kidney injury: an experimental study. Crit Care. 2011;15(5):R256.

342. Bellomo R, Kellum JA, Ronco C, Wald R, Martensson J, Maiden M, et al. Acute kidney injury in sepsis. Intens Care Med. 2017 Mar 31;43(6):816–28.

343. Maiden MJ, Otto S, Brealey JK, Finnis ME, Chapman MJ, Kuchel TR, et al. Structure and Function of the Kidney in Septic Shock. A Prospective Controlled Experimental Study. Am J Resp Crit Care. 2016 Sep 15;194(6):692–700.

344. Lankadeva YR, Kosaka J, Evans RG, Bailey SR, Bellomo R, May CN. Intrarenal and urinary oxygenation during norepinephrine resuscitation in ovine septic acute kidney injury. Kidney Int. 2016 Jul 1;90(1):100–8.

345. Langenberg C, Bellomo R, May C, Wan L, Egi M, Morgera S. Renal blood flow in sepsis. Crit Care [Internet]. 2005 May 23;9(4):R363. Available from: https://www.ncbi.nlm.nih.gov/pmc/articles/PMC1269441/pdf/cc3540.pdf

346. Langenberg C, Wan L, Egi M, May CN, Bellomo R. Renal blood flow in experimental septic acute renal failure. Kidney Int. 2006;69(11):1996–2002.

347. Giantomasso DD, Morimatsu H, May CN, Bellomo R. Intrarenal blood flow distribution in hyperdynamic septic shock: Effect of norepinephrine. Crit Care Med. 2003;31(10):2509–13.

348. Calzavacca P, Evans RG, Bailey M, Bellomo R, May CN. Cortical and Medullary Tissue Perfusion and Oxygenation in Experimental Septic Acute Kidney Injury. Crit Care Med. 2015 Oct;43(10):e431–9.

349. Watchorn J, Huang DY, Joslin J, Bramham K, Hutchings SD. Critically ILL COVID-19 Patients With Acute Kidney Injury Have Reduced Renal Blood Flow and Perfusion Despite Preserved Cardiac Function; A Case-Control Study Using Contrast Enhanced Ultrasound. Shock. 2020;Publish Ahead of Print.

350. Wharton G, Steeds R, Allen J, Phillips H, Jones R, Kanagala P, et al. A minimum dataset for a standard adult transthoracic echocardiogram: a guideline protocol from the British Society of Echocardiography. Echo Res Pract. 2015 Mar 1;2(1):G9–24.

351. Khwaja A. KDIGO Clinical Practice Guidelines for Acute Kidney Injury. Nephron Clin Pract. 2012;120(4):c179–84.

352. Hsu CY, Ordoñez JD, Chertow GM, Fan D, McCulloch CE, Go AS. The risk of acute renal failure in patients with chronic kidney disease. Kidney Int. 2008;74(1):101–7.

353. Levey AS, Stevens LA. Estimating GFR Using the CKD Epidemiology Collaboration (CKD-EPI) Creatinine Equation: More Accurate GFR Estimates, Lower CKD Prevalence Estimates, and Better Risk Predictions. Am J Kidney Dis. 2010;55(4):622–7.

354. Hellebrekers LJ, Liard JF, Laborde AL, Greene AS, Cowley AW. Regional autoregulatory responses during infusion of vasoconstrictor agents in conscious dogs. Am J Physiol-Hear Circ Physiol. 1990;259(4):H1270–7.

355. Bellomo R, Wan L, May C. Vasoactive drugs and acute kidney injury. Crit Care Med. 2008;36(4):S179–86.

356. Denic A, Lieske JC, Chakkera HA, Poggio ED, Alexander MP, Singh P, et al. The Substantial Loss of Nephrons in Healthy Human Kidneys with Aging. J Am Soc Nephrol. 2017;28(1):313–20.

357. James MT, Hemmelgarn BR, Wiebe N, Pannu N, Manns BJ, Klarenbach SW, et al. Glomerular filtration rate, proteinuria, and the incidence and consequences of acute kidney injury: a cohort study. Lancet. 2010;376(9758):2096–103.

358. Prowle JR, Molan MP, Hornsey E, Bellomo R. Measurement of renal blood flow by phase-contrast magnetic resonance imaging during septic acute kidney injury. Crit Care Med. 2012 Jun;40(6):1768–76.

359. TAKEUCHI J, ISHIKAWA I, INASAKA T, SAKAI S, SHINODA A, TAKADA A, et al. Intrarenal Distribution of Blood Flow in Man. Circulation. 1970;42(2):347–60.

360. Wu L, Tiwari MM, Messer KJ, Holthoff JH, Gokden N, Brock RW, et al. Peritubular capillary dysfunction and renal tubular epithelial cell stress following lipopolysaccharide administration in mice. Am J Physiol-renal. 2007;292(1):F261–8.

361. Seely KA, Holthoff JH, Burns ST, Wang Z, Thakali KM, Gokden N, et al. Hemodynamic changes in the kidney in a pediatric rat model of sepsis-induced acute kidney injury. Am J Physiol-renal. 2011;301(1):F209–17.

362. Reynès C, Vinet A, Maltinti O, Knapp Y. Minimizing the duration of laser Doppler flowmetry recordings while maintaining wavelet analysis quality: A methodological study. Microvascular research. 2020 Sep;131:104034.

363. Garrison RN, Wilson MA, Matheson PJ, Spain DA. Nitric Oxide Mediates Redistribution of Intrarenal Blood Flow during Bacteremia. J Trauma Inj Infect Critical Care. 1995;39(1):90-97.

364. AUGUSTE LJ, STONE AM, WISE L. The Effects of Escherichia coli Bacteremia on in Vitro Perfused Kidneys. Ann Surg. 1980;192(1):65–8.

365. Schurek HJ, Jost U, Baumgartl H, Bertram H, Heckmann U. Evidence for a preglomerular oxygen diffusion shunt in rat renal cortex. Am J Physiol-renal [Internet]. 2002 Aug 20;259(6):F910–5. Available from: https://www.physiology.org/doi/pdf/10.1152/ajprenal.1990.259.6.F910

366. Molitoris BA, Sandoval RM. Kidney Endothelial Dysfunction: Ischemia, Localized Infections and Sepsis. Contrib Nephrol. 2011;174:108–18.

367. O'Connor PM, Anderson WP, Kett MM, Evans RG. RENAL PREGLOMERULAR ARTERIAL–VENOUS O2 SHUNTING IS A STRUCTURAL ANTI-OXIDANT DEFENCE MECHANISM OF THE RENAL CORTEX. Clin Exp Pharmacol P. 2006;33(7):637–41.

368. Vilander LM, Kaunisto MA, Vaara ST, Pettilä V, Laru-Sompa R, Pulkkinen A, et al. Genetic variants in SERPINA4 and SERPINA5, but not BCL2 and SIK3 are associated with acute kidney injury in critically ill patients with septic shock. Crit Care. 2017;21(1):47.

369. Zarbock A, Nadim MK, Pickkers P, Gomez H, Bell S, Joannidis M, et al. Sepsis-associated acute kidney injury: consensus report of the 28th Acute Disease Quality Initiative workgroup. Nat Rev Nephrol. 2023;19(6):401–17.

370. Vilander LM, Kaunisto MA, Pettilä V. Genetic predisposition to acute kidney injury – a systematic review. BMC Nephrol. 2015;16(1):197.

371. Heemskerk S, Masereeuw R, Russel FGM, Pickkers P. Selective iNOS inhibition for the treatment of sepsis-induced acute kidney injury. Nat Rev Nephrol. 2009;5(11):629–40.

372. Schrier RW, Wang W. Acute Renal Failure and Sepsis. New Engl J Medicine. 2004;351(2):159–69.

373. Tsukahara Y, Morisaki T, Kojima M, Uchiyama A, Tanaka M. iNOS expression by activated neutrophils from patients with sepsis. Anz J Surg. 2001;71(1):15–20.

374. Wu F, Tyml K, Wilson JX. iNOS expression requires NADPH oxidase-dependent redox signaling in microvascular endothelial cells. J Cell Physiol. 2008;217(1):207–14.

375. Bultinck J, Sips P, Vakaet L, Brouckaert P, Cauwels A, Bultinck J, et al. Systemic NO production during (septic) shock depends on parenchymal and not on hematopoietic cells: in vivo iNOS expression pattern in (septic) shock. Faseb J. 2006;20(13):2363–5.

376. Trzeciak S, Cinel I, Dellinger RP, Shapiro NI, Arnold RC, Parrillo JE, et al. Resuscitating the Microcirculation in Sepsis: The Central Role of Nitric Oxide, Emerging Concepts for Novel Therapies, and Challenges for Clinical Trials. Acad Emerg Med. 2008;15(5):399–413.

377. Spain DA, Wilson MA, Bar-Natan MF, Garrison RN. NITRIC OXIDE SYNTHASE INHIBITION AGGRAVATES INTESTINAL MICROVASCULAR VASOCONSTRICTION AND HYPOPERFUSION OF BACTEREMIA. J Trauma Inj Infect Critical Care. 1994;36(5):720–5.

378. Spain DA, Wilson MA, Garrison RN. Nitric oxide synthase inhibition exacerbates sepsis-induced renal hypoperfusion. Surgery. 1994;116(2):322–30; discussion 330-1.

379. Spain DA, Wilson MA, Bloom ITM, Garrison RN. Renal Microvascular Responses to Sepsis Are Dependent on Nitric Oxide. J Surg Res. 1994;56(6):524–9.

380. Avontuur JAM, Bruining HA, Ince C. Inhibition of Nitric Oxide Synthesis Causes Myocardial Ischemia in Endotoxemic Rats. Circ Res. 1995;76(3):418–25.

381. Zhang H, Rogiers P, Smail N, Cabral A, Preiser JC, Peny MO, et al. Effects of nitric oxide on blood flow distribution and O2 extraction capabilities during endotoxic shock. J Appl Physiol. 1997;83(4):1164–73.

382. Caterina RD, Libby P, Peng HB, Thannickal VJ, Rajavashisth TB, Gimbrone MA, et al. Nitric oxide decreases cytokine-induced endothelial activation. Nitric oxide selectively reduces endothelial expression of adhesion molecules and proinflammatory cytokines. J Clin Invest. 1995;96(1):60–8.

383. Gundersen Y, Corso CO, Leiderer R, Dörger M, Lilleaasen P, Aasen AO, et al. The nitric oxide donor sodium nitroprusside protects against hepatic microcirculatory dysfunction in early endotoxaemia. Intens Care Med. 1998;24(12):1257–63.

384. Zhou M, Wang P, Chaudry IH. Endothelial nitric oxide synthase is downregulated during hyperdynamic sepsis. Biochimica Et Biophysica Acta Bba - Gen Subj. 1997;1335(1–2):182–90.

385. Tiwari MM, Brock RW, Megyesi JK, Kaushal GP, Mayeux PR. Disruption of renal peritubular blood flow in lipopolysaccharide-induced renal failure: role of nitric oxide and caspases. Am J Physiol-renal. 2005;289(6):F1324–32.

386. Schramm L, Weierich T, Heldbreder E, Zimmermann J, Netzer KO, Wanner C. Endotoxin-induced acute renal failure in rats: effects of L-arginine and nitric oxide synthase inhibition on renal function. J Nephrol. 2005;18(4):374–81.

387. Hinder F, Booke M, Traber LD, Matsumoto N, Nishida K, Rogers S, et al. Nitric oxide synthase inhibition during experimental sepsis improves renal excretory function in the presence of chronically increased atrial natriuretic peptide. Crit Care Med. 1996;24(1):131–6.

388. ROSSELET A, FEIHL F, MARKERT M, GNAEGI A, PERRET C, LIAUDET L. Selective iNOS Inhibition Is Superior to Norepinephrine in the Treatment of Rat Endotoxic Shock. Am J Resp Crit Care. 1998;157(1):162–70.

389. Szabó C, Southan GJ, Thiemermann C. Beneficial effects and improved survival in rodent models of septic shock with S-methylisothiourea sulfate, a potent and selective inhibitor of inducible nitric oxide synthase. Proc National Acad Sci. 1994;91(26):12472–6.

390. Mitaka C, Hirata Y, Masaki Y, Takei T, Yokoyama K, Imai T. S-Methylisothiourea sulfate improves renal, but not hepatic dysfunction in canine endotoxic shock model. Intens Care Med. 2000;26(1):117–24.

391. Jarisch A. Kreislauffragen. Dtsch Med Wochenschr. 1928;(29):1211–3.

392. Badin J, Boulain T, Ehrmann S, Skarzynski M, Bretagnol A, Buret J, et al. Relation between mean arterial pressure and renal function in the early phase of shock: a prospective, explorative cohort study. Crit Care. 2011;15(3):R135–R135.

393. Dünser MW, Takala J, Ulmer H, Mayr VD, Luckner G, Jochberger S, et al. Arterial blood pressure during early sepsis and outcome. Intens Care Med. 2009;35(7):1225–33.

394. Poukkanen M, Wilkman E, Vaara ST, Pettilä V, Kaukonen KM, Korhonen AM, et al. Hemodynamic variables and progression of acute kidney injury in critically ill patients with severe sepsis: data from the prospective observational FINNAKI study. Crit Care. 2013;17(6):R295.

395. Asfar P, Meziani F, Hamel JF, Grelon F, Megarbane B, Anguel N, et al. High versus Low Blood-Pressure Target in Patients with Septic Shock. New Engl J Medicine. 2014;370(17):1583–93.

396. Lamontagne F, Richards-Belle A, Thomas K, Harrison DA, Sadique MZ, Grieve RD, et al. Effect of Reduced Exposure to Vasopressors on 90-Day Mortality in Older Critically Ill Patients With Vasodilatory Hypotension. Jama. 2020;323(10):938–49.

397. Langenberg C, Wan L, Egi M, May CN, Bellomo R. Renal blood flow and function during recovery from experimental septic acute kidney injury. Intens Care Med. 2007;33(9):1614–8.

398. Giantomasso DD, May CN, Bellomo R. Vital Organ Blood Flow During Hyperdynamic Sepsis. Chest. 2003;124(3):1053–9.

399. Benes J, Chvojka J, Sykora R, Radej J, Krouzecky A, Novak I, et al. Searching for mechanisms that matter in septic acute kidney injury: an experimental study. Crit Care. 2011;15(Suppl 1):P97.

400. BELLOMO R, KELLUM JA, WISNIEWSKI SR, PINSKY MR, Ondulik B. Effects of Norepinephrine on the Renal Vasculature in Normal and Endotoxemic Dogs. Am J Resp Crit Care. 1999;159(4):1186–92.

401. Brenner M, Schaer GL, Mallory DL, Suffredini AF, Parrillo JE. Detection of Renal Blood Flow Abnormalities in Septic and Critically III Patients Using a Newly Designed Indwelling Thermodilution Renal Vein Catheter. Chest. 2016 Feb 19;98(1):170–9.

402. Bergström J, Bucht H, Josephson B. Determination of the Renal Blood Flow in Man-By Means of Radioactive Diodrast and Renal Vein Catheterization. Scand J Clin Laboratory Investigation. 2010;11(1):71–81.

403. Lankadeva YR, Kosaka J, Evans RG, May CN. Traumatic and Ischemic Injury, Methods and Protocols. Methods Mol Biology. 2018;1717:207–18.

404. Lankadeva YR, Kosaka J, Iguchi N, Evans RG, Booth LC, Bellomo R, et al. Effects of Fluid Bolus Therapy on Renal Perfusion, Oxygenation, and Function in Early Experimental Septic Kidney Injury. Critical Care Medicine. 2018 Oct 31;Publish Ahead of Print:1.

405. Lankadeva YR, May CN, Cochrane AD, Marino B, Hood SG, McCall PR, et al. Influence of blood haemoglobin concentration on renal haemodynamics and oxygenation during experimental cardiopulmonary bypass in sheep. Acta Physiol. 2021;231(3):e13583.

406. Iguchi N, Lankadeva YR, Mori TA, Osawa EA, Cutuli SL, Evans RG, et al. Furosemide reverses medullary tissue hypoxia in ovine septic acute kidney injury. Am J Physiology-regulatory Integr Comp Physiology. 2019;317(2):R232–9.

407. Lankadeva YR, Kosaka J, Evans RG, Bellomo R, May CN. Urinary Oxygenation as a Surrogate Measure of Medullary Oxygenation During Angiotensin II Therapy in Septic Acute Kidney Injury. Crit Care Med. 2018;46(1):e41–8.

408. Zhen J, Li L, Yan J. Advances in biomarkers of myocardial injury in sepsis. Chin Critical Care Medicine. 2018;30(7):699–702.

409. Chen KP, Cavender S, Lee J, Feng M, Mark RG, Celi LA, et al. Peripheral Edema, Central Venous Pressure, and Risk of AKI in Critical Illness. Clin J Am Soc Nephro. 2016;11(4):602–8.

410. Husain-Syed F, Birk H, Ronco C, Schörmann T, Tello K, Richter MJ, et al. Doppler-Derived Renal Venous Stasis Index in the Prognosis of Right Heart Failure. J Am Heart Assoc. 2019;8(21):e013584.

411. Beaubien-Souligny W, Rola P, Haycock K, Bouchard J, Lamarche Y, Spiegel R, et al. Quantifying systemic congestion with Point-Of-Care ultrasound: development of the venous excess ultrasound grading system. Ultrasound J. 2020;12(1):16.

412. Brunkhorst FM, Engel C, Bloos F, Meier-Hellmann A, Ragaller M, Weiler N, et al. Intensive Insulin Therapy and Pentastarch Resuscitation in Severe Sepsis. New Engl J Medicine. 2008;358(2):125–39.

413. Perner A, Haase N, Guttormsen AB, Tenhunen J, Klemenzson G, Åneman A, et al. Hydroxyethyl Starch 130/0.42 versus Ringer's Acetate in Severe Sepsis. New Engl J Medicine. 2012;367(2):124–34.

414. Myburgh JA, Finfer S, Bellomo R, Billot L, Cass A, Gattas D, et al. Hydroxyethyl Starch or Saline for Fluid Resuscitation in Intensive Care. New Engl J Medicine. 2012;367(20):1901–11.

415. Schick MA, Isbary TJ, Schlegel N, Brugger J, Waschke J, Muellenbach R, et al. The impact of crystalloid and colloid infusion on the kidney in rodent sepsis. Intens Care Med. 2010;36(3):541–8.

416. Chowdhury AH, Cox EF, Francis ST, Lobo DN. A Randomized, Controlled, Double-Blind Crossover Study on the Effects of 2-L Infusions of 0.9% Saline and Plasma-Lyte® 148 on Renal Blood Flow Velocity and Renal Cortical Tissue Perfusion in Healthy Volunteers. Ann Surg. 2012;256(1):18–24.

417. Self WH, Semler MW, Wanderer JP, Wang L, Byrne DW, Collins SP, et al. Balanced Crystalloids versus Saline in Noncritically Ill Adults. New Engl J Medicine. 2018;378(9):819–28.

418. Semler MW, Self WH, Wanderer JP, Ehrenfeld JM, Wang L, Byrne DW, et al. Balanced Crystalloids versus Saline in Critically Ill Adults. New Engl J Medicine. 2018;378(9):829–39.

419. Inkinen N, Jukarainen S, Wiersema R, Poukkanen M, Pettilä V, Vaara ST. Fluid management in patients with acute kidney injury – A post-hoc analysis of the FINNAKI study. J Crit Care. 2021;64:205–10.

420. Grams ME, Estrella MM, Coresh J, Brower RG, Liu KD, Lung and BIARDSN for the NH. Fluid Balance, Diuretic Use, and Mortality in Acute Kidney Injury. Clin J Am Soc Nephro. 2011;6(5):966–73.

421. Prowle JR, Echeverri JE, Ligabo EV, Ronco C, Bellomo R. Fluid balance and acute kidney injury. Nat Rev Nephrol. 2010;6(2):107–15.

422. Cruces P, Salas C, Lillo P, Salomon T, Lillo F, Hurtado DE. The renal compartment: a hydraulic view. Intensive Care Medicine Exp. 2014;2(1):26.

423. Lankadeva YR, Ma S, Iguchi N, Evans RG, Hood SG, Farmer DGS, et al. Dexmedetomidine reduces norepinephrine requirements and preserves renal oxygenation and function in ovine septic acute kidney injury. Kidney Int. 2019;96(5):1150–61.

424. Schneider AG, Goodwin MD, Schelleman A, Bailey M, Johnson L, Bellomo R. Contrast-enhanced ultrasound to evaluate changes in renal cortical perfusion around cardiac surgery: a pilot study. Crit Care. 2013 Jul 12;17(4):R138.

425. Bersten ADM, Rutten AJBs. Renovascular interaction of epinephrine, dopamine, and intraperitoneal sepsis. Crit Care Med. 1995;23(3):537-544.

426. Fink MP, Nelson R, Roethel R. Low-dose dopamine preserves renal blood flow in endotoxin shocked dogs treated with ibuprofen. J Surg Res. 1985;38(6):582–91.

427. Post EH, Su F, Taccone FS, Hosokawa K, Herpain A, Creteur J, et al. THE EFFECTS OF FENOLDOPAM ON RENAL FUNCTION AND METABOLISM IN AN OVINE MODEL OF SEPTIC SHOCK. Shock. 2016;45(4):385–92.

428. Ishikawa K, Calzavacca P, Bellomo R, Bailey M, May CN. Effect of selective inhibition of renal inducible nitric oxide synthase on renal blood flow and function in experimental hyperdynamic sepsis* Crit Care Med. 2012;40(8):2368–75.

429. Ishikawa K, Bellomo R, May CN. The impact of intrarenal nitric oxide synthase inhibition on renal blood flow and function in mild and severe hyperdynamic sepsis* Crit Care Med. 2011;39(4):770–6.

430. Okazaki N, Iguchi N, Evans RG, Hood SG, Bellomo R, May CN, et al. Beneficial Effects of Vasopressin Compared With Norepinephrine on Renal Perfusion, Oxygenation, and Function in Experimental Septic Acute Kidney Injury. Crit Care Med. 2020;48(10):e951–8.

431. Albert M, Losser MR, Hayon D, Faivre V, Payen D. Systemic and renal macro- and microcirculatory responses to arginine vasopressin in endotoxic rabbits* Crit Care Med. 2004;32(9):1891–8.

432. Ishikawa K, Wan L, Calzavacca P, Bellomo R, Bailey M, May CN. The Effects of Terlipressin on Regional Hemodynamics and Kidney Function in Experimental Hyperdynamic Sepsis. Plos One. 2012;7(2):e29693.

433. Edwards RM, Trizna W, Kinter LB. Renal microvascular effects of vasopressin and vasopressin antagonists. Am J Physiol-renal. 1989;256(2):F274–8.

434. Sacha GL, Lam SW, Bauer SR. Did the beneficial renal outcomes with vasopressin VANISH? Ann Transl Medicine. 2016;4(S1):S67–S67.

435. Tamaki T, Kiyomoto K, He H, Tomohiro A, Nishiyama A, Aki Y, et al. Vasodilation induced by vasopressin V2 receptor stimulation in afferent arterioles. Kidney Int. 1996;49(3):722–9.

436. Wan L, Langenberg C, Bellomo R, May CN. Angiotensin II in experimental hyperdynamic sepsis. Crit Care. 2009;13(6):R190–R190.

437. Gordon AC, Russell JA, Walley KR, Singer J, Ayers D, Storms MM, et al. The effects of vasopressin on acute kidney injury in septic shock. Intens Care Med [Internet]. 2009 Oct 20;36(1):83–91. Available from: https://link.springer.com/content/pdf/10.1007%2Fs00134-009-1687-x.pdf

438. Russell JA, Walley KR, Singer J, Gordon AC, Hébert PC, Cooper DJ, et al. Vasopressin versus Norepinephrine Infusion in Patients with Septic Shock. New Engl J Medicine. 2008;358(9):877–87.

439. Backer DD, Creteur J, Dubois MJ, Sakr Y, Vincent JL. Microvascular alterations in patients with acute severe heart failure and cardiogenic shock. American heart journal. 2004 Jan;147(1):91–9.

440. Levy B, Gibot S, Franck P, Cravoisy A, Bollaert PE. Relation between muscle Na+K+ ATPase activity and raised lactate concentrations in septic shock: a prospective study. Lancet (London, England). 2005 Mar;365(9462):871–5.

441. Levy B, Perez P, Gibot S, Gerard A. Increased muscle-to-serum lactate gradient predicts progression towards septic shock in septic patients. Intens Care Med. 2010;36(10):1703–9.

442. Tammaro A, Kers J, Scantlebery AML, Florquin S. Metabolic Flexibility and Innate Immunity in Renal Ischemia Reperfusion Injury: The Fine Balance Between Adaptive Repair and Tissue Degeneration. Front Immunol. 2020;11:1346.

443. El-Achkar TM, Huang X, Plotkin Z, Sandoval RM, Rhodes GJ, Dagher PC. Sepsis induces changes in the expression and distribution of Toll-like receptor 4 in the rat kidney. Am J Physiol-renal. 2006;290(5):F1034–43.

444. Toro J, Manrique-Caballero CL, Gómez H. Metabolic Reprogramming and Host Tolerance: A Novel Concept to Understand Sepsis-Associated AKI. J Clin Medicine. 2021;10(18):4184.

445. Zager RA, Johnson ACM, Hanson SY, Lund S. Ischemic proximal tubular injury primes mice to endotoxin-induced TNF-α generation and systemic release. Am J Physiol-renal. 2005;289(2):F289–97.

446. Naito M, Bomsztyk K, Zager RA. Endotoxin Mediates Recruitment of RNA Polymerase II to Target Genes in Acute Renal Failure. J Am Soc Nephrol. 2008;19(7):1321–30.

447. Nakano D, Kitada K, Wan N, Zhang Y, Wiig H, Wararat K, et al. Lipopolysaccharide induces filtrate leakage from renal tubular lumina into the interstitial space via a proximal tubular Toll-like receptor 4–dependent pathway and limits sensitivity to fluid therapy in mice. Kidney Int. 2020;97(5):904–12.

448. Nakano D, Doi K, Kitamura H, Kuwabara T, Mori K, Mukoyama M, et al. Reduction of Tubular Flow Rate as a Mechanism of Oliguria in the Early Phase of Endotoxemia Revealed by Intravital Imaging. J Am Soc Nephrol. 2015;26(12):3035–44.

449. Nakano D. Septic acute kidney injury: a review of basic research. Clin Exp Nephrol. 2020;24(12):1091–102.

450. Knotek M, Rogachev B, Wang W, Ecder T, Melnikov V, Gengaro PE, et al. Endotoxemic renal failure in mice: Role of tumor necrosis factor independent of inducible nitric oxide synthase. Kidney Int. 2001;59(6):2243.

451. Wu X, Guo R, Chen P, Wang Q, Cunningham PN. TNF induces caspase-dependent inflammation in renal endothelial cells through a Rho- and myosin light chain kinase-dependent mechanism. Am J Physiol-renal. 2009;297(2):F316–26.

452. Xu C, Chang A, Hack BK, Eadon MT, Alper SL, Cunningham PN. TNF-mediated damage to glomerular endothelium is an important determinant of acute kidney injury in sepsis. Kidney Int. 2014;85(1):72–81.

453. Salmon AHJ, Ferguson JK, Burford JL, Gevorgyan H, Nakano D, Harper SJ, et al. Loss of the Endothelial Glycocalyx Links Albuminuria and Vascular Dysfunction. J Am Soc Nephrol. 2012;23(8):1339–50.

454. McMahon BA, Galligan M, Redahan L, Martin T, Meaney E, Cotter EJ, et al. Biomarker Predictors of Adverse Acute Kidney Injury Outcomes in Critically Ill Patients: The Dublin Acute Biomarker Group Evaluation Study. Am J Nephrol. 2019;50(1):19–28.

455. Kalakeche R, Hato T, Rhodes G, Dunn KW, El-Achkar TM, Plotkin Z, et al. Endotoxin Uptake by S1 Proximal Tubular Segment Causes Oxidative Stress in the Downstream S2 Segment. J Am Soc Nephrol. 2011;22(8):1505–16.

456. Hato T, Winfree S, Day R, Sandoval RM, Molitoris BA, Yoder MC, et al. Two-Photon Intravital Fluorescence Lifetime Imaging of the Kidney Reveals Cell-Type Specific Metabolic Signatures. J Am Soc Nephrol. 2017;28(8):2420–30.

457. Zager RA. 'Biologic memory' in response to acute kidney injury: cytoresistance, toll-like receptor hyper-responsiveness and the onset of progressive renal disease. Nephrol Dial Transpl. 2013;28(8):1985–93.

458. Zager RA, Johnson ACM. Renal ischemia-reperfusion injury upregulates histone-modifying enzyme systems and alters histone expression at proinflammatory/profibrotic genes. Am J Physiol-renal. 2009;296(5):F1032–41.

459. Gómez H, Kellum JA, Ronco C. Metabolic reprogramming and tolerance during sepsis-induced AKI. Nat Rev Nephrol. 2017;13(3):143–51.

460. Hallows KR, Mount PF, Pastor-Soler NM, Power DA. Role of the energy sensor AMP-activated protein kinase in renal physiology and disease. Am J Physiol-renal. 2010;298(5):F1067–77.

461. Larsen R, Gozzelino R, Jeney V, Tokaji L, Bozza FA, Japiassú AM, et al. A Central Role for Free Heme in the Pathogenesis of Severe Sepsis. Sci Transl Med. 2010;2(51):51ra71-51ra71.

462. Figueiredo N, Chora A, Raquel H, Pejanovic N, Pereira P, Hartleben B, et al. Anthracyclines Induce DNA Damage Response-Mediated Protection against Severe Sepsis. Immunity. 2013;39(5):874–84.

463. Ferreira A, Balla J, Jeney V, Balla G, Soares MP. A central role for free heme in the pathogenesis of severe malaria: the missing link? J Mol Med. 2008;86(10):1097–111.

464. Medzhitov R, Schneider DS, Soares MP. Disease Tolerance as a Defense Strategy. Science. 2012;335(6071):936–41.

465. Bolisetty S, Agarwal A. Neutrophils in acute kidney injury: not neutral any more. Kidney Int. 2009;75(7):674–6.

466. Lee S, Huen S, Nishio H, Nishio S, Lee HK, Choi BS, et al. Distinct Macrophage Phenotypes Contribute to Kidney Injury and Repair. J Am Soc Nephrol. 2011;22(2):317–26.

467. Zhang ZX, Wang S, Huang X, Min WP, Sun H, Liu W, et al. NK Cells Induce Apoptosis in Tubular Epithelial Cells and Contribute to Renal Ischemia-Reperfusion Injury. J Immunol. 2008;181(11):7489–98.

468. Li L, Huang L, Ye H, Song SP, Bajwa A, Lee SJ, et al. Dendritic cells tolerized with adenosine A2AR agonist attenuate acute kidney injury. J Clin Invest. 2012;122(11):3931–42.

469. Wan L, Bagshaw SM, Langenberg C, Saotome T, May C, Bellomo R. Pathophysiology of septic acute kidney injury: What do we really know? Crit Care Med. 2008 Apr;36(4):S198–203.

470. Langenberg C, Bagshaw SM, May CN, Bellomo R. The histopathology of septic acute kidney injury: a systematic review. Crit Care. 2008;12(2):R38.

471. Hotchkiss RS, Swanson PE, Freeman BD, Tinsley KW, Cobb JP, Matuschak GM, et al. Apoptotic cell death in patients with sepsis, shock, and multiple organ dysfunction. Crit Care Med. 1999;27(7):1230-1251.

472. Peerapornratana S, Manrique-Caballero CL, Gómez H, Kellum JA. Acute kidney injury from sepsis: current concepts, epidemiology, pathophysiology, prevention and treatment. Kidney Int. 2019;96(5):1083–99.

473. Heiden MGV, Cantley LC, Thompson CB. Understanding the Warburg Effect: The Metabolic Requirements of Cell Proliferation. Science. 2009;324(5930):1029–33.

474. Frauwirth KA, Riley JL, Harris MH, Parry RV, Rathmell JC, Plas DR, et al. The CD28 Signaling Pathway Regulates Glucose Metabolism. Immunity. 2002;16(6):769–77.

475. Smith JA, Stallons LJ, Schnellmann RG. Renal cortical hexokinase and pentose phosphate pathway activation through the EGFR/Akt signaling pathway in endotoxin-induced acute kidney injury. Am J Physiol-renal. 2014;307(4):F435–44.

476. Patil NK, Parajuli N, MacMillan-Crow LA, Mayeux PR. Inactivation of renal mitochondrial respiratory complexes and manganese superoxide dismutase during sepsis: mitochondria-targeted antioxidant mitigates injury. Am J Physiol-renal. 2014;306(7):F734–43.

477. Waltz P, Carchman E, Gomez H, Zuckerbraun B. Sepsis results in an altered renal metabolic and osmolyte profile. J Surg Res. 2016;202(1):8–12.

478. Cheng SC, Quintin J, Cramer RA, Shepardson KM, Saeed S, Kumar V, et al. mTOR- and HIF-1α–mediated aerobic glycolysis as metabolic basis for trained immunity. Science. 2014;345(6204):1250684–1250684.

479. Jin K, Li H, Volpe J, Emlet D, Pastor-Soler N, Pinsky M, et al. Is acute kidney injury in the early phase of sepsis a sign of metabolic downregulation in tubular epithelial cells? Crit Care. 2015;19(Suppl 1):P286.

480. Han SH, Malaga-Dieguez L, Chinga F, Kang HM, Tao J, Reidy K, et al. Deletion of Lkb1 in Renal Tubular Epithelial Cells Leads to CKD by Altering Metabolism. J Am Soc Nephrol. 2016;27(2):439–53.

481. Bartz RR, Fu P, Suliman HB, Crowley SD, MacGarvey NC, Welty-Wolf K, et al. Staphylococcus aureus Sepsis Induces Early Renal Mitochondrial DNA Repair and Mitochondrial Biogenesis in Mice. Plos One. 2014;9(7):e100912.

482. Hsiao HW, Tsai KL, Wang LF, Chen YH, Chiang PC, Chuang SM, et al. The Decline of Autophagy Contributes to Proximal Tubular Dysfunction During Sepsis. Shock. 2012;37(3):289–96.

483. Endre ZH, Mehta RL. Identification of acute kidney injury subphenotypes. Curr Opin Crit Care. 2020;26(6):519–24.

484. Huang CT, Liu KD. Exciting developments in the field of acute kidney injury. Nat Rev Nephrol. 2020;16(2):69–70.

485. Garofalo AM, Lorente-Ros M, Goncalvez G, Carriedo D, Ballén-Barragán A, Villar-Fernández A, et al. Histopathological changes of organ dysfunction in sepsis. Intensive Care Medicine Exp. 2019;7(Suppl 1):45.

486. Xu K, Rosenstiel P, Paragas N, Hinze C, Gao X, Shen TH, et al. Unique Transcriptional Programs Identify Subtypes of AKI. J Am Soc Nephrol. 2017;28(6):1729–40.

487. Bhatraju PK, Cohen M, Nagao RJ, Morrell ED, Kosamo S, Chai XY, et al. Genetic variation implicates plasma angiopoietin-2 in the development of acute kidney injury sub-phenotypes. Bmc Nephrol. 2020;21(1):284.

488. Go AS, Parikh CR, Ikizler TA, Coca S, Siew ED, Chinchilli VM, et al. The assessment, serial evaluation, and subsequent sequelae of acute kidney injury (ASSESS-AKI) study: design and methods. Bmc Nephrol. 2010;11(1):22.

489. Bhatraju PK, Prince DK, Mansour S, Ikizler TA, Siew ED, Chinchilli VM, et al. Data Driven Analysis of Molecular Data Classifies AKI Patient and Predicts Clinical Outcomes. Ssrn Electron J. 2021;

490. Wiersema R, Jukarainen S, Vaara ST, Poukkanen M, Lakkisto P, Wong H, et al. Two subphenotypes of septic acute kidney injury are associated with different 90-day mortality and renal recovery. Crit Care. 2020;24(1):150.

491. Chaudhary K, Duffy A, Poojary P, Saha A, Chauhan K, Do R, et al. Unsupervised Machine learning to subtype Sepsis-Associated Acute Kidney Injury. Biorxiv. 2018;447425.

492. Chaudhary K, Vaid A, Duffy Á, Paranjpe I, Jaladanki S, Paranjpe M, et al. Utilization of Deep Learning for Subphenotype Identification in Sepsis-Associated Acute Kidney Injury. Clin J Am Soc Nephro. 2020;15(11):1557–65.

493. Malhotra R, Siew ED. Biomarkers for the Early Detection and Prognosis of Acute Kidney Injury. Clin J Am Soc Nephro. 2017;12(1):149–73.

494. Levey AS, Grams ME, Inker LA. Uses of GFR and Albuminuria Level in Acute and Chronic Kidney Disease. N Engl J Med. 2022;386(22):2120–8.

495. Benzing T, Salant D. Insights into Glomerular Filtration and Albuminuria. N Engl J Med. 2021;384(15):1437–46.

496. Wang Y, Zou Z, Jin J, Teng J, Xu J, Shen B, et al. Urinary TIMP-2 and IGFBP7 for the prediction of acute kidney injury following cardiac surgery. Bmc Nephrol. 2017;18(1):177.

497. Bagshaw SM, Laupland KB, Doig CJ, Mortis G, Fick GH, Mucenski M, et al. Prognosis for long-term survival and renal recovery in critically ill patients with severe acute renal failure: a population-based study. Crit Care. 2005;9(6):R700–9.

498. Uchino S, Bellomo R, Goldsmith D, Bates S, Ronco C. An assessment of the RIFLE criteria for acute renal failure in hospitalized patients* Crit Care Med. 2006;34(7):1913–7.

499. Bagshaw SM, George C, Dinu I, Bellomo R. A multi-centre evaluation of the RIFLE criteria for early acute kidney injury in critically ill patients. Nephrol Dial Transpl. 2008;23(4):1203–10.

500. Hoste EA, Clermont G, Kersten A, Venkataraman R, Angus DC, Bacquer DD, et al. RIFLE criteria for acute kidney injury are associated with hospital mortality in critically ill patients: a cohort analysis. Crit Care. 2006;10(3):R73–R73.

501. Ikizler TA, Parikh CR, Himmelfarb J, Chinchilli VM, Liu KD, Coca SG, et al. A prospective cohort study of acute kidney injury and kidney outcomes, cardiovascular events, and death. Kidney Int. 2021;99(2):456–65.

502. Lafrance JP, Miller DR. Acute Kidney Injury Associates with Increased Long-Term Mortality. J Am Soc Nephrol. 2010;21(2):345–52.

503. James MT, Bhatt M, Pannu N, Tonelli M. Long-term outcomes of acute kidney injury and strategies for improved care. Nat Rev Nephrol. 2020;16(4):193–205.

504. Fiorentino M, Tohme FA, Wang S, Murugan R, Angus DC, Kellum JA. Long-term survival in patients with septic acute kidney injury is strongly influenced by renal recovery. Plos One. 2018;13(6):e0198269.

505. Chawla LS, Amdur RL, Amodeo S, Kimmel PL, Palant CE. The severity of acute kidney injury predicts progression to chronic kidney disease. Kidney Int. 2011;79(12):1361–9.

506. Thakar CV, Christianson A, Himmelfarb J, Leonard AC. Acute Kidney Injury Episodes and Chronic Kidney Disease Risk in Diabetes Mellitus. Clin J Am Soc Nephro. 2011;6(11):2567–72.

507. Wu VC, Huang TM, Lai CF, Shiao CC, Lin YF, Chu TS, et al. Acute-on-chronic kidney injury at hospital discharge is associated with long-term dialysis and mortality. Kidney Int. 2011;80(11):1222–30.

508. Schmitt R, Coca S, Kanbay M, Tinetti ME, Cantley LG, Parikh CR. Recovery of Kidney Function After Acute Kidney Injury in the Elderly: A Systematic Review and Meta-analysis. Am J Kidney Dis. 2008;52(2):262–71.

509. Wang HE, Jain G, Glassock RJ, Warnock DG. Comparison of absolute serum creatinine changes versus Kidney Disease: Improving Global Outcomes consensus definitions for characterizing stages of acute kidney injury. Nephrol Dial Transpl. 2013;28(6):1447–54.

510. Zarbock A, Kellum JA, Schmidt C, Aken HV, Wempe C, Pavenstädt H, et al. Effect of Early vs Delayed Initiation of Renal Replacement Therapy on Mortality in Critically Ill Patients With Acute Kidney Injury: The ELAIN Randomized Clinical Trial. Jama [Internet]. 2016 May 24;315(20):2190. Available from: https://jamanetwork.com/journals/jama/fullarticle/2522434

511. Gaudry S, Hajage D, Schortgen F, Martin-Lefevre L, Pons B, Boulet E, et al. Initiation Strategies for Renal-Replacement Therapy in the Intensive Care Unit. New Engl J Medicine. 2016 Jul 14;375(2):122–33.

512. Investigators SA, Group CCCTG the Australian and New Zealand Intensive Care Society Clinical Trials Group, the United Kingdom Critical Care Research Group, the Canadian Nephrology Trials Network, and the Irish Critical Care Trials, Bagshaw SM, Wald R, Adhikari NKJ, Bellomo R, et al. Timing of Initiation of Renal-Replacement Therapy in Acute Kidney Injury. New Engl J Med. 2020;383(3):240–51.

513. Barbar SD, Clere-Jehl R, Bourredjem A, Hernu R, Montini F, Bruyère R, et al. Timing of Renal-Replacement Therapy in Patients with Acute Kidney Injury and Sepsis. New Engl J Med. 2018 Oct 11;379(15):1431–42.

514. Molema G, Zijlstra JG, Meurs M van, Kamps JAAM. Renal microvascular endothelial cell responses in sepsis-induced acute kidney injury. Nat Rev Nephrol. 2022;18(2):95–112.

515. Li T, Ji X, Liu J, Guo X, Pang R, Zhuang H, et al. Ulinastatin Improves Renal Microcirculation by Protecting Endothelial Cells and Inhibiting Autophagy in a Septic Rat Model. Kidney Blood Press Res. 2022;47(4):256–69.

516. Coca SG, Singanamala S, Parikh CR. Chronic kidney disease after acute kidney injury: a systematic review and meta-analysis. Kidney Int. 2012;81(5):442–8.

517. Kuilman T, Michaloglou C, Mooi WJ, Peeper DS. The essence of senescence. Gene Dev. 2010;24(22):2463–79.

518. Ruiz-Torres MP, Bosch RJ, O'Valle F, Moral RGD, Ramírez C, Masseroli M, et al. Age-related increase in expression of TGF-beta1 in the rat kidney: relationship to morphologic changes. J Am Soc Nephrol. 1998;9(5):782–91.

519. Karam Z, Tuazon J. Anatomic and Physiologic Changes of the Aging Kidney. Clin Geriatr Med. 2013;29(3):555–64.

520. Kang HM, Huang S, Reidy K, Han SH, Chinga F, Susztak K. Sox9-Positive Progenitor Cells Play a Key Role in Renal Tubule Epithelial Regeneration in Mice. Cell Reports. 2016;14(4):861–71.

521. Bonventre JV. Dedifferentiation and Proliferation of Surviving Epithelial Cells in Acute Renal Failure. J Am Soc Nephrol. 2003;14(6):S55–61.

522. Lazzeri E, Angelotti ML, Peired A, Conte C, Marschner JA, Maggi L, et al. Endocycle-related tubular cell hypertrophy and progenitor proliferation recover renal function after acute kidney injury. Nat Commun. 2018;9(1):1344.

523. Venkatachalam MA, Griffin KA, Lan R, Geng H, Saikumar P, Bidani AK. Acute kidney injury: a springboard for progression in chronic kidney disease. Am J Physiol-renal. 2010;298(5):F1078–94.

524. Kulkarni OP, Hartter I, Mulay SR, Hagemann J, Darisipudi MN, VR SK, et al. Toll-Like Receptor 4–Induced IL-22 Accelerates Kidney Regeneration. J Am Soc Nephrol. 2014;25(5):978–89.

525. Cheng Y, Luo R, Wang K, Zhang M, Wang Z, Dong L, et al. Kidney disease is associated with in-hospital death of patients with COVID-19. Kidney Int. 2020 May;97(5):829–38.

526. Zhou F, Yu T, Du R, Fan G, Liu Y, Liu Z, et al. Clinical course and risk factors for mortality of adult inpatients with COVID-19 in Wuhan, China: a retrospective cohort study. Lancet (London, England). 2020 Mar 28;395(10229):1054–62.

527. Richardson S, Hirsch JS, Narasimhan M, Crawford JM, McGinn T, Davidson KW, et al. Presenting Characteristics, Comorbidities, and Outcomes Among 5700 Patients Hospitalized With COVID-19 in the New York City Area. Jama. 2020 Apr 22;323(20):2052–9.

528. icnarc07. ICNARC report on COVID-19 in critical care 29 May 2020. 2020 May 29;1–35.

529. Adamczak M, Surma S, Więcek A. Acute kidney injury in patients with COVID-19: Epidemiology, pathogenesis and treatment. Adv Clin Exp Medicine Official Organ Wroclaw Medical Univ. 2022;31(3):317–26.

530. Fu EL, Janse RJ, Jong Y de, Endt VHW van der, Milders J, Willik EM van der, et al. Acute kidney injury and kidney replacement therapy in COVID-19: a systematic review and meta-analysis. Clin Kidney J. 2020;13(4):550–63.

531. Tian L, Shao X, Hang Y, Yang W, Mou S, Zhu C. Risk Factors for Acute Kidney Injury in Patients with Coronavirus Disease 2019 (COVID-19): A Meta-Analysis. 2020;

532. Su H, Yang M, Wan C, Yi LX, Tang F, Zhu HY, et al. Renal histopathological analysis of 26 postmortem findings of patients with COVID-19 in China. Kidney Int. 2020 Apr 9;98(1):219–27.

533. Roufosse C, Curtis E, Moran L, Hollinshead M, Cook T, Hanley B, et al. Electron microscopic investigations in COVID-19: not all crowns are coronas. Kidney Int. 2020;98(2):505–6.

534. Radzikowska U, Ding M, Tan G, Zhakparov D, Peng Y, Wawrzyniak P, et al. Distribution of ACE2, CD147, CD26 and other SARS-CoV-2 associated molecules in tissues and immune cells in health and in asthma, COPD, obesity, hypertension, and COVID-19 risk factors. Allergy. 2020;75(11):2829–45.

535. Nasr SH, Kopp JB. COVID-19-Associated Collapsing Glomerulopathy: An Emerging Entity. Kidney Int Reports. 2020;5(6):759–61.

536. Pons S, Fodil S, Azoulay E, Zafrani L. The vascular endothelium: the cornerstone of organ dysfunction in severe SARS-CoV-2 infection. Critical Care Lond Engl. 2020;24(1):353.

537. Hirsch JS, Ng JH, Ross DW, Sharma P, Shah HH, Barnett RL, et al. Acute kidney injury in patients hospitalized with COVID-19. Kidney Int. 2020;98(1):209–18.

538. Varga Z, Flammer AJ, Steiger P, Haberecker M, Andermatt R, Zinkernagel AS, et al. Endothelial cell infection and endotheliitis in COVID-19. Lancet (London, England). 2020 May 2;395(10234):1417–8.

539. Bagshaw SM, Uchino S, Bellomo R, Morimatsu H, Morgera S, Schetz M, et al. Septic Acute Kidney Injury in Critically Ill Patients: Clinical Characteristics and Outcomes. Clin J Am Soc Nephro. 2007 May;2(3):431–9.

540. Fabrizi F, Alfieri CM, Cerutti R, Lunghi G, Messa P. COVID-19 and Acute Kidney Injury: A Systematic Review and Meta-Analysis. Pathogens. 2020;9(12):1052.

541. Ronco C, Reis T, Husain-Syed F. Management of acute kidney injury in patients with COVID-19. Lancet Respir Medicine. 2020 May 14;8(7):738–42.

542. Ottolina D, Zazzeron L, Trevisi L, Agarossi A, Colombo R, Fossali T, et al. Acute kidney injury (AKI) in patients with Covid-19 infection is associated with ventilatory management with elevated positive end-expiratory pressure (PEEP). J Nephrol. 2022;35(1):99–111.

543. Multiorgan and Renal Tropism of SARS-CoV-2.

544. Schurink B, Roos E, Radonic T, Barbe E, Bouman CSC, Boer HH de, et al. Viral presence and immunopathology in patients with lethal COVID-19: a prospective autopsy cohort study. Lancet Microbe. 2020;1(7):e290–9.

545. Braun F, Lütgehetmann M, Pfefferle S, Wong MN, Carsten A, Lindenmeyer MT, et al. SARS-CoV-2 renal tropism associates with acute kidney injury. Lancet. 2020;396(10251):597–8.

546. Kwiatkowska E, Kwiatkowski S, Dziedziejko V, Tomasiewicz I, Domański L. Renal Microcirculation Injury as the Main Cause of Ischemic Acute Kidney Injury Development. Biology. 2022;12(2):327.

547. Ferrara G, Edul VSK, Martins E, Canales HS, Canullán C, Murias G, et al. Intestinal and sublingual microcirculation are more severely compromised in hemodilution than in hemorrhage. J Appl Physiol. 2016;120(10):1132–40.

548. Revelly JP, Tappy L, Martinez A, Bollmann M, Cayeux MC, MD MMB, et al. Lactate and glucose metabolism in severe sepsis and cardiogenic shock* Crit Care Med. 2005;33(10):2235–40.

549. Wiersema R, Forte JNC, Kaufmann T, Haas RJ de, Koster G, Hummel YM, et al. Observational Study Protocol for Repeated Clinical Examination and Critical Care Ultrasonography Within the Simple Intensive Care Studies. Journal of visualized experiments : JoVE. 2019 Jan 16;(143).